Brain neurokinin-1 receptors in depression and interactions with the serotonin system

Sepehr Hafizi

Thesis submitted in partial fulfilment of the requirements for the degree of Doctor of Philosophy in the Faculty of Medicine

University of Oxford

University Department of Pharmacology

Linacre College

Trinity Term 2009

ABSTRACT

Sepehr Hafizi, Linacre College, Oxford, D. Phil., Trinity Term 2009

Brain neurokinin-1 receptors in depression and interactions with the serotonin system

Emerging evidence suggests neurokinin-1 receptors (NK_1Rs) may be altered in depression and NK_1R antagonists may have antidepressant properties. In addition, blockade or deletion of NK_1Rs has been shown to increase neuronal firing in the dorsal raphe nucleus suggestive of an interaction with the serotonin (5-HT) system. Against this background, one main aim of this thesis was to investigate anatomical interactions in the rat brain between NK_1Rs and the 5-HT system. The second main aim was to use the positron emission tomography (PET) radioligand [^{18}F] SPA-RQ to study NK_1Rs *in vivo* in normal human volunteers and in patients with depression.

In the animal studies, immunofluorescence experiments found NK_1Rs colocalised with 5-HT_{1A} receptors to a high degree in many forebrain regions, in particular in the medial septum and hippocampus. Colocalisation was also present in the prefrontal cortex, frontal cortex and lateral/basolateral amygdala, but to a lesser degree. NK_1Rs were found to mostly colocalise with 5-HT_{2A} receptors in hippocampus only. Colocalisation between NK_1Rs and 5-HT_{1A} receptors was much greater than that between NK_1Rs and 5-HT_{2A} receptors. In separate experiments, using retrograde tracing combined with immunohistochemistry and light and electron microscopy, NK_1Rs were found on the cell bodies of some of the neurons within the lateral habenula and locus coeruleus that project to the dorsal raphe nucleus, but were not found on the cell bodies of afferent neurons in the prefrontal cortex.

In the human studies, a comparison of a reversible two-tissue, four rate constants compartment model using plasma input function was made with a transient equilibrium model for the *in vivo* quantification of NK_1Rs in humans using the PET radioligand [^{18}F]SPA-RQ. The regional brain uptake of [^{18}F]SPA-RQ was found to be consistent with the known distribution of NK_1Rs: highest in the striatum, moderate in cortex and thalamus and low in the cerebellum. Furthermore, using the transient equilibrium model and a simplified PET imaging protocol with [^{18}F]SPA-RQ, there was no difference in binding potential in any of the brain regions studied between depressed patients, patients recovered from depression and controls. However, a negative correlation was found between age and binding potential for global and regional NK_1Rs (in particular, anterior temporal lobe).

Collectively these data provide evidence for an interaction between NK_1Rs and the 5-HT system at both the presynaptic and postsynaptic levels. In addition, they confirm the utility of the PET radioligand [^{18}F] SPA-RQ for studying NK_1Rs *in vivo* in humans. However, they do not support the idea of altered NK_1R numbers in depression.

DECLARATION

I confirm I was the principal researcher in each of the studies in this thesis, conducted in collaboration with a number of colleagues. A number of abstracts and an editorial have been published from this thesis as follows:

Chapter 1:

Hafizi S, Chandra P & Cowen PJ (2007): Neurokinin-1 receptor antagonists as novel antidepressants: trials and tribulations. *Br J Psych* **191** (4): 282-284.

Chapter 2:

Hafizi S, Serres F, Pei Q, Totterdell S, Grasby PM & Sharp T (2004). Evidence for co-localisation of neurokinin-1 and 5-HT_{1A} receptors in rat forebrain. *J. Psychopharm.* Supp. **18** (3): A28.

Hafizi S, Serres FM, Pei Q, Totterdell S, Grasby PM & Sharp T (2004). Evidence for the differential co-localization of neurokinin-1 receptors with 5-HT receptor subtypes in rat forebrain. *Society for Neuroscience annual meeting* Program No. 1027.7.

Chapter 3:

Hafizi S, Boothman LJ, Totterdell S, Grasby PM & Sharp T (2005). Neurokinin-1 receptors on the afferents to the raphe. *J. Psychopharm.* Supp. **19** (5): A50.

Chapter 4:

Hinz R, **Hafizi S**, Bhagwagar Z, Hargreaves R & Grasby PM (2004). Methods of quantification for PET studies of human NK1 receptors with [^{18}F]SPA-RQ. *Neuroimage* **22** (2): T75.

Chapter 5:

Hafizi S, Hinz R, Bhagwagar Z, Fancy S, Hargreaves R, Cowen PJ & Grasby PM (2006): Imaging Brain Neurokinin-1 Receptors in Depression using the Positron Emission Tomography Radiotracer [^{18}F]SPA-RQ. *J. Psychopharm* Supp. **20** (5): A55.

ACKNOWLEDGEMENTS

Firstly, I thank the Medical Research Council (UK) for providing funding for this project in the form of an MRC Clinical Research Training Fellowship held at the University Department of Pharmacology, Oxford.

At the University Dept. of Pharmacology (Oxford), I am indebted to my supervisor Dr Trevor Sharp for his support and guidance with this work. I also thank Dr Sue Totterdell for her invaluable input and suggestions with regards to chapter 3. My further thanks go to Ms Sarah Busby for her help with surgical procedures, and Qi, Florence and Wendy for their help in the laboratory. At the University Dept. of Psychiatry (Oxford), I thank Alison Reed for plasma cortisol meausurements and Prof. Phil Cowen, Dr Bhagwagar and Dr Selvaraj for their help and advice.

At the Hammersmith Hospital (London), I thank my supervisor Prof. Grasby for all his help, support and guidance; Julian Goggi for confocal microscopy; Rainer Hinz for mathematical modelling and help with image analysis; and Sabrina Fancy for help with recruitment of subjects. I also thank Dr Murthy for the [^{11}C] WAY-100635 image in chapter 5, physicist Terry Spinks; radiographers Andy Blythe and team; chemists Sajinder Luthra and Zhao Yongjun for synthesis of [^{18}F]SPA-RQ; and Safiye Osman and team for radiochemical quality control and metabolite analysis. Further thanks go to Merck Laboratories for providing the precursor for [^{18}F]SPA-RQ. Very importantly I thank all of the subjects who participated in the clinical studies, without whose participation much of this thesis would not have been possible.

Finally, I thank my friends and family for their emotional support through these years.

CONTENTS

Title i

Abstract ii

Declaration iii

Acknowledgements iv

Contents v

List of figures xii

List of tables xvi

Abbreviations xviii

CHAPTER 1- GENERAL INTRODUCTION.....1

1.1. Scope of thesis 1
1.2. Substance P and tachykinin receptors 3
1.3. Neuroanatomy of tackykinin and tachykinin receptor systems 8
1.3.1. Neuroanatomical studies in rodents 8
1.3.1.1. Tachykinin cell-bodies.....8
1.3.1.2. Tachykinin pathways 11
1.3.1.3. Tachykinin receptors.....13
1.3.2. Neuroanatomical studies in humans and non-human primates.....14
1.3.2.1. Tachykinins.....14
1.3.2.2. Tachykinin receptors.....15
1.4. Substance P and NK_1 receptors in anxiety and depression.....19
1.4.1. Animal studies 19
1.4.1.1. Behavioural effects of substance P and substance P agonists 19
1.4.1.2. Effects of stress on substance P and NK_1 receptors.....20
1.4.1.3. Effects of psychotropic drugs on substance P and NK_1 receptors.....21
1.4.1.4. Effects of electroconvulsive shock on substance P and NK_1 receptors.....23
1.4.1.5. NK_1receptor antagonism.....24
1.4.1.5.1. *Pharmacological blockade* 24
1.4.1.5.2. *Genetic deletion* 26
1.4.1.5.3. *Substance P-saporin* 27
1.4.2. Human studies.....27
1.4.2.1. Studies of substance P.....27
1.4.2.2. Studies of NK_1 receptors.....28
1.4.2.2.1. *NK_1 receptor antagonism*.....28
1.4.2.2.2. *Postmortem studies* 28
1.5. The central 5-HT system 30

1.5.1. 5-Hydroxytryptamine 30
1.5.2. Major 5-HT pathways 30
1.5.2.1. Brainstem and cerebellar 5-HT projections 30
1.5.2.2. 5-HT fibres innervating the forebrain 31
1.5.2.3. Afferent projections to the dorsal raphe nucleus 32
1.5.3. 5-HT receptors 35
1.5.3.1. 5-HT_1 receptors 35
1.5.3.1.1. *5-HT_{1A} receptors* 35
1.5.3.1.2. *5-HT_{1B-1F} receptors* 36
1.5.3.2. 5-HT_2 receptors 36
1.5.3.2.1. *5-HT_{2A} receptors* 36
1.5.3.2.2. *5-HT_{2B} and 5-HT_{2C} receptors* 38
1.5.3.3. Other 5-HT receptors 38
1.6. 5-HT and depression 41
1.6.1. The role of 5-HT receptors in depression 41
1.6.1.1. 5-HT_{1A} receptors in depression 41
1.6.1.2. 5-HT_{2A} receptors in depression 43
1.7. Interactions between NK_1 receptors and 5-HT 45
1.7.1. Coexistence of 5-HT receptors and tachykinins 45
1.7.2. NK_1 receptor blockade and alterations in 5-HT 45
1.8. Summary 48
1.9. Aims of thesis 49

CHAPTER 2- INVESTIGATION INTO COLOCALISATION OF NK_1 RECEPTORS WITH 5-HT_{1A} AND 5-HT_{2A} RECEPTORS IN RAT FOREBRAIN 50

2.1. Introduction 50
2.1.1. Interactions between NK_1 receptors and 5-HT system 50
2.1.2. Aims of this chapter 52
2.2. Materials and methods 53
2.2.1. Animals 53
2.2.2. Immunohistochemistry 53
2.2.2.1. 5-HT_{1A} receptor and NK_1 receptor colocalisation 53
2.2.2.2. 5-HT_{2A} receptor and NK_1 receptor colocalisation 54
2.2.3. Image acquisition and analysis of material 56
2.3. Results 59
2.3.1. Distribution of NK_1 receptor immunoreactivity 59
2.3.2. Distribution of 5-HT_{1A} receptor immunoreactivity 59
2.3.3. Distribution of 5-HT_{2A} receptor immunoreactivity 60
2.3.4. NK_1 and 5-HT_{1A} receptor colocalisation in rat forebrain regions 60
2.3.5. NK_1 and 5-HT_{2A} receptor colocalisation in rat forebrain regions 60
2.4. Discussion 75
2.4.1. Colocalisation of NK_1 and 5-HT_{1A} receptors in rat forebrain 75
2.4.1.1. Septum 76
2.4.1.2. Hippocampus 76
2.4.1.3. Amygdala 77
2.4.1.4. Prefrontal cortex 77

2.4.2. Colocalisation of NK_1 and 5-HT_{2A} receptors in rat forebrain.....78
2.4.2.1. Hippocampus 78
2.4.2.2. Amygdala.....79
2.4.3. Methodological issues.....79
2.4.3.1. Specificity of the NK_1 receptor antibody.....79
2.4.3.2. Specificity of the 5-HT_{1A} receptor antibody.....80
2.4.3.3. Specificity of the 5-HT_{2A} receptor antibody.....83
2.4.3.4. Other technical considerations.....86
2.4.4. Functional effects of NK_1 and 5-HT_{1A} receptor colocalisation 87
2.4.4.1. Septum 87
2.4.4.2. Hippocampus 88
2.4.4.3. Amygdala.....90
2.4.4.4. Prefrontal cortex.....91
2.4.5. Functional effects of NK_1 and 5-HT_{2A} receptor colocalisation 91
2.5. Conclusions.....93

CHAPTER 3- INVESTIGATION OF NK_1 RECEPTORS ON AFFERENT PROJECTIONS TO DORSAL RAPHE NUCLEUS.....94

3.1. Introduction.....94
3.1.1. Major afferent projections of dorsal raphe nucleus 95
3.1.1.1. Prefrontal cortex.....95
3.1.1.2. Lateral habenula.....95
3.1.1.3. Locus coeruleus 97
3.1.2. Tackykinins and NK_1 receptors on afferent projections of dorsal raphe nucleus 97
3.1.3. Aims of this chapter.....98
3.2. Materials and methods 99
3.2.1. Animals.....99
3.2.2. Antibodies.....99
3.2.3. Choice of retrograde tracer 100
3.2.4. Stereotaxic injection of retrograde tracer.....100
3.2.4.1. Fast Blue 101
3.2.4.2. Wheat germ agglutinin-horseradish peroxidase.....102
3.2.5. Visualisation of tracers and single immunohistochemistry 106
3.2.5.1. Visualisation of tracer at injection sites 106
3.2.5.1.1 *Fast Blue* 106
3.2.5.1.2 *Wheat germ agglutinin-horseradish peroxidase*...106
3.2.5.2. Fluorescence immunohistochemistry for NK_1 receptors 106
3.2.5.3. Immunohistochemistry for tryptophan hydroxylase in dorsal raphe nucleus.....107
3.2.5.4. Histochemistry for wheat germ agglutinin-horseradish peroxidase in prefrontal cortex 108
3.2.5.5. Immunohistochemistry for tyrosine hydroxylase in locus coeruleus.....108
3.2.6. Double-labelling immunohistochemistry.....109
3.2.6.1. Double fluorescence immunohistochemistry for NK_1 receptors and tyrosine hydroxylase.....109

3.2.6.2. Double-labelling immunohistochemistry for wheat germ agglutinin-horseradish peroxidase and NK_1 receptors 110
3.2.7. Electron microscopy 111
3.2.8. Image acquisition and analysis of material 114
3.2.8.1. Labelling with Fast Blue 114
3.2.8.2. Labelling with wheat germ agglutinin-horseradish peroxidase 114
3.2.8.2.1. *Light microscopy* 114
3.2.8.2.2. *Electron microscopy* 114
3.3. Results 116
3.3.1. Dorsal raphe nucleus 116
3.3.1.1. Tryptophan hydroxylase in dorsal raphe nucleus 116
3.3.1.2. Injection sites 116
3.3.1.2.1. *Fast Blue* 116
3.3.1.2.2. *Wheat germ agglutinin-horseradish peroxidase* .. 116
3.3.2. Light microscopic examination of NK_1 receptors on afferents to dorsal raphe nucleus 117
3.3.2.1. Afferents from prefrontal cortex 117
3.3.2.1.1. *Fast Blue* 117
3.3.2.1.2. *Wheat germ agglutinin-horseradish peroxidase* .. 118
3.3.2.2. Afferents from lateral habenula 118
3.3.2.2.1. *Fast Blue* 118
3.3.2.2.2. *Wheat germ agglutinin-horseradish peroxidase* .. 118
3.3.2.3. Afferents from locus coeruleus 119
3.3.2.3.1. *Fast Blue* 119
3.3.2.3.2. *Wheat germ agglutinin-horseradish peroxidase* .. 119
3.3.3. Electron microscopic examination of NK_1 receptors on afferents to dorsal raphe nucleus 131
3.3.3.1. NK_1 receptors on afferents from lateral habenula 131
3.3.3.2. NK_1 receptors on afferents from locus coeruleus 132
3.3.4. Confocal microscopy for NK_1 receptors on tyrosine hydroxylase immunoreactive neurons in the locus coeruleus 136
3.3.5. Immunoreactivity for tyrosine hydroxylase in the locus coeruleus ... 136
3.4. Discussion 139
3.4.1. Localisation of NK_1 receptors on afferents to dorsal raphe nucleus .. 139
3.4.1.1. Afferents from lateral habenula 139
3.4.1.2. Afferents from locus coeruleus 140
3.4.1.3. Afferents from prefrontal cortex 141
3.4.2. Technical considerations 142
3.4.2.1. Retrograde labelling 142
3.4.2.2. Comparison of TMB and DAB 145
3.4.2.3. Specificity of the NK_1 receptor antibody 146
3.4.2.4. Electron microscopy 146
3.4.2.5. Other considerations 147
3.4.3. Functional significance of NK_1 receptors on neurons afferent to dorsal raphe nucleus 148
3.4.3.1. Lateral habenula 148
3.4.3.2. Locus coeruleus 150
3.4.3.3. Prefrontal cortex 152
3.5. Conclusions 153

CHAPTER 4- METHODS FOR QUANTIFICATION OF HUMAN NK_1 RECEPTORS USING POSITRON EMISSION TOMOGRAPHY AND [^{18}F]SPA-RQ 154

4.1. Introduction 154
4.1.1. Positron emission tomography-an overview 154
4.1.1.1. Data reconstruction 157
4.1.1.2. Kinetic modelling 157
4.1.1.3. Region of interest analysis 160
4.1.1.4. Sources of error in positron emission tomography 161
4.1.1.5. Limitations of positron emission tomography 161
4.1.2. NK_1 receptors in the human brain in vivo 162
4.1.2.1. Positron emission tomography radioligands for NK_1 receptors 162
4.1.2.2. [^{18}F]Substance P Antagonist-Receptor Quantifier 162
4.1.3. Aims of this chapter 164
4.2. Methods 165
4.2.1. Radio-synthesis of [^{18F}]SPA-RQ 165
4.2.2. Human subjects 165
4.2.3. Positron emission tomography and magnetic resonance imaging scanning protocols 166
4.2.4. Image analysis 169
4.2.5. Radioligand kinetic modelling 169
4.2.6. Statistical analysis 171
4.3. Results 172
4.3.1. Subject demographics and radioligand-related data 172
4.3.2. Brain uptake of [^{18}F]SPA-RQ 173
4.3.2.1. Summed positron emission tomography scan images and magnetic resonance imaging scans 173
4.3.2.2. Regions of interest 173
4.3.2.3. Regional time activity curves 177
4.3.3. Plasma analysis of radioligand 185
4.3.3.1. Arterial versus venous radioligand activities 186
4.3.4. Volumes of distribution and binding potential estimates 187
4.4. Discussion 191
4.4.1. Comparison of kinetic and transient equilibrium models for [^{18F}]SPA-RQ 191
4.4.2. Limitations of this study 194
4.5. Conclusions 196

CHAPTER 5- IMAGING BRAIN NK_1 RECEPTORS IN DEPRESSION USING POSITRON EMISSION TOMOGRAPHY AND [^{18}F]SPA-RQ 197

5.1. Introduction 197
5.1.1. NK_1 receptors in human depression 197
5.1.2. Aims of this chapter 199
5.2. Methods 200

5.2.1. Radio-synthesis of [^{18F}]SPA-RQ....200
5.2.2. Human subjects....200
5.2.3. Positron emission tomography and magnetic resonance imaging scanning protocols....204
5.2.4. Image analysis....205
5.2.5. Localisation of the raphe region....209
5.2.6. Generation of time activity curves....211
5.2.7. Mathematical modeling and binding potential estimates....211
5.2.8. Measurements of stress....212
5.2.8.1. Physiological measures of stress....212
5.2.8.1.1. *Measurement of plasma cortisol*....212
5.2.8.1.2. *Measurement of blood pressure and heart rate*....212
5.2.8.2. Subjective measures of stress....212
5.2.9. Statistical analysis....212
5.3. Results....215
5.3.1. Subject demographics and radioligand-related data....215
5.3.2. Measures of mood and anxiety....216
5.3.3. Clinical characteristics....216
5.3.4. Measures of personality and parental bonding....217
5.3.5. NK_1 receptor binding....218
5.3.5.1. Effect of gender....218
5.3.5.2. Activity in the cerebellum....218
5.3.5.3. Effect of magnet strength....218
5.3.5.4. Regional time activity curves....222
5.3.5.5. NK_1 receptor binding potentials in depressed, recovered depressed and control subjects....231
5.3.5.6. Effect of age on NK_1 receptor binding potential....235
5.3.5.7. Correlation of NK_1 receptor binding potentials with clinical characteristics....238
5.3.5.8. Correlation of NK_1 receptor binding potentials with mood and personality....239
5.3.6. Measures of stress....239
5.3.6.1. Physiological measures of stress....240
5.3.6.2. Subjective measures of stress....240
5.3.6.3. Correlation of measures of stress with NK_1 receptor binding potentials....240
5.4. Discussion....243
5.4.1. No difference in NK_1 receptor binding potentials between depressed, recovered depressed and control subjects....243
5.4.2. Comparison of binding potentials in control subjects with Nyman et al. (2006)....245
5.4.3. Decline of NK_1 receptor binding with age....248
5.4.4. Effect of gender on NK_1 receptor binding....249
5.4.5. NK_1 receptor binding and personality scores....249
5.4.6. NK_1 receptor binding and clinical parameters....250
5.4.7. NK_1 receptor binding and measures of stress....250
5.4.8. Strengths and weaknesses of the study....251
5.5. Conclusions....252

CHAPTER 6- GENERAL DISCUSSION 253

6.1. Review of thesis background.....253
6.2. Summary of main aims and findings 254
6.2.1. Investigation into colocalisation of NK_1 receptors with 5-HT_{1A} and 5-HT_{2A} receptors in rat forebrain 254
6.2.1.1. Aim 254
6.2.1.2. Findings.....254
6.2.2. Investigation of NK_1 receptors on afferent projections to dorsal raphe nucleus.....254
6.2.2.1. Aim 254
6.2.2.2. Findings.....255
6.2.3. Methods for quantification of human NK_1 receptors using positron emission tomography and [^{18}F]SPA-RQ.....255
6.2.3.1. Aim 255
6.2.3.2. Findings.....255
6.2.4. Imaging brain NK_1 receptors in depression using positron emission tomography and [^{18}F] SPA-RQ 256
6.2.4.1. Aim 256
6.2.4.2. Findings.....256
6.3. Discussion.....257
6.3.1. Interactions between NK_1 receptors and the 5-HT system in brain regions postsynaptic and presynaptic to the raphe.....257
6.3.2. NK_1 receptors in human depression 264
6.4. Future studies 267
6.5. Conclusions.....269

BIBLIOGRAPHY 271

APPENDICES 326

Appendix A: Radio-synthesis of [^{18F}]SPA-RQ.....326
Appendix B: Measurement of [^{18}F] SPA-RQ and its metabolites in plasma.....328
Appendix C: Correction of activity concentrations in the cerebellum 329
Appendix D: Tissue over parent in plasma ratios for [^{18}F] SPA-RQ 330

LIST OF FIGURES

CHAPTER 1- GENERAL INTRODUCTION

Fig. 1.1. Chemical structure and amino acid sequence of substance P 3
Fig. 1.2. Schematic diagram of the structure of human NK_1 receptor 6
Fig. 1.3. Substance P/ Neurokinin A cell bodies in the rodent brain 10
Fig. 1.4. Tachykinin pathways in the rodent brain 12
Fig. 1.5. NK_1 receptor mRNA in human brain 16
Fig. 1.6. NK_1 receptor binding in the rostral orbitofrontal cortex of postmortem depressed patients and normal control subjects 29
Fig. 1.7. Schematic diagram of ascending and descending projections of midbrain raphe nuclei in the rat in sagittal section 33
Fig. 1.8. Schematic diagram of afferent connections to mesencephalic raphe nuclei in the rat brain in sagittal section 34

CHAPTER 2- INVESTIGATION INTO COLOCALISATION OF NK_1 RECEPTORS WITH 5-HT_{1A} AND 5-HT_{2A} RECEPTORS IN RAT FOREBRAIN

Fig. 2.1. Schematic diagrams of coronal rat forebrain sections of brain regions examined for colocalisation 58
Fig. 2.2. Photomicrographs of NK_1 and 5-HT_{1A} receptor immunoreactivities in medial septum 63
Fig. 2.3. Photomicrographs of NK_1 and 5-HT_{1A} receptor immunoreactivities in vertical diagonal band of Broca 64
Fig. 2.4. Photomicrographs of NK_1 and 5-HT_{1A} receptor immunoreactivities in horizontal diagonal band of Broca 65
Fig. 2.5. Photomicrographs of NK_1 and 5-HT_{1A} receptor immunoreactivities in CA1 region of hippocampus 66
Fig. 2.6. Photomicrographs of NK_1 and 5-HT_{1A} receptor immunoreactivities in CA3 region of hippocampus 67
Fig. 2.7. Photomicrographs of NK_1 and 5-HT_{1A} receptor immunoreactivities in dentate gyrus of hippocampus 68
Fig. 2.8. Photomicrographs of NK_1 and 5-HT_{1A} receptor immunoreactivities in basolateral region of amygdala 69
Fig. 2.9. Photomicrographs of NK_1 and 5-HT_{1A} receptor immunoreactivities in prelimbic region of prefrontal cortex (I) 70
Fig. 2.10. Photomicrographs of NK_1 and 5-HT_{1A} receptor immunoreactivities in prelimbic region of prefrontal cortex (II) 71
Fig. 2.11. Photomicrographs of NK_1 and 5-HT_{2A} receptor immunoreactivities in CA3 region of hippocampus 72
Fig. 2.12. Photomicrographs of NK_1 and 5-HT_{2A} receptor immunoreactivities in prelimbic cortex, horizontal diagonal band of Broca and basolateral amygdala 73
Fig. 2.13. Confocal photomicrographs of NK_1 and 5-HT_{1A} receptor immunoreactivities in CA3 region of the hippocampus 74

CHAPTER 3- INVESTIGATION OF NK_1 RECEPTORS ON AFFERENT PROJECTIONS TO DORSAL RAPHE NUCLEUS

Fig. 3.1. Flow chart of experiments with 'Fast Blue' and wheat germ agglutinin-horseradish peroxidase 104
Fig. 3.2. Flow chart of additional immunohistochemical experiments in dorsal raphe and locus coeruleus 105
Fig. 3.3. Summary flow chart of procedures for electron microscopy 113
Fig. 3.4. Tryptophan hydroxylase immunohistochemistry in dorsal raphe nucleus 120
Fig. 3.5. Photomicrographs of injection sites for 'Fast Blue' and wheat germ agglutinin-horseradish peroxidase in dorsal raphe nucleus 121
Fig. 3.6. Schematic representation of spread of retrograde tracer wheat germ agglutinin-horseradish peroxidase in dorsal raphe nucleus 122
Fig. 3.7. Photomicrographs of NK_1 receptor-immunoreactivity and of neurons labeled with 'Fast Blue' in prefrontal cortex (I) 123
Fig. 3.8. Photomicrographs of NK_1 receptor-immunoreactivity and of neurons labeled with 'Fast Blue' in prefrontal cortex (II) 124
Fig. 3.9. Photomicrographs of neurons labeled with wheat germ agglutinin-horseradish peroxidase in prefrontal cortex 125
Fig. 3.10. Photomicrographs of NK_1 receptor-immunoreactivity and of neurons labeled with 'Fast Blue' in lateral habenula 126
Fig. 3.11. Photomicrographs of neurons labeled with wheat germ agglutinin-horseradish peroxidase and NK_1 receptors in lateral habenula (I) 127
Fig. 3.12. Photomicrographs of neurons labeled with wheat germ agglutinin-horseradish peroxidase and NK_1 receptors in lateral habenula (II) 128
Fig. 3.13. Photomicrographs of neurons labeled with 'Fast Blue', NK_1 receptor and tyrosine hydroxylase-immunoreactivities in locus coeruleus 129
Fig. 3.14. Photomicrographs of neurons labeled with wheat germ agglutinin-horseradish peroxidase and NK_1 receptors in locus coeruleus 130
Fig. 3.15. A correlated study of a cell in lateral habenula that projects to dorsal raphe nucleus and expresses NK_1 receptor-immunoreactivity 133
Fig. 3.16. Cells in lateral habenula that project to dorsal raphe nucleus 134
Fig. 3.17. Cell in locus coeruleus that projects to dorsal raphe nucleus and expresses NK_1 receptor protein 135
Fig. 3.18. Confocal photomicrographs of cells in locus coeruleus colocalising tyrosine hydroxylase and NK_1 receptor immunoreactivities 137
Fig. 3.19. Photomicrographs of tyrosine hydroxylase immunoreactivity in the locus coeruleus 138

CHAPTER 4- METHODS FOR QUANTIFICATION OF HUMAN NK_1 RECEPTORS USING POSITRON EMISSION TOMOGRAPHY AND [^{18}F]SPA-RQ

Fig. 4.1. Signal detection in a positron emission tomography camera 156
Fig. 4.2. Compartmental modelling 158
Fig. 4.3. Positron emission tomography scanning protocol for brain NK_1 receptors in normal human subjects *in vivo* using [^{18}F] SPA-RQ 168
Fig. 4.4. Positron emission tomography images with [^{18}F] SPA-RQ and co-registered magnetic resonance images.....174
Fig. 4.5. Reference region maps of the cerebellum 175
Fig. 4.6. Object maps for regions of interest.....176
Fig. 4.7. Time activity curves of [^{18}F]SPA-RQ for subject 1 179
Fig. 4.8. Time activity curves of [^{18}F]SPA-RQ for subject 2 180
Fig. 4.9. Time activity curves of [^{18}F]SPA-RQ for subject 3 181
Fig. 4.10. Time activity curves of [^{18}F]SPA-RQ for subject 4 182
Fig. 4.11. Time activity curves of [^{18}F]SPA-RQ for subject 5 183
Fig. 4.12. Time activity curves of [^{18}F]SPA-RQ for subject 6 184
Fig. 4.13. Fraction of unmetabolised [^{18}F]SPA-RQ in arterial plasma.....185
Fig. 4.14. Arterial versus venous [^{18}F]SPA-RQ activity 186
Fig. 4.15. Average binding potential estimates from compartmental modelling and the ratio method 189
Fig. 4.16. Simplified positron emission tomography scanning protocol for study of brain NK_1 receptors in human subjects *in vivo* using [^{18}F] SPA-RQ 196

CHAPTER 5- IMAGING BRAIN NK_1 RECEPTORS IN DEPRESSION USING POSITRON EMISSION TOMOGRAPHY AND [^{18}F]SPA-RQ

Fig. 5.1. Study protocol on day of the positron emission tomography scan with [^{18}F]SPA-RQ.....203
Fig. 5.2. Procedure for image analysis (I).....207
Fig. 5.3. Procedure for image analysis (II) 208
Fig. 5.4. Determination of the position of the raphe nucleus.....210
Fig. 5.5. Individual [^{18}F]SPA-RQ time activity curves for control subjects 223
Fig. 5.6. Individual [^{18}F]SPA-RQ time activity curves for subjects with major depressive disorder 227
Fig. 5.7. Individual [^{18}F]SPA-RQ time activity curves for subjects recovered from depression 228
Fig. 5.8. Example of a [^{18}F]SPA-RQ time activity curve for the raphe.....230
Fig. 5.9. Comparison of NK_1 receptor binding potentials in the amygdala between healthy controls, subjects with major depressive disorder and subjects recovered from depression 233
Fig. 5.10. Comparison of NK_1 receptor binding potentials in selected brain regions between healthy controls, subjects with major

depressive disorder and subjects recovered from depression 234
Fig. 5.11. Negative correlations between age and binding potential globally and in anterior temporal lobe (medial) 237
Fig. 5.12. Comparison of measures of stress versus time during PET scan 242
Fig. 5.13. Correlation of binding potentials obtained from transient equilibrium versus those of Nyman et al. (2006) in normal volunteers.....247

CHAPTER 6- GENERAL DISCUSSION

Fig. 6.1. Schematic summary diagram of the interactions between NK_1 receptors and the 5-HT system 257
Fig. 6.2. Interactions between NK_1 receptors and 5-HT system in the septohippocampal pathway of the rat 259
Fig. 6.3. Schematic diagram illustrating agonist and antagonist actions on 5-HT_{1A} and NK_1 receptors on a colocalised cell.....260
Fig. 6.4. Schematic representation of NK_1 receptors on neurons afferent to the dorsal raphe nucleus 5-HT system.....262

APPENDICES

Fig. A.1. Structure of [^{18}F]SPA-RQ, its precursor and its intermediate 327
Fig. C.1. Correction of activity concentrations in the cerebellum 329
Fig. D.1. Tissue over parent in plasma ratio versus time for [^{18}F] SPA-RQ in controls, depressed and recovered depressed subjects.....330

LIST OF TABLES

CHAPTER 1- GENERAL INTRODUCTION

Table 1.1. Amino acid sequences of mammalian tachykinins 4
Table 1.2. Human tachykinin peptide genes 4
Table 1.3. Neurokinin receptors in rodent central nervous system 7
Table 1.4. Tachykinin cell bodies in rodent central nervous system 9
Table 1.5. Effects of stress on substance P levels in rat central nervous system 21
Table 1.6. Effects of psychotropic drugs on substance P and NK_1 receptors in the rat brain 22
Table 1.7. 5-HT receptors located in central nervous system 40

CHAPTER 2- INVESTIGATION INTO COLOCALISATION OF NK_1 RECEPTORS WITH 5-HT_{1A} AND 5-HT_{2A} RECEPTORS IN RAT FOREBRAIN

Table 2.1. Antibodies used against NK_1, 5-HT_{1A} and 5-HT_{2A} receptors 55
Table 2.2. NK_1 and 5-HT_{1A} receptor colocalisation in rat forebrain 61
Table 2.3. NK_1 and 5-HT_{2A} receptor colocalisation in rat forebrain 62

CHAPTER 3- INVESTIGATION OF NK_1 RECEPTORS ON AFFERENT PROJECTIONS TO DORSAL RAPHE NUCLEUS

Table 3.1. Antibodies for immunohistochemistry 99

CHAPTER 4- METHODS FOR QUANTIFICATION OF HUMAN NK_1 RECEPTORS USING POSITRON EMISSION TOMOGRAPHY AND [^{18}F]SPA-RQ

Table 4.1. Descriptive statistics for subjects 172
Table 4.2. Volumes of distribution and binding potentials estimates from compartmental modelling versus the ratio method for all 6 subjects 188
Table 4.2. Coefficient of variation for volumes of distribution and binding potential estimates from compartmental modelling versus the ratio method for all 6 subjects 190

CHAPTER 5- IMAGING BRAIN NK_1 RECEPTORS IN DEPRESSION USING POSITRON EMISSION TOMOGRAPHY AND [^{18}F]SPA-RQ

Table 5.1. Demographics, radioligand-related data and clinical characteristics

of healthy controls, subjects with major depressive disorder and subjects recovered from depression 220
Table 5.2. Measures on personality and parental bonding for healthy controls, subjects with major depressive disorder and subjects recovered from depression 221
Table 5.3. Binding potentials in brain regions for healthy controls, subjects with major depressive disorder and subjects recovered from depression 232
Table 5.4. Correlations of binding potential with age in brain regions 236
Table 5.5. Comparison of measures of stress between healthy controls, subjects with major depressive disorder and subjects recovered from depression 241
Table 5.6. Comparison of binding potentials in controls versus Nyman et al. 246

ABBREVIATIONS

3D	three dimensional
3V	third ventricle
4V	fourth ventricle
5-HT	5-hydroxytryptamine
5-HTP	5-hydroxytryptophan
5-HT_{1A}R	5-HT_{1A} receptor
5-HT_{2A}R	5-HT_{2A} receptor
ABC	avidin-biotin-peroxidase complex
ACE	Angiotensin I converting enzyme
AC-PC	anterior commissure-posterior commissure
ACTH	adrenocorticotrophic hormone
ANOVA	analysis of variance
ARSAC	Administration of Radioactive Substances Advisory Committee
AUC	area under curve
BDI	Beck Depression Inventory
BIS	Barrat Impulsivity Scale
BLA	basolateral amygdala
BMI	body mass index
B-P	band pass
BNST	bed nuclei of the stria terminalis
BP	binding potential
BPa	apparent binding potential
BSA	bovine serum albumin
cAMP	cyclic adenosine monophosphate
Cb	specific binding compartment
CB	calbindin
CCK	cholecystokinin
ChAT	choline acetyl transferase
CMS	chronic mild stress
Cn	non-displaceable compartment
CNS	central nervous system
Cp	plasma compartment
CR	calretinin
CSF	cerebrospinal fluid
CV	coefficient of variation
DAB	3,3'–diaminobenzidine tetrahydrochloride
DAS	Dysfunctional Attitudes Scale
DBB	diagonal band of Broca
DG	dentate gyrus
DRD	dorsal raphe nucleus dorsal
DRN	dorsal raphe nucleus
DRV	dorsal raphe nucleus ventral
DRVL	dorsal raphe nucleus venterolateral
DSM-IV	Diagnostic and Statistical Manual of Mental Disorders-Fourth Edition
ECS	electroconvulsive shock
EM	electron microscope
EPM	elevated plus maze

EPN	entopeduncular nucleus
EPQ	Eysenck Personality Questionnaire
EPQ-E	Eysenck Personality Questionnaire-extroversion
EPQ-L	Eysenck Personality Questionnaire-lie
EPQ-N	Eysenck Personality Questionnaire-neurotism
EPQ-P	Eysenck Personality Questionnaire-psychoticism
FOV	field of view
FST	forced swim test
FWHM	full width half maximum
GABA	gamma-aminobutyric acid
GAD	glutamic acid decarboxylase
GLM	general linear model
GM	grey matter
GST	glutathione *S*-transferase
HCl	hydrochloride
HDBB	horizontal diagonal band of Broca
HDRS	Hamilton Depression Rating Scale
HPLC	high perfrormance liquid chromatography
HPA	hypothalamic-pituitary-adrenal
HRP	horseradish peroxidase
I/D	insertion/deletion
IL	infralimbic
i.m.	intramuscular
IP3	inositol triphosphate
i.p.	intraperitoneal
ir	immunoreactivity
i.v.	intravenous
IPN	interpeduncular nucleus
LA	lateral amygdala
Lat	lateral
LC	locus coeruleus
LdTg	laterodorsal tegmental nucleus
LHb	lateral habenula
LS	lateral septum
MAOI	monoamine oxidase inhibitor
MAP	mean arterial pressure
MeA	medial amygdala
Med	medial
MDD	major depressive disorder
MDE	major depressive episode
MFB	medial forebrain bundle
MHb	medial habenula
MNI	Montreal Neurological Institute
MRI	magnetic resonance imaging
MRN	median raphe nucleus
mRNA	messenger ribonucleic acid
MRTM	multilinear reference tissue model
MRTM2	multilinear reference tissue model two-parameter version
MS	medial septum
MS-DBB	medial septum-diagonal band of Broca complex

NA	noradrenergic
NART	National Adult Reading Test
NGS	normal goat serum
NHS	normal horse serum
NKA	neurokinin A
NKB	neurokinin B
NK_1R	neurokinin-1 receptor
NK_1RA	neurokinin-1 receptor antagonist
$NK_1R–/–$	neurokinin-1 receptor knockout
NK_2R	neurokinin-2 receptor
NK_2RA	neurokinin-2 receptor antagonist
NK_3R	neurokinin-3 receptor
NPY	neuropeptide Y
NRS	normal rabbit serum
NSA	number of signal acquisitions
PAG	periaqueductal grey
PB	phosphate buffer
PBI	Parental Bonding Inventory
PBS	phosphate buffered saline
PCR	polymerase chain reaction
PET	positron emission topography
PFC	prefrontal cortex
PKC	protein kinase C
PL	prelimbic cortex
PLC	phospholipase C
PPT-A	preprotachykinin-A
PPT-B	preprotachykinin-B
PV	parvalbumin
PVN	paraventricular nucleus
r	Pearson's product moment correlation coefficient
rCBF	regional cerebral blood flow
RD	recovered depressed
RF	radiofrequency
ROI	region of interest
RT	room temperature
RT-PCR	reverse transcriptase polymerase chain reaction
SCID	Structured Clinical Interview Schedule for DSM-IV
SD	standard deviation
s.e.	standard error
SEM	standard error of the mean
SN	substantia nigra
SOM	somatostatin
SON	supraoptic nucleus
SP	substance P
SPA-RQ	Substance P Antagonist-Receptor Quantifier
SPE	solid-phase extraction
SPM	statistical parametric mapping
SPSS	Statistical package for Social Sciences
SSRI	selective serotonin reuptake inhibitor
STAI	Spielberger State-Trait Anxiety Inventory

TAC	time activity curve
TE	echo time
TH	tyrosine hydroxylase
TMB	tetramethylbenzidine
TPH	tryptophan hydroxylase
TPQ	Tridimensional Personality Questionnaire
TR	repetition time
VAS	visual analogue scales
VD	volume of distribution
VDa	apparent volume of distribution
VDBB	vertical diagonal band of Broca
VTA	ventral tegmental area
WGA-HRP	wheat germ agglutinin-horseradish peroxidase
WM	white matter

CHAPTER 1

GENERAL INTRODUCTION

1.1. SCOPE OF THESIS

Depression is a common and debilitating psychiatric disorder and estimated to become the second leading cause of medical morbidity worldwide by the year 2020 (Murray and Lopez 1997). In the last 50 years, disturbances in brain monoamines such as serotonin (5-hydroxytryptamine; 5-HT) have been thought to play an important role in the aetiology of depressive illness. However, in more recent years, substance P (SP) and the neurokinin-1 receptor (NK_1R) have also been implicated. Pre-clinical data suggest that NK_1 receptor antagonists (NK_1RA) may have antidepressant properties. Indeed, electrophysiological experiments showed that NK_1R blockade or NK_1R deletion can increase neuronal firing in the dorsal raphe nucleus (DRN) suggestive of an interaction with the 5-HT system (Conley et al 2002; Santarelli et al 2001). Although a postmortem study showed a decrease in NK_1Rs in the orbitofrontal cortex in depression (Stockmeier et al 2002), NK_1Rs remain to be fully investigated in human depression *in vivo*.

One of the main aims of this thesis was to investigate anatomical interactions between NK_1Rs and brain systems presynaptic and postsynaptic to the DRN. Thus, immunohistochemistry was used to examine for colocalisation between NK_1Rs and 5-HT_{1A} receptors (5-$HT_{1A}Rs$) and 5-HT_{2A} receptors (5-$HT_{2A}Rs$) in postsynaptic forebrain regions. In addition, retrograde tracing was combined with immunohistochemistry at the light and electron microscope (EM) levels to identify NK_1Rs on neurons afferent to the DRN. The other main aim of this thesis was to

develop a protocol for quantification of NK_1Rs in humans *in vivo* using the positron emission tomography (PET) radioligand [^{18}F] Substance P Antagonist-Receptor Quantifier (SPA-RQ) and to study alterations in NK_1Rs in depression.

In this introduction, a description of SP and related tachykinins and their receptors is first given (section 1.2). This is followed by a description of the neuroanatomy of the tachykinins and tachykinin receptors in the rodent, primate and human brain (section 1.3). Evidence for SP and NK_1RAs in depression and anxiety from animal and human studies is then presented (section 1.4). The next section presents the anatomy of the 5-HT system and its receptors (section 1.5), followed by the role of 5-HT in depression (section 1.6). The following section presents anatomical and functional evidence for NK_1R and 5-HT system interactions in the brain. The importance of these interactions with respect to depression and anxiety is also discussed (section 1.7). The last section lays out the aims of this thesis (section 1.8).

1.2. SUBSTANCE P AND TACHYKININ RECEPTORS

SP was first discovered by von Euler and Gaddum in 1931 in equine intestinal and brain tissue extracts and found to stimulate smooth muscle contraction in rabbit jejunum and to lower blood pressure. Its activity was retained even when the extract was evaporated to a dry 'powder' or 'preparation' and hence was named 'substance P' by Gaddum and Schild (Harrison and Geppetti 2001; Hokfelt et al 2003; Hokfelt et al 2001). However, it was not until the 1970s, when SP was identified as an undecapeptide in bovine hypothalamus (see Fig. 1.1) and first synthesised (Chang and Leeman 1970; Chang et al 1971).

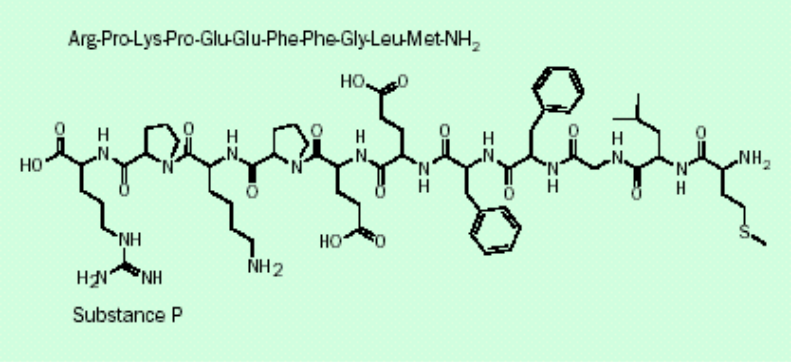


Fig. 1.1. Chemical structure and amino acid sequence of substance P. Adapted from (Hokfelt et al 2003).

SP belongs to the tachykinin group of peptides as it produces rapid contractions in smooth muscle. Tachykinins are defined by the common hydrophobic carboxy-terminal amino acid sequence Phe-X-Gly-Leu-Met-NH_2 (Baby et al 1999; Harrison and Geppetti 2001; Severini et al 2002; Takahashi et al 1992) where X is either an aromatic or beta-branched chain aliphatic residue (Page 2005). Neurokinin A (NKA) and neurokinin B (NKB) are other members of this group (Table 1.1). In addition,

hemokinins and endokinins are tachykinins found in non-neuronal tissues and important for B cell development (Brain and Cox 2006; Page 2005).

Table 1.1. Amino acid sequences of mammalian tachykinins

Substance P:	Arg-Pro-Lys-Pro-Glu-Glu-**Phe**-Phe-**Gly-Leu-Met-NH2**
Neurokinin A:	His-Lys-Thr-Asp-Ser-**Phe-**Val-**Gly-Leu-Met-NH2**
Neurokinin B:	Asp-Met-His-Asp-Phe-**Phe**-Val-**Gly-Leu-Met-NH2**

Different genes are responsible for the formation of the above tachykinins in mammals. These include TAC1 gene, formerly referred to as the preprotachykinin-A (PPT-A) gene, and TAC 3 gene, formerly known as the preprotachykinin-B (PPT-B) gene. TAC1 contains seven exons and is differentially spliced to alpha, beta, gamma and delta TAC1 messenger ribonucleic acid (mRNA). The alpha and delta mRNA lead to the formation of an SP precursor, while the beta and gamma forms code for both SP and NKA precursors. The TAC3 gene only encodes for NKB (Page 2005; Takahashi et al 1992). In addition, the TAC4 gene is responsible for the production of hemokinin-1, first discovered in the mouse and then discovered in humans as endokinin-A and endokinin-B (see Table 1.2) (Zhang et al 2000).

Table 1.2. Human tachykinin peptide genes

Tachykinin	Gene	Alternative name	Chromosome
Substance P/ Neurokinin A	TAC1	PPT-A	7q21-q22
Neurokinin B	TAC3	PPT-B	12q13-q21
Endokinin-A/ Endokinin-B	TAC4	PPT-C	17q21,33

PPT= preprotachykinin. Adapted from (Pennefather et al 2004).

Tachykinins are found in both the central nervous system (CNS) and peripheral nervous system. They play a role in smooth muscle contraction, inflammation, pain, autonomic reflexes and emotional behaviours-for reviews see: (Page 2005; Siemion et al 2005). They activate 3 types of receptors: NK_1R (see Fig. 1.2), NK_2 receptor (NK_2R) and NK_3 receptor (NK_3R). These receptors belong to the class 1 (rhodopsin-like) G-protein-coupled receptors, with seven trans-membrane domains, 3 intracellular loops, 3 extra-cellular loops, an extra-cellular amino-terminus and an intracellular carboxy-terminus (Page 2005; Pennefather et al 2004).

SP, NKA and NKB bind preferentially, but not exclusively, to NK_1R, NK_2R and NK_3R, respectively (Saria 1999; Tooney et al 2001). Species variations exist in tachykinins with regards to brain distribution, receptor pharmacology (Beresford et al 1991; Sachais et al 1993) and receptor protein sequence (Fong et al 1992b). For example, the NK_1R is the main tachykinin receptor in the human brain (Dietl and Palacios 1991; Mileusnic et al 1999a; Mileusnic et al 1999b; Mounir and Parent 2002), while both NK_1R and NK_3R are extensively expressed in rat and guinea-pig brain (Elde et al 1990; Mileusnic et al 1999a; Nakaya et al 1994; Nalivaiko et al 1997; Quirion and Dam 1986; Saffroy et al 2001; Saffroy et al 2003; Yip and Chahl 2001). The NK_1R is consistently described as a 407 amino acid residue protein with a molecular weight of 58,000 and in the human is localised to chromosome 2 (Gerard et al 1990; Hopkins et al 1991; Takeda et al 1991). Human NK_1R has 97% homology with the guinea-pig NK_1R and 95% homology with the rat NK_1R (Saria 1999; Takahashi et al 1992). The different homologies become important when non-peptide antagonists are tested (Engberg et al 2007).

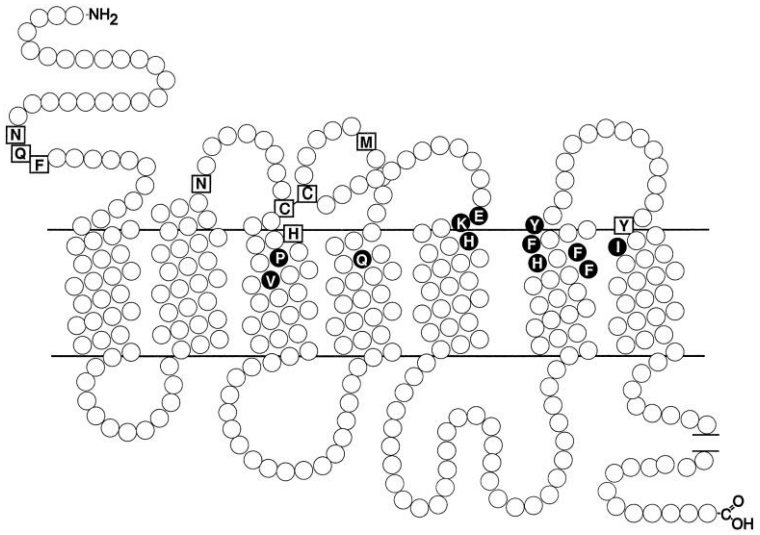


Fig. 1.2. Schematic diagram of the structure of human NK_1 receptor. The receptor has an extracellular N-terminus, 7 hydrophobic membrane-spanning regions, intervening extracellular and cytoplasmic loops and a cytoplasmic C terminal tail. Also shown are the presumed contact sites for binding of the non-peptide antagonist CP96,345 (*black letters* on *white squares*) and for binding of SP (*white letters* on *black dots*). From (Turcatti et al 1997).

Second messenger systems (see Table 1.3) that come into play after tachykinin receptor activation include calcium, phospholipase C (PLC), inositol triphosphate (IP3), phospholipase A2, p42/44 and p38 mitogen-activated protein kinases, cyclic adenosine monophosphate (cAMP), protein kinase C, nuclear factor kappa B and nuclear factor interleukin-6 (Hamke et al 2006; Mitsuhashi et al 1992; Nakajima et al 1992; Satake and Kawada 2006). Agonist activation also results in receptor internalisation (Hokfelt et al 2003).

NKA acts mainly via NK_2Rs expressed in peripheral tissues, while NK_2R antagonists (NK_2RA) alter contraction of human airways, urinary bladder and gastrointestinal smooth muscle (Cialdai et al 2006). On the other hand, NKB is involved in pain, emesis, asthma, anxiety, epilepsy, schizophrenia and Parkinson's disease (Massi et al 2000).

Table 1.3. Neurokinin receptors in rodent central nervous system.

Neurokinin receptor	Known Agonists & Antagonists	Intracellular mechanism	Main location in central nervous system	Behavioural effects
NK_1R	*Agonists:* Substance P *Antagonists:* CGP 49823;CP-122721; CP 96345; CP-99,994; FK888; GR 205171; L-733060; L-742694; L-759274; L-760735; LY303870; MK-869; NKP608; RP 67580; SSR240600; WIN51708	cAMP, PLC, calcium, IP3, p42/p44, p38 mitogen activated protein kinases, protein kinase C, nuclear factor kappa B & interleukin-6, reduced K^+ conductance	*Highest:* striatum, stria terminalis, septohippocampal nucleus, nucleus accumbens *Moderate:* PAG, amygdala, habenula, periventricular nucleus, olfactory bulb, prefrontal cortex (layers I & II)	*Agonists:* anxiogenic on EPM *Antagonists:* anxiolytic on EPM, social interaction test, open field, separation-induced vocalisation, FST, tail suspension
NK_2R	*Agonists:* NK-A; NKP; GR64349 *Antagonists:* MEN15596; SR48968; GR94800	Calcium, cAMP	Hippocampus, septum, thalamus, pituitary gland	*Agonists:* grooming, anxiogenic *Antagonists:* anxiolytic on EPM, antidepressant on FST
NK_3R	*Agonists:* NK-B; Senktide *Antagonists:* Osanetant; Talnetant; SR142801; SB-223412	Calcium mobilisation via IP3, cAMP	Neocortex (deep layers): frontal, parietal, cingulate; septum, amygdala, zona incerta, hupothalamus, hippocampus, substantia nigra, ventral tegmental nucleus, raphe	*Agonists:* yawning, chewing, head twitches, forepaw treading, hindlimb splaying; tachycardia; increased blood pressure *Antagonists:* antidepressant on FST

cAMP=cyclic adenosine monophosphate; EPM=elevated plus maze; FST=forced swim test; IP3=inositol trihosphate; PAG=periaqueductal grey; PLC=phospholipase C

1.2. NEUROANATOMY OF TACHYKININ AND TACHYKININ RECEPTOR SYSTEMS

NK_1Rs are expressed by only a small percentage of neurons (5-7%) in brain and spinal cord. The brain distribution of tachykinins and their receptors in rodents and humans has been examined using autoradiographic, immunohistochemical and *in-situ* hybridisation techniques (Adell 2004) and recently reviewed (Harding et al 2004; Ribeiro-da-Silva and Hokfelt 2000).

1.3.1. Neuroanatomical studies in rodents

The CNS distribution of tachykinins has been examined using immuno-histochemistry, while tachykinin tissue levels have been measured in brain extracts using high performance liquid chromatography (HPLC) and radioimmunoassay (Hokfelt et al 1975; Pernow 1983). However, regional specific antisera directed against the C-terminal region of tachykinins has made discrimination between the various tachykinins difficult (Severini et al 2002). The rat has been the most studied rodent species (Otsuka and Yoshioka 1993).

1.3.1.1. Tachykinin cell-bodies

SP is the most abundant tachykinin in rat CNS and is distributed in cell bodies in the brainstem, several hypothalamic nuclei, epithalamus, basal forebrain, striatum, limbic system (amygdala and hippocampus) and neocortex (Otsuka and Yoshioka 1993; Severini et al 2002). The distribution of SP/NKA cell bodies is illustrated in Fig. 1.3 and contrasted with that of NKB cell bodies in Table 1.4. Essentially, SP/NKA cell bodies are more widely distributed in the rodent brain than NKB, especially in the brainstem, epithalamus and septum.

Table 1.4. Tachykinin cell bodies in rodent central nervous system.

Brain regions	Neurokinin cell bodies	
	SP/NKA	***NKB***
Brainstem	Dorsal tegmental nucleus, LdTg, pontine reticular formation, parabrachial nucleus, LC, raphe cells (B5/8 and B6, dorsal raphe B7, B9), medullary raphe, IPN, superficial layers of the superior colliculus, deep layers of both colliculi, central PAG, pedunculopontine tegmental nucleus, the Edinger-Westphal nucleus. *Minor presence:* VTA, dorsal parts of the mesenchephalic tegmentum	superficial layers of the superior colliculus, dorsal PAG, raphe cells (B9) *Minor presence:* reticular formation
Cerebellum	Negligible	Negligible
Hypothalamus	Many hypothalamic nuclei	Many hypothalamic nuclei
Epithalamus	Habenula complex	Medial Habenula
Basal forebrain	All parts of septum	Medial and lateral septal nuclei *Minor presence:* Diagonal band of Broca
Striatum	Throughout the striatum	Throughout the striatum
Amygdala	Anterior, cortical, central and medial nuclei	Central and basolateral nuclei
Hippocampus	Throughout hippocampus (esp. subiculum and entorhinal cortex	Throughout hippocampus
Neocortex	Layer 4	Layers 2-4

Data from: (Borhegyi and Leranth 1997b; Harlan et al 1989; Hokfelt et al 1975; Ljungdahl et al 1978a; Marksteiner et al 1992; Nussdorfer and Malendowicz 1998; Shults et al 1984; Warden and Young 1988). IPN=interpeduncular nucleus; LC=locus coeruleus; LdTg=laterodorsal tegmental nucleus; PAG=periaqueductal grey; VTA=ventral tegmental area.

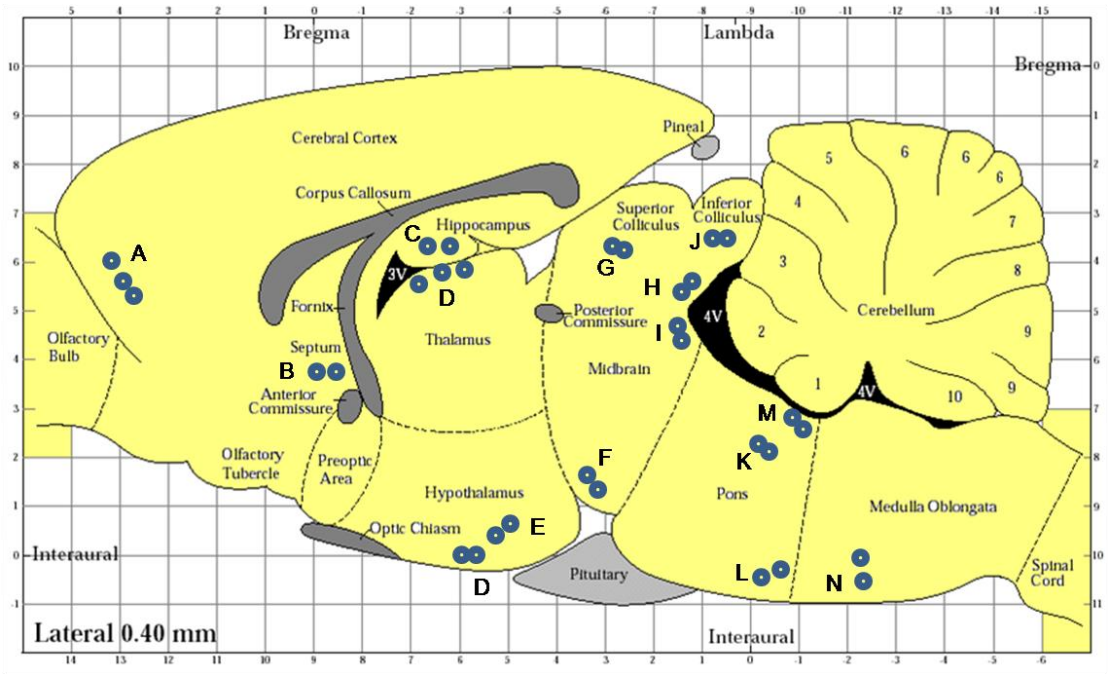


Fig. 1.3. Substance P / Neurokinin A cell bodies in the rodent brain. Schematic diagram of a sagittal brain section at 0.40 mm lateral to the midline illustrating the distribution of SP/NKA cell bodies in the rodent brain (A-N). Note the lack of cell bodies in the cerebellum. A=prefrontal cortex; B=septum; C=hippocampus; D=hypothalamus; F=interpeduncular nucleus; G=superior colliculus; H=periaqueductal grey; I=midbrain raphe nuclei; J=inferior colliculus; K=laterodorsal tegmental nucleus; L=pontine reticular nuclei; M=locus coeruleus; N=medullary raphe. Information from: (Harding et al 2004). Diagram adapted from: (Paxinos and Watson 1998).

1.3.1.2. Tachykinin pathways

Tachykinins form descending and ascending pathways as well as regional circuits. The hypothalamus, amygdala and the epithalamus send descending tachykinin pathways to the brainstem. In turn, many tachykinin fibres ascend within the medial forebrain bundle (MFB) to target the septum, prefrontal cortex (PFC), hypothalamus, amygdala and thalamus. In addition, there are circuits within the brainstem, e.g. a reciprocal circuit between the locus coeruleus (LC) and the raphe. Connections within the forebrain are also observed e.g. between the hypothalamus and septum (Fig. 1.4).

The amygdala contains tachykinin fibres with intrinsic and extrinsic origins. Tracing studies in the guinea-pig have demonstrated that the ventrolateral hypothalamus sends a modest SP projection to the medial nucleus (Ricciardi and Blaustein 1994), while the rat central nucleus receives SP projections from the parabrachial nuclei, caudal laterodorsal tegmental nuecleus (LdTg), periaqueductal grey (PAG) and DRN (Block et al 1989; Li et al 1990a; Petrov et al 1994; Yamano et al 1988). In turn, fibres from the amygdala innervate the bed nuclei of the stria terminalis (BNST) (Sakanaka et al 1981b) and parabrachial nuclei (Ljungdahl et al 1978b; Marksteiner et al 1992; Shults et al 1984). Intrinsic SP fibers course between the medial, central and basolateral nuclei (Roberts et al 1982). Within the hippocampus, a direct septo-hippocampal SP projection (Peterson and Shurlow 1992) is observed in the dentate gyrus (DG), CA1 and CA2 (Iritani et al 1989). Also, an SP projection from the supramammilary nucleus of the hypothalamus has been observed in both guinea-pig (Gall and Moore 1984) and rat (Borhegyi and Leranth 1997a; Borhegyi and Leranth 1997b). Furthermore, intrinsic SP fibres are observed in the CA3 (Marksteiner et al 1992).

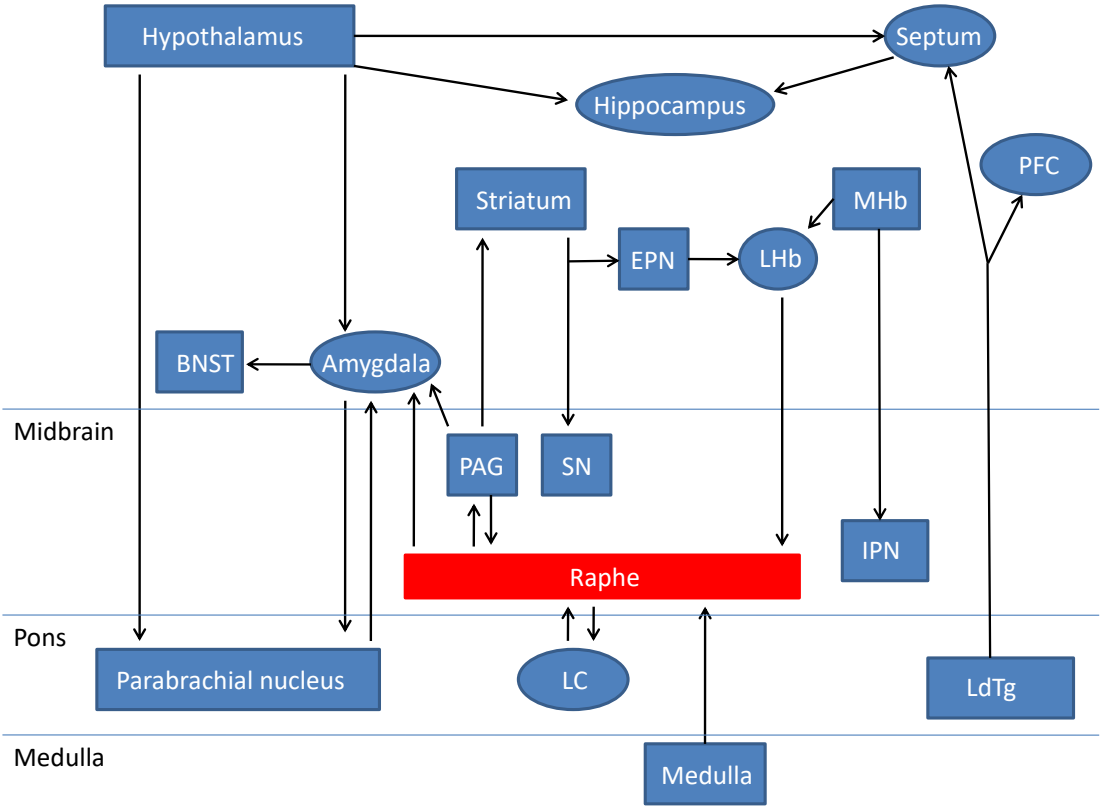


Fig. 1.4. Tachykinin pathways in the rodent brain. Schematic diagram of tachykinin connections in rodent brain. Raphe is in 'red' and represents caudal and dorsal DRN. Brain regions in 'oval' were studied in this thesis. The hypothalamus, amygdala and epithalamic regions (MHb and LHb) send SP/NKA fibres to the brainstem and in turn brainstem regions send up axons to the forebrain (e.g. septum and PFC). Intrinsic circuits are seen within the brainstem e.g. reciprocal circuit between LC and raphe, and between parabrachial nucleus and amygdala (central nucleus). Although not shown, fibres have also been observed in the hypothalamus, reticular formation, superior colliculus, thalamus and ventral tegmental area. Information from: (Bolam and Smith 1990; Emson et al 1977; Harding et al 2004; Hong et al 1977; Kanazawa et al 1980; Li et al 1990b; Ljungdahl et al 1978b; Marksteiner et al 1992; Milner and Pickel 1986; Murakami et al 1989; Neckers et al 1979; Ronnekleiv and Kelly 1984; Sakanaka et al 1982a; Sakanaka et al 1982b; Sakanaka et al 1981a; Sakanaka et al 1983; Shimada et al 1989; Shults et al 1984; Vincent et al 1983; Yamano et al 1988).

1.3.1.3. Tachykinin receptors

Autoradiographic studies in rodents have shown NK_1Rs distributed thoughout the CNS (Dam et al 1990b; Dam et al 1991; Danks et al 1986; Mantyh et al 1989; Mantyh PW 1984; Mantyh et al 1984; Saffroy et al 1994; Saffroy et al 2003; Shults et al 1984; Shults et al 1982). The distribution of SP binding generally shows a close correlation with NK_1R-immunoreactivitity (-ir) (Kaneko et al 1994; Liu et al 2004; Mick et al 1995; Nakaya et al 1994; Piggins et al 2001; Shigemoto et al 1993) and NK_1R-mRNA (Maeno et al 1993; Mick et al 1994). Highest densities of NK_1Rs in the rat brain were detected in the striatum, stria terminalis, septohippocampal nucleus, and nucleus accumbens, with moderate densities in the amygdala, habenula nuclei, periventricular nucleus and olfactory bulb (Beaujouan et al 2000; Helke et al 1990; Mazzone and Geraghty 2000; Nakanishi 1991; Quartara and Maggi 1998; Saria 1999). However, there are some species differences. For example, in the gerbil only weak binding was observed in hippocampus, while in the guinea-pig DG binding was specific to granule cells (Rigby et al 2005). Furthermore, in rat hippocampus NK_1Rs are found only on gamma-aminobutyric acid (GABA) interneurons (Nakaya et al 1994; Sloviter et al 2001).

In the hypothalamus, SP binding was reported in the rat supraoptic nucleus (SON) (Rigby et al 2005; Saffroy et al 1988; Saffroy et al 2003), but was not detected in other studies (Buck et al 1986; Mantyh et al 1989). Similarly, SP binding was reported in the rat paraventricular nucleus (PVN) (Buck et al 1986; Mantyh et al 1989), but not found by others (Saffroy et al 1988; Saffroy et al 2003). Immunohistochemistry has not clarified the situation as NK_1R-ir was found in the

PVN by one group (Liu et al 2002a), while another group only detected very low levels in the SON and PVN (Nakaya et al 1994).

NK_2Rs are mostly found in peripheral tissues, but within the rat CNS these receptors are detected in relatively low densities in the cortex, hippocampus, septum (Helke et al 1990; Saffroy et al 2001), amygdala, interpeduncular nucleus (IPN), habenula, striatum (Stratton et al 1996) and thalamus (Saffroy et al 2001; Stratton et al 1996). Low levels have also been detected within the guinea-pig CNS (Dam et al 1991; Rigby et al 2005).

NK_3Rs are relatively abundant in the brains of rats, gerbils and guinea-pigs using both autoradiography (Bergstrom et al 1987; Dam et al 1990a; Danks et al 1986; Dietl and Palacios 1991; Langlois et al 2001; Rigby et al 2005) and immunohistochemistry (Mileusnic et al 1999a) NK_3Rs are mostly found in neocortex, septum, diagonal band of Broca (DBB), hypothalamus, amygdala, zona incerta, substantia nigra (SN) and raphe nuclei (Ding et al 1996; Koutcherov et al 2000a; Massi et al 2000; Mileusnic et al 1999a; Shughrue et al 1996; Sivam and Krause 1992; Whitty et al 1995).

1.3.2. Neuroanatomical studies in humans and non-human primates

1.3.2.1. Tachykinins

In human brain, the amygdala, caudate, putamen, globus pallidus, hypothalamus, SN and LC were found to be rich in SP-ir (Severini et al 2002). SP-ir nerve cell bodies in the infant and adult human hippocampus are distributed within interneurons in the DG, Ammon's horn, subicular complex and entorhinal cortex (Lotstra et al 1988).

Intense PPT-A mRNA expression has been found in the neocortex, caudate and putamen in the monkey and human brain (Hurd et al 1999), similar to that for SP-ir in the monkey (Hayashi 1992; Jakab et al 1996). In the monkey hippocampus, SP-positive neurons were found on somatostatin (SOM)-ir, GABAergic neurons (Seress and Leranth 1996), but with the major SP input arising from the hypothalamus (Borhegyi and Leranth 1997a; Borhegyi and Leranth 1997b; Nitsch and Leranth 1994). In the DRN of colchicine-treated squirell monkey, SP-ir was found in register with 5-HT-ir neurons (Charara and Parent 1998). The distribution of SP-ir neurons in the monkey PAG and DG is identical to that of the rat (Ljungdahl et al 1978a).

1.3.2.2. Tachykinin receptors

Few studies of tachykinin receptor distribution have been carried out in the primate brain. Nagano et al. (2006) recently studied NK_1R and NK_3R mRNA distributions in rhesus monkey brain (Nagano et al 2006). They found NK_1R mRNA in several cortical and subcortical brain regions including hippocampus and amygdala, with the highest densities in the putamen. These findings are similar to those found in the human brain for NK_1R mRNA (Caberlotto et al 2003), NK_1R-ir (Parent et al 1995; Tooney et al 2000b) and SP binding (Dietl and Palacios 1991). On the other hand, NK_3R mRNA was only found in the cortex, hippocampus and amygdala and in lower densities (Nagano et al 2006).

More recently, Rigby et al (2005) carried out a study in rodent, non-human primate and human brain (Rigby et al 2005). In keeping with Dietl and Palacios (1991), in the human brain, the most intense binding with [^{125}I] SP was found in the superior olives (Rigby et al 2005). The next highest binding was seen in the striatum, DBB, septum,

LC, and PAG. Moderately dense binding was observed in the amygdala, frontal, visual, temporal, and entorhinal cortices. There was weak to moderate binding in PFC and raphe. Within the hippocampus, the cell bodies of the DG polymorphic layer were strongly labeled, but with moderate binding in dendritic fields of CA3-CA1. The weakest binding occurred in the thalamus and cerebellum. This distribution was similar to that in non-human primates (Rigby et al 2005). Similar results were found by Caberlotto et al (2003) who used riboprobe *in situ* hybridisation, quantitative polymerase chain reaction (PCR) and *in vitro* autoradiography to study human NK_1Rs. They found highest NK_1R mRNA levels in the LC and ventral striatum, moderate signals in the cerebral cortex, hippocampus and amygdala, and low signals in the DRN. Only very low levels of NK_1R mRNA were found in the thalamus and cerebellum (Fig. 1.5). Autoradiography with ^{3}H-SP revealed good correlations between receptor binding and NK_1R mRNA with highest levels of binding in LC (Caberlotto et al 2003).

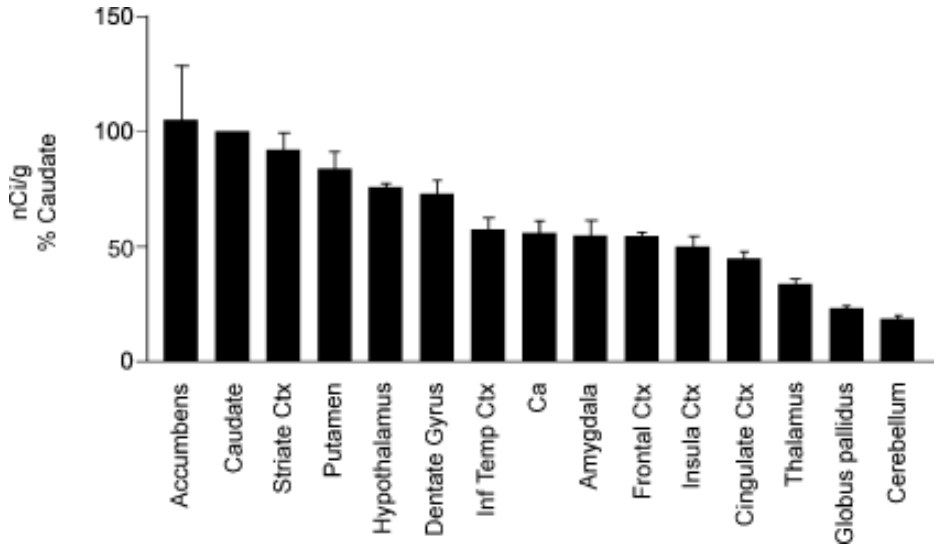


Fig. 1.5. NK_1 receptor mRNA in human brain. Percentages are mean ± standard error of the mean (SEM) of 4 subjects. Value for caudate nucleus set at 100 % (Caberlotto et al 2003).

Two receptor isoforms for the NK_1R with different lengths at the C-terminus have been detected (Fong et al 1992a). Caberlotto et al. found the long isoform to be most prevalent in the human brain, with the short form found mostly in the periphery, but also in the SN and cerebellum (Caberlotto et al 2003). However, more recently real-time reverse transcriptase-PCR (RT-PCR) showed the truncated NK_1R mRNA to be more abundant than previously thought (Lai et al 2008).

Initially, only low levels of NK_1R binding (Nilsson et al 1991) or NK_1R-ir (Kowall et al 1993) were detected in the midbrain, but more recent studies have reported NK_1R mRNA (Whitty et al 1997) and protein (Mounir and Parent 2002) in human SN.

A study of the human basolateral amygdala (BLA) using an antibody to the C-terminus of the NK_1R, which only detects the long isoform of the NK_1R, identified NK_1Rs on pyramidal cells and possible GABA interneurons (Maubach et al 2001). More recently, antibodies against the N-terminus of the NK_1R, which detect both the long and short forms of the NK_1R, were used to study NK_1Rs in the amygdala of schizophrenic patients and normal controls postmortem. Although no difference between the two groups was found, NK_1Rs were observed on large pyramidal, small stellate and large bipolar neurons (Weidenhofer et al 2006).

A double-immunoflourescent study in the human hippocampus showed colocalisation of NK_1Rs with calbindin (CB), but not with SOM, parvalbumin (PV), calretinin (CR) or cholecystokinin (CCK) (Toth et al 2007). This is in contrast to the rat, where NK_1Rs were found on a hetergenous group of inhibitory neurons (Acsady et al 1997; Sloviter et al 2001).

Using polyclonal antibodies that detect both isoforms, NK_1R-ir has been found in human PFC as a thin band at the pial surface, with dots scattered across the mid to upper cortical layers (Tooney et al 2000a; Tooney et al 2000b; Tooney et al 2001).

Specific [^{125}I]NKA binding for NK_2R has not been detected in the brains of higher mammals including humans (Rigby et al 2005), but RT-PCR has identified NK_2R mRNA in human caudate, putamen, hippocampus, SN and cortex (Bensaid et al 2001). In addition, autoradiography detected NK_3Rs in monkey cortex, but until recently has failed to detect NK_3Rs in human brain (Rigby et al 2005). Nevertheless, expression of human NK_3R mRNA was detected using RT-PCR (Buell et al 1992). The use of specific antibodies has also allowed localisation of NK_1R and NK_3R in SN and globus pallidus of squirrel monkeys (Levesque et al 2006; Levesque et al 2007) and NK_3R in human cortex (Mileusnic et al 1999a; Tooney et al 2000a) and hypothalamus (Koutcherov et al 2000b).

It thus appears that NK_1Rs are localised to many of the brain regions that are thought to have a role in mood and stress. Further evidence from physiological and pharmacological studies for a functional role for SP and NK_1Rs in mood and stress is presented below in section 1.4.

1.4. SUBSTANCE P AND NK_1 RECEPTORS IN ANXIETY AND DEPRESSION

Studies suggest a role for SP and NK_1Rs in cognition, emesis, nociception (Quartara and Maggi 1998), stress (De Felipe et al 1998; Kramer et al 1998), schizophrenia and depression (Burnet and Harrison 2000; Malek-Ahmadi 1992). Much of the evidence that links SP with stress and depression comes from pre-clinical studies. Indeed, SP and NK_1Rs are found distributed in brain regions that process emotion and stress (Harrison and Geppetti 2001; Herpfer and Lieb 2005; Honkaniemi et al 1992; Hurd et al 1999; Mantyh PW 1984; Nakaya et al 1994; Ribeiro-da-Silva and Hokfelt 2000).

1.4.1. Animal studies

1.4.1.1. Behavioural effects of substance P and substance P agonists

Centrally administrated SP and SP agonists show different effects on anxiety-related behaviours depending on dose and site of administration (Ebner and Singewald 2006). For example, anxiogenesis is observed after SP injections into the dorsal PAG, lateral septum (LS) and medial amygadala (MeA) (Aguiar and Brandao 1996; De Araujo et al 1999; Ebner et al 2004; Gavioli et al 2002; Teixeira et al 1996). In contrast, SP injections into nucleus basalis magnocellularis were associated with anxiolysis on the elevated plus maze (EPM) (Hasenohrl et al 1998; Nikolaus et al 1999). Moreover, the C-terminal fragment SP 7-11 when injected into the dorsal PAG had anxiogenic effects (De Araujo et al 2001a; De Araujo et al 2001b; De Araujo et al 1999), but when either the N-terminal fragement SP1-7 or the C-terminal fragment were injected into the ventral pallidum, anxiolysis was observed (Nikolaus et al 2000). Thus, different SP peptide fragments may have similar behavioural effects when injected into one brain region, but an opposing effect when injected into a different region.

1.4.1.2. Effects of stress on substance P and NK_1 receptors

Studies indicate that brain SP levels may be altered after exposure to stress (Bannon et al 1986; Takayama et al 1986). Indeed, the effects of stressors on SP tissue levels or SP-ir in rat CNS has recently been reviewed (Herpfer and Lieb 2005) (see Table 1.5). However, both increases and decreases (Lisoprawski et al 1981; Nakamura et al 1990; Siegel et al 1987; Takayama et al 1986) in SP tissue content have been observed after stress (Ebner and Singewald 2006). Nevertheless, more recent microdialysis experiments found stress-induced increases of SP release in the LS and MeA (Ebner et al 2004; Ebner and Singewald 2006). Similar increases in stress-induced SP transmission were found in MeA of a rat model of anxiety with a genetic polymorphism in the NK_1R (Ebner and Singewald 2006). In addition, chronic mild stress (CMS) increased SP mRNA in MeA (Sergeyev et al 2005). In other studies, immobilisation stress increased NK_1R endocytosis in the gerbil amygdala (Smith et al 1999). Furthermore, Kramer et al. also showed that neonatal separation of guinea pig pups increased SP release in the amygdala, coincident with induction of distress vocalisations (Boyce et al 2001; Kramer et al 1998).

Alterations in NK_1Rs have also been observed depending upon duration and severity of the stressor and brain area studied. For example, acute stressors decreased NK_1R binding in amygdala and hippocampus (Duric and McCarson 2005; Takayama et al 1986), while prolonged stressors increased NK_1R binding in central amygdala (Hwang et al 2005) and down-regulated NK_1R gene expression in hippocampus (Duric and McCarson 2005).

Table 1.5. Effects of stress on substance P levels in rat central nervous system.

Stressor	Brain region	SP content
Intermittent foot shock	VTA, olfactory tubercle, hypothalamus	decrease
	Septum, hippocampus (DG)	increase
Whole body vibration	Frontal cortex	decrease
	Nucleus accumbens, amygdala	increase
Immobilisation (1 hr)	Septum, striatum, hippocampus	decrease
Isolation (1 day or 1 week)	Dorsal PAG	increase
	Hippocampus, amygdala	unchanged
Saline injection	PAG	increase
	Nucleus accumbens	decrease
Adjuvant-induction of arthritis (14 days)	Median eminence/arcuate nucleus, PVN	increase

Adapted from (Herpfer and Lieb 2005) with information from: (Brodin et al 1994; Chowdrey et al 1995; Ebner and Singewald 2006; Nakamura et al 1990; Rosen et al 1992; Takayama et al 1986).

Thus, the effects of stress on SP content and NK_1Rs are mixed and depend on the stressor and the brain region studied. Nevertheless, most studies do show an alteration in SP content or NK_1Rs in limbic and cortical brain regions following stress.

1.4.1.3. Effects of psychotropic drugs on substance P and NK_1 receptors

Psychotropic drugs alter SP in different ways in different brain regions depending upon whether the psychotropic drug is administered acutely or in a subchronic or chronic fashion. The results of studies with diazepam, antidepressants and mood stabilisers are presented in Table 1.6.

Table 1.6. Effects of psychotropic drugs on substance P and NK_1 receptors in the rat brain.

Psychotropic	Treatment	Brain region	Alteration in SP/NK_1R
Anxiolytics:			
Diazepam	acute	Hippocampus	decrease in SP
		PAG	decrease in SP
		SN	increase in SP
	sub-chronic	Striatum	increase PPT-mRNA
Antidepressants:			
SSRI	acute	PAG	increase in SP
	sub-chronic	PAG	increase in SP
		Medullary raphe	decrease in PPT-mRNA
		Striatum	increase in PPT-mRNA
	chronic	Striatum, SN	decrease in SP
		Amygdala	decrease in SP
Tricyclic	chronic	Frontal cortex	decrease in SP
MAOI	chronic	LC	increase in NK_1R binding
Mood stabilisers:			
Lithium	sub-chronic	Frontal cortex	increase in SP
		Striatum	increase in SP
	chronic	Hypothalamus	increase in SP
		Striatum	increase in SP
Carbamazepine	chronic	Cortex, SN	increase in SP
		Striatum	increase in SP
		Brainstem	increase in SP
Valproic acid	acute, sub-chronic, chronic	*in vitro* astrocytes	decrease in NK_1 R function

Information from: diazepam (Brodin et al 1994; Koshiya and Kato 1983; Lucas et al 1997); antidepressants (Brodin et al 1987; Riley et al 1991; Rosen et al 1995; Sartori et al 2004; Shirayama et al 1996; Walker et al 1991); mood stabilisers (Hong et al 1983; Kuang et al 1991; Lieb et al 2003; Mathe et al 1990; Mitsushio et al 1988; Sivam et al 1989). MAOI=monoamine oxidase inhibitor.

In addition to the results in Table 1.6, chronic lithium treatment normalised the reduced striatal and elevated frontal cortical SP levels observed in Flinders Sensitive Line (a rat model of depression) (Husum et al 2001). Lithium also increased SP levels in the frontal cortex in Fischer rats (Hong et al 1983). Furthermore, carbamazepine increased responsiveness of neurons to applied SP in the cingulate cortex (Jones et al 1985).

Thus, in general, acute and subchronic treatment with antidepressants led to increases in SP content in the PAG, while chronic treatment led to reductions in SP levels in the striatum, amygdala and frontal cortex depending on the drug used. Perhaps the increase seen in NK_1R binding in the LC after chronic monoamine oxidase inhibitor (MAOI) administration may have been compensatory to a reduction in SP (Sartori et al 2004). In contrast, treatments with mood stabilisers mostly increased SP content in striatum and frontal cortex and reduced NK_1R function.

1.4.1.4. Effects of electroconvulsive shock on substance P and NK_1 receptors

Studies with repeated electroconvulsive shock (ECS) in rats have shown inconsistent results. For example, following ECS, increased SP levels or PPTA mRNA expression were observed in the frontal cortex, PAG and Edinger-Westphal nucleus (Brodin et al 1989), and either reduced or unaltered expression of PPTA mRNA was observed in caudate and putamen (Stenfors et al 1992; Zachrisson et al 1997). Furthermore, when cortical NK_1Rs were measured in rats following ECS, NK_1R binding was increased (Burnet et al 2001). Thus, ECS may alter SP and NK_1Rs in specific brain regions and these alterations may be related to its therapeutic actions.

1.4.1.5. NK_1 receptor antagonism

1.4.1.5.1. Pharmacological blockade

NK_1RAs can be either peptide or non-peptide molecules; but the majority of the studies with NK_1RAs have been carried out with non-peptide molecules (Giardina et al 2003; Swain 1998). Pre-clinical studies have shown NK_1RAs to attenuate stress-induced responses (Bannon et al 1983; Culman et al 1997; Kramer et al 1998; Unger et al 1988). For example, FK-888 was anxiolytic on the EPM (Teixeira et al 1996), while L-760,735 was anxiolytic in a fear conditioning paradigm in the mouse (Rupniak et al 2003). Similarly, NKP-608 was anxiolytic on EPM and social interaction test in the rat (File 2000; Vassout et al 2000; Vendruscolo et al 2003). Furthermore, NKP-608 had antidepressant-like effects in the rat CMS paradigm (Papp et al 2000). However, NK_1RAs with a high affinity for the human receptor have a low affinity for the rat receptor (Beresford et al 1991; Gitter et al 1991), therefore other species e.g. guinea-pig, gerbil and tree shrew have also been used (Rupniak et al 2001; van der Hart et al 2002). For example, many NK_1RAs exhibited anxiolytic and antidepressant actions in gerbils on the social interaction test (Cheeta et al 2001; Gentsch et al 2002; Salome et al 2006), EPM (Varty et al 2002), tail suspension test (Varty et al 2003) and fear-conditioning paradigms e.g. attenuation of foot tapping induced by foot shock (Ballard et al 2001). Also, single administration of an NK_1RA reduced immoblility in forced swim test (FST) in some species: e.g. CP-96,345 in rats (Dableh et al 2005), and MK-869, L-774,2694, L-733,060, CP-99994 and CP-122,721 in gerbils (Wallace-Boone et al 2008). A single dose of GR-205,171 in mice, however showed either a reduction (Zocchi et al 2003) or no change (Chenu et al 2006) in immobility in the FST.

Many brain areas have been postulated to mediate NK_1RA action including amygdala, LS, PAG (Ebner and Singewald 2006) and parietal cortex (Serres et al 2006). For example, immobilisation stress in gerbils showed an increase in NK_1R internalisation in BLA that was inhibited by pre-treatment with the NK_1RA, L-760,735 (Smith et al 1999). In addition, maternally separated guinea-pig pups emitted distress vocalisations that were inhibited by intra-amygdala infusions of L-760,735 (Boyce et al 2001) or GR73632 (Rupniak et al 2000). Also, bilateral BLA lesions in the gerbil induced anxiolysis in fear conditioning and social interaction tests. However, these lesions had no effect on systemically administered NK_1R agonist-induced foot tapping (Woolley et al 2006).

Other studies have examined the role of the MeA in mediating NK_1RA action. For example, pre-injection of the NK_1RA, L-822,429 (Compound A), abolished anxiogensis on the EPM elicited by a microinjection of SP into MeA (Ebner et al 2004). Also, injection of the NK_1RA compound A into MeA led to anxiolysis in rats previously subjected to immobilisation stress (Ebner et al 2004), while infusion into the LS reduced immobility time on FST (Ebner and Singewald 2006). Interestingly, the NK_1RA, GR205,171 was recently shown to increase intermediate early gene expression (*Arc* and *c-fos*) in the rat parietal cortex (Serres et al 2006).

A psychosocial stress paradigm has been used in tree shrews to model depression (Fuchs and Flugge 2002; van Kampen et al 2002). The NK_1RA, L-760,735 (van der Hart et al 2002) had a similar effect to clomipramine on counteracting alterations in the CNS induced by chronic psychosocial stress, e.g. changes in brain metabolites and hippocampal cytogenesis (van der Hart et al 2002). Also, treatment with both L-

760,735 and clomipramine attenuated stress-induced alterations on organ weight, but did not counteract the elevations in cortisol and noradrenaline. However, L-760,735 counteracted stress-induced reductions on marking behaviour (van der Hart et al 2005), while the NK_1RA, SLV-323 prevented stress-induced reductions in PV-ir cells in the hippocampus (Czeh et al 2005).

Thus, pre-clinical studies suggest that NK_1RAs may exhibit both anxiolytic and antidepressant actions in animal models, and that these drugs may mediate their effects via the amygdala (BLA or MeA), LS, hippocampus or parietal cortex.

1.4.1.5.2. Genetic deletion

In recent years, NK_1R knockout (NK_1R–/–) mice were generated and found to be less aggressive (De Felipe et al 1998) and less anxious (Santarelli et al 2001), e.g. fewer separation-induced ultrasonic vocalisations and less immobility in the FST (Rupniak et al 2000; Rupniak et al 2001; Santarelli et al 2001). Also, mice with selective deletion of the gene for TAC1, which encodes for both SP and NKA, were shown to be less fearful (Bilkei-Gorzo et al 2002). However, the results with EPM have been contradictory, possibly due to the use of animals with different genetic backgrounds. Santarelli et al. showed their NK_1R–/– mice (pure 129/sv) to be less anxious on this test (Santarelli et al 2001), but this was not seen in other studies where 129/sv and C57BL/6J mice were used (Murtra et al 2000; Rupniak et al 2001). Nevertheless, plasma corticosterone levels were lower in NK_1R–/– mice subjected to EPM, suggestive of an interaction with the hypothalamic-pituitary-adrenal (HPA) axis (Santarelli et al 2001). Moreover, genetic deletion of NK_1Rs led to reductions in the stress-induced expression of neuronal activation marker Fos in the LC, PAG, frontal

cortex and hypothalamic PVN (Baulmann et al 2000; Ebner and Singewald 2006; Hahn and Bannon 1999; Santarelli et al 2002). Furthermore, in other studies, NK_1R–/– mice showed increased hippocampal neurogenesis and brain-derived neurotrophic factor levels (Morcuende et al 2003), further suggestive of a role for NK_1Rs in stress.

1.4.1.5.3. Substance P-saporin

Interestingly, the use of the toxin, SP-saporin which selectively ablates NK_1R containing neurons, showed these animals to be less anxious on the EPM and less immobilised in the open field (Mantyh 2002).

1.4.2. Human Studies

1.4.2.1. Studies of substance P

A recent study of intravenous (i.v.) SP administration to healthy male subjects led to a significant worsening of mood, but this may have been due to unpleasant peripheral side effects with SP (e.g. flushing) (Lieb et al 2002). In other studies, high anxiety levels increased blood SP concentrations (Fehder et al 1997), or depressed patients showed elevated SP plasma levels (Bondy et al 2003). Also, in some studies, cerebrospinal fluid (CSF) SP levels were elevated in depression (Geracioti et al 2006; Rimon et al 1984), but this was not replicated in another study (Berrettini et al 1985). Furthermore, serum SP levels acted as a predictor of antidepressant response (Bondy et al 2003; Lieb et al 2004). However, this was not replicated in other studies for SP in the serum (Deuschle et al 2005) or CSF (Martensson et al 1989). In one study, valproic acid inhibited SP-induced adrenocorticotrophic hormone (ACTH) synthesis *in vivo* in normal men (Coiro et al 1992). Thus, SP may play a role in stress-induction via NK_1Rs and activation of the HPA axis.

1.4.2.2. Studies of NK_1 receptors

1.4.2.2.1. NK_1 receptor antagonism

The results of clinical trials with NK_1RAs have been mixed. An initial phase II randmonised and placebo-controlled clinical trial in 200 people with major depression showed that after 6 weeks of treatment, NK_1RA, MK-869 (aprepitant) at 300 mg per day was as effective as the selective serotonin reuptake inhibitor (SSRI), paroxetine (20 mg per day) in major depression (Kramer et al 1998). Both aprepitant and paroxetine were superior to placebo in lowering scores on depressive and anxiety symptoms, using the Hamilton Rating Scale for Depression (HDRS) and the Hamilton Rating Scale for Anxiety. Although both treatments were of equal efficacy, aprepitant was better tolerated. The antidepressant efficacy was replicated in clinical trials with two further NK_1RAs: L-759,274 (Compound A) (Kramer et al 2004) and CP-122,721 (Chappell 2002). However, these findings were not supported by a more recent trial (Keller et al 2006). The results from 5 randomised, double-blind, controlled studies in over 2500 people with depression revealed that 8 weeks of treatment with aprepitant at doses of 80 and 160 mg did not show any benefit over placebo. In contrast, paroxetine at 20 mg was used in 2 out of the 5 trials as a comparator and it proved better than placebo. PET imaging showed that the aprepitant doses used would have produced effective NK_1R blockade (> 95% blockade for 160 mg of aprepitant) and would have been pharmacologically active (Keller et al 2006). Despite this, NK_1RAs are also being investigated in other disorders e.g. social phobia (Furmark et al 2005).

1.4.2.2.2. Postmortem studies

An early postmortem study showed a change in the laminar ratio of NK_1Rs in the anterior cingulate cortex of depressed patients (Burnet and Harrison 2000). Another

study showed a decrease in NK_1R binding with [^{125}I]Bolton-Hunter SP in the orbitofrontal cortex in depression (Fig. 1.6), which may reflect fewer NK_1Rs coupled to G-proteins (Stockmeier et al 2002). More recently, Carletti et al. found a significant reduction in PPT-A mRNA (precursor for SP and NKA) in amygdala of patients with bipolar disorder, depression or schizophrenia. However, binding with ^{3}H-SP showed no differences compared to controls (Carletti et al 2005). Postmortem studies suffer from potential confounding factors e.g. effects of treatment, diagnosis and postmortem delay. In fact, postmortem delay negatively correlated with ^{3}H-SP binding, suggesting NK_1Rs are particularly susceptible (Carletti et al 2005). Ideally, NK_1R binding would be better studied *in vivo* using PET. Indeed, NK_1Rs have been imaged in monkeys with an ^{11}C-labeled ligand (Bergstrom et al. 2000) and in humans with [^{18}F]SPA-RQ (Bergstrom et al 2004; Hargreaves 2002).

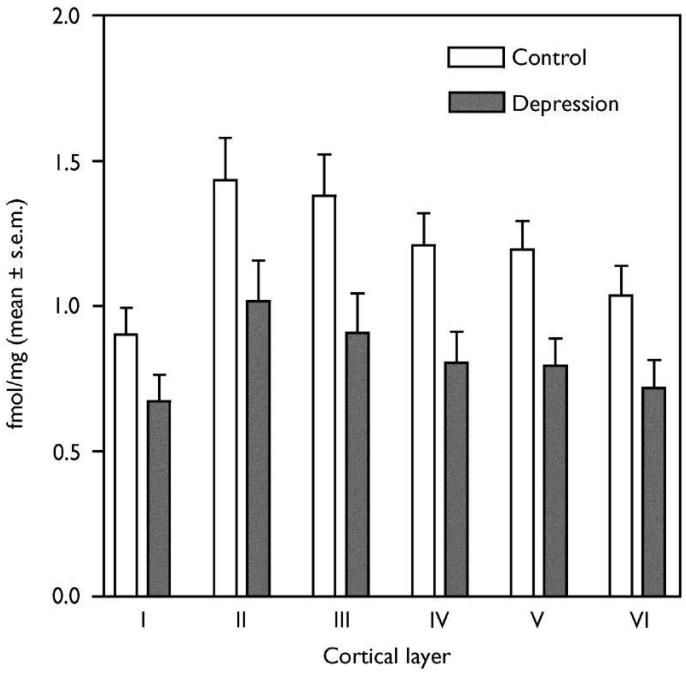


Fig. 1.6. NK_1 receptor binding in the rostral orbitofrontal cortex of postmortem depressed patients and normal control subjects. NK_1R binding is lower in depressed subjects across all cortical layers (Stockmeier et al 2002).

1.5. THE CENTRAL 5-HT SYSTEM

1.5.1. 5-Hydroxytryptamine

5-HT is an indoleamine synthesised from the amino acid tryptophan via 5-hydroxytryptophan (5-HTP). 5-HT neurons have been located in the CNS using immunohistochemistry. The 5-HT system is composed of neuronal clusters located in the raphe nuclei, PAG and brainstem reticular formation which send out projections throughout the CNS. Brainstem 5-HT neuronal clusters have been classified into 9 groups: B1-B9. The caudal group of 5-HT neurons develops into B1-B4, while the rostral group develops into B5-B9 (Tork 1990). The raphe contains the largest collection of 5-HT neurons projecting to the forebrain. The DRN in particular (mostly B6, B7) is composed of 5-HT neurons together with GABA, glutamate or dopamine neurons, which regulate the activity of the 5-HT neurons either locally or via mediating the effects of afferent inputs (Valentino and Commons 2005). The DRN mostly innervates the cortex and neostriatum, while the median raphe nucleus (MRN; B5, B8) mostly innervates limbic regions e.g. septum and hippocampus.

1.5.2. Major 5-HT pathways

Harding et al. (2004) described many of the 5-HT pathways in the rat brain (Harding et al 2004). A summary is described below and depicted in Fig. 1.7 and Fig. 1.8.

1.5.2.1. Brainstem and cerebellar 5-HT projections

In the medulla oblongata, 5-HT fibres were observed in the reticular formation, solitary complex, cranial nerve nuclei and superior and inferior olives (Kolta et al 1993; Steinbusch 1981; Takeuchi et al 1983; Woods and Azeredo 1999). In the pons, 5-HT fibres were detected in the PAG, parabrachial nucleus and cranial nerve nuclei.

In the midbrain, 5-HT fibres were found in the PAG, superior colliculus, cranial nerve nuclei, IPN and dopaminergic cell groups; whilst in the cerebellum, 5-HT fibres were found mostly in the granule cell-layer (Steinbusch 1981).

1.5.2.2. 5-HT fibres innervating the forebrain

Ascending 5-HT projections pass via the MFB to innervate structures in the forebrain, including the olfactory bulb, hypothalamus, thalamus, septum, striatum, hippocampus and cerebral cortex. In the diencephalon, the main targets include the suprachiasmatic nucleus, lateral part of the medial preoptic nucleus, and dorsal and ventral premammillary nuclei. The DRN projects to midline and intralaminar thalamic nuclei, while B9 cells project to other thalamic nuclei and subthalamic nucleus (Vertes 1991; Vertes and Martin 1988). The MRN, in contrast, projects to the lateral habenula (LHb) (Vertes et al 1999). 5-HT fibres in the septum arise from B7 and B8 and some B3 cells, with collaterals sent to the entorhinal cortex (Kohler et al 1982). Furthermore, the cholinergic basal forebrain receives projections from B7, B8 and B9 cells (Jones and Cuello 1989; Vertes 1991; Vertes and Crane 1997; Vertes and Martin 1988). The 5-HT innervation to the basal ganglia is mostly derived from the B7 cell group (Imai et al 1986; Vertes 1991), while the amygdala receives 5-HT projections from the B6, B7 and B8 cell groups. These are mainly present in the central, lateral and basolateral nuclei (Imai et al 1986; Vertes 1991).

5-HT innervation to the hippocampus is derived from both DRN and MRN cell groups (McQuade and Sharp 1997). Dense bands of 5-HT fibres are seen within the strata lacunosum moleculare and oriens, with CA1 and CA2 regions receiving more innervation than CA3 and CA4 (Ihara et al 1988). With regards to the cortex, B7 and B9 cell groups innervate the entire cortex, while B8 cells innervate outer cortical

layers (Harding et al 2004). The piriform, insular, frontal cortices receive denser innervations than the occipital, entorhinal, perirhinal, orbitofrontal, anterior cingulate and infralimbic cortices (Vertes 1991).

1.5.2.3. Afferent projections to the dorsal raphe nucleus

The activity of raphe neurons is controlled by afferent pathways from medial PFC, LHb, LC and other brainstem nuclei (Baraban and Aghajanian 1981; Peyron et al 1996; Sakai et al 1977a; Verge et al 1986) as well as by self-inhibition via 5-HT_{1A} auto-receptors (see Fig. 1.8). The inputs to the DRN from the LC are noradrenergic (NA), while those from the ventral tegmental area (VTA) are dopaminergic (Peyron et al 1996; Peyron et al 1995; Wiklund et al 1988). Other dopaminergic inputs include those from SN (Beckstead et al 1979; Sakai et al 1977a) and A11 cell group of the hypothalamus (Peyron et al 1995). There is also some evidence for dopaminergic inputs to the MRN (Beckstead et al 1979). In addition, the DRN receives major glutamatergic projections from the medial PFC and LHb, with minor inputs from the PAG, lateral hypothalamus and IPN (Aghajanian and Wang 1977; Kalen et al 1985; Kalen et al 1986; Maciewicz et al 1981).

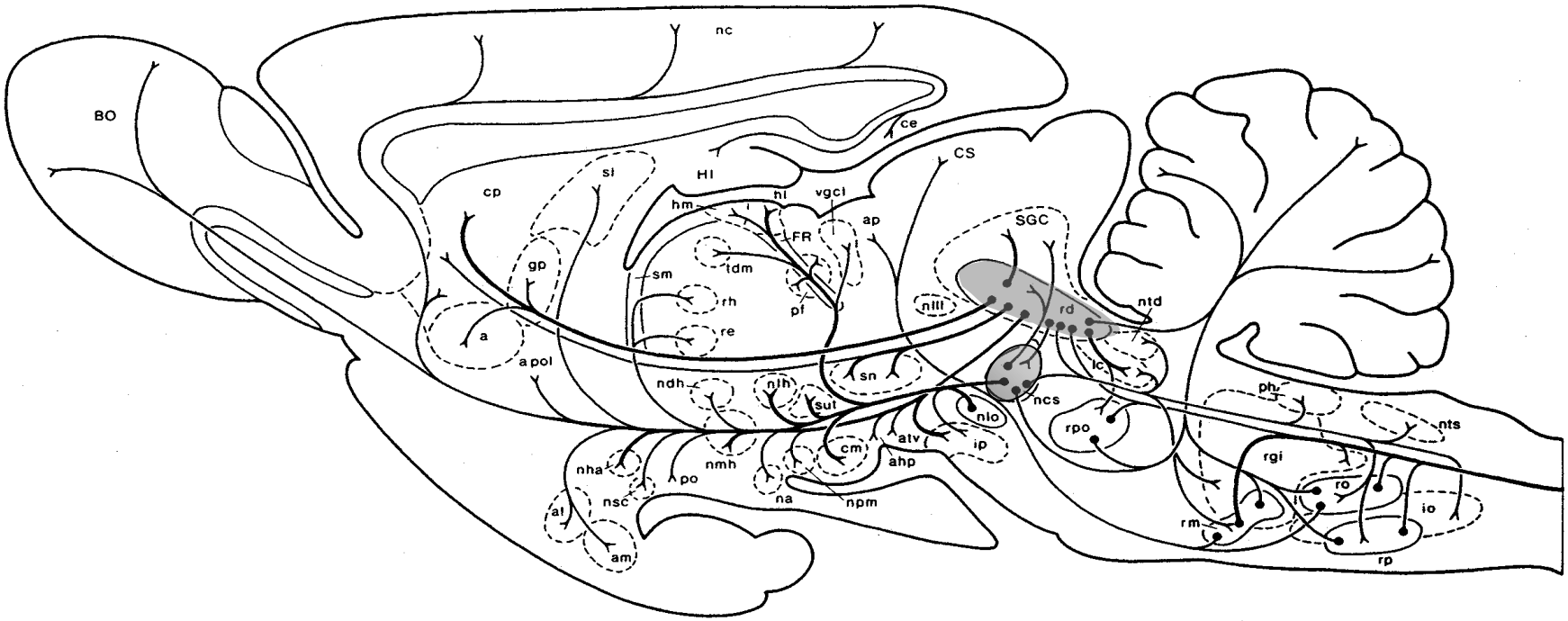


Fig. 1.7. Schematic diagram of ascending and descending projections of midbrain raphe nuclei in the rat in sagittal section. Adapted from (Steinbusch and Nieuwenhuys 1983) figure 33. The DRN (shaded) is the largest raphe nucleus and innervates many forebrain structures. The MRN (shaded) is denoted by ncs.

Abbreviations (n. = nucleus) : a, n. accumbens; ahp, area hypothalami posterior; al, n. amygdaloideus lateralis; am, n. amygdaloideus medialis; ap, area pretectalis; a pol, area preopticus lateralis; BO, bulbus olfactorius; ce, cortex entorhinalis; cm, n. centromedianus thalami; cp, n. caudatus putamen; CS, colliculus superios; FR, fasciculus retroflexus; gp, globus pallidus; HI, hippocampus; hl, n. habenulae lateralis; hm, n. habenulae medalis; io, n. olivaris inferior; ip, n. interpenduncularis; na n. arcuatus; nc, neocortex; ncs, n. centralis superior; ndh, n. dorsalis hypothalami; nf n. fastiguus; nha, n. hypothalami anterior; nlh, n. lateralis hypothalami; nlo, n. lineris oralis; nmh, n. medianus hypothalami; npd, n. parabrachialis dorsalis; npm, n. premammalaris; npv, n. paraventricular hypothalami; ntd, n. tegmentalis; nts, n. tractus solitaruis; nIII, n. motoruis nervi oculomotori; pf, n. parafascicularis; PF, cortex prefrontalis; ph, n. prepositus hypoglossi; po, n. pontis; pv, n. periventricularis thalami; rd, n. raphe dorsalis; re, n. reunions; rgi, n. reticularis gigantocellularis; rh, n. rhomboideus; rm, n. raphe magnus; ro, n. raphe obscurus; rp, n. raphe pallidus; rpo, n. raphe pontis; rpoo, n. reticularis pontis oralis; SGC, substantia grisea centralis; sl, n. lateralis septi; sm, striae medialis; sn, substantia nigra; sut, n. subthalamicus; tdm, nucleus dorsomedialis thalamis; vgcl, n. ventralis corporis geniculati lateralis; vm, n. vestibularis medialis.

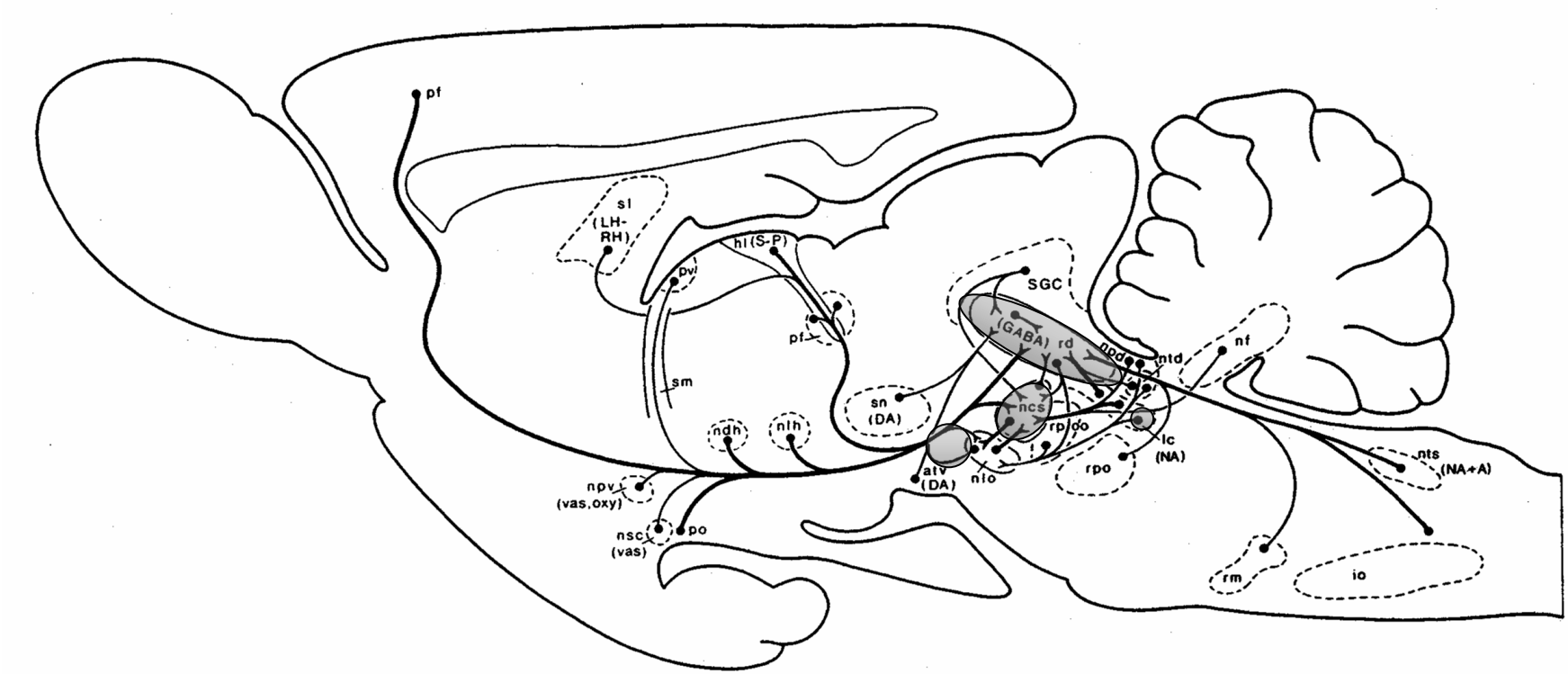


Fig. 1.8. Schematic diagram of afferent connections to mesencephalic raphe nuclei in the rat brain in sagittal section. Adapted from (Steinbusch and Nieuwenhuys 1983) figure 35. A=adrenaline; DA=dopamine; GABA=gamma-aminobutyric acid; NA=noradrenaline; oxy=oxytocin; SP=substance P; vas=vasopressin. For region abbreviations see Figure 1.7. DRN, MRN, locus coeruleus and ventral tegmental area in shade.

1.5.3. 5-HT receptors

Up to now, 7 different subclasses of 5-HT receptors with at least 14 different subtypes have been discovered (Barnes and Sharp 1999). These receptors are described below in terms of their anatomical locations and physiological actions, with an emphasis on 5-HT_{1A}Rs and 5-HT_{2A}Rs (also see Table 1.5).

1.5.3.1. 5-HT_1 receptors

5-HT_1 receptors are classified into: 5-HT_{1A}, 5-HT_{1B}, 5-HT_{1D}, 5-HT_{1E} and 5-HT_{1F}.

1.5.3.1.1. 5-HT_{1A} receptors

5-HT_{1A}Rs in the raphe nuclei are somatodendritic and act as autoreceptors to inhibit cell firing. Somatodendritic 5-HT_{1A}Rs are also found in postsynaptic regions e.g. frontal, prefrontal and entorhinal cortices, septum, hippocampus, amygdala, and hypothalamus (Collin et al 2002; Luttgen et al 2005; Martin-Ruiz et al 2001; Ou et al 2003). 5-HT_{1A}R-ir in the medial septum-diagonal band of Broca (MS-DBB) was found colocalised with PV (Aznar et al 2003) and cholinergic markers (Kia et al 1996a; Luttgen et al 2005). 5-HT_{1A}R-ir is also present on pyramidal cells and CB and PV-positive interneurons within the hippocampus and cortex (Aznar et al 2003).

5-HT_{1A}Rs modulate adenylate cyclase and stimulate N-type Ca^{2+} channels or hyperpolarising G-protein-coupled K^+ channels. 5-HT_{1A}Rs are implicated in the regulation of ACTH, cardiovascular control, anxiety and depression (Hoyer et al 2002).

1.5.3.1.2. 5-HT_{1B-1F} receptors

5-HT_{1B} receptors serve as terminal autoreceptors and heteroceptors and act via inhibiting adenylate cyclase. They are found in the rat basal ganglia, striatum, frontal cortex and cerebral arteries. 5-HT_{1D} receptors are found on axon terminals of 5-HT and non-5-HT neurons within the basal ganglia, hippocampus and cortex and act in a similar way to 5-HT_{1B} receptors. They also act as autoreceptors within the DRN. 5-HT_{1E} receptors are located in the entorhinal cortex, caudate, putamen, claustrum, subiculum and amygdala, while 5-HT_{1F} receptors are found in the entorhinal and cingulate cortices, DRN, claustrum and caudate nucleus (Barnes and Sharp 1999).

1.5.3.2. 5-HT_2 receptors

5-HT_2 receptors are subclassified into 5-HT_{2A}, 5-HT_{2B} and 5-HT_{2C} receptors. These receptor subtypes are coupled to PLC and can also mobilise intracellular calcium via hydrolysis of phosphatidyl inositol (Harding et al 2004).

1.5.3.2.1. 5-HT_{2A} receptors

In the adult rat CNS, autoradiography for 5-HT_{2A}Rs with radioligand antagonists (Appel et al 1990; Lafaille et al 1991; Leysen et al 1982; Lopez-Gimenez et al 1997; Marlier et al 1991; Pazos et al 1985; Schotte and Leysen 1988) and agonists (Altar et al 1985; Appel et al 1990; McKenna et al 1989; Mengod et al 1990; Nazarali et al 1989) has yielded the distribution of 5-HT_{2A}R binding sites. *In situ* hybridisation histochemistry for 5-HT_{2A}R mRNA has also been employed (Burnet et al 1995; Mengod et al 1990; Mijnster et al 1997; Pompeiano et al 1994; Wright et al 1995), supported by several immunohistochemical studies (Carlton and Coggeshall 1997; Hamada et al 1998; Jakab and Goldman-Rakic 1998; Jansson et al 1998; Maeshima et

al 1998a; Maeshima et al 1998b; Morilak et al 1993; Morilak et al 1994; Willins et al 1997; Wu et al 1998).

One immunohistochemical study in the rat cortex showed 5-HT_{2A}Rs in all layers of the neocortex, in particular in the pyramidal cells of layer V (Xu and Pandey 2000). An autoradiographic study also reported 5-HT_{2A}Rs in pyramidal cells in the rat cortex (Rahman et al 1995), but a later immunocytochemical study found the receptors in both pyramidal and nonpyramidal cells (Willins et al 1997). Furthermore, 5-HT_{2A}Rs were indicated in rat cortical interneurons by other immunocytochemical (Morilak et al 1993; Morilak et al 1994) and electrophysiological studies (Gellman and Aghajanian 1993; Marek and Aghajanian 1996; Sheldon and Aghajanian 1990). In the cortex of human and rhesus monkey, 5-HT_{2A}R binding and mRNA signals were found in layers III and V (Burnet et al 1995; Jakab and Goldman-Rakic 1998; Pazos et al 1987; Pompeiano et al 1994), located on pyramidal cells and PV/CR interneurons (Jakab and Goldman-Rakic 1998; Jakab and Goldman-Rakic 2000; Joyce et al 1993).

In colchicine-treated rats, 5-HT_{2A}R-ir was detected in septal cholinergic neurons, identified with an antiserum to the vesicular acetylcholine transporter, and in GABA cells in MS-DBB, identified with antisera to glutamic acid decarboxylase (GAD) and PV. In dorsal hippocampus, 5-HT_{2A}R-ir was found in pyramidal cell layers of CA1-3 and in granular cell layer of DG. 5-HT_{2A}R-ir was also present in hippocampal interneurons identified by GAD65, PV, CB, SOM and neuropeptide Y (NPY), but fewer interneurons with CCK-ir and CR-ir (Luttgen et al 2004).

5-HT_{2A}Rs depolarise membrane potential and stimulate phosphatidylinositol hydrolysis. They are down-regulated following chronic administration of antidepressants or antipsychotics (Eison and Mullins 1996).

1.5.3.2.2. 5-HT_{2B} and 5-HT_{2C} receptors

5-HT_{2B} receptors are located in cerebellum, LS, dorsal hypothalamus and MeA (Barnes and Sharp 1999). 5-HT_{2C} receptors are located in choroid plexus, cortical areas (olfactory nucleus, pyriform, cingulate and retrosplenial cortices), basal ganglia and limbic system (nucleus accumbens, amygdala, and hippocampus), while 5-HT_{2C} receptor mRNA was found in the medulla. Activation of 5-HT_{2C} receptors leads to depolarisation of pyramidal neurons in the piriform cortex (Barnes and Sharp 1999).

1.5.3.3. Other 5-HT receptors

Other 5-HT receptors include 5-HT_3 and 5-$HT_{4,5,6,7}$ receptors (Barnes and Sharp 1999). Table 1.5 describes the locations of all the 5-HT receptors, with examples of their agonists and antagonists, intracellular mechanisms of action, main locations in CNS and behavioural effects.

5-HT is implicated in a variety of functions, ranging from regulation of autonomic functions to cognition, motor behaviours, nociception, arousal and affective behaviours (Harding et al 2004).

5-HT receptor subtype	Known Agonists & Antagonists	Intracellular mechanism	Main location in central nervous system	Behavioural effects
5-HT$_{1A}$	*Agonists:* 8-OH-DPAT, U 92016A *Antagonists:* WAY 100635, (S)-UH-301	Negatively coupled to AC	Limbic areas, cortex, DRN & MRN	5-HT syndrome, hypothermia, hyperphagia, anxiolysis, sexual behaviour
5-HT$_{1B}$	*Agonists:* Sumatriptan, L 694247 *Antagonists:* SB 224289, GR 55562	Negatively coupled to AC	Basal ganglia, striatum, hippocampus, DRN & MRN	Increased locomotion, hypophagia, hypothermia (G.Pigs), myoclonic jerk (G.pigs)
5-HT$_{1D}$	*Agonists:* Sumatriptan, L 694247 *Antagonist:* BRL 15572	Negatively coupled to AC	Basal ganglia, cortex, DRN & MRN	Not known
5-HT$_{1E}$	None	Negatively coupled to AC	Cortex (monkey & human) & caudate putamen	Not known
5-HT$_{1F}$	*Agonist:* LY 334370	Negatively coupled to AC	Hippocampus, cortex & DRN	Not known
5-HT$_{2A}$	*Agonists:* DOI, alpha-Me-5-HT *Antagonists:* MDL 100907, AMI-193	Positively coupled to PLC	Cortex , nucleus accumbens, caudate nucleus & olfactory tubercle	Wet dog shakes (rats), head twitch (mouse), hyperlocomotion
5-HT$_{2B}$	*Agonists:* alpha-Me-5-HT, BW 723C86 *Antagonist:* RS 127445	Positively coupled to PLC	Low levels detected in rat and human brain	Not known
5-HT$_{2C}$	Agonists: WAY 161503, RO 60-0175, RO 60-0332 *Antagonist:* SB 242084	Positively coupled to PLC	Cortex, nucleus accumbens, hippocampus, amygdala, LHb & basal ganglia	Hypolocomotion, hypophagia, anxiety, penile erections, hyperthermia

5-HT receptor subtype	Known Agonists & Antagonists	Intracellular mechanism	Main location in central nervous system	Behavioural effects
5-HT$_3$	*Agonists:* 2-methyl-5-HT, 3-chlorophenyl-biguanide *Antagonists:* Granisetron, Ondansetron, Tropisetron	Cation channel permeable to Na+ and K+	Cortex, hippocampus & amygdala	Anxiolysis, cognition, locomotion, reward
5-HT$_4$	*Agonists:* BIMU8, ML 10302, RS67506 *Antagonists:* GR 113808, SB 204070, RS 100235	Positively coupled to AC	Septum, hippocampus & striatum	Pain, anxiolysis, anxiogenesis cognition
5-HT$_{5A}$	None	Not known	Hippocampus, hypothalamus, cortex, thalamus & striatum	Not known
5-HT$_{5B}$	None	Not known	LHb, DRN & piriform cortex	Not known
5-HT$_6$	*Antagonists:* RO 630563, SB 271046,SB 357134	Positively coupled to AC	Striatum, &hippocampus	Psychosis, anxiety, cognition
5-HT$_7$	*Antagonists:* SB 656104, SB 269970, SB 258719	Positively coupled to AC	Hypothalamus, thalamus & low levels in the cortex	Sleep, cognition, anxiety, temperature regulation

Table 1.7. 5-HT receptors located in central nervous system. AC=adenylate cyclase; DRN=dorsal raphe nucleus; LHb=lateral habenula; MRN=median raphe nucleus; PLC=phospholipase C. Adapted from: (Barnes and Sharp 1999; Lanfumey and Hamon 2004; Leysen 2004; Nelson 2004; Raley 2006; Thomas and Hagan 2004).

1.6. 5-HT AND DEPRESSION

1.6.1. The role of 5-HT in depression

5-HT has been implicated in the aetiology of depression for several decades. For example, the levels of 5-HT and its metabolites were found in some studies to be reduced in the CSF of depressed subjects and in the brain of suicide victims (Nordstrom and Asberg 1992; van Praag and Plutchik 1984). Furthermore, the MAOI, iproniazid, was found to have antidepressant properties, while the monoamine depleting agent reserpine was found to lead to depression (Owens and Nemeroff 1994). Later, it was discovered that the 5-HT precursors, tryptophan and 5-HTP could also alleviate depression (Coppen et al 1967; Hayashi et al 2001). However, tryptophan depletion was shown to precipitate depressive symptoms in healthy relatives of depressed patients (Benkelfat et al 1994) and precipitate relapse in patients successfully treated with SSRIs and recovered from depression (Leyton et al 2000; Neumeister et al 2004; Smith et al 1997; Van der Does 2001; Verastegui et al 1997). Furthermore, PET studies reported altered expression of 5-HT_{1A}Rs and 5-HT_{2A}Rs (Bhagwagar et al 2004; Drevets et al 1999; Meltzer et al 2004; Staley et al 1998; Stockmeier 2003). Moreover, preclinical studies have demonstrated that SSRIs enhance extracellular 5-HT levels in the rodent brain after chronic treatment (Hajos et al 2003b; Kreiss and Lucki 1995; Wegener et al 2003). These data are thus in keeping with the studies showing that tryptophan depletion induces relapse in SSRI-remitted patients.

1.6.1.1. 5-HT_{1A} receptors and depression

Studies suggest that 5-HT_{1A}Rs may play a role in depression. The evidence comes from studies in 5-HT_{1A}R knock out mice, postmortem human brain, human PET

studies and from pharmacological studies. For example, 5-HT_{1A}R knockout mice exhibited decreased exploratory behaviour and increased fear of open or elevated spaces as well as reduced mobility in FST (Ramboz et al 1998). Also, a recent analysis of inducible 5-HT_{1A}R knock-out mice demonstrated that the absence of 5-HT_{1A}Rs during early postnatal development had similar effects on anxiety-related behaviours as the unconditional mutation (Gross et al 2002).

In addition, 5-HT_{1A}Rs have been examined in a number of cerebral cortical and subcortical areas in suicide victims and subjects with a history of a mood disorder. Agonist binding to 5-HT_{1A}Rs appears to be increased in ventrolateral PFC (Arango et al 1995) and in the DRN (Stockmeier et al 1998) in suicide, but no consistent changes in agonist binding were detected elsewhere in PFC or hippocampus-for review see: (Stockmeier 2003). Although these *in vitro* findings are varied, PET studies of 5-HT_{1A}R are more convincing. Specifically, 5-HT_{1A}Rs as measured with PET radioligands such as [^{11}C]WAY-100635 *in vivo* were consistently reduced in numbers in human depression in presynaptic and postsynaptic brain regions in a number of independent studies (Bhagwagar et al 2004; Drevets et al 1999; Elhwuegi 2004; Sargent et al 2000).

5-HT_{1A}Rs are also involved in the actions of antidepressants (Elhwuegi 2004; Santarelli et al 2003). For example, chronic SSRI administration reduced 5-HT_{1A}R binding (Li et al 1994; Welner et al 1989) and led to 5-HT_{1A}R desensitisation (Blier and de Montigny 1994; Haddjeri and Blier 2001) in the midbrain. Also, 5-HT_{1A}R agonists such as buspirone have been shown to produce changes in the 5-HT system similar to those produced by antidepressants, e.g. desensitisation of presynaptic 5-

HT_{1A}Rs, and these changes are thought to underlie their therapeutic potential in depression (Blier and Ward 2003). Indeed clinical trials of SSRI augmentation with the 5-HT_{1A}R partial agonist pindolol have shown some benefit in the majority of studies (Segrave and Nathan 2005).

1.6.1.2. 5-HT_{2A} receptors and depression

There is evidence to suggest that 5-HT_{2A}Rs may also play a role in depression. For example, some antidepressant medications may mediate their actions partially via blockade of postsynaptic 5-HT_{2A}Rs, while atypical antipsychotics with 5-HT_{2A}R and 5-HT_{2C} receptor blocking properties can augment the efficacy of SSRIs (Boothman et al 2006; Shelton et al 2001). Also, repeated antidepressant administration can down-regulate 5-HT_{2A}Rs (Gray and Roth 2001). In support of the above, 5-HT_{2A}R knock out mice showed decreased inhibition in conflict anxiety paradigms (Weisstaub et al 2006). Additional evidence comes from studies of 5-HT_{2A}R binding density in the postmortem human brain. For example, an increase in 5-HT_{2A}R numbers was seen in the PFC in suicide victims in some studies (Arango et al 1990; Turecki et al 1999), although not seen in others (Arranz et al 1994; Gross-Isseroff et al 1989). Similarly, there was some evidence for increased cortical 5-HT_{2A}R binding in patients with depression (Hrdina et al 1993; Laruelle et al 1993).

In contrast, the results for 5-HT_{2A}R binding in the cerebral cortex of depressed patients using *in vivo* PET imaging have been varied (for review see Stockmeier 2003). This may be due to factors such as previous antidepressant treatment and issues relating to ligand specificity and modeling (Tan et al 1999). However, recently a study of drug-free acutely depressed patients found increased frontal cortical 5-

$HT_{2A}R$ binding in subjects with high Dysfunctional Attitudes Scale (DAS) scores (Meyer et al 2003). In addition, a more recent study with the PET radioligand [^{11}C]MDL 100,907 showed cortical 5-HT_{2A}Rs to be increased in number in patients recovered from depression (Bhagwagar et al 2006).

Thus, alterations in 5-HT and its receptors, in particular 5-HT_{1A}Rs and 5-HT_{2A}Rs, may play an important role in both the aetiology and the treatment of depression.

1.7. INTERACTIONS BETWEEN NK_1 RECEPTORS AND 5-HT

1.7.1. Coexistence of 5-HT and tachykinins

Studies suggest there are interactions between the SP and 5-HT systems. For example, 30-46% of the neurons in the human raphe colocalised 5-HT and SP (Baker et al 1991; Sergeyev et al 1999). Although a similar picture was seen in squirrel monkeys (Charara and Parent 1998), this degree of colocalisation was not seen in the rat (Bowker et al 1983; Chan-Palay 1981; Hokfelt et al 1978). Nonetheless, SP-ir cells and fibres were present within the DRN (Warden and Young 1988), with NK_1R-ir in the neuropil around 5-HT cells (Commons and Valentino 2002; Froger et al 2001; Leger et al 2002; Nakaya et al 1994). Also, an electrophysiological study suggested that NK_1R may be localised to glutamatergic cells in the DRN (Commons and Valentino 2002). Furthermore, a more recent study showed that a subpopulation of 5-HT cell bodies and dendrites in the caudal DRN of the rat and mouse were endowed with NK_1R-ir (Lacoste et al 2006).

1.7.2. NK_1 receptor blockade and alterations in 5-HT

Application of SP to brain slices *in vitro* induced an increase in excitatory postsynaptic currents in DRN 5-HT neurons (Liu et al 2002b). However, *in vivo* SP infused into the DRN was associated with decreased 5-HT cell firing (Valentino et al 2003). Furthermore, NK_1R deletion (Conley et al 2002; Santarelli et al 2001) and NK_1RAs increased neuronal firing in the DRN (Haddjeri and Blier 2001), although this was not confirmed in another study (Millan et al 2001). Interestingly, NK_1R–/– mice also showed 5-HT_{1A} somatodendritic autoreceptor desensitisation similar to chronic treatment with SSRIs (Froger et al 2001). Although, the desensitisation was seen after chronic treatment with the NK_1RA GR-205,171 in mice (Guiard et al 2005),

it was not seen with L-760,735 in guinea-pigs (Conley et al 2002). Furthermore, there were no direct effects on neuronal firing in guinea-pig DRN slices *in vitro* after SP or NK_1RA treatment, but local application of L-760,735 into the LHb led increased neuronal firing in the DRN possibly via disinhibition of the habenulo-raphe projection (Conley et al 2002). In addition, NK_1RAs increased the firing rate of NA neurons in LC (Maubach et al 2002), a brain region with reciprocal connections to the DRN.

Intracerebral *in vivo* microdialysis experiments with NK_1RAs did not show a change in basal 5-HT levels in the cortex in either rats (Conley et al 2002; Haddjeri and Blier 2000; Lejeune et al 2002; Millan et al 2001) or mice (Guiard et al 2005; Guiard et al 2004; Zocchi et al 2003). However, increases in cortical 5-HT overflow caused by paroxetine were higher in freely moving NK_1R-/- mutants than in wild-type mice (Herpfer et al 2005). In addition, acute or repeated (3 weeks) administration of GR-205,171 to wild-type mice potentiated paroxetine-induced increases in cortical 5-HT dialysate (Guiard et al 2005). More recently, although a single systemic dose of GR-205,171 had no effect by itself, it selectively potentiated the antidepressant-like activity of subactive doses of citalopram and paroxetine in the FST in Swiss mice (Chenu et al 2006). These data tally with the finding of increased extracellular 5-HT in the frontal cortex of awake and freely-moving mice adminstrered a combination of paroxetine and either GR-205,171 or L-733,060 (Guiard et al 2004). The increased neuronal release of 5-HT was compensated by increased 5-HT reuptake, indicating that NK_1RAs do not have an inhibitory effect on the 5-HT transporter in rodents (Guiard et al 2004). Another group found that L-733,060, in contrast to the SSRI fluvoxamine did not inhibit 5-HT uptake in human brain synaptosomes and did not modulate fluvoxamine-induced 5-HT uptake inhibition. Similarly, SP did not

modulate 5-HT uptake in human brain synaptosomes either. These results were replicated in rat cortex synaptosomes using the rat-specific NK_1RA, WIN51708. Thus, inhibition of the 5-HT transporter is probably not responsible for the assumed antidepressant activity of NK_1RAs (Lieb et al 2005). However, co-administration of an NK_1RA with an SSRI may show an advantage in the treatment of human depression (Chenu et al 2006). In fact, in animal models, compounds with dual NK_1R antagonism and serotonin reuptake inhibition showed antidepressant-like activities (Ryckmans et al 2002a; Ryckmans et al 2002b).

Although the above studies suggest interactions between NK_1Rs and the DRN, NK_1Rs may also influence afferent networks to the DRN (Blier et al 2004; Commons et al 2003; Conley et al 2002; Maubach et al 2002). Furthermore, interactions between NK_1R and 5-HT receptor subtypes in postsynaptic regions of the forebrain have yet to be investigated. Interestingly, the levels of NK_1Rs are high in brain regions receiving inputs from the DRN e.g. PFC, septum, hippocampus and amygdala (Barnes and Sharp 1999; Nakaya et al 1994). In these latter regions, 5-HT acts via postsynaptic 5-HT_{1A}Rs and 5-HT_{2A}Rs, receptors important in the aetiology of depression (Bhagwagar et al 2006; Bhagwagar et al 2004; Sargent et al 2000), and in the action of antidepressants (Santarelli et al 2003; Sargent et al 2000; Stockmeier 2003). The 5-HT_{1A}R is found in limbic areas such as the septum, hippocampus and frontal and entorhinal cortices (Aznar et al 2003). In comparison 5-HT_{2A}Rs are distributed in the olfactory region, the striatum, cortex, hippocampus and the amygdala (Cornea-Hebert et al 1999; Xu and Pandey 2000). However, it is not known whether NK_1Rs and the above 5-HT receptor subtypes colocalise to the same neurons. This may be important with respect to the antidepressant action of NK_1RAs.

1.8. SUMMARY

NK_1Rs are expressed in a lower proportion of neurons than are the receptors for classical neurotransmitters. Nevertheless, NK_1Rs are widely distributed in brain regions that regulate emotions and stress e.g. amygdala, hippocampus, PFC, septum, LC and habenula. In fact, alterations have been observed in SP content or NK_1Rs in limbic and cortical brain regions after stress. In addition, acute and subchronic treatment with antidepressants increased SP content in the PAG, while chronic treatments led to reductions in SP levels in the striatum, amygdala and frontal cortex. Also, pre-clinical studies with NK_1RAs suggest anxiolytic and antidepressant actions in animal models. These drugs may partially mediate their effects via the amygdala, LS, hippocampus or parietal cortex. Similarly, NK_1R–/– mice were shown to be less anxious on behavioural testing.

Some findings in humans suggest elevated SP level in the CSF of depressed patients and a role for SP in stress-induction via NK_1Rs and the HPA axis. Postmortem findings suggest a reduction in NK_1R numbers in the orbitofrontal cortex in depression, and a reduction of PPT-A mRNA expression in parts of the amygdala. Although, initial clinical trials showed NK_1RAs to act as antidepressants, this was not borne out in a later trial. However, animal studies suggest an interaction between the NK_1R and 5-HT systems, e.g. 5-HT_{1A} somatodendritic autoreceptor desensitisation or increased cortical 5-HT overflow caused by paroxetine in NK_1R–/– mice as well as increased neuronal firing in the DRN by NK_1RAs via disinhibition of habenulo-raphe projections or neurons in the LC. These findings may explain why NK_1RAs may act as antidepressants in animal models.

1.9. AIMS OF THESIS

Evidence thus suggests that NK_1Rs may play a role in stress and depression and that NK_1RAs may influence the 5-HT system. Therefore, the aims of this thesis were to investigate the neuroanatomical interactions between NK_1Rs and the 5-HT system in the rat and to investigate alterations in NK_1Rs in human depression *in vivo*. Thus, chapter 2 describes experiments using double fluorescence immunohistochemistry for NK_1Rs and 5-HT_{1A}Rs as well as NK_1Rs and 5-HT_{2A}Rs to investigate cellular colocalisaton of these receptors in rat forebrain regions. Chapter 3 describes experiments using retrograde tracing and immunohistochemistry to investigate for the presence of NK_1Rs on DRN afferent neurons in the habenula, PFC and LC. Chapter 4 describes brain imaging of normal volunteers using PET and the selective radioligand [^{18}F]SPA-RQ to determine an appropriate mathematical model for the quantification of brain NK_1Rs. Chapter 5 describes a clinical study using PET and [^{18}F]SPA-RQ to examine *in vivo* differences in NK_1R numbers between drug-free depressed patients, patients recovered from depression and healthy controls. Finally, chapter 6 contains a summary of the findings of the studies from the chapters 2 to 5 as well as a general discussion of these findings including future directions.

CHAPTER 2

INVESTIGATION INTO COLOCALISATION OF NK_1 RECEPTORS WITH 5-HT_{1A} AND 5-HT_{2A} RECEPTORS IN RAT FOREBRAIN

2.1. INTRODUCTION

As outlined in chapter 1, studies suggest that NK_1Rs may play a role in depression or anxiety and that NK_1RAs may modulate the 5-HT system. Interestingly, NK_1Rs and some 5-HT receptor subtypes are found in similar postsynaptic brain regions in the rat forebrain. These include the prefrontal and frontal cortices, septum, hippocampus and amygdala. Therefore, these postsynaptic brain regions may represent a site for interaction between NK_1RAs and the 5-HT system to modulate mood. However, it is not known whether 5-HT receptor subtypes colocalise to the same cells as NK_1Rs. To address this question, in this chapter double-labelled immunofluorescent microscopy was used to determine whether NK_1Rs and 5-HT_{1A}Rs or 5-HT_{2A}Rs are colocalised on the same cells in the rat forebrain.

2.1.1. Interactions between NK_1 receptors and 5-HT system

SP acts via NK_1Rs in brain regions involved in the processing of emotions and stress (Mantyh PW 1984; Nakaya et al 1994). Pre-clinical studies showed SP and its agonists to induce anxiety, while NK_1RAs exhibited anxiolytic and antidepressant properties (Papp et al 2000; Rupniak and Kramer 1999). Also, NK_1R -/- mice displayed marked reductions in anxiety and stress-related behaviours (Santarelli et al 2001). An initial phase II clinical trial showed the NK_1RA aprepitant to be more

effective than placebo and as effective as paroxetine in depression (Kramer et al 1998). Although this was not borne out in a larger trial (Keller et al 2006), the antidepressant and anxiolytic efficacy of a different NK_1RA, L-759, 274 has been confirmed in a further phase II trial (Kramer et al 2004). In addition, altered NK_1R numbers were observed in the postmortem orbitofrontal cortical regions of depressed patients (Stockmeier et al 2002).

An important question that arises is whether the NK_1Rs and the 5-HT systems interact with each other to produce an antidepressant effect. In fact, NK_1R knockout mice exhibited increased firing of 5-HT neurons and desensitisation of 5-HT_{1A} auto-receptors in raphe nuclei (Santarelli et al 2001), with similar changes found in animals treated with NK_1RAs (Haddjeri and Blier 2001). The levels of NK_1Rs are high in some brain regions that receive 5-HT innervations from the raphe e.g. PFC, septum, hippocampus and amygdala (Barnes and Sharp 1999; Nakaya et al 1994). In these regions, 5-HT acts via postsynaptic 5-HT_{1A}Rs and 5-HT_{2A}Rs, receptors important in the aetiology of depression and antidepressant action (Santarelli et al 2003; Sargent et al 2000; Stockmeier 2003). The 5-HT_{1A}R is found distributed in the septum, hippocampus and frontal and entorhinal cortices (Aznar et al 2003; Clement et al 1996; Kia et al 1996c; Pompeiano et al 1992; Wright et al 1995). In comparison 5-HT_{2A}Rs are distributed in the olfactory region, striatum, cortex, hippocampus and amygdala (Cornea-Hebert et al 1999; Xu and Pandey 2000). However, it is not known whether NK_1Rs colocalise on the same cells as these 5-HT receptor subtypes.

2.1.2. Aims of this chapter

The aim in this chapter was to examine the degree of cellular colocalisation between NK_1Rs and 5-HT_{1A}Rs and 5-HT_{2A}Rs in forebrain regions in the rat including the PFC, septum, hippocampus and amygdala.

2.2. MATERIALS AND METHODS

2.2.1. Animals

Male Sprague-Dawley rats (Harlan-Olac, Bicester, UK) were housed in cages in a temperature-controlled environment with a 12 h light/dark cycle (lights on 7:00 am) and allowed free access to food and water. Animal experiments were carried out according to Home Office guidelines and UK Animals (Scientific Procedures) Act 1986, and were designed to minimise animal suffering and number of animals used.

2.2.2. Immunohistochemistry

2.2.2.1. 5-HT_{1A} receptor and NK_1 receptor colocalisation

Six Sprague-Dawley adult male rats (250-370 g) were deeply anaesthetised with intraperitoneal (i.p.) sodium pentobarbital (Merial Animal Health Ltd, Harlow, UK; 200 mg/kg, i.p.) and transcardially perfused with 200 ml 0.9% saline followed by about 300 ml of ice-cold fixative composed of 4% (w/v) paraformaldehyde (Agar Scientific, Stansted, UK) and 0.4% (v/v) saturated aqueous picric acid in 0.1 M phosphate buffer (PB) at pH 6.9 for 20 min. The brains were then removed and post-fixed in the above solution overnight at 4 ºC. Prior to sectioning, the brains were cut into smaller blocks using a plexiglass brain matrix. Coronal sections (40 μm) were cut on a vibrating microtome (Leica, Milton Keynes, UK) and collected as free-floating sections in ice-cold phosphate-buffered saline (PBS, pH 7.4, components 0.14 M sodium chloride, 0.003 M potassium chloride, 0.01 M PB) and after washes in PBS, stored at 4 ºC in PBS with 0.1% (w/v) sodium azide preservative. Following further washes in PBS, sections were incubated for 90 min at room temperature in blocking buffer composed of 0.3% (v/v) Triton X-100, 10% (v/v) normal goat serum (NGS) and 1% (w/v) bovine serum albumin (BSA) in PBS, and then incubated

overnight at 4 ºC with rabbit NK_1R (Chemicon, CA, USA; 1:2000; AB5060) and guinea pig 5-$HT_{1A}R$ primary antibodies (Chemicon; 1:1000; AB5406). The sections were then washed in PBS followed by incubation in Alexa Fluor 488 goat anti-rabbit (Molecular Probes, Netherlands; 1:1000) and Alexa Fluor 568 goat anti-guinea pig secondary antibodies (Molecular Probes; 1:500) for 4 hrs at room temperature while protected from light. All anti-sera were diluted in PBS, 0.3% Triton X-100, 1% NGS and 1% BSA. After further washes, sections were mounted from a buffer bath onto gelatin-coated glass slides, allowed to air-dry while protected from light before being cover-slipped with Vectashield liquid mounting medium (Vector Laboratories, Peterborough, UK). Controls included omitting the primary antibody as well as comparisons for cross-reactivity between a primary antibody and the unrelated secondary antibody.

2.2.2.2. 5-HT_{2A} receptor and NK_1 receptor colocalisation

Six Sprague-Dawley adult male rats (230-250 g) were deeply anaesthetised with pentobarbital and transcardially perfused with 200 ml of PB, followed by 250 ml of ice-cold 4% (w/v) paraformaldehyde (Agar Scientific, Stansted, UK) and 0.4% (v/v) saturated aqueous picric acid in 0.1 M PB at pH 6.9 for 20 min. Brains were post-fixed at 4 ºC for 4 hours and then transferred to 30% (w/v) sucrose in PBS for cryoprotection at 4 ºC for about 36 hours. Each brain was then cut into smaller blocks prior to sectioning on a freezing sliding microtome (Leica Microsystems, Germany). Coronal sections (30 μm) were collected in ice-cold PBS and after 3 x 10 min washes in PBS, stored at 4 ºC in PBS / 0.1% sodium azide. After incubation in blocking buffer sections were then incubated with mouse 5-$HT_{2A}R$ primary antibody (Pharmingen; 1:1000; #556326) for 3 nights at 4 ºC and with rabbit NK_1R primary

antibody (Chemicon; 1:2000) added on the final night. Afterwards sections were rinsed 3 x 10 min in PBS and then incubated in Alexa Fluor 488 goat anti-rabbit antibody (Molecular Probes; 1:1000) and Alexa Fluor 568 goat anti-mouse antibody (Molecular Probes: 1:1000) for 4 hrs at room temperature. After further washes, sections were mounted and cover-slipped as described for the 5-HT_{1A}R experiments. Control comparisons were included as above. The antibodies with the dilutions used are tabulated in Table 2.1.

Table 2.1. Antibodies used against NK_1, 5-HT_{1A} and 5-HT_{2A} receptors

Receptor	**NK_1**	**5-HT_{1A}**	**5-HT_{2A}**
Primary Antibody	rabbit (1:2000)	guinea-pig (1:1000)	mouse (1:1000)
Source	Chemicon [AB5060]	Chemicon [AB5406]	Pharmingen [#556326]
Incubation	overnight/4 °C	overnight/4 °C	3 nights/4 °C
Secondary Antibody	goat anti-rabbit Alexafluor 488	goat anti-guinea-pig Alexafluor 568	goat anti-mouse Alexafluor 568
Source	Molecular probes	Molecular probes	Molecular probes
Incubation	4hr/RT	4hr/RT	4hr/RT

RT = room temperature

2.2.3. Image acquisition and analysis of material

All tissue sections were initially examined using a Leitz Diaplan (Leica, Germany) microscope fitted with an incident 50 Watt mercury arc lamp and equipped with epifluorescence optics and dichroic filters and viewed via a Leitz PL-Fluotar objective (x 40 numerical aperture=0.7). Filters used were as follows: green fluorophore 420-490 excitation band-pass and 520 nm emission long-pass; red fluorophore 530-560 nm excitation band-pass and 580 nm emission long-pass.

Data was collected at x 40 objective throughout. Cell counts for NK_1R-ir and 5-HT receptor-ir colocalisations were made bilaterally on 3 sections, which were collected alternately to avoid counting the same cells twice. All NK_1R-ir positive cells were counted in defined anatomical areas using 'The Rat Brain Atlas' (see Fig. 2.1) (Paxinos and Watson, 1998). Cell counting was carried out on slices from a number of brain regions including the PFC and frontal cortex (bregma 2.7 mm), LS and medial septum (MS) (bregma 0.70 mm), amygdala and hippocampus (bregma –3.30 mm). Within the PFC, only prelimbic and infralimbic regions were included. The frontal cortical regions examined were combined regions of M1 and M2 as depicted in the Paxinos & Watson atlas. Also as MS and DBB represent central structures with cells that cross over the hemispheres, these regions were combined together as MS-DBB for the purposes of counting. The same was done for the LS for the purpose of comparison. Within the amygdala, combined lateral and basolateral nuclei were investigated. Within the hippocampus, the CA4 region was not included as part of the DG, however, the CA3 region also included counts from CA2. Percentage colocalisation is presented as mean of 6 brains +/- SEM.

Coloured digital images of sections with NK_1R and 5-$HT_{1A}R$ double immunofluorescence histochemistry were captured using a cooled colour CCD camera (model C4742-95; Hamamatsu, Welwyn Garden City, UK) on a Leica (Wetzlar, Germany) DMRB microscope with epifluorescence illumination equipped with the following filter blocks: A4 (excitation filter band-pass (B-P), 360/40 nm; reflection short-pass filter, 400 nm; suppression filter B-P, 470/40 nm), L5 (excitation filter B-P, 480/40 nm; reflection short-pass filter, 505 nm; suppression filter B-P, 527/30 nm), Y3 (excitation filter B-P, 545/30 nm; reflection short-pass filter, 565 nm; suppression filter B-P, 610/75 nm), and Y5 (excitation filter B-P, 620/60 nm; reflection short-pass filter, 660 nm; suppression filter B-P, 700/75 nm). Coloured digital images of sections with NK_1R and 5-$HT_{2A}R$ double immunofluorescence histochemistry were obtained using a Xillix Micro Imager camera (Xillix Technologies Corp., Canada) on the Leitz Diaplan microscope described above.

Images were analysed and displayed using Openlab software (version 3.1.4; Improvision, Coventry, UK). Brightness and contrast were adjusted for the entire frame, and no part of a frame was modified in any way. Digital images were manipulated with regards to size, cropping, colour balance, brightness) using Photoshop 5.0 software (Adobe systems, San Jose, CA) on a Power Macintosh computer and later labelled using Powerpoint (Microsoft).

Selected hippocampal sections with double labelling for NK_1R and 5-$HT_{1A}R$ were also analysed by Dr Julian Goggi (Imperial College, London) with a Leica SP confocal laser-scanning microscope (Leica, Germany) through a 63 × PlanApoChromat 1.32 numerical aperture oil immersion objective. The 488 and 568 fluorophores were excited sequentially in order to avoid bleedthrough. The Alexa-

488 signal was detected by excitation with the 488-nm line of an argon laser. The signal from Alexa-568 in the same cell section was detected by excitation using the 568-nm line of a krypton laser. The emitted fluorescence was collected separately through a triple dichroic mirror 488/568/633. The confocal cell images were taken sequentially with an inter section distance of 0.5 μm over the entire depth of the cell.

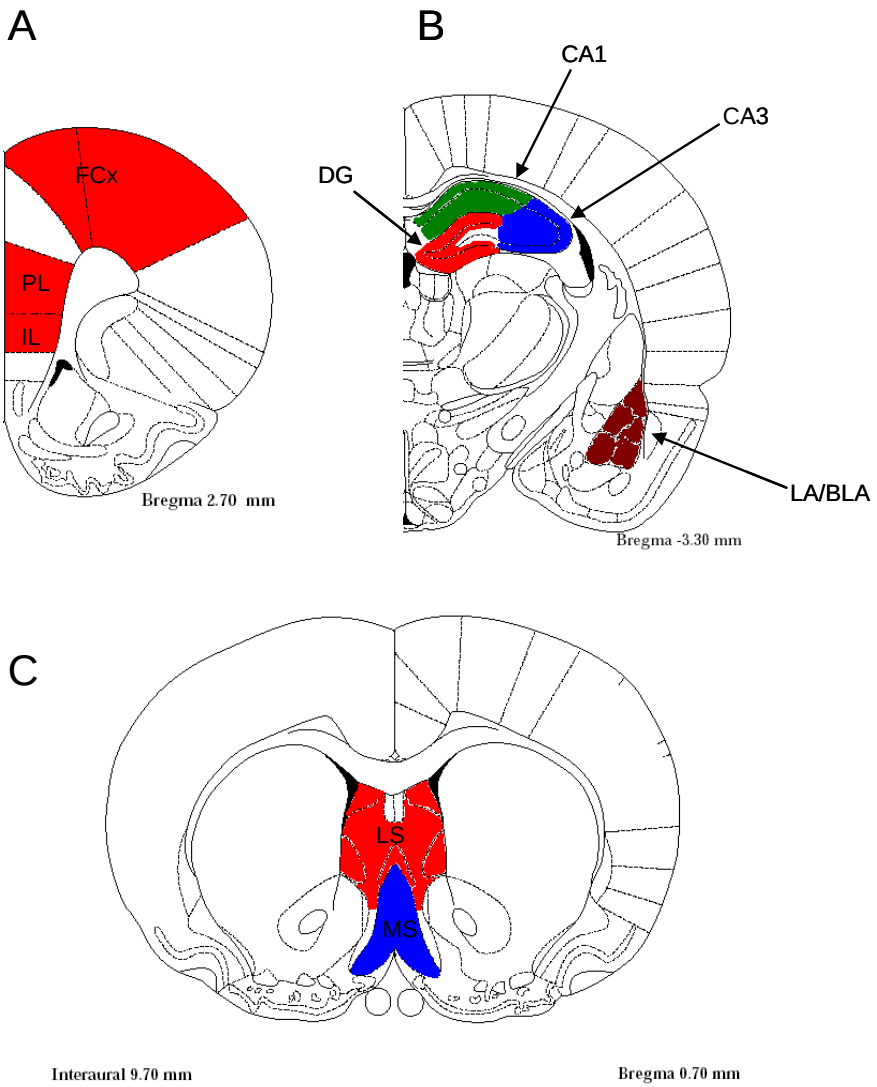


Fig. 2.1. Schematic diagrams of coronal rat forebrain sections of brain regions examined for colocalisation. (A) The infralimbic (IL) and the prelimbic (PL) regions combined to represent the prefrontal cortex; FCx represent the frontal cortex (bregma 2.70 mm). (B) Section representing the hippocampal subregions (dentage gyrus (DG), CA1 and CA3) and amygdala (lateral and basolateral aspects (LA/BLA) (bregma -3.30 mm). (C) Section of the septum (medial septum and diagonal band of Broca complex (MS) and lateral septum (LS) (bregma 0.70 mm).

2.3. RESULTS

2.3.1. Distribution of NK_1 receptor immunoreactivity

NK_1R-ir was detected throughout the rat forebrain regions studied (Fig. 2.2 to Fig. 2.10), similar to what has been shown previously (Nakaya et al 1994). Strong cellular expression for NK_1R-ir was observed in all of the sub-regions of the MS-DBB i.e. the MS (Fig. 2.2), vertical diagonal band of Broca (VDBB) (Fig. 2.3) and horizontal diagonal band of Broca (HDBB) (Fig. 2.4). NK_1R-ir was also observed on cells and fibres in hippocampal sub-regions CA1 (Fig. 2.5), CA3 (Fig. 2.6) and DG (Fig. 2.7). In the DG, strong expression of NK_1R-ir was seen on a network of fibres (Fig. 2.7). NK_1R-ir was less dense in the BLA (Fig. 2.8) and the medial PFC (Fig. 2.9 and Fig. 2.10).

2.3.2. Distribution of 5-HT_{1A} receptor immunoreactivity

5-HT_{1A}R-ir was detected throughout the rat forebrain regions studied (Fig. 2.2 to Fig. 2.10). In previous studies, 5-HT_{1A}R-ir was demonstrated on cells in the hippocampus, DRN, cortex, hypothalamus and septal complex (Collin et al 2002; Kia et al 1996a; Kia et al 1996b; Kia et al 1996c; Luttgen et al 2005; Martin-Ruiz et al 2001; Ou et al 2003). A similar distribution was observed here. 5-HT_{1A}R-ir was strong, dense and prominent on cells in the midline and lateral zones of the MS (Fig. 2.2) as well as in the VDBB (Fig. 2.3) and HDBB (Fig. 2.4). However, less intense cellular expression of 5-HT_{1A}R-ir was observed in hippocampal CA1 (Fig. 2.5), CA3 (Fig. 2.6) and DG (Fig. 2.7) as well as in the BLA (Fig. 2.8), frontal and prefrontal cortices (Fig. 2.9 and Fig. 2.10).

2.3.3. Distribution of 5-HT_{2A} receptor immunoreactivity

5-HT_{2A}R-ir was detected throughout the rat forebrain regions studied (Fig. 2.11 and Fig. 2.12). Within PFC, 5-HT_{2A}R-ir was prominent and observed on both cells bodies and fibres (Fig. 2.12 B). Cellular expression of 5-HT_{2A}R-ir was also observed in the hippocampus e.g. CA3 (Fig. 2.11), MS-DBB (Fig. 2.12 D) and BLA (Fig. 2.12 F).

2.3.4. NK_1 and 5-HT_{1A} receptor colocalisation in rat forebrain regions

Colocalisation between NK_1R-ir and 5-HT_{1A}R-ir was frequent in most areas examined. The highest percentage of colocalisation was present in MS-DBB (88.0%), DG (65.1%) and CA3 regions (62.5%). Moderate colocalisation was seen in the BLA (34.5%), hippocampal CA1 region (32.4%), frontal cortex (32.0%) and PFC (31.1%). Very little colocalisation (3.9%) was found in the LS (see Table 2.2). Fig. 2.2 to Fig. 2.10 depict 5-HT_{1AR}-ir and NK_1R-ir neurons in different forebrain regions. The merged photographs reveal colocalisation on cell bodies in: MS (Fig. 2.2), VDBB (Fig. 2.3) and HDBB (Fig. 2.4), CA1 (Fig. 2.5), CA3 (Fig. 2.6) and DG (Fig 2.7), BLA (Fig. 2.8) and PFC (Fig. 2.9 and Fig. 2.10). Also, confocal microscopy confirmed colocalisation of NK_1R-ir and 5-HT_{1A}R-ir in CA3 region (Fig. 2.13).

2.3.5. NK_1 and 5-HT_{2A} receptor colocalisation in rat forebrain regions

Colocalisation between NK_1R-ir and 5-HT_{2A}R-ir was rare or infrequent (< 8%) in most areas except for hippocampus: DG (15.9%), CA1 (24.8%) and CA3 (43.1%) as shown in Table 2.3. Fig. 2.11 and Fig. 2.12 depict 5-HT_{2A}R-ir and NK_1R-ir neurons in forebrain regions. The merged photographs reveal colocalisation on cell bodies within hippocampal CA3 region (Fig. 2.11), HDBB (Fig. 2.12 C+D) and BLA (Fig. 2.12 E+F). Examples of colocalising cells are also shown in PFC (Fig. 2.12 A+B).

Table 2.2. NK_1 and 5-HT_{1A} receptor colocalisation in rat forebrain

Brain Area	Total no. of NK_1R-ir cells	No. of NK_1R-ir cells expressing 5-HT_{1A}R-ir	Percentage colocalisation Mean (SEM)
mPFC*	415	135	31.1 (4.8)
Frontal Cortex†	1422	455	32.0 (1.7)
Lateral Septum‡	1813	76	3.9 (1.3)
Medial Septum‡	2642	2342	88.0 (0.7)
Amygdala§	384	144	34.5 (2.0)
Dentate Gyrus¶	511	317	65.1 (2.3)
CA3	459	297	62.5 (3.0)
CA1	776	233	32.4 (4.4)

The total number of NK_1R-ir cells counted (total from all animals) and the number of cells also immunoreactive for 5-HT_{1A}Rs is tabulated together with the mean (SEM) percentage colocalisation in different brain regions; in each brain region cell counts were made from both hemispheres in 3 slices for each brain–(total of 6 brains).

* infralimbic/prelimbic regions only
† M1 and M2 regions combined
‡ both hemispheres counted together as one in the septal areas.
§ Lateral/basolateral amygdala only
¶ CA4 not included as part of the dentate gyrus

Table 2.3. NK_1 and 5-HT_{2A} receptor colocalisation in rat forebrain

Brain Area	Total no. of NK_1R-ir cells	No. of NK_1R-ir cells expressing 5-HT_{2A}R-ir	Percentage colocalisation Mean (SEM)
mPFC*	414	9	1.7 (1.1)
Frontal Cortex†	1429	71	5.1 (1.1)
Medial Septum‡	1684	113	6.2 (1.2)
Amygdala§	384	36	8.1 (2.7)
Dentate Gyrus¶	740	124	15.9 (4.6)
CA3	667	290	43.1 (5.5)
CA1	882	218	24.8 (3.9)

The total number of NK_1R-ir cells counted (total from all animals) and the number of cells also immunoreactive for 5-HT_{2A}Rs is tabulated together with the mean (SEM) percentage colocalisation in different brain regions; in each brain region cell counts were made from both hemispheres in 3 slices for each brain–(total of 6 brains).

* infralimbic/prelimbic regions only
† M1 and M2 regions combined
‡ both hemispheres counted together as one in the septal areas.
§ Lateral/basolateral amygdala only
¶ CA4 not included as part of the dentate gyrus

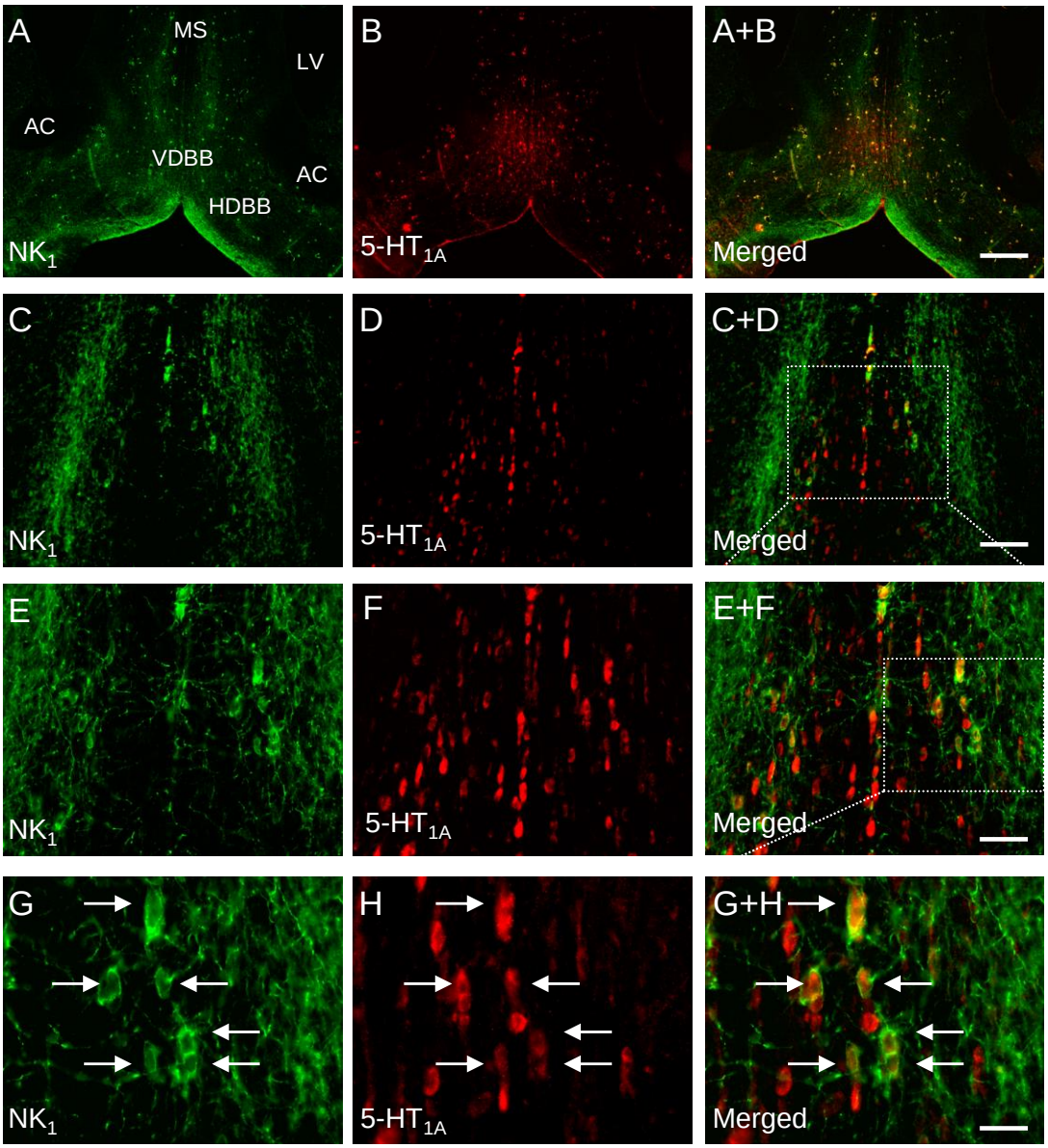


Fig. 2.2. Photomicrographs of NK_1 and 5-HT_{1A} receptor immunoreactivities in medial septum. The medial septum-diagonal band of Broca complex is depicted with its subregions, medial septum (MS), vertical limb of the diagonal band of Broca (VDBB) and horizontal diagonal band of Broca (HDBB) (A, B and A+B). 5-HT_{1A}R- and NK_1R-ir cell bodies are observed in the MS (C, D and C+D). Higher magnification photographs of the square in C+D are shown in E, F and E+F. Cells colocalised for both NK_1R-ir and 5-HT_{1A}R-ir are observed (arrows in G, H, G+H). Scale bars in A+B: 480 μm; C+D: 120 μm; E+F: 60 μm; G+H: 30 μm. AC=anterior commissure; LV=lateral ventricle.

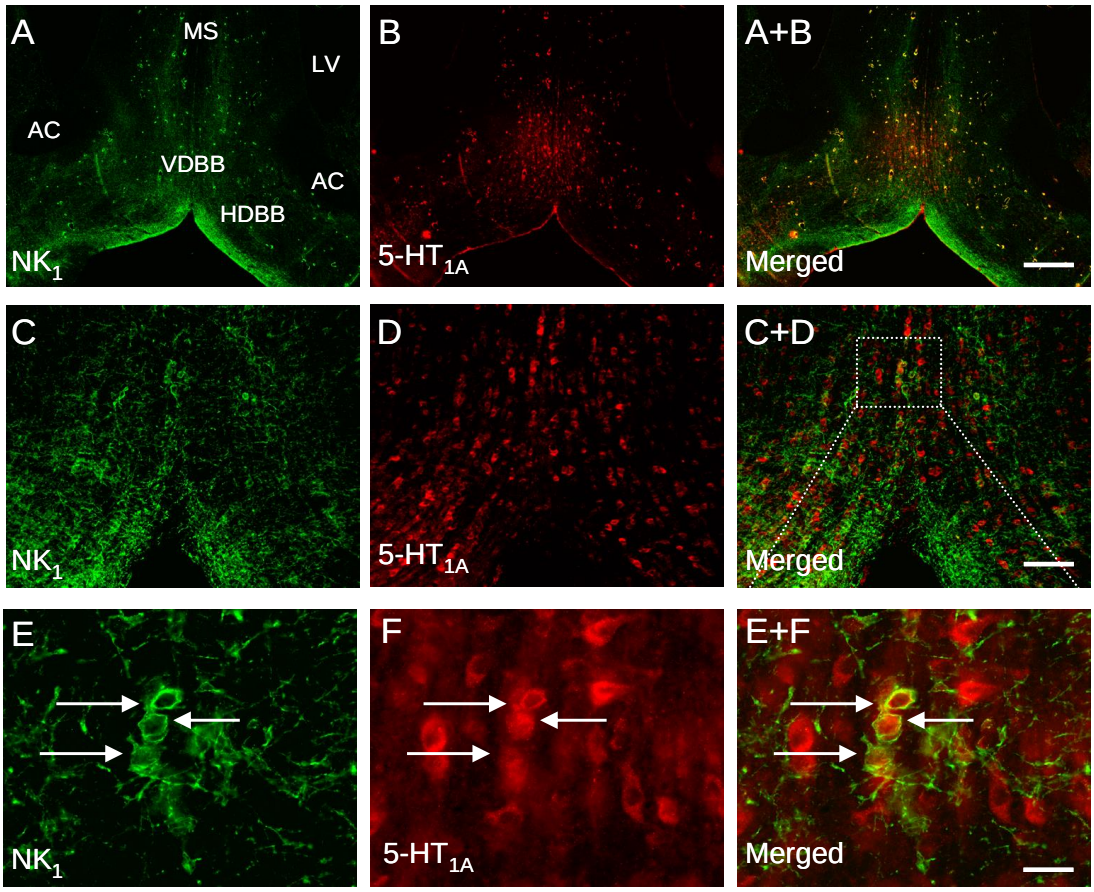


Fig. 2.3. Photomicrographs of NK_1 and 5-HT_{1A} receptor immunoreactivities in vertical diagonal band of Broca. The medial septum-diagonal band of Broca complex is depicted with its subregions, medial septum (MS), vertical limb of the diagonal band of Broca (VDBB) and horizontal diagonal band of Broca (HDBB) (A, B and A+B). 5-HT_{1A}R- and NK_1R-ir cell bodies are observed in the VDBB (C, D and C+D). Higher magnification photographs of the square in C+D are shown in E, F and E+F. Cells colocalised for both NK_1R-ir and 5-HT_{1A}R-ir are observed (arrows). Scale bars in A+B: 480 μm; C+D: 120 μm; E+F: 30 μm. AC=anterior commissure; LV=lateral ventricle.

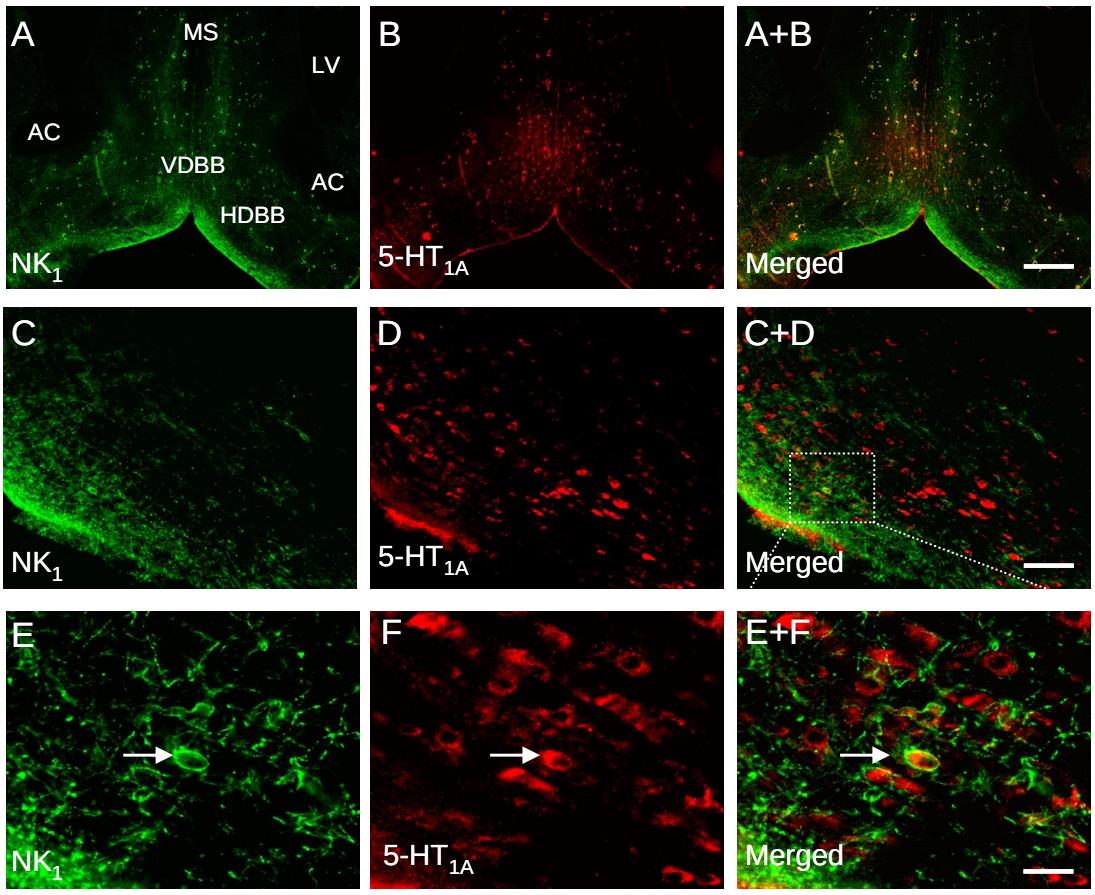


Fig. 2.4. Photomicrographs of NK_1 and 5-HT_{1A} receptor immunoreactivities in horizontal diagonal band of Broca. The medial septum-diagonal band of Broca complex is depicted with its subregions, medial septum (MS), vertical limb of the diagonal band of Broca (VDBB) and horizontal diagonal band of Broca (HDBB) (A, B and A+B). 5-HT_{1A}R- and NK_1R-ir cell bodies are observed in the HDBB (C, D and C+D). Higher magnification photographs of the square in C+D are shown in E, F and E+F. A cell colocalised for both NK_1R-ir and 5-HT_{1A}R-ir is observed (arrows). Scale bars in A+B: 480 μm; C+D: 120 μm; E+F: 30 μm. AC=anterior commissure; LV=lateral ventricle.

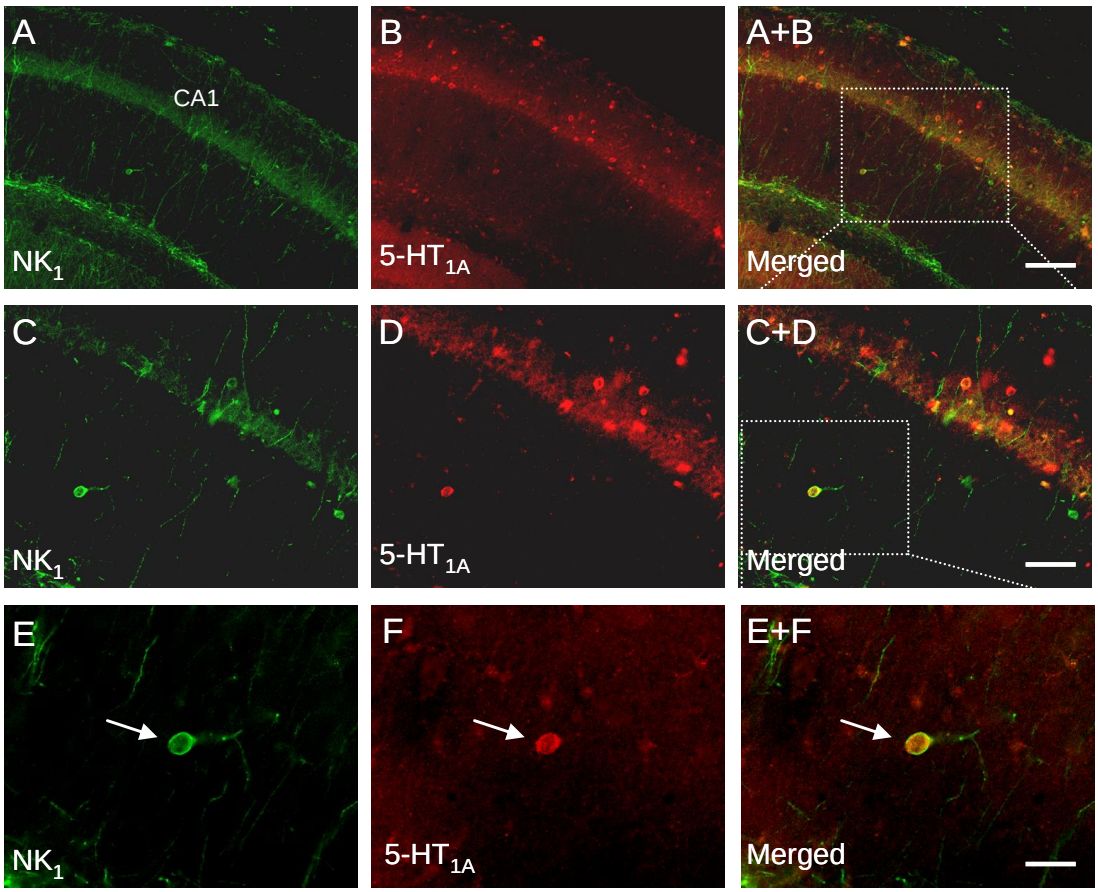


Fig. 2.5. Photomicrographs of NK_1 and 5-HT_{1A} receptor immunoreactivities in CA1 region of hippocampus. Lower magnification photomicrographs reveal NK_1R-ir (A, C) and 5-HT_{1A}R-ir (B, D). Higher magnification photographs of the square in C+D are shown in E, F and E+F. A cell colocalising both NK_1R-ir and 5-HT_{1A}R-ir is observed (arrowed in E, F and E+F). Scale bars in A+B: 125 μm; C+D: 60 μm: E+F: 30 μm.

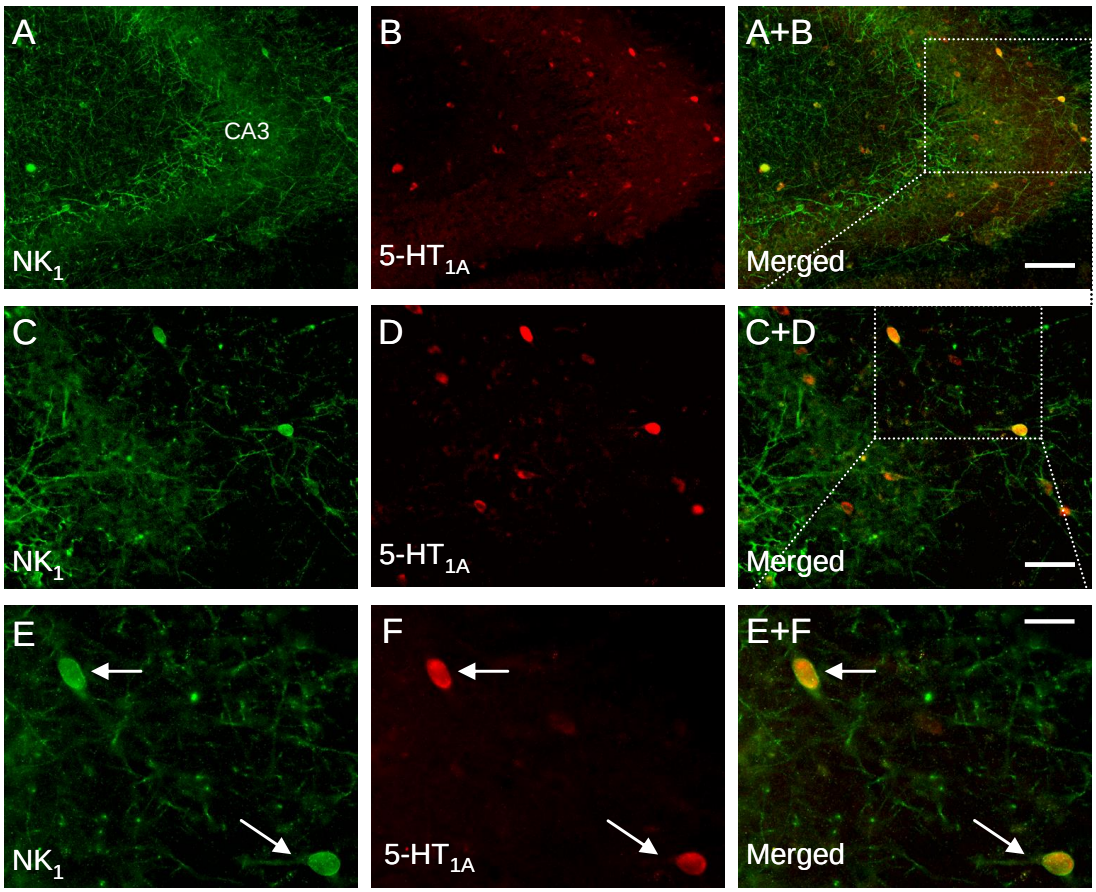


Fig. 2.6. Photomicrographs of NK_1 and 5-HT_{1A} receptor immunoreactivities in CA3 region of hippocampus. Lower magnification photomicrographs reveal extensive NK_1R-ir (A, C), but sparser 5-HT_{1A}R-ir (B, D). Higher magnification photographs of the square in C+D are shown in E, F and E+F. Cell colocalising both NK_1R-ir and 5-HT_{1A}R-ir are observed (arrowed in E, F and E+F). Scale bars in A+B: 125 μm; C+D: 60 μm: E+F: 30 μm.

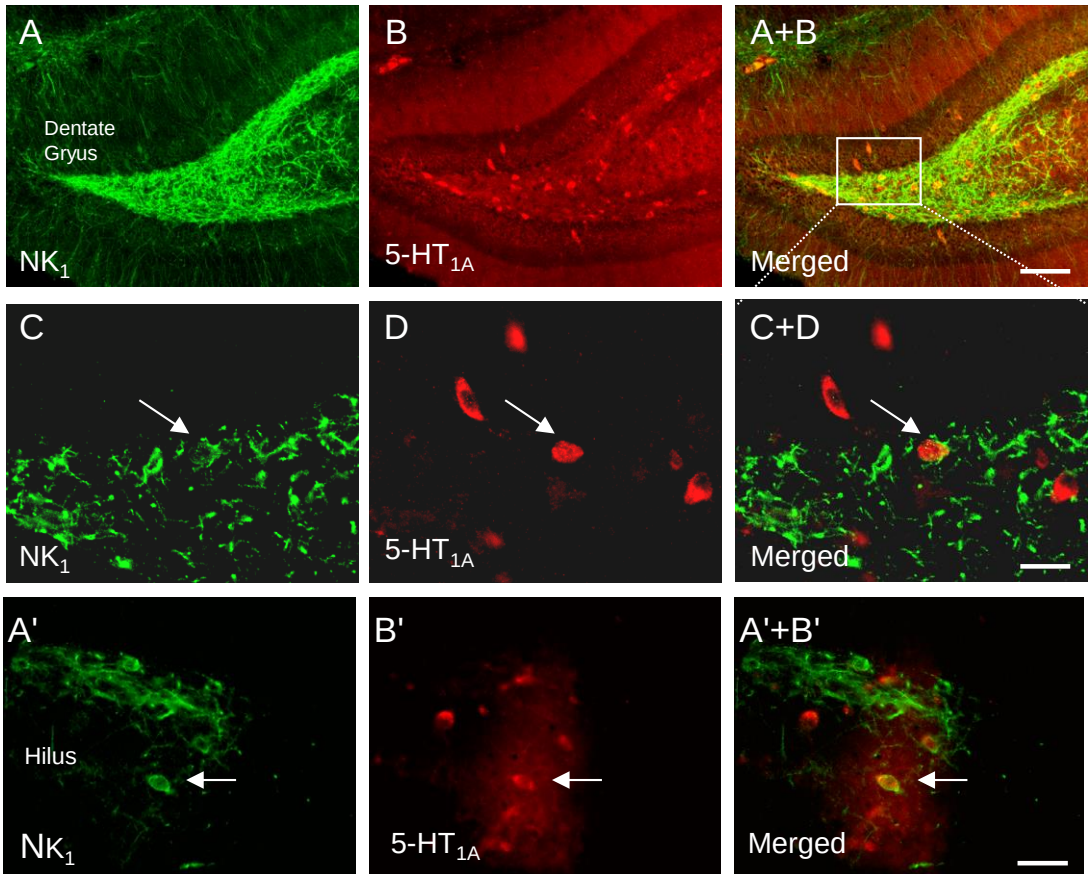


Fig. 2.7. Photomicrographs of NK_1 and 5-HT_{1A} receptor immunoreactivities in dentate gyrus of hippocampus. Lower magnification photomicrographs reveal extensive NK_1R-ir in fibres (A, C) and extensive 5-HT_{1A}R-ir in cell bodies (B, D). Higher magnification photographs of the square in A+B are shown in C, D and C+D. The cell arrowed reveals weak NK_1R-ir and strong 5-HT_{1A}R-ir (C+D). The hilus of the dentate gyrus reveals a cell colocalising NK_1R-ir and 5-HT_{1A}R-ir (arrow, A', B' and A'+B'). Scale bars in A+B: 120 μm; C+D: 30 μm: A'+B': 50 μm.

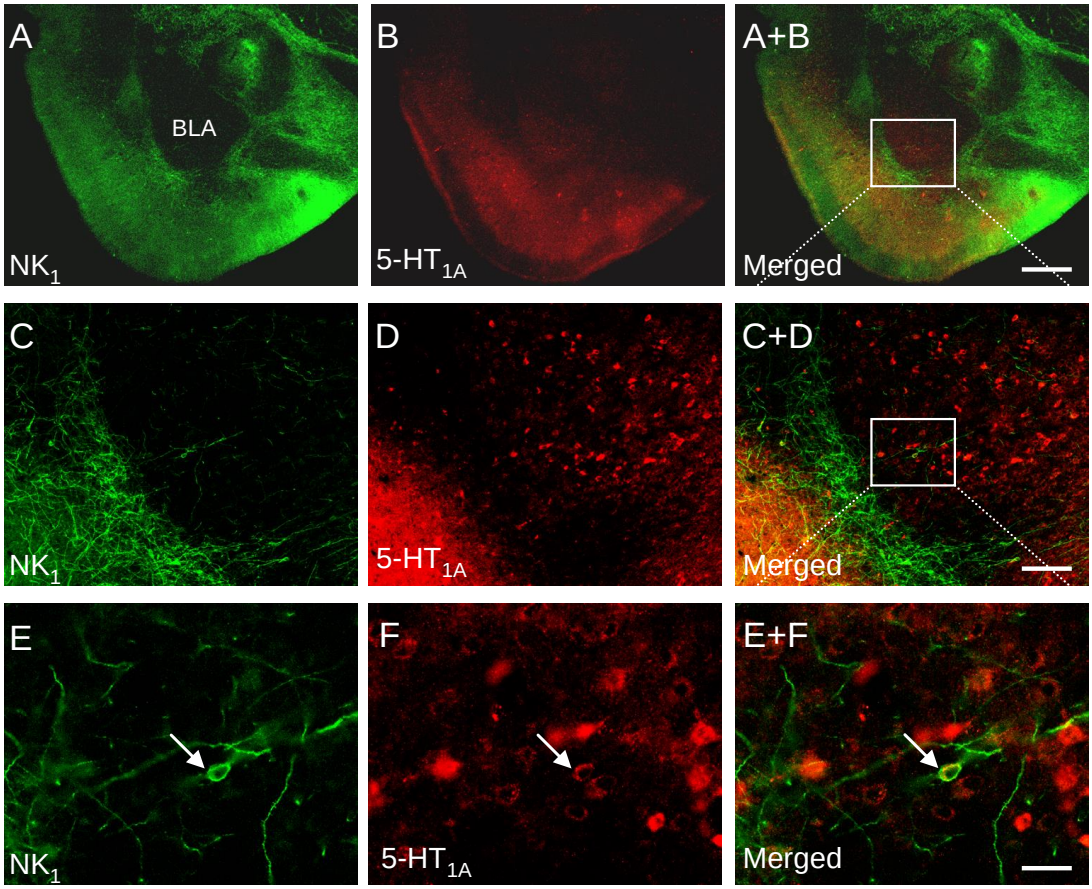


Fig. 2.8. Photomicrographs of NK_1 and 5-HT_{1A} receptor immunoreactivities in basolateral region of amygdala. Lower magnification photomicrographs reveal sparse NK_1R-ir (A, C) and extensive 5-HT_{1A}R-ir in cell bodies (B, D). Higher magnification photographs of the square in C+D are shown in E, F and E+F. A cell colocalising both NK_1R-ir and 5-HT_{1A}R-ir is observed (arrowed in E, F and E+F). Scale bars in A+B: 480 μm; C+D: 120 μm: E+F: 30 μm. BLA=lateral/basolateral amygdala.

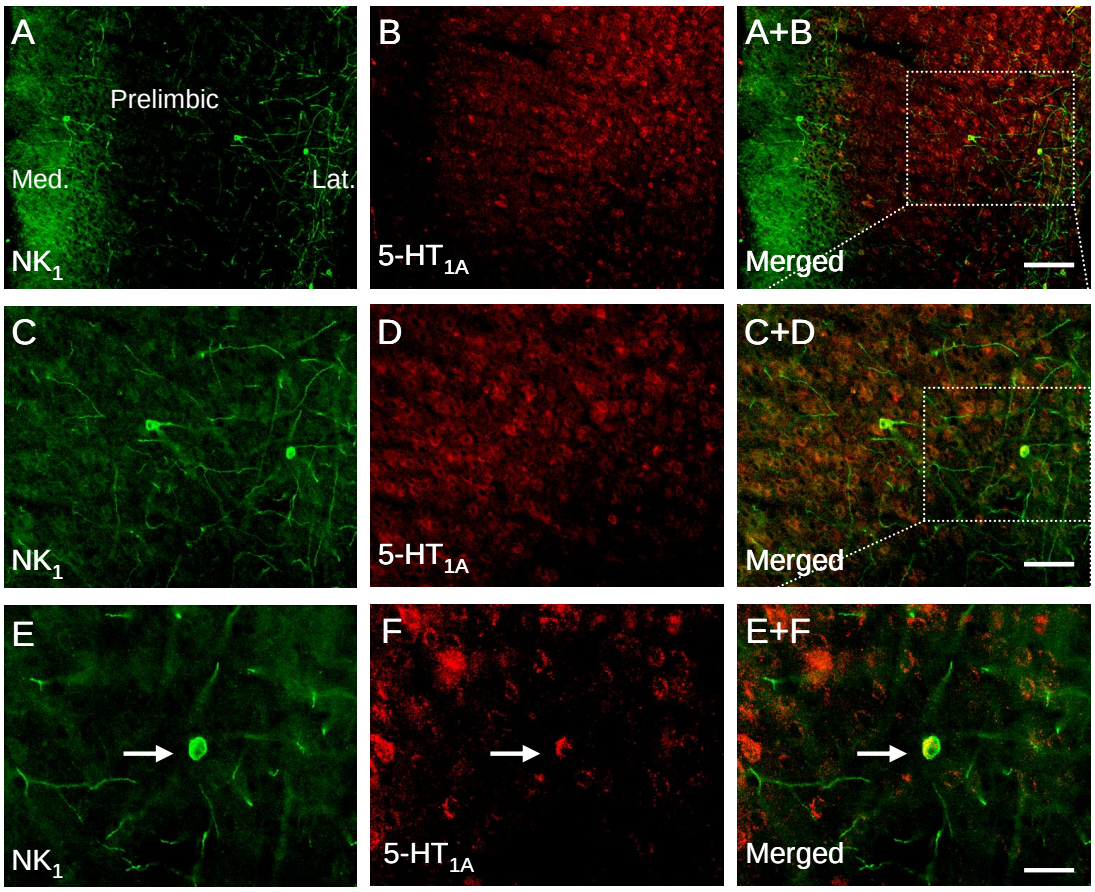


Fig. 2.9. Photomicrographs of NK_1 and 5-HT_{1A} receptor immunoreactivities in prelimbic region of prefrontal cortex (I). Lower magnification photomicrographs reveal sparse NK_1R-ir in cell bodies with extensive NK_1R-ir in fibres (A, C) and weak, but extensive 5-HT_{1A}R-ir in cell bodies (B, D). Higher magnification photographs of the square in C+D are shown in E, F and E+F. A cell colocalising both NK_1R-ir and 5-HT_{1A}R-ir is observed (arrowed in E, F and E+F). Scale bars in A+B: 120 μm; C+D: 60 μm: E+F: 30 μm.

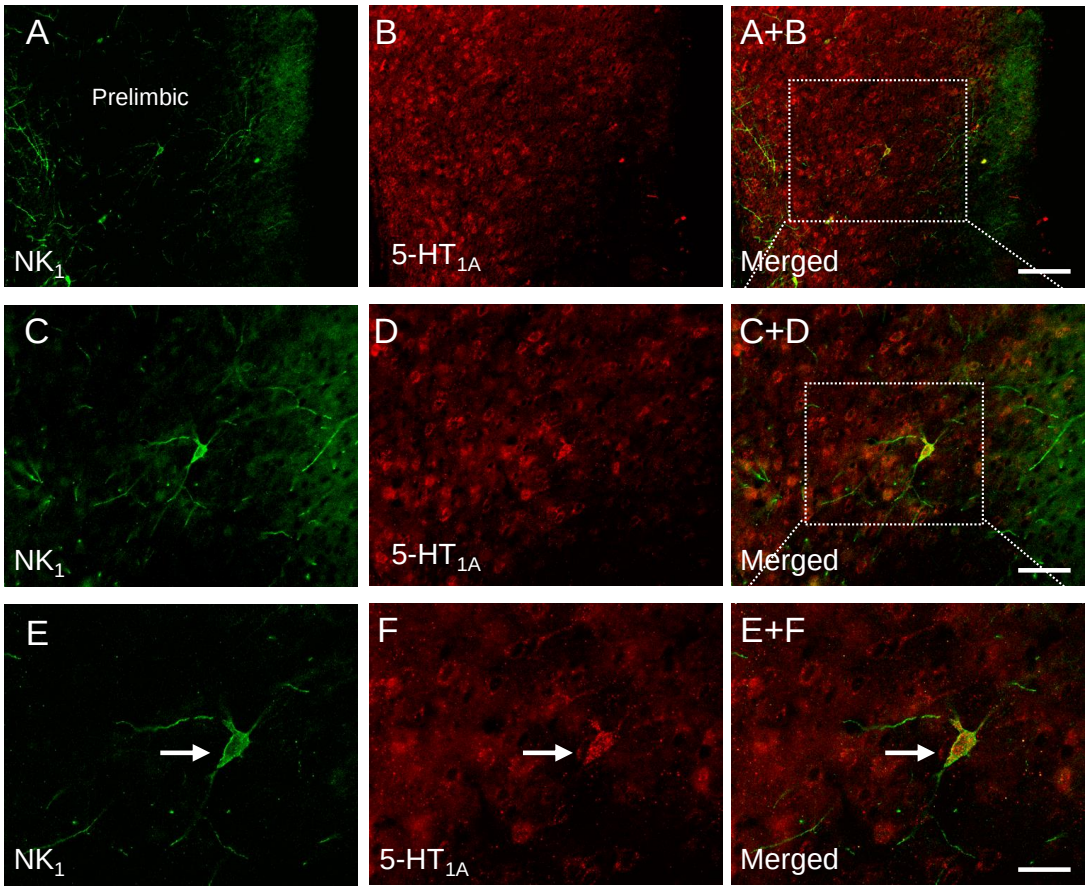


Fig. 2.10. Photomicrographs of NK_1 and 5-HT_{1A} receptor immunoreactivities in prelimbic region of prefrontal cortex (II). Lower magnification photomicrographs reveal sparse NK_1R-ir in cell bodies with extensive NK_1R-ir in fibres (A, C) and weak, but extensive 5-HT_{1A}R-ir in cell bodies (B, D). Higher magnification photographs of the square in C+D are shown in E, F and E+F. A cell colocalising both NK_1R-ir and 5-HT_{1A}R-ir is observed (arrowed in E, F and E+F). Scale bars in A+B: 120 μm; C+D: 60 μm: E+F: 30 μm.

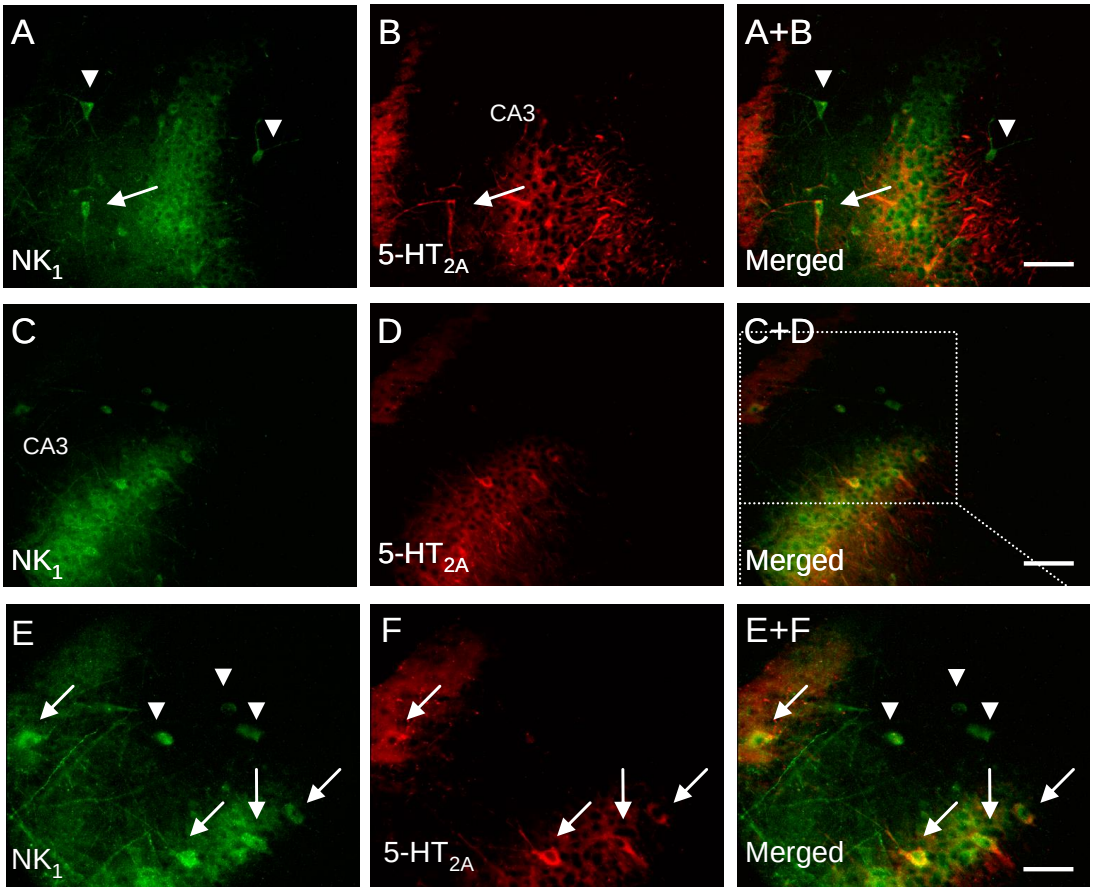


Fig. 2.11. Photomicrographs of NK_1 and 5-HT_{2A} receptor immunoreactivities in CA3 region of hippocampus. A lower magnification photomicrograph reveals NK_1R-ir in some cell bodies (A). A cell colocalising both NK_1R-ir and 5-HT_{2A}R-ir is observed (arrows in A, B and A+B) as well as cells with only NK_1R-ir (arrow heads in A, A+B). In another coronal section, higher magnification photomicrographs of the square in C+D are shown in E, F and E+F. Cell colocalising both NK_1R-ir and 5-HT_{2A}R-ir are again observed (arrowed in E, F and E+F). Cells with only NK_1R-ir are also observed (arrowheads in E and E+F). Scale bars in A+B: 80 μm; C+D: 80 μm; E+F: 50 μm.

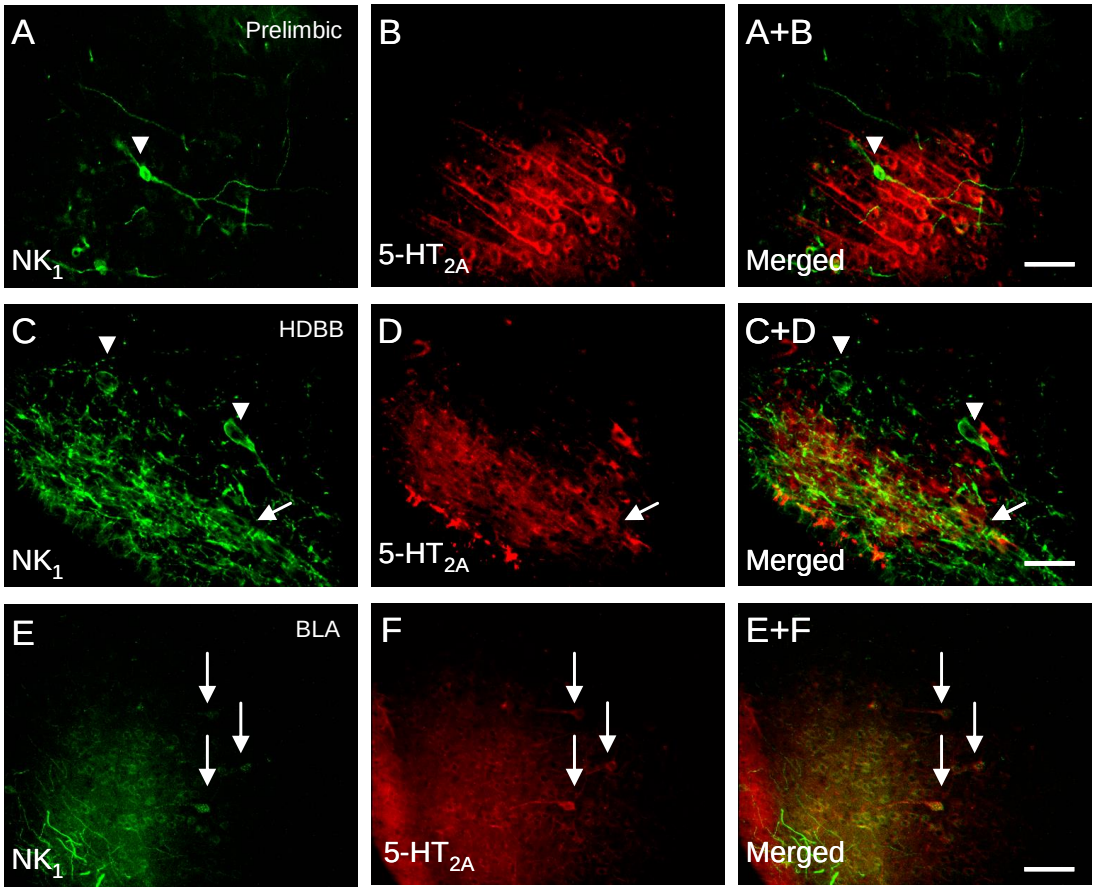


Fig. 2.12. Photomicrographs of NK_1 and 5-HT_{2A} receptor immunoreactivities in prelimbic cortex, horizontal diagonal band of Broca and basolateral amygdala. NK_1R-ir neurons are sparse in the prelimbic region (arrow head in A), while 5-HT_{2A}R-ir neurons are more frequently observed (B). The NK_1R-ir neuron in the prelimbic region does not colocalise 5-HT_{2A}R-ir (arrowhead in A+B). In the HDBB, neurons with only NK_1R-ir are also observed (arrowheads in C and C+D) together with an example of a neuron colocalising NK_1R-ir and 5-HT_{2A}R-ir (arrow in C, D and C+D). In the BLA, neurons colocalising NK_1R-ir and 5-HT_{2A}R-ir are observed (arrows in E, F and E+F). Scale bars in A+B: 50 μm ; C+D: 50 μm; E+F: 50 μm. BLA=basolateral amygdala; HDBB=horizontal diagonal band of Broca.

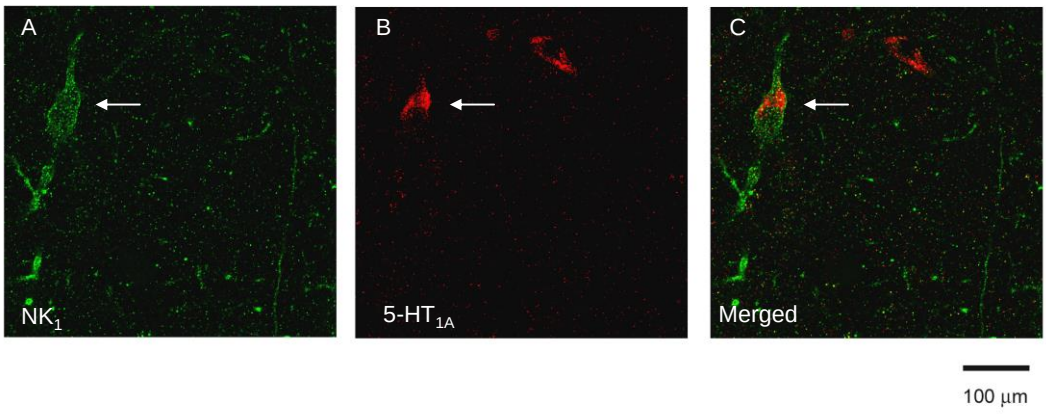


Fig. 2.13. Confocal photomicrographs of NK_1 and 5-HT_{1A} receptor immunoreactivities in CA3 region of the hippocampus. A cell with somatodendritic NK_1R-ir (A) is observed to display 5-HT_{1A}R-ir in the somatic cytoplasm (B). The merged microphotograph shows clearly that the NK_1R-ir and the 5-HT_{1A}R-ir are colocalised on the same cell. Scalebar: 100 µm.

2.4. DISCUSSION

Studies suggest that NK_1Rs interact with the raphe 5-HT system (Blier et al 2004; Commons et al 2003; Conley et al 2002; Lacoste et al 2006; Maubach et al 2002). However, NK_1R interactions with forebrain postsynaptic 5-HT receptors have not been previously investigated. NK_1Rs are found in brain regions that receive 5-HT innervations from the raphe, but it has not been clear whether NK_1Rs and 5-HT receptor subtypes colocalise onto the same cells. This may be important with regards to the antidepressant action of NK_1RAs. The aim of this chapter was therefore to investigate the degree of colocalisation between NK_1Rs and 5-HT_{1A}Rs as well as NK_1Rs and 5-HT_{2A}Rs in the rat forebrain.

The main findings in this chapter were: 1) NK_1R-ir and 5-HT_{1A}R-ir were colocalised to a high degree in many forebrain regions, in particular in the MS-DBB and hippocampus. Colocalisation was also present in PFC, frontal cortex and the BLA, but to a lesser degree. 2) NK_1R-ir was found to mostly colocalise with 5-HT_{2A}Rs in hippocampal subregions only. 3) The degree of colocalisation between NK_1R and 5-HT_{1A}Rs was much greater than the degree of colocalisation between NK_1R and 5-HT_{2A}Rs. The results suggest that 5-HT_{1A}Rs and NK_1Rs are expressed in a co-ordinated fashion within the rat forebrain and so they may act as common sites of action for NK_1RAs and 5-HT targeted antidepressants.

2.4.1. Colocalisation of NK_1 and 5-HT_{1A} receptors in rat forebrain

Extensive colocalisation between NK_1R-ir and 5-HT_{1A}R-ir was observed in many different brain regions as discussed in more detail below.

2.4.1.1. Septum

The highest degree of colocalisation (88%) was found between NK_1Rs and 5-HT_{1A}Rs in the MS-DBB. NK_1Rs in the MS-DBB complex are mostly found on cholinergic neurons (Chen et al 2001), while 5-HT_{1A}Rs are found on both PV-positive GABAergic cells (Aznar et al 2003) and cholinergic cells (Kia et al 1996a). NK_1Rs and 5-HT_{1A}Rs are thus likely to be colocalised on cholinergic cells within the MS-DBB. In contrast, although there was a high level of NK_1R-ir in the LS, very little colocalisation was found with 5-HT_{1A}Rs. Therefore, within the septum colocalisation between NK_1Rs and 5-HT_{1A}Rs was specific to the MS-DBB. The high degree of colocalisation between NK_1Rs and 5-HT_{1A}Rs suggests that SP and 5-HT share common cellular targets within the rat MS-DBB complex (also see Fig. 6.2 in chapter 6).

2.4.1.2. Hippocampus

Moderate to high levels of colocalisation between NK_1Rs and 5-HT_{1A}Rs were found in the hippocampus ranging from 65.1% in the DG to 62.5% in the CA3 and 32.4% in the CA1 regions, respectively. Within the hippocampus NK_1R-ir is found on GABAergic interneurons, but not on pyramidal cells (Acsady et al 1997; Freund and Buzsaki 1996; Sloviter et al 2001). In fact, CA3 axon collaterals have been shown to preferentially innervate the aspiny subgroup of NK_1R-ir interneurons in all hippocampal subregions (Wittner et al 2006). These include PV- and CCK-positive perisomatic (basket and chandelier), NPY-positive dendritic inhibitory cells and CR- and VIP-positive interneuron-specific interneurons (Acsady et al 1997; Sloviter et al 2001). However, the spiny NK_1R-ir and SOM-positive interneurons in CA1 are largely under the control of CA1 pyramidal cells instead (Blasco-Ibanez and Freund

1995). In contrast, 5-HT_{1A}Rs are located on both principal cells and CB and PV-containing neurons in the hippocampus (Aznar et al 2003; Gulyas et al 1999).

Thus, NK_1Rs and 5-HT_{1A}Rs are colocalised on GABAergic cells in the hippocampus representing a shared anatomical target for the SP and 5-HT systems.

2.4.1.3. Amygdala

The percentage of NK_1R-ir positive cells that colocalised with 5-HT_{1A}Rs was 34.5% in the BLA, indicative of an interaction between the two receptors in this brain region. NK_1Rs are found in the amygdala on subsets of GABAergic interneurons, in particular neurons containing NPY, CB and SOM, but not PV or CR (Levita et al 2003). In contrast, 5-HT_{1A}Rs are located on both principal cells and CB and PV-containing neurons in the amygdala (Aznar et al 2003). NK_1Rs and 5-HT_{1A}Rs are thus likely to be colocalised on GABAergic cells within the BLA.

2.4.1.4. Prefrontal cortex

The degree of colocalisation within the medial PFC between NK_1Rs and 5-HT_{1A}Rs was 31.1%. The medial PFC receives extensive 5-HT innervation from the raphe nuclei (Azmitia and Segal 1978) and is enriched with 5-HT_{1A}Rs (Amargos-Bosch et al 2004; Santana et al 2004). 5-HT_{1A}Rs are found on pyramidal cells and GABAergic interneurons (Aznar et al 2003), while NK_1Rs are found only on GABAergic neurons within the medial PFC (Kaneko et al 1994). NK_1Rs and 5-HT_{1A}Rs are thus likely to be colocalised on GABAergic cells within the medial PFC.

The immunofluorescence results above suggest that 5-HT_{1A}Rs and NK_1Rs are expressed in a co-ordinated fashion within a number of regions including the MS-DBB, hippocampus, amygdala and PFC. Based upon this finding, NK_1RAs and 5-HT targeted antidepressants may thus share a common anatomical site of action.

2.4.2. Colocalisation of NK_1 and 5-HT_{2A} receptors in rat forebrain

The degree of colocalisation between NK_1R and 5-HT_{2A}Rs was much smaller than the degree of colocalisation between NK_1Rs and 5-HT_{1A}Rs. NK_1R-ir was found to mostly colocalise with 5-HT_{2A}Rs in the hippocampus and to some extent in the amygdala.

2.4.2.1. Hippocampus

Colocalisation between NK_1R-ir and 5-HT_{2A}R-ir for hippocampal subregions was greatest in the CA3 region: DG (15.9%), CA1 (24.8%) and CA3 (43.1%). Many GABAergic neurons have been shown to display labeling for 5-HT_{2A}Rs (Luttgen et al 2004; Meltzer et al 2003). Interestingly, a recent study also showed 5-HT_{2A}R mRNA in 13–46% of GABAergic neurons of the monkey and human PFC (de Almeida and Mengod 2007). Similarly, 5-HT_{2A}Rs were found on a subpopulation of GABAergic neurons in the rat cortex (Willins et al 1997). Other studies have shown that 5-HT_{2A}Rs are found in a proportion of, but not all cells with GABAergic profiles within the hippocampus and other brain regions (Geurts et al 2002; Jakab and Goldman-Rakic 2000; Peddie et al 2008). Indeed, a recent study suggested that 5-HT_{2A}Rs are colocalised to both the dendrites of excitatory glutamatergic granule cells and inhibitory GABAergic interneurons (Peddie et al 2008). However, only 12% of 5-HT_{2A}R positive profiles within the DG were found to be GABAergic (Peddie et al 2008).

2.4.2.2. Amygdala

The degree of colocalisation in this chapter between NK_1R-ir and 5-$HT_{2A}R$-ir in the amygdala was 8.1%. Previous studies showed that most amygdala nuclei show low-moderate levels of 5-$HT_{2A}R$ binding and mRNA (Pazos and Palacios 1985; Pompeiano et al 1994; Wright et al 1995). Also, immunohistochemistry has revealed 5-$HT_{2A}Rs$ on the dendrites of pyramidal neurons and on mostly PV-positive interneurons in the BLA (Cornea-Hebert et al 1999; McDonald and Mascagni 2007; Morilak et al 1993; Xu and Pandey 2000). However, NK_1Rs in the amygdala are found on GABAergic interneurons, containing NPY, CB and SOM, but not PV or CR (Levita et al 2003). Thus, the small degree of colocalisation between NK_1Rs and 5-$HT_{2A}Rs$ is likely to be on GABAergic neuronal subsets.

2.4.3. Methodological issues

Methodological issues in this study concern whether the antibodies used were selective for their respective receptors and whether the distribution of immunofluorescent staining matched those of previous studies.

2.4.3.1. Specificity of the NK_1 receptor antibody

NK_1R-ir was detected throughout the rat forebrain regions studied (Fig. 2.2 to Fig. 2.10), similar to a previous study (Nakaya et al 1994). Polyclonal rabbit anti-NK_1R serum raised by immunising rabbits with C-terminal peptide fragments (e.g. amino acids 385-407) has been used to provide specific labelling for NK_1R-ir neurons in studies at both light microscopic and EM levels (Barbaresi 1998; Commons et al 2003; Commons and Valentino 2002; Halasz et al 2008; Lacoste et al 2006; Li et al 2000a; Liu et al 2002b; Myohanen et al 2008; Nakaya et al 1994; Shigemoto et al

1993; Wittner et al 2006). The antibodies have been characterised and their specificity reported (Ardelt et al 1996; Grady et al 1996; Kaneko et al 1994; Lacoste et al 2006; Mantyh et al 1996; Piggins et al 2001; Ribeiro-da-Silva and Hokfelt 2000; Shigemoto et al 1993; Yokota et al 1989). In pre-adsorption tests, excess of the fusion protein containing the NK_1R C-terminal completely blocked immunoreactivity (Piggins et al 2001; Shigemoto et al 1993), while in another study, polyclonal rabbit anti-NK_1R serum recognised a broad protein band on Western blots of membranes prepared from cells expressing NK_1R, but not from cells transfected with vector alone (Vigna et al 1994). In addition, antibody specificity has been tested by the processing of sections from NK_1R knockout mice (Lacoste et al 2006). Furthermore, control experiments in this chapter excluding the primary antibody for NK_1R, but including the secondary antibody, did not result in any labelling.

2.4.3.2. Specificity of the 5-HT_{1A} receptor antibody

Attempts to study the anatomical localisation of 5-HT_{1A}Rs in the brain have included the use of *in situ* hybridisation for mRNA, selective radioligands for receptor binding and selective antibodies for receptor protein. However, different techniques yield slightly different results due to technical reasons. For example, the binding of the radioligand agonist [^{3}H]8-OH-DPAT is limited to the pool of receptors coupled to G proteins. In addition, although selective antibodies to different epitopes of the 5-HT_{1A}R yield labelling in similar cellular populations, the cellular distribution of staining does vary depending upon the antibody used (Anthony and Azmitia 1997).

Commonly used polyclonal antibodies to the rat 5-HT_{1A}R either target extracellular or intracellular epitopes. The specificity of the guinea-pig polyclonal antibody used in

this chapter has been confirmed when preabsorption of 5-HT_{1A}R antiserum with immunogen peptide (10^{-5} M) corresponding to amino acids 248–262 located within the third intracellular loop of the rat 5-HT_{1A}R and the hapten thyroglobulin (0.5 mg/μl undiluted antiserum) resulted in marked reduction in immunostaining (Collin et al 2002; Luttgen et al 2005). The pattern of immunohistochemical staining found in this chapter was similar to those found in other studies when using the same antibody in the hippocampus, DRN, cortex, hypothalamus and septum (Collin et al 2002; Luttgen et al 2005; Ou et al 2003). As in the other studies, 5-HT_{1A}R-ir was predominantly seen in cell soma and occasionally also seen in dendrites.

Within the DG only very faint 5-HT_{1A}R-ir was seen within the granule cell layer, with more prominent immunoreactivity in hilar regions. Similarly, Kia et al. (1996) used a rabbit antibody to the third intracellular loop of the rat 5-HT_{1A}R (amino acids 243-268) and found that cell body staining was restricted to the hilus, with dendritic staining in the molecular layer of the DG (Kia et al 1996c). These results were consistent with those of Gerard et al. (1994) who used an antibody raised to the entire third intracellular loop of the rat 5-HT_{1A}R (Gerard et al 1994). Interestingly, immunohistochemistry with the same antibody used in this chapter did not result in staining of granule cells in the gerbil either (Kim et al 2007).

The above results in the DG do not however concur with the findings of other studies. For example, a colocalisation study using a polyclonal rabbit antibody to the third intracellular loop (amino acids 258-274) revealed that most of the 5-HT_{1A}R-ir positive cells in the hippocampus and cortex were principal cells (Aznar et al 2003). Nevertheless, colocalisation with GABA-ergic cells was also observed in these

regions, especially with CB positive cells in the hippocampus. Here, these cells were located mostly in the stratum radiatum and in the inner side of the granule cell layer, while PV positive cells were located close to the pyramidal and granule cell layers (Aznar et al 2003). In another study that used antibody raised against the second extracellular loop of the 5-HT_{1A}R (amino acids 170-186), the immunoreactivity within the granule cell layer and the hilus was equally prominent (Patel et al 1996). This latter antibody also revealed 5-HT_{1A}R-ir in glial cells throughout the CNS (Azmitia et al 1992; Whitaker-Azmitia et al 1993). Furthermore, early autoradiographic studies also revealed 5-HT_{1A}R binding in pyramidal and granular cells within the hippocampus (Pompeiano et al 1992). Similarly, 5-HT_{1A}R mRNA was also found in high levels in the perikarya of both pyramidal and granule cells (Miquel et al 1992; Wright et al 1995).

Similar discrepancies were also found in other brain regions including the PFC and LS. Colocalisation of NK_1Rs in the PFC with 5-HT_{1A}Rs in this chapter as detected with the guinea-pig polyclonal antibody to the third intracellular loop of the rat 5-HT_{1A}R (amino acids 248-262) must be detecting 5-HT_{1A}R-ir on GABA-ergic cells. This is because, NK_1Rs in the PFC are only found on GABA-ergic cells. An *in situ* hybridisation study also clearly showed 5-HT_{1A}R mRNA on GABA-ergic interneurons (Santana et al 2004). These results however, do not tally with the results found with the rabbit polyclonal antibody which recognises epitopes of the second extracellular loop of the rat 5-HT_{1A}R (amino acids 170-186) (Anthony and Azmitia 1997; Azmitia et al 1992). This antibody mostly labels the short, thin, smooth and mostly vertically oriented fragments of cortical neurons in the PFC, with the density being prominent in the layers II/III and V/VI. Lower densities of staining were also

observed on the periphery and cytoplasm of cell bodies of glutamatergic neurons (Czyrak et al 2003). In the LS brain region, only weak immunostaining of 5-HT_{1A}R was found in LS neurons, in concordance with a previous study that utilised the same guinea-pig polyclonal antibody (Luttgen et al 2005). However, Kia et al. (1996) reported strong somatodendritic staining in this region (Kia et al 1996c), while other investigators have also detected strong 5-HT_{1A}R mRNA (Chalmers and Watson 1991; Luttgen et al 2005; Pompeiano et al 1992; Wright et al 1995) and ^{3}H-8-OH-DPAT binding (Chalmers and Watson 1991; Pompeiano et al 1992) within the LS.

Different staining patterns from the use of different antibodies may be related to differences in the epitopes recognised by the antibodies. For example, it may be that the antibody recognising the binding site of the 5-HT_{1A}R (amino acids 170-186) will mostly only allow for the visualisation of functionally active membrane-bound receptors, and less likely to allow for the visualisation of cytoplasmic receptors that may be in the process of synthesis or degradation (Anthony and Azmitia 1997; Azmitia et al 1992; Czyrak et al 2003). Thus, the choice of different antigenic epitopes can result in minor variations in immunohistochemical staining.

As NK_1Rs are known to be only found on GABA-ergic neurons within the rat hippocampus and PFC in particular, then the above discrepancies do not have a bearing on the results of this chapter.

2.4.3.3. Specificity of the 5-HT_{2A} receptor antibody

As with 5-HT_{1A}Rs, a number of different techniques have been used to localise 5-HT_{2A}Rs in the brain. Some of these include *in situ* hybridisation (Amargos-Bosch et

al 2004; Burnet et al 1995; Mengod et al 1990; Pompeiano et al 1994), autoradiography (Fischette et al 1987; Lopez-Gimenez et al 1997; Pazos et al 1985; Pazos et al 1987) and immunohistochemistry. With the latter technique, both polyclonal and monoclonal antibodies have been previously employed.

The antibody used in this chapter was a monoclonal antibody (Wu et al 1998) as opposed to polyclonal antibodies used in some other studies (Berry et al 1996; Maeshima et al 1998b; Miner et al 2003; Morilak et al 1993; Nocjar et al 2002). This commercially purchased antibody was a monoclonal mouse antiserum generated against a recombinant hybridoma fusion protein between glutathione *S*-transferase (GST) and the first extracellular domain of the human 5-HT_{2A}R (amino acids 1–72 of the amino terminus; #556326, BD PharMingen, BD Biosciences, Cowley, UK). The hybridomas were screened by PharMingen using an enzyme-linked immunosorbent assay, immunocytochemistry of frozen rat brain sections, and Western blot analysis: the 5-HT_{2A}R antibody recognised the receptor as a 55-kDa band. The specificity of the band was verified by competition with a 5-HT_{2A}R fusion protein and lack of competition with an irrelevant fusion protein. The supernatant was also tested against GST protein to rule out reactivity to this part of the immunogen. The antibody was purified from hybridoma culture supernatant by protein G affinity chromatography. In addition, the antibody has specifically been shown to react with human, monkey, and rat 5-HT_{2A}R (Jakab and Goldman-Rakic 1998). Other investigators confirmed the specificity of the antibody by Western blot analysis of rat brain membranes, human brain and transfected NIH 3T3 cell lysates, and immunofluorescence of rat Schwann cells in culture (Wu et al 1998; Xu and Pandey 2000). The antisera utilised has been characterised and applied in brain tissues, with specificity of labelling demonstrated in

many different studies (Cornea-Hebert et al 1999; Doherty and Pickel 2000; Garlow et al 1993; Jakab and Goldman-Rakic 1998; Jakab and Goldman-Rakic 2000; Jansson et al 2001; Jansson et al 1998; Luttgen et al 2004; Martin-Ruiz et al 2001; McDonald and Mascagni 2007; Miner et al 2003; Willins et al 1999; Wu et al 1998; Xu and Pandey 2000).

The cellular distribution of 5-HT_{2A}R-ir in this chapter using the monoclonal mouse antiserum to 5-HT_{2A}Rs showed a predominantly somatodendritic neuronal localisation as described in previous studies. However, axonal staining and glial localisation has also been seen with this antibody in another study in the VTA (Doherty and Pickel 2000). As in a previous study, 5-HT_{2A}R-ir was detected in cell bodies within the MS-DBB, cells located in the pyramidal cell layers CA1-3 of the hippocampus and in the granular cell layer of the DG as well as hippocampal interneurons (Luttgen et al 2004). 5-HT_{2A}R-ir was also observed in the BLA in cell bodies and some neuronal fibres as seen before (Xu and Pandey 2000). Within the cerebral cortex, 5-HT_{2A}R was highly expressed with particular staining of cell bodies and apical dendrites of pyramidal neurons (Wu et al 1998), similar to the pattern found with *in situ* hybridisation (Amargos-Bosch et al 2004).

Martin-Ruiz et al. (2001) compared the staining patterns of a rabbit polyclonal 5-HT_{2A}R antibody generated against amino acids 22-41 in the N-terminus (Berry et al 1996) with that of a commercially available monoclonal antibody and found similar results in the PFC (Martin-Ruiz et al 2001). Nocjar et al. (2002) carried out a similar comparison in the midbrain between the above antibodies and found them to label identical cells (Nocjar et al 2002). They did however find minor differences in the

cellular distribution of the labelling. The monoclonal PharMingen antibody only resulted in intracellular labelling, while the polyclonal antibody also labelled the plasma membrane (Nocjar et al 2002). Similarly, Miner et al. (2003) compared the ultrastructural labelling of the monoclonal PharMingen antibody with a rabbit polyclonal antibody raised against amino acids 428-443 of the rat carboxyl-terminus and found the latter antibody to reveal more extensive immunoreactivity including spinal processes on pyramidal cells within the PFC (Miner et al 2003). Nocjar et al. (2002) have suggested that these differences are likely to be due to variations in the molecular species detected by the various antisera (Nocjar et al 2002).

As the purpose of the experiments in this chapter was to examine for cellular colocalisation between receptors, the prominent somatodendritic labelling achieved with the PharMingen monoclonal antibody for 5-HT_{2A}Rs did allow for the successful quantitation of receptor colocalisation at the light microscopic level.

2.4.3.4. Other technical considerations

The degree of NK_1R-ir/5-HT_{1A}R-ir and NK_1R-ir/5-HT_{2A}R-ir colocalisation found in the present study is assumed to be representative of the colocalisation throughout the rostro-caudal axis of each brain region. However, for practical purposes brain regions at specific levels from bregma were examined. Therefore, only detailed analysis would fully confirm the exact degree of receptor colocalisation at each rostro-caudal level for each brain region. Also, as NK_1R-positive neurons were sparse in many of the regions examined except for the septum, cells had to be counted within whole anatomical areas rather than in a standard square. This means that although one can

compare the percentages across regions, these are not amenable to statistical tests, because the areas measured were not comparable.

Also, as epifluorescence light microscopy and not laser confocal microscopy was used for quantification, there was a risk of over-counting of colocalised cells. However, cells were not counted in adjacent sections. Also, colocalisation was determined by observing cells through all the focal planes at 40 x magnification to ensure cells were not simply superimposed. In addition, the same observer did all of the counting throughout the study. Nevertheless, laser confocal microscopy was used to confirm cellular colocalisation between NK_1R-ir and 5-HT_{1A}R-ir in at least one brain region: hippocampal CA3 (see Fig. 2.13).

2.4.4. Functional effects of NK_1 and 5-HT_{1A} receptor colocalisation

Evidence from behavioural and electrophysiological studies after local applications of 5-HT_{1A}R agonists or NK_1RAs at specific brain sites are described below.

2.4.4.1. Septum

Local application of 5-HT_{1A}R agonists such as 8-OH-DPAT in the septum shows anti-depressive effects in the learned helplessness model of depression (Martin et al 1991) as well as in the FST (Schreiber and De Vry 1993). In addition, pretreatment with the 5-HT_{1A}R partial agonist ipsapirone attenuated the anti-immobility effects of 8-OH-DPAT when both compounds were given into the LS, but not when given into the DRN, suggesting a predominant role for postsynaptic 5-HT_{1A}Rs (Schreiber and De Vry 1993). Septal injections of 8-OH-DPAT also increased maternal aggression (De Almeida and Lucion 1997) and influenced anxiety (De Almeida et al 1998; Menard

and Treit 1998; Micheau and Van Marrewijk 1999). However, the results of studies on anxiety have been mixed. One study reported intraseptal injections of 8-OH-DPAT were anxiogenic on EPM in mice (Micheau and Van Marrewijk 1999). A similar effect was seen in female rats (De Almeida et al 1998), but in male rats anxiolysis was seen in the shock-probe burying test (Menard and Treit 1998). Thus, 5-HT_{1A}R agonism in the septum may have anxiolytic and antidepressive effects.

Studies of local injections of SP and NK_1RAs in the septum are very limited. For example, SP applied to cultured cholinergic neurons of basal forebrain resulted in cellular excitation (Bajic et al 2002; Yamaguchi et al 1990), while infusion of NK_1RA, compound A into the LS reduced immobility time on the FST (Ebner and Singewald 2006). It is possible that some of the drug may have diffused into the MS-DBB, having its behavioural effect via this region. However, studies with direct local injections of an NK_1RA into the MS-DBB have yet to be carried out.

Thus, separate studies suggest that both 5-HT_{1A}R agonists and NK_1RAs may in some circumstances show anti-depressive effects when applied into septal regions.

2.4.4.2. Hippocampus

5-HT_{1A}Rs are found in high densities in the hippocampus (Khawaja 1995; Raurich et al 1999), and their responsiveness is enhanced by tricyclic antidepressants and electroconvulsive shock therapy, accounting for the therapeutic effect of these treatments (Chaput et al 1991; de Montigny 1984). Similarly, the selective noradrenaline reuptake inhibitor, reboxetine increases the tonic activation of 5-HT_{1A}Rs in the hippocampus (Invernizzi and Garattini 2004; Szabo and Blier 2001a).

More selective 5-HT_{1A}R agonists such as 8-OH-DPAT and buspirone inhibit hippocampal unit activity and mimic the inhibitory effects of 5-HT (Martin and Mason 1987; Rowan and Anwyl 1986). Also, these 5-HT_{1A}R agonists were anxiolytic on the EPM and the open-field test when injected into the hippocampus (Kostowski et al 1989; Stefanski et al 1993). In addition, infusions of the 5-HT_{1A}R antagonist NAN-190 into dorsal hippocampus blocked the anti-conflict effect of systemic ipsapirone, suggesting that post-synaptic 5-HT_{1A}R activation at this site may be critical to the anxiolytic effects of 5-HT_{1A}R agonists (Przegalinski et al 1994). Furthermore, 5-HT_{1A}R null mice were insensitive to neurogenesis and behavioural effects of fluoxetine (Santarelli et al 2003).

In contrast, early work in rat hippocampal slices showed SP to excite CA1 hippocampal interneurons (Dreifuss and Raggenbass 1986; Teixeira et al 1996). SP by acting on the somatodendritic membranes increases the excitability of CA1 GABAergic interneurons via the suppression of a resting K^+ conductance. This was suppressed by the NK_1RA, SR140,333. By acting on interneurons, SP may therefore indirectly inhibit the activity of CA1 pyramidal neurons (Ogier and Raggenbass 2003). More recent experiments investigating the effects of SP and the NK_1RA (L-822,429) on hippocampal CA3 pyramidal neurons using direct microiontophoretic applications *in vivo*, showed SP to produce either a decrease in activity or a rapid decrease followed by an excitation. However, in NK_1R knockout mice, the most prevalent response was excitatory (Gobbi and Blier 2005). At low ejection currents, L-822,429 was able to only block the inhibitory response produced by SP. The excitatory response was blocked by an NK_2R antagonist. Thus, in mouse

hippocampus, NK_1Rs mediate the inhibitory responses to SP, and NK_2Rs mediate the excitatory responses (Gobbi and Blier 2005).

Thus, 5-HT_{1A}R agonists have inhibitory actions on hippocampal neurons, while SP leads to cellular excitation blocked by NK_1RAs. In addition, long-term treatment with the NK_1RA CP-96,345 enhanced the tonic activation of postsynaptic 5-HT_{1A}Rs (Haddjeri and Blier 2001) as seen with other antidepressants (Haddjeri et al 1998).

2.4.4.3. Amygdala

5-HT_{1A}Rs are present in the BLA (Wright et al 1995), and maternal separation stress in rats can alter their levels (Vicentic et al 2006). Also, 5-HT depresses excitatory transmission and depolarisation-evoked Ca^{2+} influx in the BLA via 5-HT_{1A}Rs (Cheng et al 1998). Indeed, 8-OH-DPAT inhibited the firing rate of the neurons in the BLA, while the inhibitory actions of 5-HT on BLA neurons was prevented by 5-HT_{1A}R antagonist co-application (Stein et al 2000; Wang et al 1999). In addition, local BLA injections of the selective 5-HT_{1A}R agonist flesinoxan decreased expression of conditioned fear (Li et al 2006), while 8-OH-DPAT was anxiolytic in the elevated T-maze (Zangrossi et al 1999). In contrast, SP stimulated inhibitory synaptic transmission in the guinea pig BLA *in vitro* (Maubach et al 2001). Also, SP in the BLA had anxiogenic effects on the EPM (Teixeira et al 1996), while NK_1RA, L-760,735 in the amygdala inhibited neonatal vocalisation in guinea-pigs (Boyce et al 2001). Thus, 5-HT_{1A}R agonists in the BLA result in anxiolysis and neuronal inhibition, while NK_1R antagonism in the amygadala also results in anxiolysis.

2.4.4.4. Prefrontal cortex

Electrophysiological studies have shown that 5-HT_{1A}Rs mediate the hyperpolarising action of 5-HT on prefrontal neurons *in vitro* (Aghajanian and Marek 1997; Zhou and Hablitz 1999) and *in vivo* (Amargos-Bosch et al 2004; Hajos et al 1999; Hajos et al 1998). In addition, direct application of 8-OH-DPAT into the medial PFC inhibited neuronal firing (Araneda and Andrade 1991; Ashby et al 1994; Borsini et al 1995; Cai et al 2002). This action was reversed by the 5-HT_{1A}R antagonist WAY 100635 (Cai et al 2002; Casanovas et al 1999; Hajos et al 2003a; Tanaka and North 1993). In contrast, SP excites cortical neurons (Albus et al 1992; Lamour et al 1983; Phillis and Limacher 1974). Therefore, 5-HT_{1A}R agonism is inhibitory, while NK_1R agonism is excitatory in the cortex.

Thus, both 5-HT_{1A}R agonists and NK_1RAs may have anti-depressive effects when applied into the septum or amygdala. In addition, 5-HT_{1A}R agonists have inhibitory actions on neurons in the hippocampus, amygdala and cortex. In contrast, SP is excitatory in these brain regions, and this excitation is blocked by NK_1RAs in the hippocampus.

2.4.5. Functional effects of NK_1 and 5-HT_{2A} receptor colocalisation

Infusion of the non-selective 5-HT_2R agonist mCPP into dorsal hippocampus decreased social interaction in the rat (Whitton and Curzon 1990). Also, the antidepressant efficacy of drugs with 5-HT_{2A}R antagonist properties (e.g. mirtazapine) suggests that 5-HT_{2A}Rs may serve to promote anxiety (Millan 2003). However, data on the effects of 5-HT_{2A}R stimulation upon neuronal circuitry appears contradictory. Several studies showed excitation (Beique et al 2004; Rahman and Neuman 1993),

whereas others showed inhibition (Piguet and Galvan 1994; Shen and Andrade 1998) or biphasic facilitatory-inhibitory actions (Arvanov et al 1999a; Arvanov et al 1999b; Zhou and Hablitz 1999). Indeed, recent ultrastructural evidence from DG supports such contrasting roles, as demonstrated by the localisation of 5-HT_{2A}Rs to both the dendrites of excitatory glutamatergic granule cells and inhibitory GABAergic interneurons (Peddie et al 2008). However, within the hippocampus NK_1R-ir is only found on GABAergic cells (Sloviter et al 2001). Therefore, the colocalisation of NK_1Rs and 5-HT_{2A}Rs in the hippocampus must occur on GABAergic cells, and this may be the pathway by which NK_1R blockade may lead to antidepressant action.

5-HT_{2A}Rs may also serve to promote anxiety in the amygdala. In fact, infusion of methysergide, a 5-HT_2R antagonist, into the BLA produced anti-conflict effects (Hodges et al 1987). Within the BLA, acute 5-HT release activated GABA interneurons, via 5-HT_2Rs, and increased inhibitory synaptic events in projection neurons (Rainnie 1999). As with 5-HT_{2A}Rs, SP was anxiogenic in the BLA (Teixeira et al 1996), acting via NK_1Rs on GABA interneurons (Levita et al 2003). Thus blockade of 5-HT_2Rs and NK_1Rs in the BLA may result in anxiolytic and antidepressant actions partly via shared GABA interneuron targets.

2.5. CONCLUSIONS

In conclusion the present study found significant degrees of colocalisation between NK_1Rs and 5-HT_{1A}Rs in the rat forebrain. In addition, there was a more region specific colocalisation between NK_1Rs and 5-HT_{2A}Rs. The NK_1R and 5-HT_{1A}R colocalisation was prominent in forebrain regions involved in the modulation of stress and affect, especially the septo-hippocampal system. Also except for the MS-DBB where NK_1Rs and 5-HT_{1A}Rs are most likely colocalised on cholinergic neurons, in other regions NK_1Rs and 5-HT_{1A}Rs are likely to be colocalised on GABAergic neurons. Interestingly, functional studies suggest that 5-HT_{1A}R agonism is inhibitory, but that NK_1R agonism with SP is excitatory and that this excitation can be blocked by NK_1RAs. Thus, NK_1RAs and 5-HT targeted antidepressant may share common sites of action within the forebrain.

CHAPTER 3

INVESTIGATION OF NK_1 RECEPTORS ON AFFERENT PROJECTIONS TO DORSAL RAPHE NUCLEUS

3.1. INTRODUCTION

Pre-clinical studies suggest NK_1RAs may have antidepressant actions, via an influence on the DRN 5-HT system. Indeed, SP colocalised with 5-HT neurons in raphe nuclei of monkey (Charara and Parent 1998) and human (Sergeyev et al 1999) species, but to a lesser extent in the rat (Hokfelt et al 1978). Nevertheless, SP fibres and terminals were present in the rat DRN (Cuello and Kanazawa 1978; Ljungdahl et al 1978a). Also, DRN 5-HT neurons of NK_1R knockout mice exhibited altered firing rates (Santarelli et al 2002), while acute systemic NK_1RAs increased DRN neuronal activity in mice and guinea-pigs (Froger et al 2001; Haddjeri and Blier 2001). Furthermore, NK_1R-ir colocalised with glutamate in rostral DRN (Commons and Valentino 2002) and with 5-HT neurons in caudal DRN in rat and mouse (Lacoste et al 2006). Indeed, neurokinins excited DRN 5-HT neurons indirectly via local glutamatergic inputs (Liu et al 2002), resulting in 5-HT release and subsequent autoinhibition via 5-HT_{1A}Rs (Valentino et al 2003; Valentino and Commons 2005).

NK_1Rs may also influence regions postsynaptic or presynaptic to the DRN. Indeed, in chapter 2, NK_1Rs and 5-HT_{1A}Rs colocalised in many postsynaptic forebrain regions in the rat. However, it is not known if NK_1Rs interact with the 5-HT system at the presynaptic level, i.e. on neurons that project to the DRN.

3.1.1. Major afferent projections of dorsal raphe nucleus

Raphe neurons are controlled by a number of afferent pathways, investigated mostly using anterograde and retrograde tracers (Buchanan et al 1994; Peyron et al 1998). Indeed, other raphe nuclei are a large source of afferents to the DRN (Aghajanian and Wang 1977), but other incoming projections include the PFC, LHb and LC (Baraban and Aghajanian 1981; Peyron et al 1996; Sakai et al 1977a; Verge et al 1986).

3.1.1.1. Prefrontal cortex

The frontal cortex has extensive projections to the DRN (Buchanan et al 1994; Jankowski and Sesack 2004; Lee et al 2003; Peyron et al 1998; Sesack et al 1989; Vertes 2004), with the majority of afferent projections arising from the medial PFC (Hajos et al 1998; Peyron et al 1998; Vertes 2004). These afferent neurons are largely glutamatergic as shown by combined retrograde tracing and glutamate immunohistochemistry (Lee et al 2003), and mostly synapse onto GABA neurons in the DRN (Jankowski and Sesack 2004; Varga et al 2003). Imaging studies have indeed found disturbances in the PFC in depression (Coffey et al 1993; Drevets 2000).

3.1.1.2. Lateral habenula

The habenula complex, is an epithalamic structure that links forebrain and midbrain/hindbrain areas (Lecourtier and Kelly 2007) and regulates ascending monoamine pathways including those of 5-HT (Concha and Wilson 2001). It is implicated in reward, social behaviours, pain (Klemm 2004), depression and schizophrenia (Shepard et al 2006; Shumake and Gonzalez-Lima 2003; Sutherland 1982).

The habenula complex consists of medial and lateral components, with largely non-overlapping connections and distinct functions. In the rat, the MHb receives inputs from the septum and sends a projection to the IPN. The MHb contains cholinergic (Eckenrode et al 1987) and SP neurons (Cuello et al 1978; Hokfelt et al 1975). On the other hand, the LHb consists of a medial subdivision with limbic afferents from the post-commissural septum and entopeduncular nucleus (EPN) (Herkenham and Nauta 1977; Herkenham and Nauta 1979; Li et al 1993), and a lateral subdivision with pallidal afferents. The LHb is mostly composed of glutamatergic neurons (Kiss et al 2002) with some GABAergic neurons (Contestabile et al 1987; Vincent et al 1980).

Efferents from LHb project to the midbrain (Aghajanian and Wang 1977; Araki et al 1988; Behzadi et al 1990; Conley et al 2002; Ferraro et al 1996; Herkenham and Nauta 1979; Kalen et al 1985; Matsuda and Fujimura 1992; Morris et al 1999; Nishikawa and Scatton 1985; Stern et al 1979; Varga et al 2003; Wang and Aghajanian 1977). Indeed, retrograde tracing with horseradish peroxidase (HRP) showed dense projections from the LHb to DRN (Aghajanian and Wang 1977). Thus, alterations in the LHb nucleus may contribute to depression (Sartorius and Henn 2007). Indeed, LHb neurons were strongly activated by stress e.g. immobilisation (Chastrette et al 1991; Wirtshafter et al 1994) or food deprivation (Timofeeva and Richard 2001). In addition, regional cerebral blood flow (rCBF) in the habenula was elevated in several rat models of depression (Caldecott-Hazard et al 1988), with similar increases in habenula metabolism (Shumake et al 2004; Shumake et al 2003; Thornton et al 1985). In contrast, habenula lesions improved the behavioural response of depressed rats (Yang et al 2008) and prevented learned helplessness (Amat et al 2001). Furthermore, in a tryptophan depletion study, Morris et al. examined 5-HT

responders with a history of depression and found rCBF was increased in the habenula, correlating negatively with plasma tryptophan levels and positively with depressed mood. Patients with a strong increase in depressive symptoms after tryptophan depletion showed a positive linear correlation in the rCBF between the habenula and DRN (Morris et al 1999).

3.1.1.3. Locus coeruleus

Tracing studies suggest reciprocal anatomical connections between the DRN and pontine LC (Anderson et al 1977; Baraban and Aghajanian 1981; Kim et al 2004; Lee et al 2005; Pasquier et al 1977; Peyron et al 1996; Sakai et al 1977b; Sim and Joseph 1989). In fact, the DRN sends inhibitory projections to the LC (Morgane and Jacobs 1979; Segal 1979) and NA terminals innervate 5-HT neurons in the DRN (Baraban and Aghajanian 1981). In addition, LC targeted the rostral and ventro-lateral DRN in the cat (Sakai et al 1977a; Sakai et al 1977b). The LC is implicated in the sleep–wake cycle, analgesia, cognition (Usher et al 1999), depression (Harro and Oreland 2001) and anxiety (Tanaka et al 2000). In fact, antidepressants (Mateo et al 2000; Szabo and Blier 2001b) and anxiolytics (Tanaka et al 2000) modified LC neuronal activity *in vivo*.

3.1.2. Tachykinins and NK_1 receptors on afferent projections to dorsal raphe nucleus

Early studies using *in-situ* hybridisation histochemistry with labelled oligodeoxynucleotides revealed cell labelling for SP and NK B throughout the rat brain including the MHb (Burgunder and Young 1989; Warden and Young 1988). Other studies revealed tachykinin fibres in the LHb (Ljungdahl et al 1978a; Shults et

al 1984), while EM revealed SP fibres forming axo-dendritic synapses in the LC (Ljungdahl et al 1978b; Pickel et al 1979). In addition, NK_1Rs were detected in LHb, LC (Nakaya et al 1994; Saffroy et al 1994; Shults et al 1984) and PFC (Harding et al 2004). For example, radioligand binding and *in situ* hybridisation demonstrated NK_1Rs and their mRNA in the LC (Dam et al 1990b; Maeno et al 1993), and immunohistochemisty showed most NA neurons in the LC express NK_1Rs (Chen et al 2000; Hahn and Bannon 1999; Ma and Bleasdale 2002). In addition, SP activated LC neurons (Cheeseman et al 1983). Also, interestingly, using *in vivo* electrophysiology in the guinea pig, Conley et al. (2002) found the NK_1RA, L-760,735 increased DRN neuronal firing. Electrophysiology *in vitro* showed this was an indirect action, as local application of L-760,735 into the LHb led to an increase in DRN firing (Conley et al 2002). Thus, NK_1RAs may modulate the 5-HT system at the presynaptic level. However, it is not known if NK_1Rs are located in the LHb, LC and medial PFC on afferent neurons projecting to the DRN.

3.1.3. Aims of this chapter

The main aim in this chapter was to use retrograde tracing from the DRN to identify cell bodies of neurons in regions afferent to the DRN (e.g. PFC, LHb and LC) and to use NK_1R immunohistochemistry to examine if NK_1Rs are localised to these afferent neurons. Multiple labelling was combined at the light microscope and EM levels.

Tyrosine hydroxylase converts L-tyrosine to dihydroxyphenylalanine, a precursor for dopamine, which in the LC is further converted to noradrenaline. Therefore, tyrosine hydroxylase-ir can act as NA marker in the LC. Thus, a minor aim was also to investigate if any NK_1R-ir afferent neurons in the LC may be NA in origin.

3.2. MATERIALS AND METHODS

3.2.1. Animals

Male Sprague-Dawley rats (275-300 g) purchased from Harlan-Olac (Bicester, UK), were housed in cages in a room with a 12 h light/dark cycle and allowed free access to food and water. All animal experiments were carried out according to Home Office guidelines and the UK Animals (Scientific Procedures) Act 1986.

3.2.2. Antibodies

A list of antibodies, including sources, dilutions and combined use is given below in Table 3.1.

Table 3.1. Antibodies for immunohistochemistry

	Primary Antibody	**Fluorescence Secondary Antibody**	**Biotinylated Secondary Antibody**
NK_1R	rabbit (1:2000) [Chemicon, USA]	goat anti-rabbit Alexafluor 488 (1:1000) [Molecular Probes]	goat anti-rabbit (1:500) [Vector, UK]
Tyrosine Hydroxylase	mouse (1:5000) [Sigma, UK]	goat anti-mouse Alexafluor 568 (1:1000) [Molecular Probes]	horse anti-mouse (1:500) [Vector, UK]
Tryptophan Hydroxylase	sheep (1:1000) [Chemicon, UK]	----	rabbit anti-sheep (1:500) [Vector, UK]

3.2.3. Choice of retrograde tracer

Two retrograde tracers were used in this study: 'Fast Blue' (Diamidino-compound 253/50), and wheat germ agglutinin-horseradish peroxidase (WGA-HRP). Initial intra-DRN injections were with 'Fast Blue', as it was fluorescent and did not require a chemical or immunological reaction. 'Fast Blue' was useful for visualisation of afferent neurons in the PFC. However WGA-HRP was required at EM as it resulted in permanent electron dense staining. WGA-HRP is taken up by neurons at their terminals and transported by axonal transport to the soma and stored in lysosomes. WGA-HRP did not diffuse far from the injection site and produced labelling suitable for combination with immunohistochemical studies and further EM.

3.2.4. Stereotaxic injection of retrograde tracer

A flowchart summarising experiments with 'Fast Blue' and WGA-HRP is depicted in Fig. 3.1. In addition, 2 adult male rats (Sprague-Dawley) weighing 275-300 g were used in other experiments without tracer injection. These experiments included immunohistochemistry for tryptophan hydroxylase in DRN and for tyrosine hydroxylase in LC, as well as immunofluorescent confocal microscopy for colocalisation of NK_1R with tyrosine hydroxylase in the LC (see flow chart in Fig. 3.2). The fixative used for the immunohistochemical experiments was 4% (w/v) paraformaldehyde (Agar Scientific, Stansted, UK), 0.2% (v/v) glutaraldehyde and 20% (v/v) saturated aqueous picric acid in 0.1 M PB at pH 7.4, while that used for the immunofluorescent experiments was 4% (w/v) paraformaldehyde and 0.4% (v/v) saturated aqueous picric acid in 0.1 M PB at pH 6.9.

3.2.4.1. Fast Blue

Three adult male rats (Sprague-Dawley) weighing 275-300 g were used. Surgical procedures were carried out by Ms Sarah Busby. In general, the procedures for stereotaxic injection of 'Fast Blue' were similar to those of WGA-HRP (see section 3.2.3.2). Briefly, each rat was anaesthetised using Hypnorm/Hypnovel. The head was placed in a stereotaxic frame, a midline skin incision revealed the skull and a burr hole was made above the co-ordinates (related to Bregma) A/P= – 7.5 mm, M/L= Midline, D/V= –5.8 mm (Paxinos and Watson 1998). A glass micropipette with a tip diameter of 25-30 μm was used to introduce 30-50 nl of 'Fast Blue' (1% in distilled water, Sigma, UK) using positive pressure injection. The pipette was kept in place for 5 min after the injection before being removed to reduce spread back up the injection track. The animals were allowed to recover with free access to food and water.

Five days after the injection of tracer and following an overdose of sodium pentobarbital (200 mg/kg, i. p.), the rats were transcardially perfused with 200 ml of 0.9% saline followed by 500 ml solution of fixative for 20 min. Brains were removed and post-fixed in the same solution overnight at 4 ºC. Separate blocks were then cut from the brains. These contained the injection site, PFC, habenula and LC. Coronal sections (40 μm) were then cut on a vibrating microtome (Leica, Milton Keynes, UK) and collected in ice-cold PBS and after washes in PBS, stored at 4 ºC in PBS with 0.1% (w/v) sodium azide preservative. Some sections were then processed for single fluorescent NK_1R immunohistochemistry in PFC, LHb and LC (see section 3.2.5.2). Some LC sections were also stained for tyrosine hydroxylase (see section 3.2.6.1).

3.2.4.2. Wheat germ agglutinin-horseradish peroxidase

Four adult male rats (Sprague-Dawley) weighing 275-300 g were used. Injection micropipettes were pulled from glass capillary tubing (1.2-1.5 mm outer diameter, 0.94-1.2 mm inner diameter; Clark Electromedical Instruments, Reading, UK) using a micropipette puller (Micro Instruments Ltd, Oxford, UK) and tips trimmed to a diameter of 30-50 μm. Glass micropipettes were then filled with WGA-HRP (7%; Sigma, UK**;** L-3892) solution in 0.9% sodium chloride.

Rats were deeply anaesthetised (0.3ml/100g i.p. for induction and 0.2 ml intramuscular (i.m.) for maintenance) with injections of Hypnorm (Janssen Pharmaceuticals Ltd, Oxford, UK) and Hypnovel (Roche Products Ltd, Welwyn Garden City, UK) mixture with water (1:1:2). All surgical procedures were carried out with the animals under deep anaesthesia, regularly assessed by checking for limb-withdrawal and corneal reflexes.

After subcutaneous administration of local anaesthetic lignocaine hydrochloride (HCl) (Martindale Pharmaceuticals, Romford, UK; 2% w/v) into the scalp and shaving of scalp fur, animals were mounted onto a stereotaxic frame (Kopf Instruments, CA, USA) and a midline incision made into the scalp. A micropipette was positioned over bregma and then moved to above the DRN using co-ordinates derived from the atlas of Paxinos and Watson (1986; co-ordinates relative to bregma and from dura; A/P –7.5 mm, M/L 0.0 mm and D/V –5.5 mm). A hole was drilled in the skull above the DRN and the micropipette lowered 5.0 mm from the dura, directly though the sinus into the DRN. The rats then received about 50 nl of WGA-HRP (7%) into the DRN over a 30 sec period via a pressure injection system. Following the tracer injection,

the micropipette was left in place for 3 min and then withdrawn slowly to avoid tracer leakage. The bone window was sealed with bone wax (Ethicon Ltd, UK) and the midline incision sutured. Some rats were administered buprenorphine (Alstoe Ltd, Melton Mowbray, UK; 10 μg/Kg i.m.) for post-operative analgesia. The animals were allowed to recover from the anaesthesia under a heat lamp and after recovery were placed together onto blankets in their normal cages and given food and water *ad libitum*.

After a survival period of about 40 hrs, the animals were terminally anaesthetised with sodium pentobarbital (Merial Animal Health Ltd, Harlow, UK; 200 mg/kg, i.p.) and transcardially perfused via a peristaltic pump, firstly with 200 ml of 0.9% (w/v) saline, followed by 500 ml of fixative over 20 min. The brains were then removed from the cranium and post-fixed in the same fixative for up to 20 min at 4 ºC, and then washed in 0.1 M PB and transferred to PBS before further processing. Prior to sectioning the brains were cut into smaller blocks using a plexiglass brain matrix. Coronal sections were cut on a vibrating microtome (Leica, Milton Keynes, UK) and collected as free-floating sections in vials containing ice-cold PBS and then washed in PBS before further processing. Sections of 50 μm thickness were collected for parallel processing for either EM or light microscopy for NK_1R immunohistochemistry and/or WGA-HRP peroxidase reactions, while 70 μm thick sections were collected through the DRN to reveal injection sites.

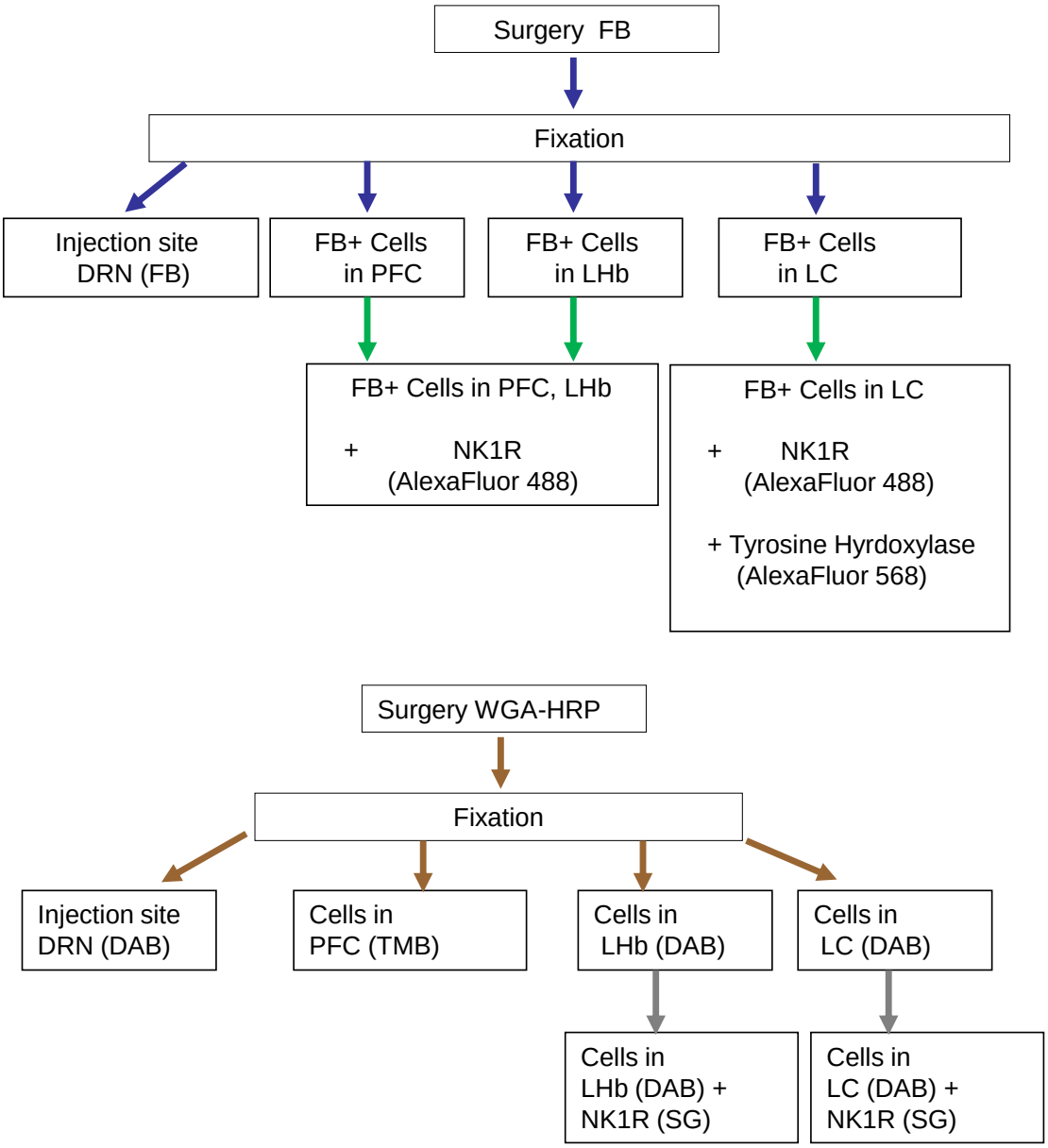


Fig. 3.1. Flow chart of experiments with 'Fast Blue' and wheat germ agglutinin-horseradish peroxidase. Surgical procedures were followed by fixation of brain. Injection sites in DRN and afferent neurons in PFC, LHb and LC were identified with immunofluorescence for 'Fast Blue' and DAB or TMB for WGA-HRP. This was followed by immunohistochemistry for NK_1R (Alexafluor 488 or Vector SG) and tyrosine hydroxylase (some LC sections).

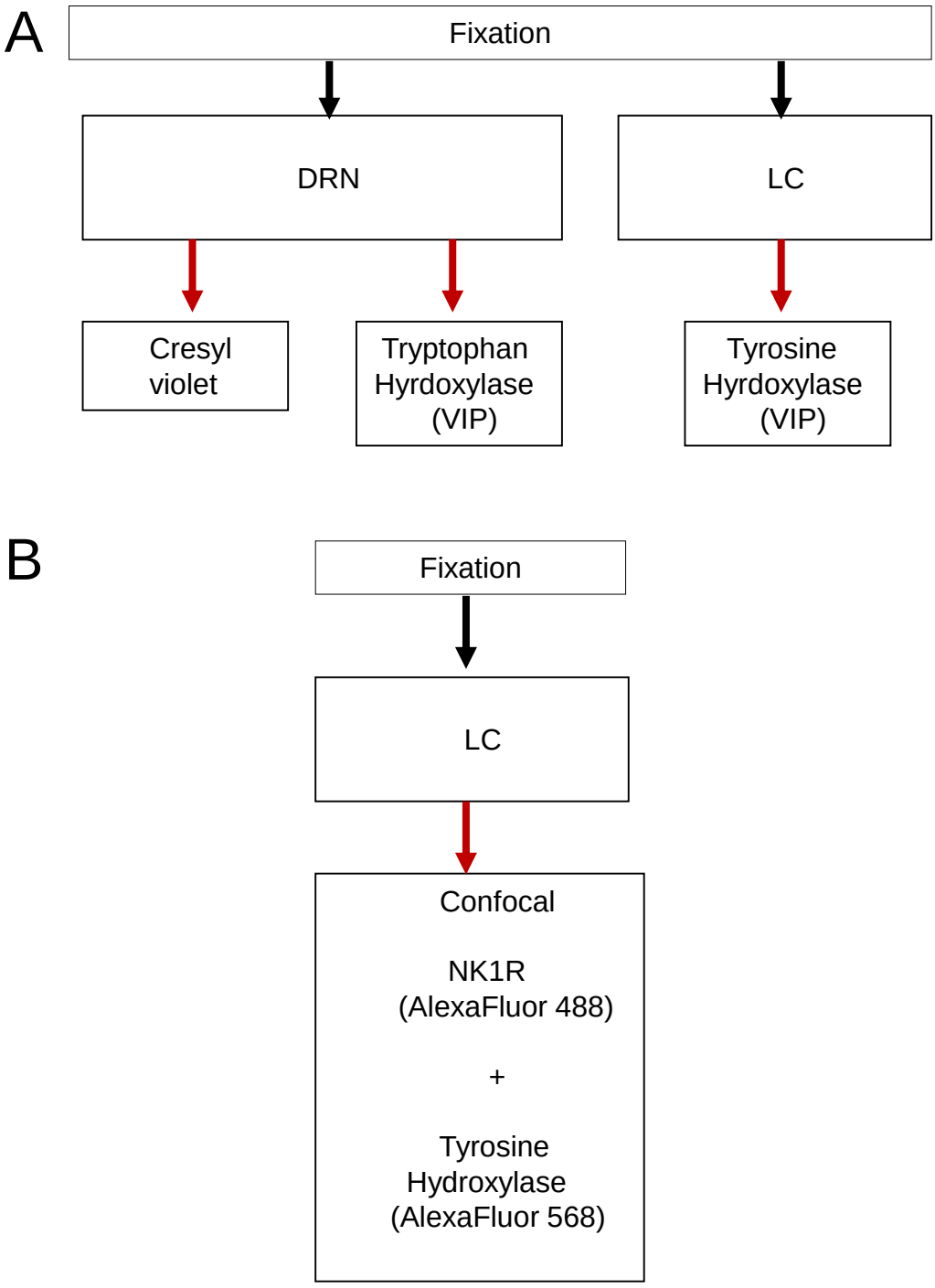


Fig. 3.2. Flow chart of additional immunohistochemical experiments in dorsal raphe and locus coeruleus. A: Permanent staining: After fixation of brain, DRN slices were stained for cresyl violet and for tryptophan hydroxylase using VIP. LC slices were stained for tyrosine hydroxylase using VIP. B: After fixation, some LC sections were stained for colocalisation of NK_1R (Alexafluor 488) and tyrosine hydoxylase (Alexafluor 568) and examined with confocal microscopy.

3.2.5. Visualisation of tracers and single immunohistochemistry

3.2.5.1. Visualisation of tracer at injection sites

3.2.5.1.1. Fast blue

Sections were collected onto microscope slides, air dried, and coversliped with Vectashield (Vector Laboratories, UK). Slides were stored in the dark at 4 ºC until required. 'Fast Blue' was visualised directly with a fluorescence microscope.

3.2.5.1.2. Wheat germ agglutinin-horseradish peroxidase

Raphe sections were processed for visualisation of injection sites using 3,3'–diaminobenzidine tetrahydrochloride (DAB; Sigma).

3.2.5.2. Fluorescence immunohistochemistry for NK_1 receptors

Light was excluded throughout to minimise bleaching of fluorescence. Brain section were washed in PBS before a 90 min incubation in blocking buffer composed of 0.3% (v/v) Triton X-100, 10% (v/v) NGS and 1% (w/v) BSA in PBS, and then incubated overnight at 4 ºC with rabbit anti-NK_1R primary antibody (Chemicon, CA, USA; 1:2000). The sections were then washed in PBS followed by incubation in Alexa Fluor 488 goat anti-rabbit (Molecular Probes, Netherlands; 1:1000) for 4 hrs. All anti-sera were diluted in 0.3% Triton X-100, 1% NGS and 1% BSA in PBS. After further washes, sections were mounted from a buffer bath onto gelatin-coated glass slides, allowed to dry before being cover-slipped with Vectashield liquid mounting medium (Vector Laboratories, Peterborough, UK). In parallel control sections, the primary antibody was omitted.

3.2.5.3. Immunohistochemistry for tryptophan hydroxylase in dorsal raphe nucleus

To define 5-HT boundaries, DRN sections were washed in PBS before further processing. Sections were treated with 1% (w/v) sodium borohydride in PBS for 10 min to reduce excess background staining and the excess aldehyde groups created by the fixatives. Sections were then washed in PBS until all bubbles had disappeared. After quenching of endogenous peroxidase with a mixture of 10% (v/v) methanol and 3% (v/v) hydrogen peroxide in distilled water for 5 min, and further washing in PBS, sections were incubated for 90 min in blocking buffer composed of PBS, 0.3% (v/v) Triton X-100, 10% (v/v) normal rabbit serum (NRS). The sections were then incubated overnight at 4 ºC with sheep anti-tryptophan hydroxylase (Chemicon, Watford, UK; 1:1000). After PBS washes, the sections were incubated in biotinylated rabbit anti-sheep secondary antibody (Vector; 1: 500) for 2 hrs. After further washes in PBS and 90 min incubation in avidin-biotin-peroxidase complex (ABC, Vector), sections were rinsed initially 3 times in PBS and then once in 0.05 M Tris-HCl (pH 7.6) and bound peroxidase revealed using VIP substrate kit (Vector). As in previous literature, a more dilute solution than suggested by the manufacturer was used (Lanciego et al 1998). One drop of each of the four reagents was added to 3.5 ml of 0.05 M Tris-HCl (pH 7.6) buffer and sections incubated for 1 min. The reaction was stopped by rinsing sections with Tris buffer. Sections were then mounted and allowed to air-dry. The slides were immersed in two changes of toluene (4 min. each) before being cover-slipped with Entellan (VWR) mounting medium and prepared for light microscopic viewing.

3.2.5.4. Histochemistry for wheat germ agglutinin-horseradish peroxidase in prefrontal cortex

Initial staining with DAB for PFC neurons with retrogradely transported WGA-HRP was either very faint or non-existent. Therefore, a reaction with ammonium paratungstate-stabilised tetramethylbenzidine (TMB) was used instead (Weinberg and van Eyck 1991). Here sections were pre-incubated in a solution of 5% (v/v) ammonium paratungstate (Sigma Aldrich, UK) with 2.5% (v/v) TMB in 0.1 M PB (pH 6.0) for 25-30 min. This solution was replaced with fresh pre-incubation solution containing 0.003% (v/v) hydrogen peroxide, and the reaction terminated after 5-15 min with washes in 0.1M PB (pH 6.0). TMB reaction product was stabilised by incubation in fresh DAB-Cobalt mixture (0.1% (w/v) DAB and 2% (v/v) cobalt chloride) together with 0.003% (v/v) hydrogen peroxide for 10 min (van der Want et al 1997). The reaction mixture was removed with washes in 0.1 M PB (pH 6.0). Sections were then processed for immediate viewing.

3.2.5.5. Immunohistochemistry for tyrosine hydroxylase in locus coeruleus

LC sections were washed in PBS, treated with sodium borohydride and endogenous peroxidase quenched. After 90 min in blocking buffer composed of 0.3% (v/v) Triton X-100, 10% (v/v) normal horse serum (NHS) in PBS, sections were incubated overnight at 4 ºC with monoclonal mouse anti-tyrosine hydroxylase (Sigma; 1:5000) in PBS with 0.3% (v/v) Triton X-100, 1% (v/v) NHS. After washes in PBS, the sections were incubated in biotinylated goat anti-mouse secondary antibody (Vector; 1:500) for 2 hrs. After rinsing, sections were incubated in ABC Elite kit (Vector) for 90 min and bound peroxidase revealed using VIP kit (Vector) for 2-3 min and then prepared for viewing (see section 3.2.5.3).

3.2.6. Double-labelling immunohistochemistry

3.2.6.1. Double fluorescence immunohistochemistry for NK_1 receptors and tyrosine hydroxylase

Some LC brain sections were washed in PBS before being incubated for 90 min at in blocking buffer composed of 0.3% (v/v) Triton X-100, 10% (v/v) NGS and 1% (w/v) BSA in PBS, and then incubated overnight at 4 ºC with rabbit NK_1R primary antibody (Chemicon, CA, USA; 1:2000) and mouse anti-tyrosine hydroxylase primary antibody (Sigma, T2928; 1:5000). The sections were then washed in PBS followed by incubation in Alexa Fluor 488 goat anti-rabbit secondary antibody (Molecular Probes, Netherlands; 1:1000) and Alexa Fluor 568 goat anti-mouse secondary antibody (Molecular Probes, Netherlands; 1:1000) for 4 hrs while protected from light. All anti-sera were diluted in 0.3% Triton X-100, 1% NGS and 1% BSA in PBS. After further washes, sections were mounted onto slides, allowed to air-dry while protected from light before being cover-slipped with Hydromount (National Diagnostics, Hull, UK) or Vectashield liquid mounting medium (Vector Laboratories, Peterborough, UK). Appropriate controls were included. Method specificity was tested by omitting the primary antibodies in the incubation sequence, and no immunostaining was observed in these slices. To control for cross reactivity between immunoglobulins in double fluorescence immunolabeling, some sections were processed through the same immunohistotochemical sequence, except that only one primary antibody was applied, but the complement of secondary antibodies was maintained.

3.2.6.2. Double-labelling immunohistochemistry for wheat germ agglutinin-horseradish peroxidase and NK_1 receptors

Double-labelling of WGA-HRP and NK_1R combined a DAB reaction for staining of WGA-HRP and an SG peroxidase substrate kit (Vector Laboratories, Burlingame, CA, USA; SK-4700) for labelling of NK_1Rs. Firstly, sections were transferred from PBS into 0.05 M Tris-HCl buffer (pH 7.6). The vials were then transferred to a fume cupboard and the sections incubated for 10-15 min in 0.05% DAB in 0.05 M Tris-HCl (filtered) before addition of 0.01% hydrogen peroxide and incubation for 10-12 min followed by incubation in a fresh solution of DAB-hydrogen peroxide mixture for a further 5-10 min. Reaction was terminated by rinsing the sections in Tris-HCl buffer. For immediate viewing, some sections were washed in PBS and mounted onto slides and allowed to air dry. They were then dehydrated through serial ethanol dilutions (10 min each) followed by two changes in xylene (20 min each) before being cover-slipped with DPX mounting medium (BDH Laboratory Supplies, Poole, UK).

Other sections were further processed for NK_1R immunohistochemistry. Triton X-100 was omitted at all steps for sections that were destined for EM, because of its damaging effect on membrane ultrastructure. Otherwise, sections were first treated with 1% (w/v) sodium borohydride in PBS for 10 min and washed as previously described. This was followed by incubation in 10% (v/v) methanol and 3% (v/v) hydrogen peroxide for 5 min to eliminate endogenous peroxidase. The sections were then thoroughly rinsed in PBS until all bubbles had fully disappeared. This was followed by 2 hr incubation in blocking buffer. LC sections were then incubated overnight, while LHb sections were incubated for 3 nights, at 4 ºC with rabbit NK_1R primary antibody (Chemicon; 1:2000). After washes in PBS the sections were

incubated in biotinylated goat anti-rabbit secondary antibody (Vector; BA-1000; 1: 500) for 2 hrs. Sections were then incubated in ABC Elite kit (Vector; 1:1:50) for 2 hrs. After further washing in PBS the bound peroxidase was revealed using a Vector SG kit (Vector) and 3-5 min incubation. The sections were then washed in PBS and mounted onto slides, air-dried overnight and dehydrated through an ascending ethanol series before being cleared in xylene and cover-slipped with DPX.

3.2.7. Electron microscopy

Some coronal sections containing LHb or LC destined for EM examination were first reacted to demonstrate WGA-HRP and then incubated overnight at 4 ºC in cryoprotectant solution composed of 25% (w/v) sucrose and 10% (v/v) glycerol in 0.05 M PB pH 7.4). These sections were then subjected to a freeze-thaw procedure designed to enhance penetration of immunological reagents into fixed tissue (Totterdell et al 1992). To do this, the sections were flattened in a mesh basket containing cryoprotectant solution. Care was taken to make sure that sections were not folded at this stage to prevent them breaking along the line of the fold when frozen. The mesh baskets were blot dried to remove traces of cryoprotectant. The baskets containing the flattened sections were first dipped into cooled isopentane (10-20 sec) and then into liquid nitrogen (30 sec). Sections containing LHb were frozen, thawed and then frozen again, while those containing LC were only subjected to freezing once. The sections were then thawed in cryoprotectant, and washed in PBS to remove all traces of cryoprotectant. After this freeze-thaw treatment, sections were processed to reveal NK_1R immunolabelling as described above (section 3.2.6.2). After the final SG reaction, sections were transferred to 0.1 M PB (pH 7.4) overnight at 4 ºC.

Sections were then placed flat at the bottom of a watch glass and post-fixed in 1% osmium tetroxide (Oxchem, UK; in 0.1 M PB, pH 7.4) for 40 min. The sections were then washed in distilled water and dehydrated through an ascending series of graded ethanol solutions (70%, 90% and absolute ethanol, 15 min each). To enhance the contrast of the tissue in the EM, the sections were stained, while protected from light, with filtered 1% uranyl acetate (TAAB, reading, UK) at the 70% ethanol phase. The sections were washed twice for 15 min in propylene oxide and left in resin (Durcupan; Fluka: Sigma, UK) at room temperature overnight to allow the resin to fully penetrate the sections. Finally the sections were embedded in resin on microscope slides, and placed in an oven at 60 ºC for > 48 hrs to polymerise the resin.

Areas of interest identified in the light microscope were recorded, and then the coverslips removed and selected areas excised and glued to blank resin blocks and serial ultrathin (60-70 nm) sections cut on an Ultracut E ultramicrotome (Leica, Milton Keynes, UK) using a diamond knife (DIATOME, Switzerland), with the guidance and assistance of Dr Susan Totterdell. These sections were collected serially onto Piloform-coated, copper, single-slot grids, contrasted with lead citrate for 2-4 min (Reynolds 1963). Progress through the block was monitored periodically in the light microscope so that the sections containing the area of interest could be rapidly identified.

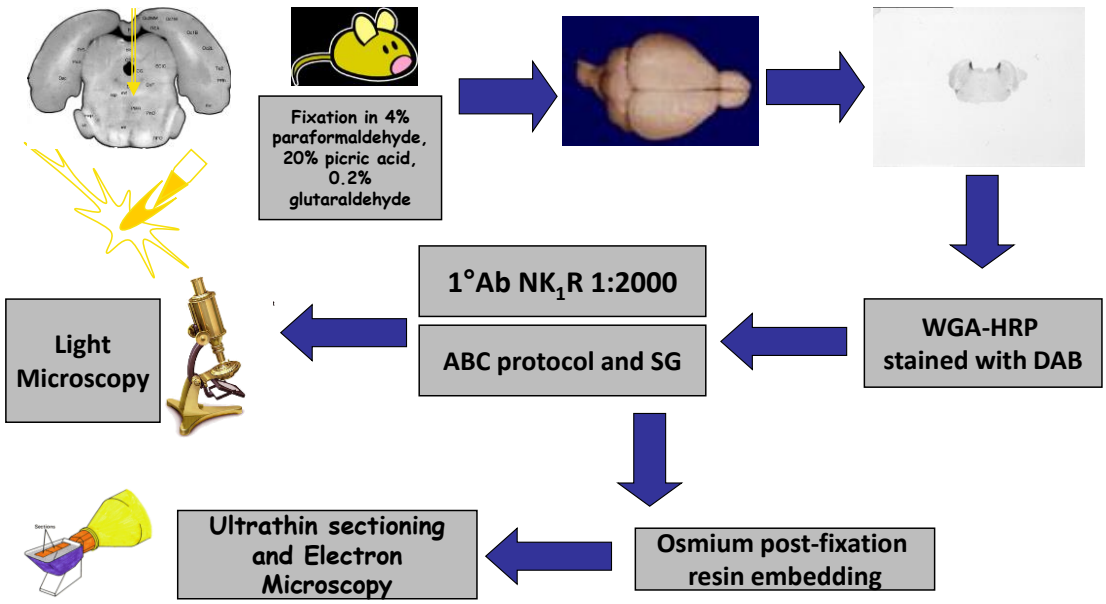


Fig. 3.3. Summary flow chart of procedures for electron microscopy. WGA-HRP was injected into DRN. After a survival period, animals were anaesthetised and transcardially perfused with fixative (4% paraformaldehyde, 20% picric acid, 0.2% glutaraldeyde). Coronal sections were cut and stained for WGA-HRP using DAB. Sections were stained for NK_1R (anti-rabbit primary antibody 1:2000) with ABC protocol and Vector SG. Some sections were processed for light microscopy, while others were processed for EM (omission of Triton-X). These latter sections were processed with osmium post-fixation, treatment in ethanol and uranyl acetate and then embedded in resin. Ultrathin sections were then prepared and after lead staining examined.

3.2.8. Image acquisition and analysis of material

3.2.8.1. Labelling with Fast Blue

Tissue sections were examined, with images captured using a CCD camera on a Leica DMRB microscope, and analysed and displayed using Openlab software as described for NK_1R and 5-$HT_{1A}R$ colocalisation in section 2.2.3. Also, selected LC sections with double labelling for NK_1R and tyrosine hyroxylase were analysed by Dr Julian Goggi (Imperial College, London) with a Leica SP confocal laser-scanning microscope as described in section 2.2.3.

3.2.8.2. Labelling with wheat germ agglutinin-horseradish peroxidase

3.2.8.2.1. Light microscopy

The location and extent of the tracer injections were assessed in the light microscope (Leica Dialux 20). The sections with the greatest spread of tracer in the raphe were photographed. In addition, photographs were taken of neurons in brain regions (PFC, LHb and LC) afferent to DRN neurons. Coloured digital images were captured using a cooled colour CCD camera (Micropublish 3.3 RTV; Qimaging, Canada) and analysed and displayed using Qcapture Pro software (version 5.0; Qimaging, Canada) or Scion Image software (Scion Corp., Frederick, USA). Digital images were manipulated with regards to size, cropping, colour balance, brightness using Photoshop 6.0 software (Adobe systems, San Jose, CA) and labelled using Powerpoint (Microsoft 2003).

3.2.8.2.2. Electron microscopy

Sections prepared for EM, which contained the WGA-HRP labelled neurons and processed to reveal NK_1R-ir, were examined in the light microscope first (Leica

Dialux 20). Initial photographs were taken with 50 ASA film and the prints digitised using an Epson GT-900 scanner (Epson). Photographs were adjusted for brightness and contrast, by eye using Photoshop 6.0 software (Adobe systems, San Jose, CA). Serial ultrathin sections were examined in a Phillips (Eindhoven, The Netherlands) 410 electron microscope. Neurons of interest were captured on a digital camera (Multiscan, Gatan, UK) running Digital Micrograph software. These images were converted to TIFF files and imported into Adobe Photoshop, where adjustments were made to size, contrast and brightness, and then assembled into plates. These plates were then imported into Powerpoint (Microsoft) and labels applied.

3.3. RESULTS

3.3.1. Dorsal raphe nucleus

3.3.1.1. Tryptophan hydroxylase in dorsal raphe nucleus

Immunolabelling with tryptophan hydroxylase revealed a population of neurons in the DRN (Fig. 3.4). These were large, with a few smooth dendrites and resembled previous reports for 5-HT neurons. Their distribution mostly overlapped with the boundaries of the DRN as in the atlas (Paxinos and Watson, 1986).

3.3.1.2. Injection sites

3.3.1.2.1. Fast Blue

Injections of 'Fast Blue' were found to be restricted to the DRN (Fig. 3.5 A). There was some variation between the rostral/caudal spread of the tracer between animals, but there was no involvement of adjacent brain regions. There was a central core to the injection sites, but the intensity of staining was otherwise quite consistent. At the injection site it was possible to identify neurons that had taken up the tracer since it was visible throughout their dendrites.

3.3.1.2.2. Wheat germ agglutinin-horseradish peroxidase

Similarly, injections of WGA-HRP did not spread beyond the boundaries of the DRN in any animal (Fig. 3.6). The DRN is highlighted on a coronal atlas section in Fig. 3.4. An example of a WGA-HRP injection site within the DRN is seen in Fig. 3.5 B.

3.3.2. Light microscopic examination of NK_1 receptors on afferents to dorsal raphe nucleus

WGA-HRP was used to identify cell bodies in regions afferent to the DRN and immunohistochemistry for NK_1Rs was used to investigate cellular colocalisation. In this study, WGA-HRP-labelled neurons presented a clear cytoplasm with an amorphous brown DAB-reaction product within. Neurons with NK_1R-ir were identified by a blue/grey cytoplasm resulting from Vector SG. Double-labelled WGA-HRP-NK_1R-ir neurons exhibited a blue/grey cytoplasm with a dense brown reaction product within. There was also some evidence of anterograde WGA-HRP transport in some areas as brown fibres with no staining in cell bodies (see section 3.3.2.2.2). Where fixation had not fully denatured them, endogenous peroxidases on red blood cells resulted in labelling on some sections.

3.3.2.1. Afferents from prefrontal cortex

3.3.2.1.1. Fast Blue

'Fast blue' labelling was abundant in the infralimbic cortex, prelimbic cortex, cingulate cortex, ventral orbital cortex and lateral orbital cortex. In the medial PFC, cells retrogradely labelled were seen in layers III and V. The label filled the cell bodies and some dendrites, and by their morphology these were pyramidal neurons, although not all neurons were labelled. There was no evidence of colocalisation between 'Fast Blue' and NK_1R-ir. However, NK_1R-ir was found on neurons or fibres close to cells containing 'Fast Blue' (Fig. 3.7 and Fig. 3.8).

3.3.2.1.2. Wheat germ agglutinin-horseradish peroxidase

In this study, the histochemical stain DAB was not sensitive enough to reveal PFC cells retrogradely labelled with WGA-HRP. However, with TMB as the chromogen, PFC neurons containing retrogradely transported WGA-HRP were labelled with an amorphous grey-black cytoplasmic deposit. These neurons were pyramidal in shape and found in the deep layers of the infralimbic and prelimbic regions (see Fig. 3.9).

3.3.2.2. Afferents from lateral habenula

3.3.2.2.1. Fast Blue

Retrograde tracing resulted in labelling in neurons mostly concentrated in the medial aspect of the LHb (see Fig. 3.10). The label filled the cell bodies and in some cells also the dendrites. In the double-labelled material, these projection neurons, as well as some unlabelled neurons, were surrounded by NK_1R-ir fibres. However, colocalisation between 'Fast Blue' and NK_1R was not found (Fig. 3.10).

3.3.2.2.2. Wheat germ agglutinin-horseradish peroxidase

After a post-injection survival time of 40 hrs, retrogradely-labelled neurons were present in the LHb in 3 rats. As with the 'Fast Blue' labelling, these neurons were mostly in the medial aspects of the LHb and of similar morphology, but with brown deposits inside the soma due to the DAB reaction product (Fig. 3.11 and Fig. 3.12). Although not quantified, retrogradely-labelled neurons appeared less frequent compared to those labelled with 'Fast Blue'.

Double-labelling for WGA-HRP and NK_1R-ir revealed some DRN afferent cells to be immunoreactive for NK_1Rs. These cells had a slate greyish/blue boundary and

cytoplasm and contained brown deposits inside the cytoplasm from the DAB reaction product for WGA-HRP (Fig. 3.11 and Fig. 3.12). Other cells with NK_1R-ir did not contain WGA-HRP (Fig. 3.12 D). In addition, there was some anterograde transport of WGA-HRP in the form of discrete brown fibres, presumably axons (Fig. 3.11 D).

3.3.2.3. Afferents from the locus coeruleus

3.3.2.3.1. Fast Blue

Within the LC, retrogradely transported 'Fast Blue' was present in neurons throughout the nucleus, especially laterally. In general, these neurons were large, with 'Fast Blue' restricted to the cell bodies, but with a few cases also in the dendrites. Unlabelled neurons were also present. Some 'Fast Blue'-containing neurons were also tyrosine hydroxylase-ir. In triple-labelled sections, these neurons appeared to be surrounded by NK_1R-ir fibres. However, at the light microscopic level, it was not clear if NK_1R was present on the plasma membrane or in the intercellular space.

3.3.2.3.2. Wheat germ agglutinin-horseradish peroxidase

After a post-injection survival time of 40 hrs, WGA-HRP was found in neurons throughout the LC in 2 rats. As with 'Fast Blue', these neurons were large and the DAB reaction product mostly restricted to cell bodies. Few unlabelled neurons were present. In double-labelled sections, neurons also appeared to be surrounded by extensive NK_1R-ir. It was not clear at the light microscopic level whether NK_1Rs were present on the plasma membrane or in the surrounding intercellular space.

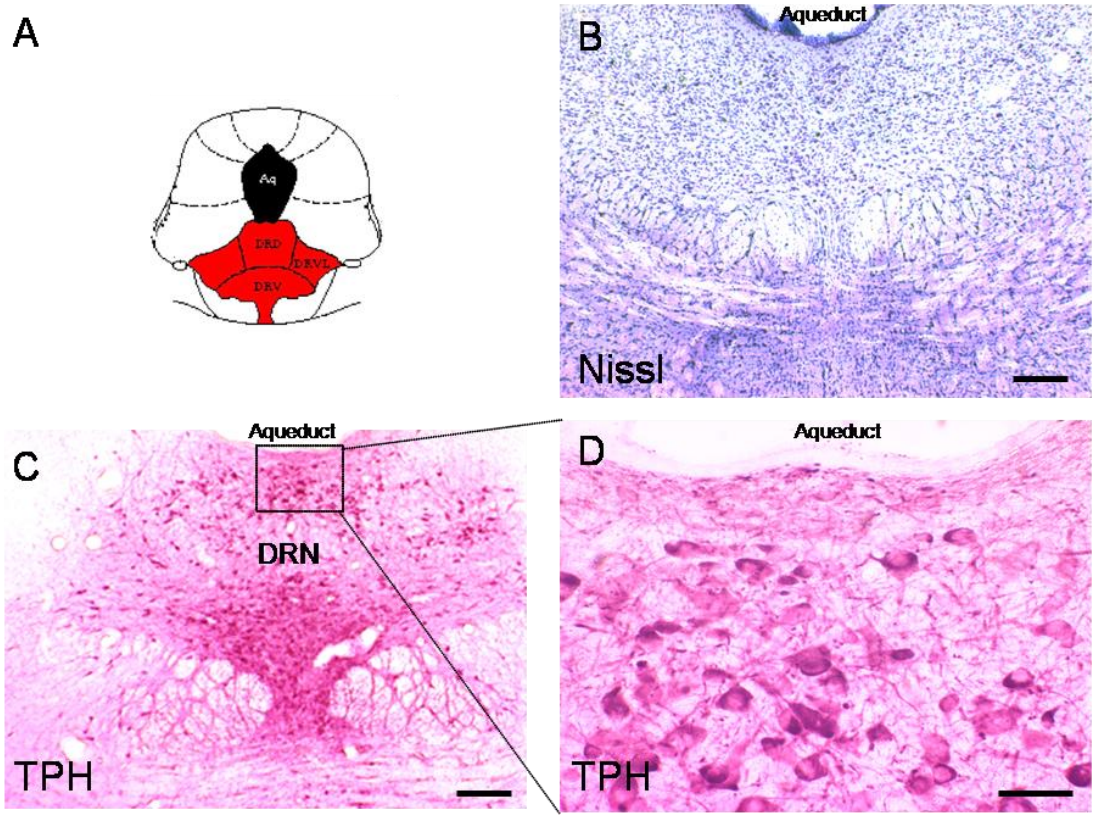


Fig. 3.4. Tryptophan hydroxylase immunohistochemistry in dorsal raphe nucleus. The DRN is represented in red in a schematic diagram together with its subregions at -8.00 from bregma; picture from Paxinos and Watson (1998) (A). Nissl staining of a corresponding DRN section (B). Immunohistochemistry for tryptophan hydroxylase stained with VIP (C). Higher magnification photograph of square in C (D). Scale bars in B: 200 μm; C: 200 μm; D: 25 μm. DRD=dorsal raphe nucleus dorsal; DRV=dorsal raphe nucleus ventral; DRVL=dorsal raphe nucleus ventrolateral; TPH=tryptophan hydroxylase.

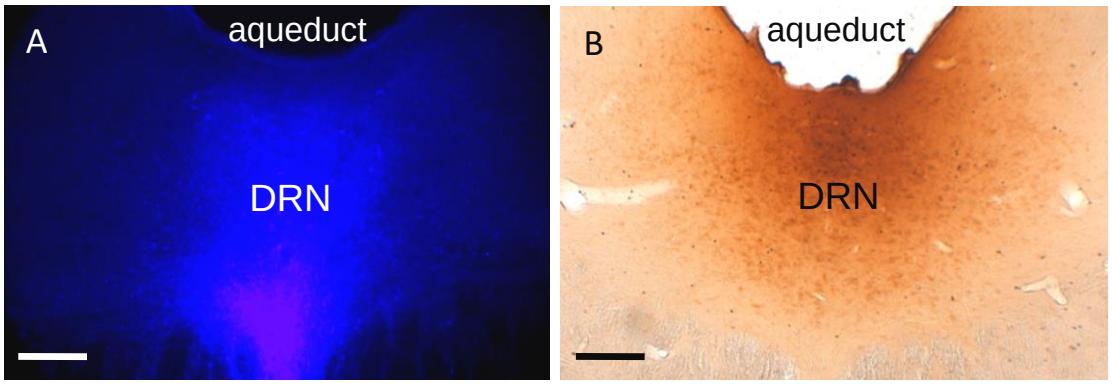


Fig. 3.5. Photomicrographs of injection sites for 'Fast Blue' and wheat germ agglutinin-horseradish peroxidase in dorsal raphe nucleus. Example of an injection site with 'Fast Blue' in DRN (A). Example of an injection site with WGA-HRP in DRN (B). Scale bars in A: 100 μm; B: 200 μm.

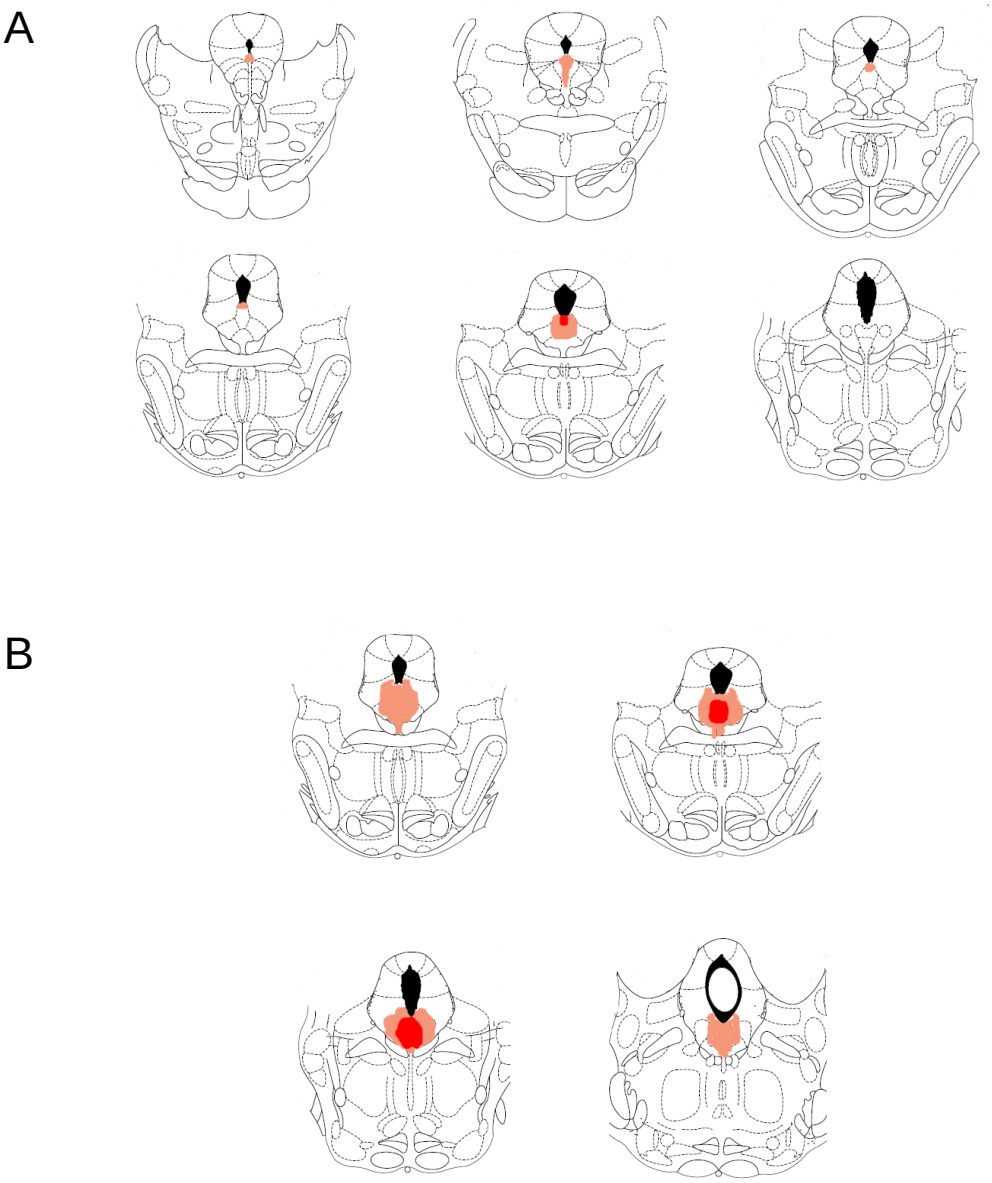


Fig. 3.6. Schematic representation of spread of retrograde tracer wheat germ agglutinin-horseradish peroxidase in dorsal raphe nucleus. Two different examples (A) and (B) of injection sites in DRN with retrograde tracer WGA-HRP. Red indicates the injection site and pink represents the spread of the tracer. Plates shown at -7.04 to 8.30 mm from bregma (A) -7.80 to 8.72 mm from bregma (B). Pictures edited from Paxinos and Watson (1998).

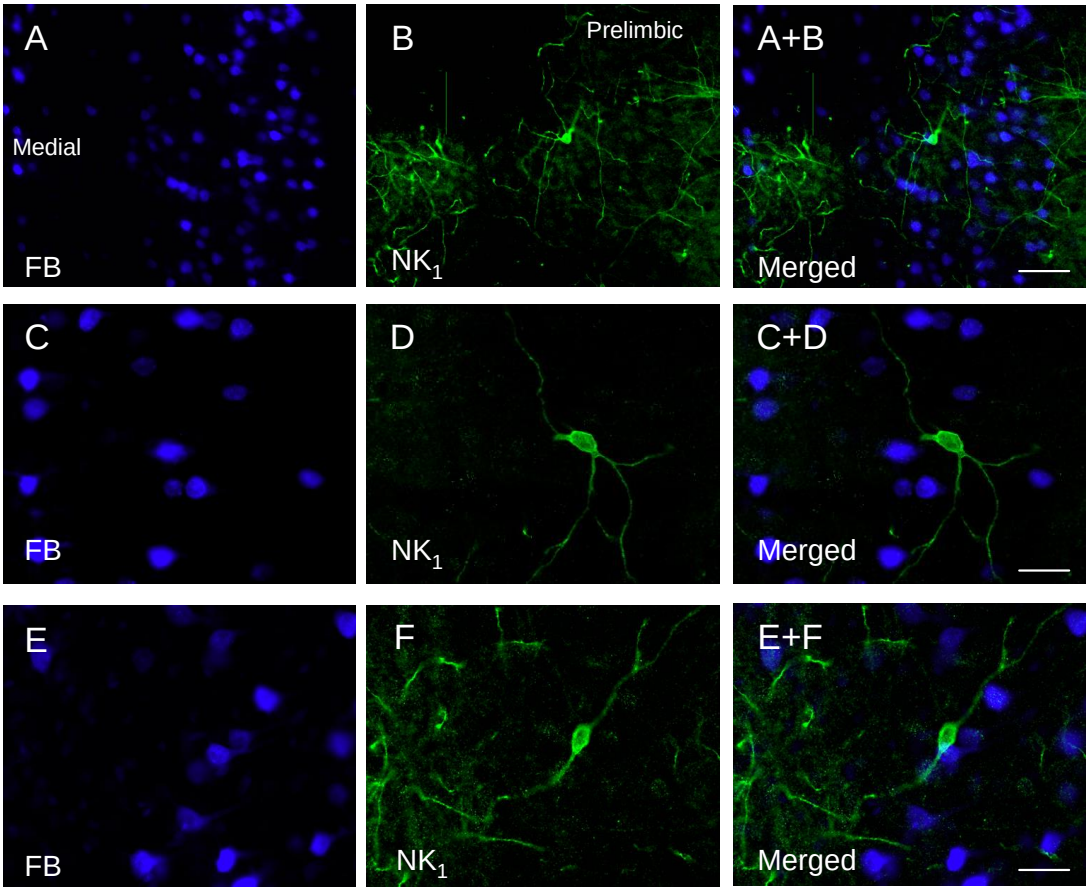


Fig. 3.7. Photomicrographs of NK_1 receptor-immunoreactivity and of neurons labeled with 'Fast Blue' in prefrontal cortex (I). Neurons containing 'Fast Blue' represent neurons afferent to DRN and are seen in the prelimbic region- at about +2.70 mm from bregma (A, C, E). Cells within the same section were also stained for NK_1R-ir (B, D, F). In merged photomicrographs, afferent neurons containing 'Fast Blue' did not show NK_1R-ir (A+B, C+D, E+F). Scale bars in A+B: 60 μm; C+D: 30 μm; E+F: 30 μm.

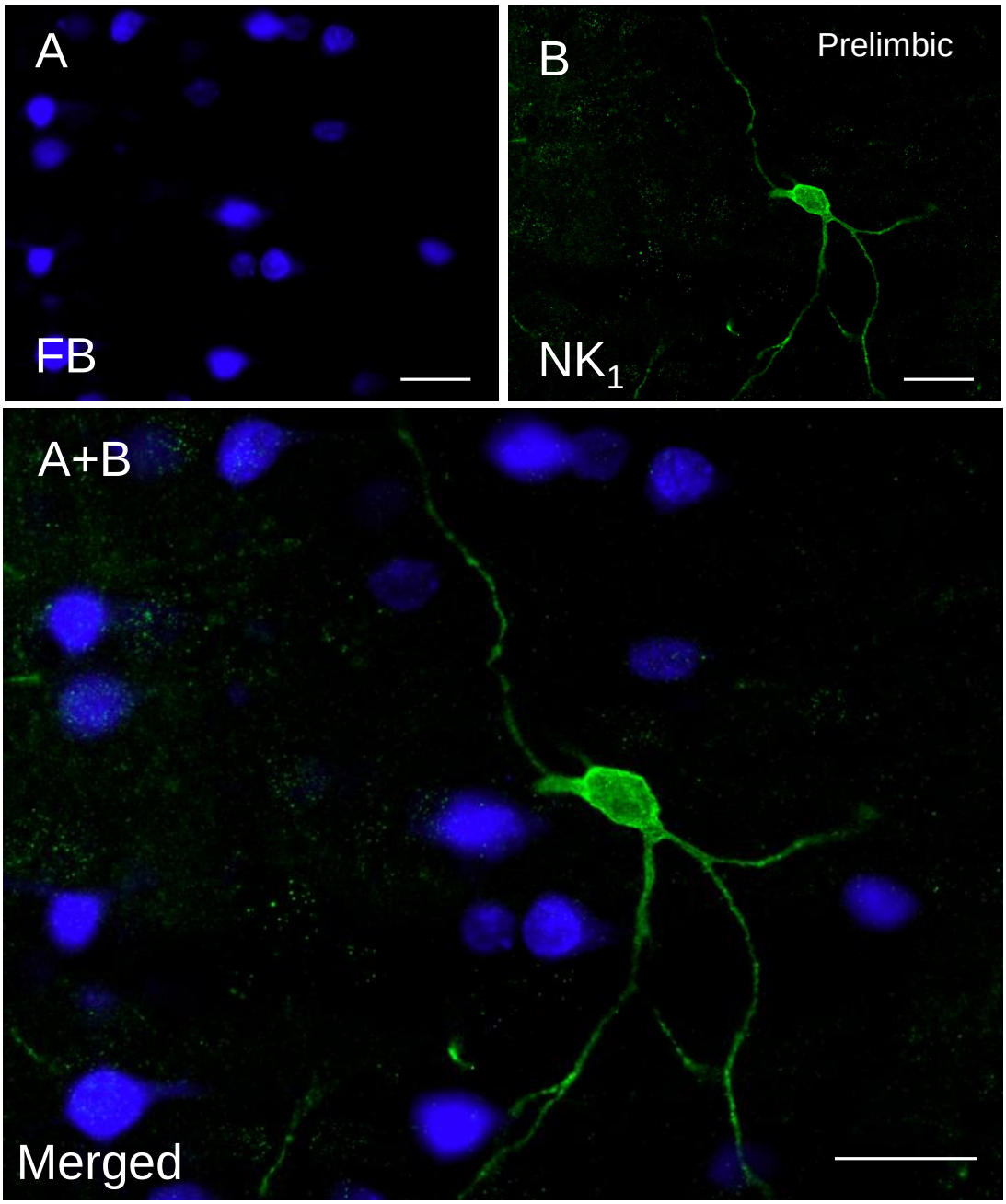


Fig. 3.8. Photomicrographs of NK_1 receptor-immunoreactivity and of neurons labeled with 'Fast Blue' in prefrontal cortex (II). Photographs from Fig. 3.7 (C, D, C+D) are represented again at higher magnification. Afferent neurons containing 'Fast Blue' are shaped like pyramidal cells (A, A+B) and surround a multipolar neuron with NK_1R-ir (A+B), suggesting close proximity, but no colocalisation between 'Fast Blue' and NK_1R-ir. Scale bars in A, B, A+B: 30 µm.

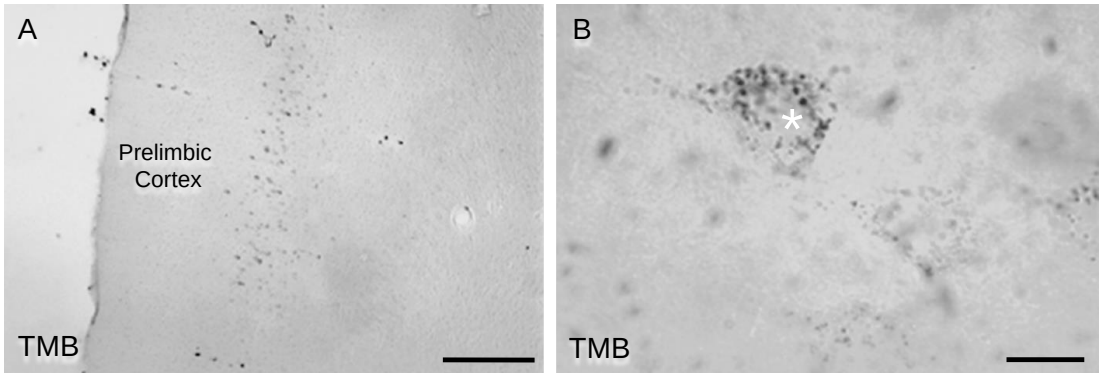


Fig. 3.9. Photomicrographs of neurons labeled with wheat germ agglutinin-horseradish peroxidase in prefrontal cortex. A) A low power micrograph of the prelimbic cortex (about +2.70 mm from bregma) showing the region containing neurons that project to the PFC. B) At higher magnification, the asterisk indicates presence of a pyramidal-like neuron in the prelimbic region of the PFC, labeled with WGA-HRP and thus afferent to DRN. In this region, WGA-HRP was revealed using TMB as the staining procedure. Scale bars in A: 300 µm; B: 10 µm.

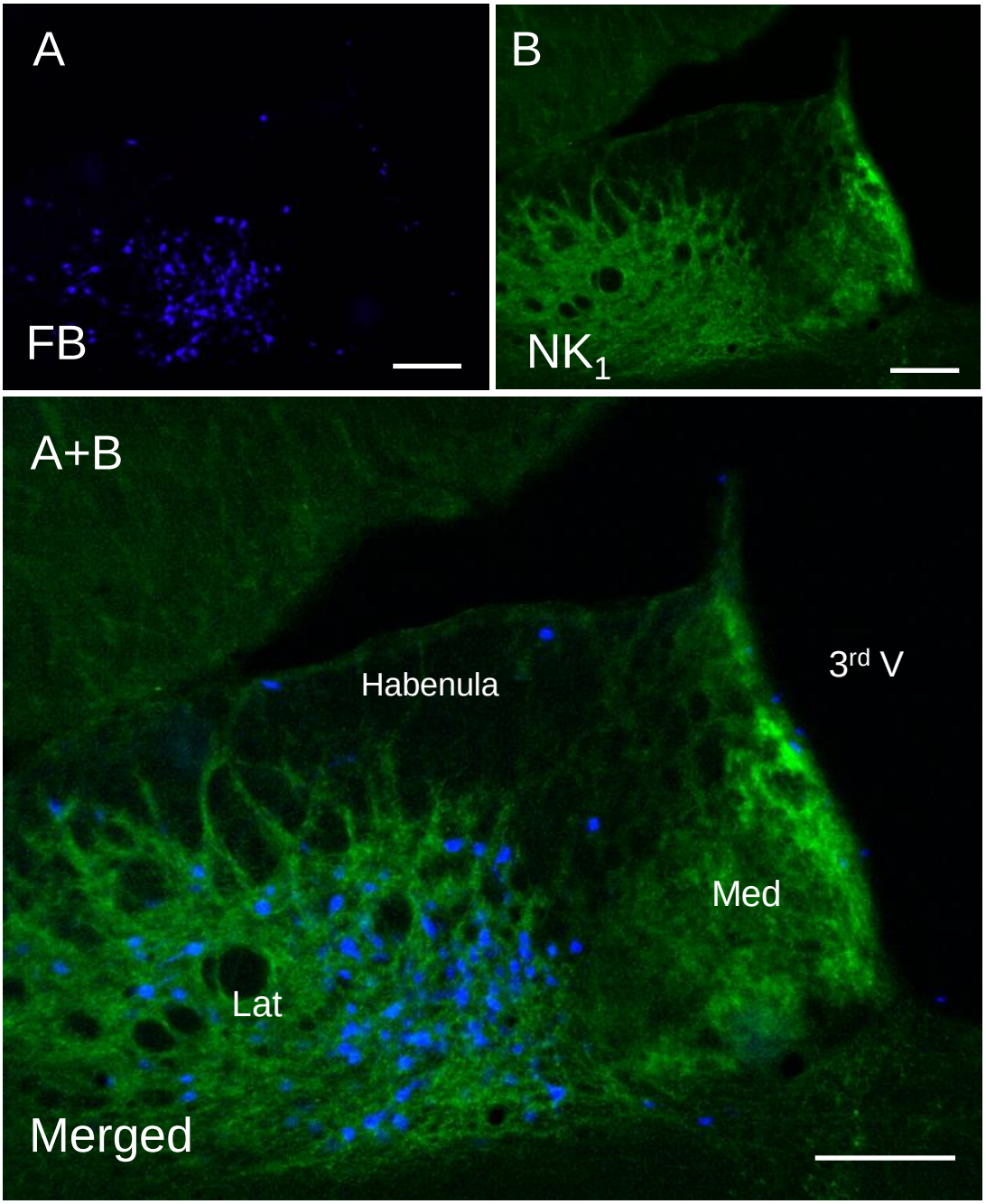


Fig. 3.10. Photomicrographs of NK_1 receptor-immunoreactivity and of neurons labeled with 'Fast Blue' in lateral habenula. Afferent neurons containing 'Fast Blue' are seen in the medial aspect of the LHb- at about -3.14 mm from bregma (A, A+B) and are seen surrounded by NK_1R-ir fibres (A+B). Colocalisation between 'Fast Blue' and NK_1R-ir is not evident. Scale bars in A, B, A+B: 30 μm. Lat=lateral; Med=medial.

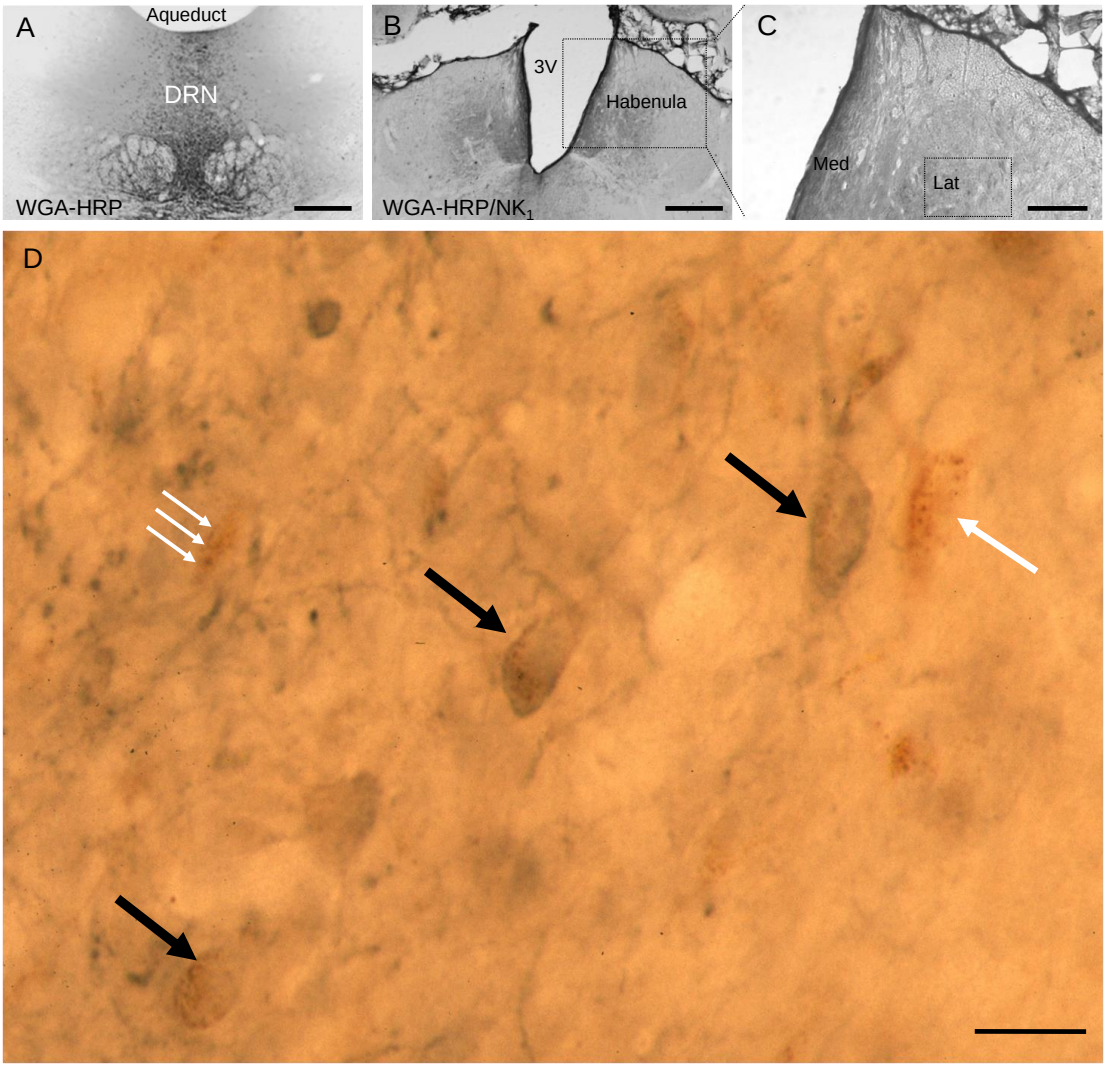


Fig. 3.11. Photomicrographs of neurons labeled with wheat germ agglutinin-horseradish peroxidase and NK_1 receptors in lateral habenula (I). The site of injection for WGA-HRP was in the DRN (A). WGA-HRP was retrogradely transported to the LHb (about -3.30 to -3.60 mm from bregma). Tissue was then processed for NK_1R-ir (B and C). A higher magnification photomicrograph of the square in B is shown in C. In turn, a higher magnification photomicrograph of the square in C is shown in D. Cells that had taken up WGA-HRP presented with brown deposits inside the soma due to the DAB reaction product. Some of these cells did not show NK_1R-ir (large white arrow), while other cells did (black arrows). These latter cells appeared to have a slate greyish/blue boundary and cytoplasm due to the Vector SG reaction, but also contained brown deposits due to DAB inside the cytoplasm and so were afferent to the DRN. Anterograde tracing of WGA-HRP was also observed by the presence of the DAB reaction product in fibres only (small white arrows). Scalebars in A: 300 µm; B: 300 µm: C: 125 µm; D: 15 µm.

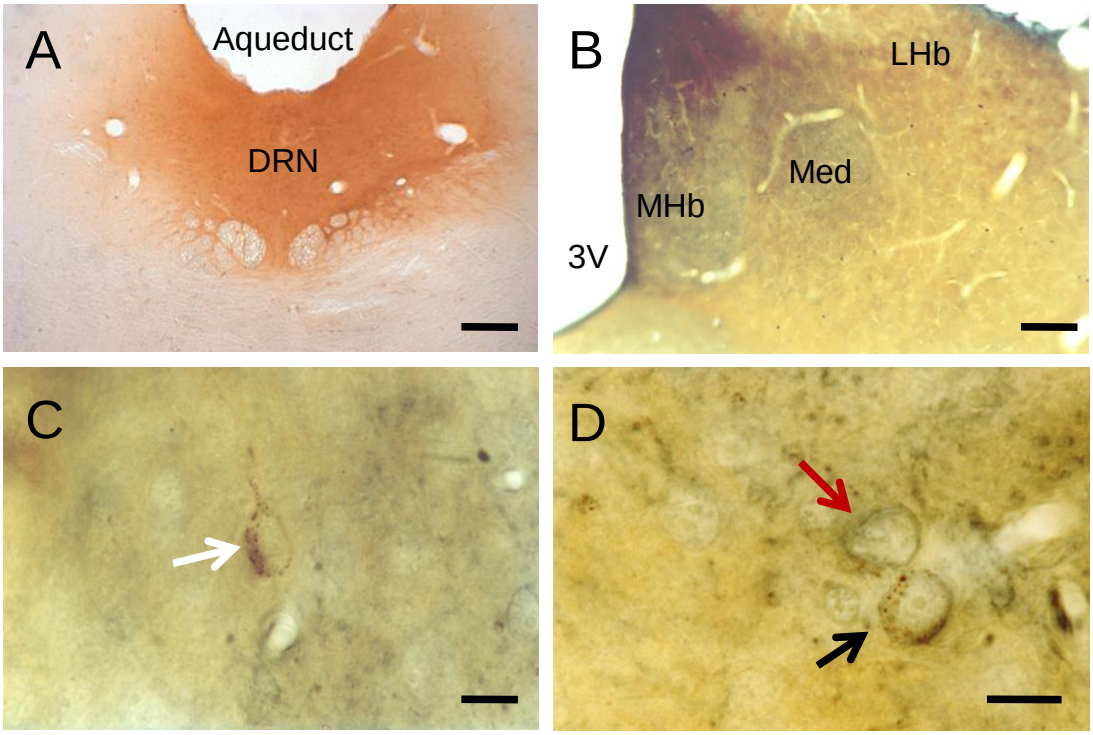


Fig. 3.12. Photomicrographs of neurons labeled with wheat germ agglutinin-horseradish peroxidase and NK_1 receptors in lateral habenula (II). The injection site for WGA-HRP was in the DRN as shown up by the DAB reaction in brown (A). WGA-HRP was then retrogradely transported to the LHb. NK_1R-ir is evident in the MHb and the medial aspect of the LHb as seen by the blue/grey colouration (B). High magnification photomicrographs of cells in the medial aspect of the LHb are seen in C and D. A cell that had taken up WGA-HRP has brown deposits inside its soma (white arrow in C). Two cells with NK_1R-ir show a slate greyish/blue boundary (D). One cell was afferent to the DRN as evidenced by brown deposits inside the cytoplasm (black arrow), while the other cell was not (red arrow). Scale bars in A: 300 μm; B: 100 μm; C: 10 μm; D: 10 μm. 3V=third ventricle; Med=medial.

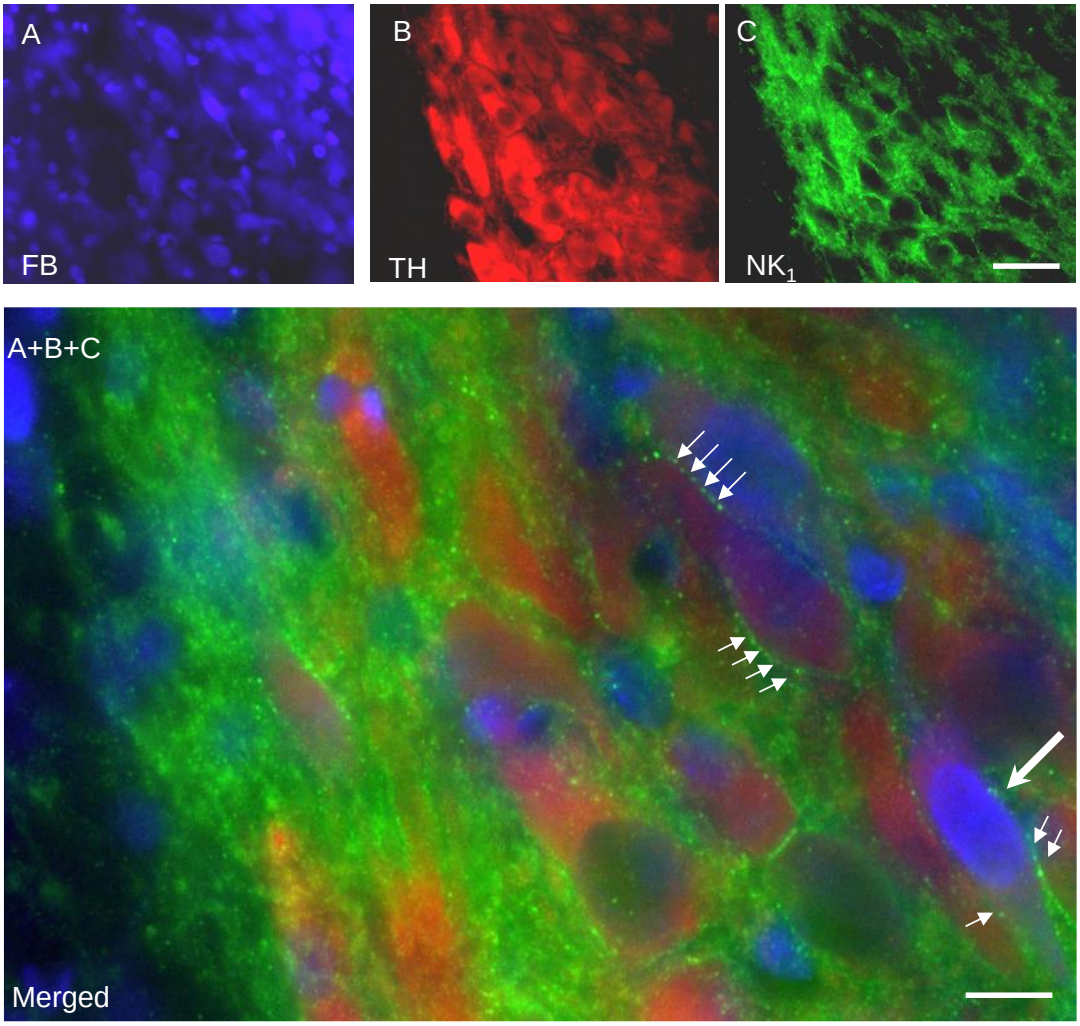


Fig. 3.13. Photomicrographs of neurons labeled with 'Fast Blue', NK_1 receptor and tyrosine hydroxylase-immunoreactivities in locus coeruleus. 'Fast Blue' was retrogradely transported into numerous neurons within the LC (A). Immunofluorescence for tyrosine hydroxylase revealed much of the LC to be composed of noradrenergic neurons (B). NK_1R-ir was also extensive within the LC, but it was unclear whether this was on fibres or on the plasma membrane (C, small white arrows in D). An afferent neuron positive for 'Fast Blue' and tyrosine hydroxylase (large white arrow) together with NK_1R-ir (small white arrows) was observed (D). Here, LC located at about -10.04 mm from bregma. Scale bars in A: 40 µm; B: 10 µm. FB= Fast Blue; TH=tyrosine hydroxylase.

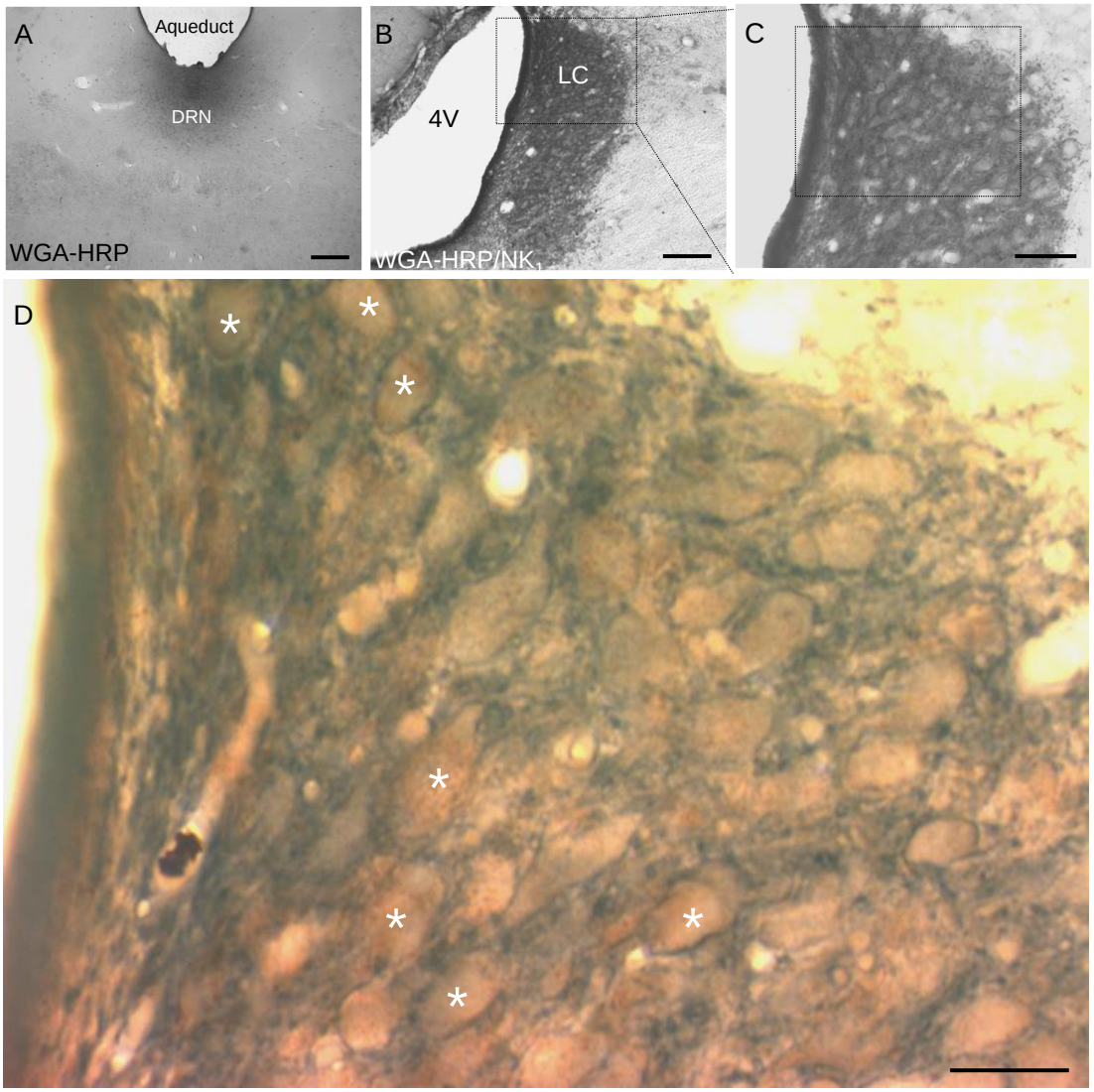


Fig. 3.14. Photomicrographs of neurons labeled with wheat germ agglutinin-horseradish peroxidase and NK_1 receptors in locus coeruleus. The injection site for WGA-HRP was in the DRN as shown up by the DAB reaction (A). Double-staining revealed extensive and dense NK_1R-ir within the LC- at about -10.04 mm from bregma (B, C, D). Higher magnification photomicrograph of the square in B is shown in C. In turn a higher magnification photomicrograph of the square in C is shown in D. Examples of afferent neurons containing the brown DAB reaction product within their cytoplasm are shown (white asterisk) with extensive Vector SG labeling for NK_1Rs surrounding them, but it was unclear whether this was on fibres or on the plasma membrane (D). Scale bars in A: 300 μm; B: 100 μm; C: 50 μm; D: 20 μm.

3.3.3. Electron microscopic examination of NK_1 receptors on afferents to dorsal raphe nucleus

Although with light microscopy it was possible to identify neurons in the LHb and LC that were either immunolabelled for, or closely apposed by NK_1R-ir profiles, it was not possible to determine whether this immunolabelling was associated with specific regions of the cell membrane, e.g. at points of synaptic contact. Hence, sections from the LHb and LC were prepared for EM examination.

3.3.3.1. NK_1 receptors on afferents from the lateral habenula

In the LHb, cells that contained WGA-HRP were identified at the light microscopic level and sections through these neurons examined in the EM. Retrogradely labelled neurons were of medium size, with deeply indented nuclei (Fig. 3.15 C and Fig. 3.16 A, D). They received a few synaptic inputs to their cell bodies. The DAB reaction product was mainly associated with cytoplasmic organelles, which was consistent with the granular appearance in the light microscope. In some retrogradely labelled neurons there were apparent accumulations of electron-dense material along the inside of the external cytoplasmic membrane. These were present in serial sections in approximately the same locations, but were not found along all of the membrane and were not associated with regions of synaptic contact (Fig. 3.15 D and Fig. 3.16 F). The accumulations resembled the reaction product for Vector SG. In one correlated example, at the light microscopic level, the neuron contained intensely brown WGA-HRP granules (Fig. 3.15 A) which related to organelles containing reaction product identified at EM (Fig. 3.15 D). The NK_1R-associated Vector SG reaction product apparently surrounded the labelled neuron at the light microscopic level, but there was no direct equivalent labelling in the EM images, although there were examples of

Vector SG-like accumulations along the membrane (Fig. 3.15 D and Fig. 3.16 F). There was no Vector SG reaction product associated with the intercellular space.

3.3.3.2. NK_1 receptors on afferents from the locus coeruleus

In the LC, retrogradely labelled neurons in the light microscope appeared as amorphous brown with some granular staining. The NK_1R immunolabel surrounded the cells and their processes (Fig. 3.17 A). In EM, these retrogradely labelled cells appeared larger than in the LHb, had relatively smooth nuclear envelopes and cytoplasm rich in organelles (Fig. 3.17 B, D) some of which were labelled with DAB reaction product. Again, along the internal side of some of the cells' exterior membranes, there were deposits of SG-like reaction product. In one case (Fig. 3.17 C) this was close to a synaptic contact, but the accumulation was located on the membrane of an adjacent structure, not one directly participating in the synapse. There was no labelling in the intercellular space.

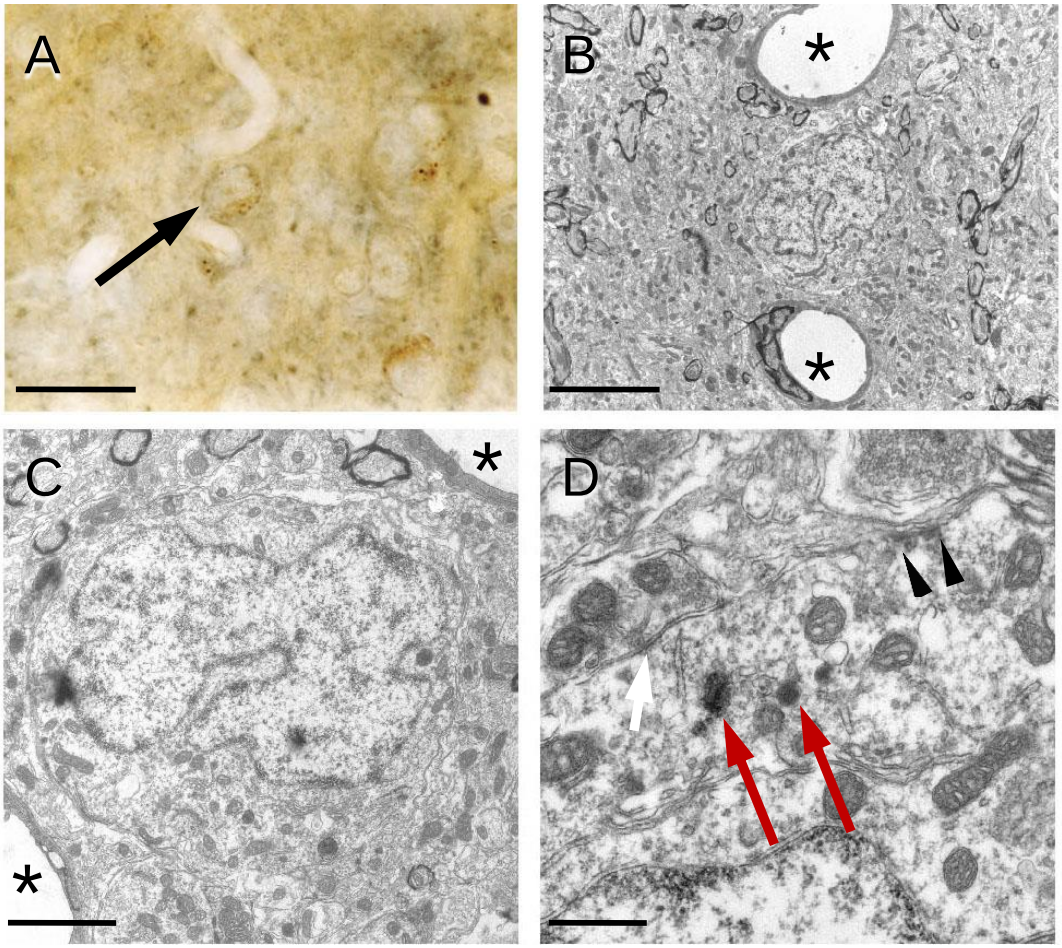


Fig. 3.15. A correlated study of a cell in lateral habenula that projects to dorsal raphe nucleus and expresses NK_1 receptor-immunoreactivity. A) Light micrograph of a cell (arrow) that contains WGA-HRP granules (brown dots) and expresses NK_1R-ir (grey Vector SG deposit in the peripheral cytoplasm). Note the capillaries immediately adjacent to this cell. B) Low power electron micrograph of the same neuron. Note the capillaries (asterisks) for orientation. C) This same neuron, slightly rotated, has a deeply indented nucleus. Note that there is no apparent labelling in the intercellular space. D) In serial section this same neuron has WGA-HRP granules (arrows) in the cytoplasm and possible SG reaction product (arrowheads) associated with the external membrane, but not at same location as the synaptic input (white arrow). Scale bars in A: 20 µm; B: 5 µm; C: 2 µm; D: 0.5 µm.

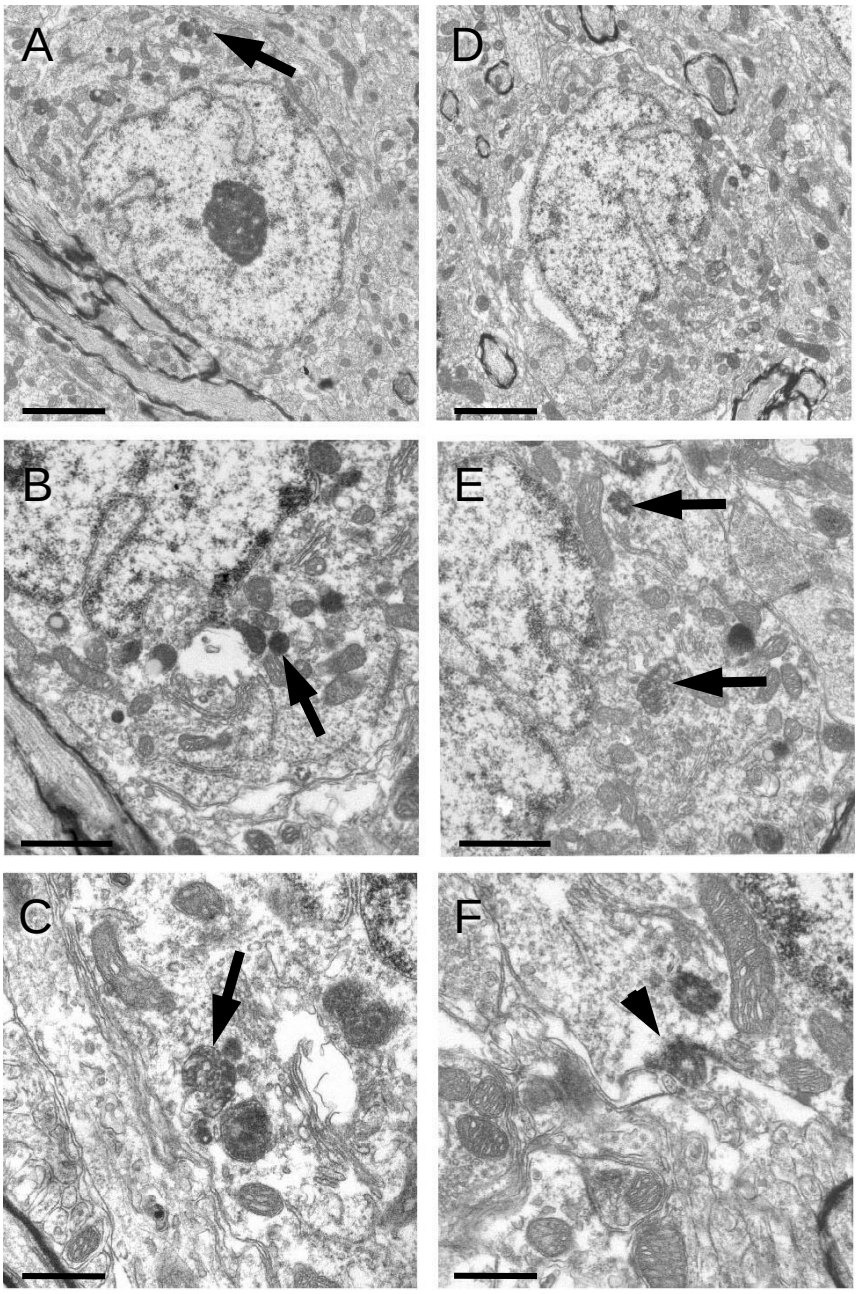


Fig. 3.16. Cells in lateral habenula that project to dorsal raphe nucleus. A) Low power EM photomicrograph of a retrogradely-labelled cell containing WGA-HRP granules (arrow). Note the deep nuclear indentations and prominent nucleolus. Also note the myelinated fibres which help with orientation and identification of this neuron in serial sections. B) Same labelled neuron at a different level, again note the WGA-HRP granules (arrow) and nuclear indentation. C) Higher power micrograph showing localisation of DAB reaction product in organelles of this neuron. D) Low power EM photomicrograph of another projection neuron in the LHb, again with a deeply indented nucleus. E) At higher power in a serial section there are WGA-HRP-labelled granules (arrows). F) A deposit of electron dense material, possibly Vector SG-reaction product (arrowhead) on the membrane of the same retrogradely-labelled neuron. Note that this labelling is not associated with any synaptic input. Scale bars in A: 2 µm; B: 1 µm; C: 0.5 µm; D: 2 µm; E 1 µm; F: 0.5 µm.

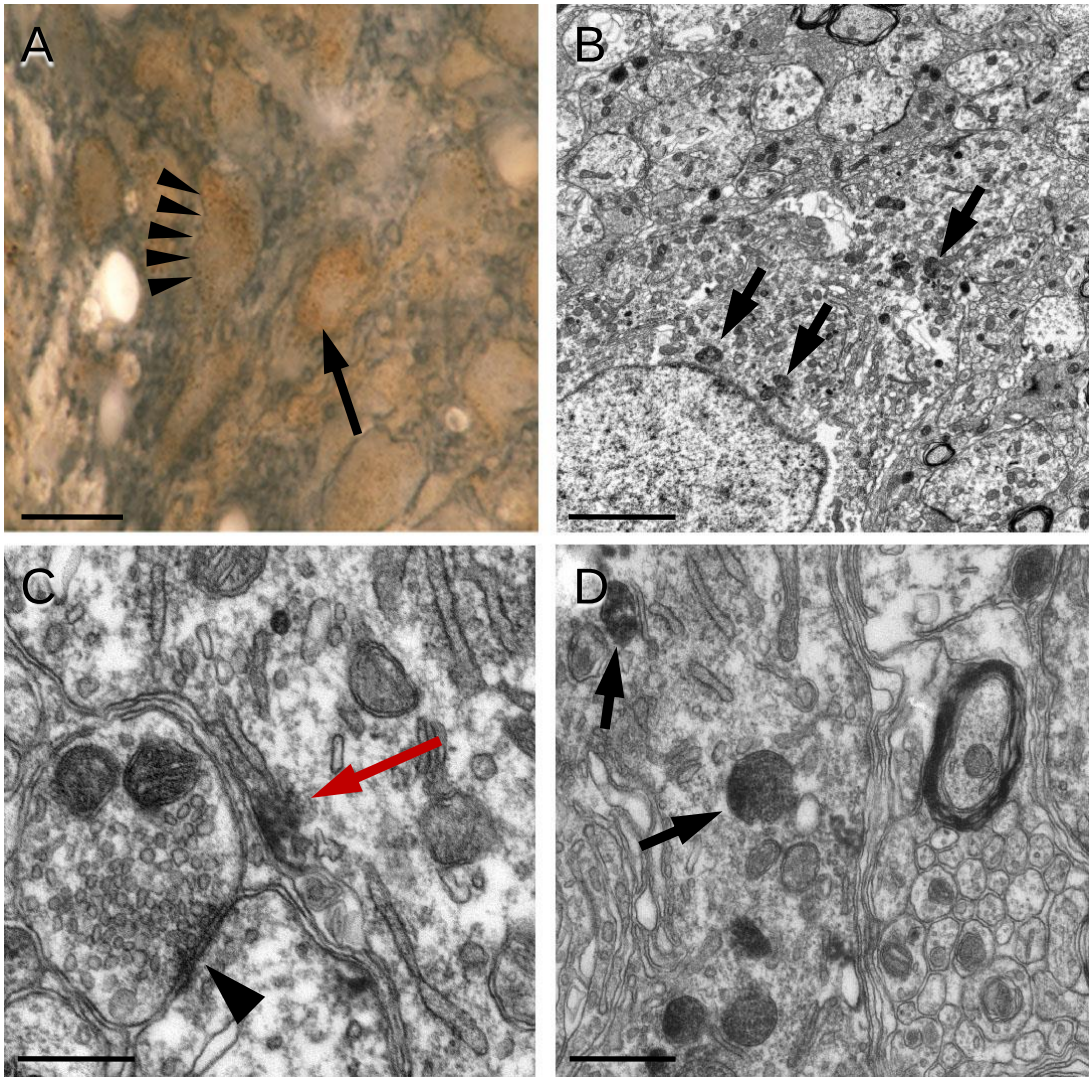


Fig. 3.17. Cell in locus coeruleus that projects to dorsal raphe nucleus and expresses NK_1 receptor protein. A) Light micrograph showing cells with brown, DAB-labelled WGA-HRP granules (arrow) and the characteristic Vector SG grey deposit around the cell peripheries (arrowheads). B) A low power electron micrograph of a part of a neuron that contains WGA-HRP granules (arrows). This cell has a relatively smooth nuclear envelope. C) High power electron micrograph showing deposit of SG-like reaction product along the external membrane of this cell (red arrow). Note that a synaptic bouton (arrowhead) is near this labelling, but not associated with the NK_1R-labelled membrane. D) A high power electron micrograph showing DAB reaction product in organelles of this projection neuron. Scale bars in A: 40 µm; B: 2 µm; C: 30 nm; D: 0.5 µm.

3.3.4. Confocal microscopy for NK_1 receptors on tyrosine hydroxylase immunoreactive neurons in the locus coeruleus

Double immunofluorescence labelling for NK_1R and tyrosine hydroxylase with confocal microscopy in the LC showed that NK_1R-ir was not simply non-specific labelling in the extracellular space, or on fibres in the region, but present on plasma membranes of tyrosine hydroxylase positive cells (see Fig. 3.18).

3.3.5. Immunoreactivity for tyrosine hydroxylase in the locus coeruleus

Immunohistochemistry for tyrosine hydroxylase immunoreactivity within the LC showed extensive and dense staining throughout much of the nucleus, helping to identify the nucleus in further experiments (Fig. 3.19).

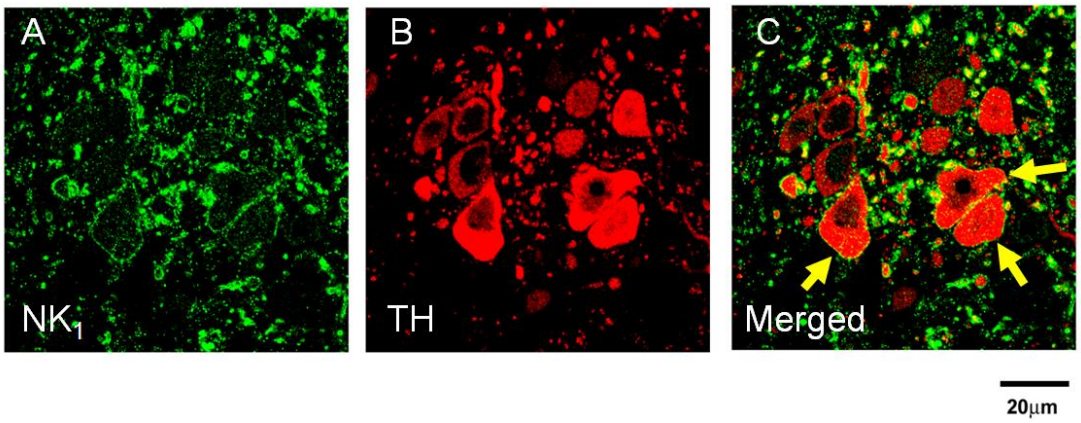


Fig. 3.18. Confocal photomicrographs of cells in locus coeruleus colocalising tyrosine hydroxylase and NK_1 receptor immunoreactivities. Extensive NK_1R-ir is observed in the LC (A). Similarly many of the cells in the LC are observed to show tyrosine hydroxylase-ir (B). Merged microphotograph suggests that the NK_1R-ir is on the plasma membranes of tyrosine hydroxylase-ir cells (yellow arrows in C). LC at about -10.04 mm from bregma. Scale bar: 20 μm. TH=tyrosine hydroxylase.

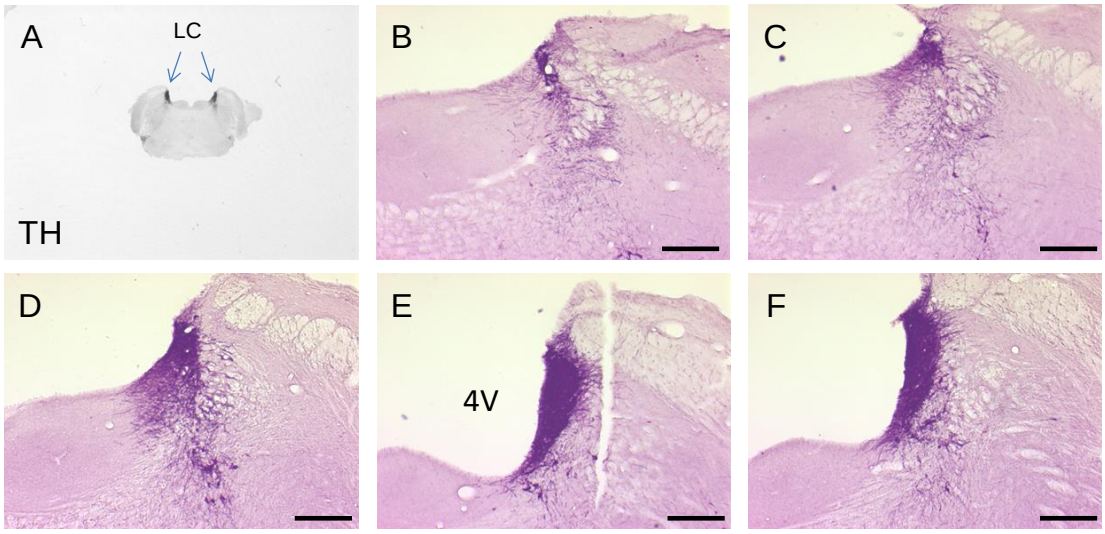


Fig. 3.19. Photomicrographs of tyrosine hydroxylase immunoreactivity in the locus coeruleus. The LC is a bilateral nucleus that can be identified with tyrosine hydroxylase-ir (blue arrows in A). Higher magnification photomicrographs of the LC in one hemisphere from bregma -9.16 to -10.04 showing the extent of the VIP reaction product (very intense purple) representing tyrosine hydroxylase-ir throughout the LC (B to F). Scale bar: 300 µm. 4V=fourth ventricle; TH=tyrosine hydroxylase.

3.4. DISCUSSION

The main experiments in this chapter used neuroanatomical tracing combined with NK_1R immunohistochemistry to investigate localisation of NK_1Rs on PFC, LHb and LC neurons afferent to the DRN. Initial experiments used the fluorescent tracer 'Fast Blue' at the light microscope level. In later experiments, immunohistochemical methods at both light and EM levels were utilised with the tracer WGA-HRP.

The main findings of this study were: 1) NK_1Rs were found present on DRN afferent neurons within the LHb and LC, 2) NK_1Rs were not found on DRN afferent neurons in the PFC, but were found in close proximity to them.

3.4.1. Localisation of NK_1 receptors on neurons afferent to dorsal raphe nucleus

3.4.1.1. Afferents from lateral habenula

Retrograde tracing with DRN injections of 'Fast Blue' or of WGA-HRP resulted in tracer transport to cells bodies of neurons within the medial LHb. However, there were discrepancies between the methods as to whether these neurons expressed NK_1R-ir. Immunofluorescence revealed extensive NK_1R-ir fibres surrounding afferents identified by 'Fast Blue', whereas immunohistochemistry at light and EM levels, revealed double-labelling of neurons for NK_1R-ir and WGA-HRP, suggesting that some of the LHb cells that project to DRN are immunoreactive for NK_1Rs. Interestingly, the origin of the SP fibres within the lateral LHb is from the rostral EPN, while that of the medial LHb is from the dorsal part of the MHb (Murakami et al 1989; Ronnekleiv and Kelly 1984; Shinoda et al 1984).

3.4.1.2. Afferents from locus coeruleus

Retrograde tracing from the DRN with either 'Fast Blue' or WGA-HRP resulted in transport of tracer to neurons in the LC, with some of the neurons being NA in origin. There was also close apposition between NK_1R-ir fibres and the cell membranes of the LC cells. Moreover, using immunohistochemical double labelling, some of the projection cells appeared to express NK_1Rs. This was confirmed at EM, where in serial sections, immunoreaction product appeared associated with cell membranes, albeit not at synaptic specialisations. Interestingly, NK_1Rs have also been observed on non-synaptic parts of the plasma membrane in other brain regions e.g. trigeminal dorsal horn (Aicher et al 2000), medullary dorsal horn (Li et al 2000a), striatum (Lee et al 1997; Li et al 2000b), hippocampus (Wittner et al 2006), PAG (Barbaresi 1998), pre-Botzinger complex (Liu et al 2004) and caudal DRN (Lacoste et al 2006). Thus, suggesting that SP may act in a diffuse, non-synaptic manner (Mazzone et al 1997; Zoli et al 1998).

Further confirmation that NK_1Rs are found on cell membranes of NA cells in the LC came from confocal microscopy for NK_1R-ir and tyrosine hydroxylase-ir (Fig. 3.18). This was a replication of a previous study (Hahn and Bannon 1999) and supported by another study where SP-ir axon terminals formed synapses with dendrites of catecholaminergic neurons (Pickel et al 1979). Previous studies have also suggested a topographical organisation for afferent projections to the DRN. For example, Kim et al. found reciprocal connections between DRN subdivisions and the LC (Kim et al 2004). In addition, Peyron et al. showed the strongest projection from the LC to the DRN was mostly to the dorsal parts of the rostral DRN (Peyron et al 1996). Similarly, in this chapter, a small injection site in the dorsal DRN (see Fig. 3.6A) resulted in

afferent labelling in the LC (see Fig. 3.14 and 3.17). However, not all of the cells in the LC that are afferent to the DRN are NA in origin. These cells tend to be smaller (10-15 µm) than the tyrosine hydroxylase-ir positive cells (15-25 µm) (Peyron et al 1996).

Thus, some of the cells in the LC that project to DRN show NK_1R-ir and consequently physiological or pharmacological action on NK_1Rs on these particular neurons may affect the function of the DRN 5-HT system.

3.4.1.3. Afferents from prefrontal cortex

Retrograde tracing with injections of 'Fast Blue' in the DRN resulted in uptake of tracer in the cells bodies in infralimbic cortex, prelimbic cortex, cingulate cortex, ventral orbital cortex and lateral orbital cortex. In the medial PFC, these pyramidal-like cells are found in layers III and V. There was no colocalisation between NK_1R-ir and 'Fast Blue'. The pyramidal nature of the projection neurons was confirmed using WGA-HRP injections, with TMB as the chromogen. Initial double labelling experiments with TMB for WGA-HRP and DAB for NK_1R-ir were not successful and in view of the clear results with 'Fast Blue', they were not pursued. Nevertheless, location of retrogradely labelled cells in the PFC was consistent with previous studies in rat and monkey (Arnsten and Goldman-Rakic 1984; Hajos et al 1998).

Lack of colocalisation between NK_1Rs and PFC afferents to the DRN is consistent with other studies. For example, PFC afferents are known to be largely glutamatergic pyramidal cells (Lee et al 2003), while NK_1Rs are found on GABAergic cells, in particular SOM-positive neurons (Kaneko et al 1994; Nakaya et al 1994). The

findings in this chapter also tally with those of chapter 2 where colocalisation between NK_1Rs and 5-HT_{2A}Rs within the PFC was found to be minimal. This may be explained by the fact that 5-HT_{2A} Rs within the PFC are mostly located on glutamatergic neurons (Willins et al 1997). Thus, although NK_1Rs are not localised on DRN afferents in the PFC, it is possible that they may yet influence these glutamatergic afferents via actions on modulatory GABAergic neurons.

3.4.2. Technical considerations

3.4.2.1. Retrograde labelling

The results of retrograde tracing obtained in this chapter resembled those of previous studies (Peyron et al 1996; Peyron et al 1998) confirming projections from the LHb (Aghajanian and Wang 1977; Kalen et al 1985; Peyron et al 1998) and LC (Peyron et al 1996). These observations were confirmed by anterograde tracing studies (Hurley et al 1991; Sesack et al 1989). Although, a previous study showed comparable results for 'Fast Blue' and HRP in tracing thalamo-cortical neurons (Aschoff and Hollander 1982), data obtained with different tracers differs depending upon the fixative used, molecular size of the tracer, solubility, injection method, volume administered and the size of the injection sites (Ader et al 1980; Ding et al 2001).

The methods of fixation with 'Fast Blue' and WGA-HRP were necessarily different and this may partly explain the differences in the results obtained. Perfusion with paraformaldehyde leads to good preservation of enzymes in immunohistochemistry (Berod et al 1981), but with increasing concentrations it reduces the visualisation of HRP-based tracers (Rosene and Mesulam 1978). Glutaraldehyde, on the other hand, gives better preservation of the enzyme activity of WGA-HRP (Malmgren and Olsson

1978; Rosene and Mesulam 1978). However, it can destroy the luminous power of fluorescent dyes, which is why only paraformaldehyde was used for fixation with 'Fast Blue'. In addition, most fixatives reduce the optimal enzymatic activity of HRP even after short fixation times. Nevertheless, HRP localisation is compatible with some variation in the fixatives (van der Want et al 1997). In this chapter, storage of tissue over a prolonged period was avoided and pre-perfusion with saline was always used to wash out erythrocytes to produce satisfactory fixation. Examination of tissue is difficult if erythrocytes are present as they express peroxidase enzymatic activity and stain brown with DAB. In addition, brain tissue may have endogenous peroxidase activity that is only denatured with good fixation. A proper perfusion is also essential, as poor perfusion would lead to enhanced overall background activity. In addition, excessive blood cells at the injection site may endocytose the injected WGA-HRP and reduce the amount of transported tracer resulting in weaker labelling (van der Want et al 1997).

'Fast Blue' has been used in the rodent and cat brain as it is able to travel rapidly and efficiently over long distances (Bentivoglio et al 1980) at rates < 110 mm per day (Itaya and van Hoesen 1982; van der Want et al 1997). The fairly low solubility of 'Fast Blue' prevents excessive diffusion from the injection site and overt changes in size with differing post-injection survival times. However, 'Fast Blue' can fade over time or on exposure to light, and could be partially washed out with further incubations (e.g. receptor immunofluorescence), which may lead to an under-estimation of retrogradely-labelled cells. In addition, tracing with 'Fast Blue' may result in glial labelling, which represents tracer leakage from labelled neurons (transneuronal labelling). However, this is reduced by keeping post-injection survival

times to a minimum and maintaining specimens under 4 °C (Bentivoglio et al 1980). Also, although anterograde transport with 'Fast Blue' may occur, it is not associated with neuronal labelling (Bullier et al 1984). Despite the above, previous retrograde tracing with 'Fast Blue' from the parabrachial nucleus, combined with NK_1R immunofluorescence using the anti-rabbit primary antibody, did show successful double-labelling in the medullary dorsal horn (Li and Li 2000).

Compared with other tracers, e.g. cholera toxin B subunit (Peyron et al 1996; Peyron et al 1998), WGA-HRP produced a well-circumscribed injection site. However, the apparent size of the injection site depends upon the amount of tracer injected, the area of injection and the survival time after the injection, as well as the chromogens used (van der Want et al 1997). Despite some diffusion here, previous studies suggest that retrograde transport of WGA-HRP occurs mainly from the core injection site (Allen and Hopkins 1998). Hence, the LHb was not labelled with a smaller injection site, where the core was confined to the dorsal DRN, whereas injection sites with larger cores that included more ventral and caudal DRN (Fig.3.6B), did label cells in the LHb. This topography suggests that afferents from the LHb may preferentially target certain subdivisions of the DRN. This is in contrast to the suggestion that the LHb projects to all of the subdivisions of the DRN (Peyron et al 1998). However, other factors may come into play, e.g. slow injections with WGA-HRP were much more likely to result in retrograde labelling than other injections. In addition, WGA-HRP is less absorbed and transported via fibres of passage (Kim et al 2004). Nevertheless, the dimensions of the injection site did vary between animals, possibly due to micropipette tip size variations and tissue conditions.

WGA-HRP has a strong affinity for *N*-acetylglucosamine in the plasma membrane and undergoes active receptor-mediated uptake and adsorptive endocystosis (Gonatas et al 1979). Retrogradely transported WGA-HRP is found in lysosome-like vacuoles and Golgi-apparatus. These vesicles fuse and accumulate WGA-HRP in high densities making them easier to visualise (Broadwell et al 1980). On the other hand, dendritic labelling is less complete (Vetter and Mugnaini 1992). Also, anterograde tracing of axon terminals, might be difficult to distinguish from retrogradely labelled distal dendrites. The extent of anterograde tracing depends on the amounts of tracer used and post-injection survival times. However, in this chapter, somatic labelling with WGA-HRP allowed for successful examination of colocalisation with Vector SG.

3.4.2.2. Comparison of TMB and DAB

Although TMB may be a more sensitive chromogen than DAB (van der Want et al 1997), it requires a stabiliser to prevent loss of reaction product and to preserve ultrastructure (Holstege 1987). However, crystals are not always restricted to cellular components, and excess crystal formation may distort ultrastructure. Moreover, identification of neurites by TMB is complicated by the granular and discontinuous nature of the TMB product. In contrast, the DAB product is non-crystalline and diffuses freely through fibres allowing an even and continuous labelling. Also, the amorphous DAB reaction product remains stable at different pH values and is insensitive to temperature changes. Furthermore, despite its greater sensitivity, TMB staining is much more complicated than the DAB procedure (van der Want et al 1997).

3.4.2.3. Specificity of the NK_1 receptor antibody

The evidence for the specificity of the NK_1R primary antibody is outlined in section 2.4.3.1. It should be noted that control experiments did not result in any labelling.

3.4.2.4. Electron microscopy

WGA-HRP was labelled with a DAB peroxidase reaction product. Although it has been suggested that the electron density of DAB labelled and unlabelled lysosomal structures are very similar (van der Want et al 1997), in this study, the DAB labelled reaction product was clearly visible at EM. At light microscopic level, the reaction product from the DAB reaction was visible as an amorphous brown material, but osmication helped to produce an electron dense dark brown precipitate with a diffuse distribution visible at EM (van der Want et al 1997).

Antibodies are large molecules that do not penetrate easily into fixed tissue. However, Triton X-100 was not used to enhance penetration in EM as detergents destroy ultrastructural integrity. One method to enhance epitope retrieval would be the use of microwave irradiation (Hayat 2000; Login and Dvorak 1993), however, here a freeze-thaw method was used instead to allow antibody penetration. It is thought that the ice crystals, slightly larger in volume than the water they replace, disrupt the cell membrane allowing better antibody penetration. This freeze-thaw method was used successfully with the LC tissue sections, but required modification for the LHb: double-freeze thaw and longer incubation with the primary antibody. This was however at the expense of loss of some ultrastructure (see Fig. 3.15 and Fig. 3.16).

With double immunohistochemistry deposition of the first peroxidase reaction product may hinder the deposition of the second within the same neuron (steric hindrance), leading to false negatives. However, retrograde labelling using DAB has been successfully combined with immunohistochemistry using Vector SG in other brain regions (Hussain et al 1996). Vector SG can be distinguished in the EM as it forms a characteristic fine grainy deposit over labelled profiles (Hussain et al 1996). In fact, although NK_1Rs have been examined at EM using other methods e.g. immunogold-silver staining (Aicher et al 2000; Commons and Valentino 2002; Lacoste et al 2006; Li et al 2000a; Liu et al 2004; Pickel et al 2000) or DAB reaction (Barbaresi 1998; Wittner et al 2006), the Vector SG method was effective and simple to apply. In comparison, the pre-embedding immunogold technique is known to be less sensitive than the immunoperoxidase reactions (Lacoste et al 2006). In most CNS regions studied, the NK_1R has been described as a membrane-bound receptor (Commons and Valentino 2002; Mantyh et al 1995; Ribeiro-da-Silva and Hokfelt 2000), except for the caudal DRN where it was also observed in the cytoplasm (Lacoste et al 2006). However, immunolabelling in the EM can be difficult as antibody penetration is often limited and cell membranes are somewhat compromised, and small accumulations of electron density within the cytoplasm often exist. Nevertheless, in this chapter, possible NK_1R was observed as membrane-bound in both the LHb and the LC and this was confirmed on several serial sections.

3.4.2.5. Other considerations

Relatively few rats were used in this study and there was no quantitative analysis of either the proportion of projection neurons identified using the different methods, or of the proportion of projection neurons that might express NK_1R. In addition, the

barbiturate anaesthetics used may reduce uptake and transport of HRP-based tracers (van der Want et al 1997), although doses used here were not large. Nevertheless, the projections seen in this study largely agree with earlier reports, although the observations of double labelling, particularly at EM, would benefit from being repeated.

3.4.3. Functional significance of NK_1 receptors on neurons afferent to dorsal raphe nucleus

3.4.3.1. Lateral habenula

There are two different pathways from the LHb to the DRN: one is a monosynaptic GABAergic pathway (Herkenham and Nauta 1979; Park 1987), while the other uses excitatory amino acids e.g. SP or glutamate (Kalen et al 1985; Kalen et al 1986). These excitatory inputs in turn synapse onto GABA interneurons in the raphe, which inhibit 5-HT projections from the DRN (Ferraro et al 1997; Kalen et al 1986; Nishikawa and Scatton 1985; Sabatino et al 1991; Speciale et al 1980; Zagami et al 1995). Indeed, stimulation of the LHb in rats induced inhibition of 5-HT neurons in the DRN (Stern et al 1979; Stern et al 1981; Wang and Aghajanian 1977). In addition, LHb and medial PFC outputs converge onto the GABAergic neurons in the DRN (Varga et al 2003).

Reducing habenula influence may be beneficial in mood disorders e.g. ablation of the habenula blocks learned helplessness (Amat et al 2001). Similarly, habenula lesions resulted in increased 5-HT transmission and decreased immobility time on FST for rats previously exposed to CMS (Yang et al 2008). Such lesions also prevented cocaine-induced inhibition of 5-HT cell firing in the DRN (Paris and Cunningham

1994) and decreased SP levels in the DRN (Neckers et al 1979). There is also evidence for a habenulo-raphe glutamatergic pathway (Geisler et al 2003), e.g. reduced glutamate uptake in the DRN after LHb lesions (Kalen et al 1986) or increased glutamate levels in the LHb in a rat model of depression (Yang et al 2008). The habenulo-raphe projection thus serves to control 5-HT transmission.

The habenula may thus be overactivated in depression. Indeed, in a human imaging study, Morris et al. proposed that the balance between excitatory and inhibitory inputs from the LHb to the DRN may favour the excitatory pathway in depression (Morris et al 1999). In addition, electrophysiological and *c-fos*-ir studies in rodents demonstrated habenula activation in response to stress, e.g. stimulation of the tail, restraint, novel environments, or footshock (Benabid and Jeaugey 1989; Gao et al 1996; Wirtshafter et al 1994). Also, hyper-metabolism of the habenula was found in animal models of depression (Caldecott-Hazard et al 1988) and congenitally helpless rats (Shumake et al 2003). Moreover, MAOIs prevented the hypermetabolism (Caldecott-Hazard et al 1988). Thus, functional inhibition of the LHb via stimulation of its afferent fibres using deep brain stimulation may show therapeutic potential in the future (Hauptman et al 2008; Sartorius and Henn 2007).

A change in habenula activity in response to local electrical stimulation or local injection of NK_1RAs altered activity of DRN 5-HT cells (Conley et al 2002; Ferraro et al 1996) leading to changes in activities of forebrain neurons in the amygdala and cingulate cortex (Conley et al 2002). Thus, NK_1RAs via blockade of excitatory transmission from the LHb may reduce the inhibitory effects of GABA neurons on 5-HT neurons within the DRN, leading to increased 5-HT transmission.

3.4.3.2. Locus coeruleus

The functional significance of the finding of NK_1Rs on LC afferents to the DRN is best examined with reference to previous literature on the effects of SP or NK_1RA on LC neurons. For example, application of SP increased LC neuronal firing rate both *in vivo* (Guyenet and Aghajanian 1977) and *in vitro* (Cheeseman et al 1983). Physiologically, SP depolarises LC neurons by increasing an inward non-specific cation current and decreasing an inwardly rectifying K^+ current (Koyano et al 1993; Otsuka and Yoshioka 1993; Shen and North 1992). The SP-containing afferents to the LC may arise from the BNST, amygdala, hypothalamus (dorsomedial, paraventricular and lateral areas) and PAG (Ebner and Singewald 2007; Tamiya et al 1994).

The results from studies of NK_1RAs on LC neurons have been inconsistent. For example, in one study GR-205,171 did not affect extra-cellular NA in rats and gerbils (Renoldi and Invernizzi 2006), while NK_1RA, RP 67580, at the dose of 2–4 mg/kg, i.p., blocked LC activation (Allam et al 1992). However, other studies have shown an increase in the firing rate of NA neurons of the LC *in vivo* after NK_1RA administration (Blier et al 2004; Haddjeri and Blier 2000; Millan et al 2001). In another study, chronic but not acute treatment of guinea pigs with the NK_1RA, L-760,735, increased the burst firing of LC neurons *in vitro* in a similar fashion to imipramine. The mechanism was shown not to be due to α_2 receptor desensitisation of LC neurons (Maubach et al 2002). More recently, NK_1R -/- mice also showed an increase in burst activity of NA neurons in the LC compared to wild-type mice (Gobbi and Blier 2005).

Some NK_1RAs have antidepressant or anxiolytic effects that involve the LC. For example, i.c.v. administration of NK_1RAs, RP 67580 and L-760,735, prevented restraint-induced LC *c-fos* expression (Hahn and Bannon 1999). In a more recent microdialysis study, systemic NK_1RA increased NA release in the medial PFC (Millan et al 2001). In another study, local NK_1RA (L-822,429) in the LC of unstressed rats, increased NA release in the medial PFC indicating that the NA pathway from the LC is to some degree under tonic inhibitory control by SP (Ebner and Singewald 2007), perhaps via GABAergic interneurons within the LC (Iijima and Ohtomo 1988; Van Bockstaele 1998). In fact, administration of a $GABA_A$ agonist into the LC decreased NA release in the medial PFC, while the administration of a $GABA_A$ antagonist increased NA release in the medial PFC indicating that NA neurons of the LC terminating in the medial PFC are under inhibitory GABAergic tone (Kawahara et al 1999). However, rodent exposure to FST enhanced the release of SP and NA in the LC. Thus, SP changes activity of NA neurons in the LC in different ways under basal and stress conditions, respectively. Administration of L-822,429 into the LC potentiated this NA response in the LC, but abolished stress-induced increases in NA release within the medial PFC (Ebner and Singewald 2007).

Both the genetic deletion and the pharmacological blockade of the NK_1R increase 5-HT neuronal firing (Gobbi et al 2007). The increase was mediated by NA neurons: in fact a selective lesion of the NA neurons prevented the enhancement of 5-HT firing activity by NK_1RAs (Gobbi et al 2007). Also, facilitation of NA activity in the LC by NK_1R blockade (Millan et al 2001) might indirectly affect the activity of DRN neurons through α_1 receptors (Vandermaelen and Aghajanian 1983). Thus the NA system via the LC may play an important role in how NK_1RAs affect 5-HT neurons.

3.4.3.3. Prefrontal cortex

Numerous studies have suggested a role for cortico-raphe projections in 5-HT feedback regulation. More recently, *in vivo* electrical stimulation of the PFC led to inhibition of firing of DRN 5-HT neurons probably via excitation of local GABA neurons (Celada et al 2001; Hajos et al 1998; Varga et al 2003; Varga et al 2001). In this chapter however, NK_1Rs were not found on PFC afferents to the DRN. Nevertheless, NK_1Rs were present on cell bodies and fibres close to these glutamatergic output neurons. Given that NK_1Rs are present on GABA neurons within the PFC and that these GABA neurons play an important role in the control of gltutamatergic pyramidal neurons in the PFC (Freund 2003), it is thus likely NK_1Rs may modulate PFC afferents to the DRN via GABA interneurons.

3.5. CONCLUSIONS

The retrograde tracers, ‘Fast Blue’ and WGA-HRP were used to identify cell bodies in regions afferent to the DRN. Immunohistochemistry for NK_1Rs was combined to investigate cellular colocalisation. In the medial PFC, NK_1Rs were found on neurons close to but separate from those with ‘Fast Blue’ suggesting an indirect interaction. With the aid of EM, NK_1 Rs were found in the LHb and LC on neurons afferent to the DRN. Some of the afferent cells in the LC were also immunoreactive for tyrosine hydroxylase. Thus, there is neuroanatomical evidence for the localisation of NK_1Rs on afferent neurons in the LHb and LC, which in turn are positioned to influence the DRN and its 5-HT system.

CHAPTER 4

METHODS FOR QUANTIFICATION OF HUMAN NK_1 RECEPTORS USING POSITRON EMISSION TOMOGRAPHY AND [^{18}F]SPA-RQ

4.1. INTRODUCTION

Chapters 2 and 3 discussed the pre-synaptic and post-synaptic interactions between the NK_1R and 5-HT systems in the normal rodent brain. However, studies measuring NK_1Rs in the human brain have been rare and have mostly been conducted in postmortem tissue (chapter1) using a number of techniques including quantitative PCR, *in situ* hybridisation and *in vitro* auto-radiography (Caberlotto et al 2003). However, a better approach would be to study human NK_1Rs *in vivo* (Bergstrom et al 2004). In view of this, chapters 4 and 5 present data on the measurement of human brain NK_1Rs *in vivo* using PET and the radio-ligand [^{18}F]SPA-RQ. This chapter (chapter 4) describes different methods for the quantification of brain NK_1Rs in normal human volunteers. The data obtained here were then used to devise a simplified and valid protocol for use in depressed subjects (chapter 5).

4.1.1. Positron emission tomography–an overview

PET is a highly sensitive and quantitative imaging technique used in clinical and research settings. PET can examine rCBF, metabolism, and pharmacology *in vivo*, both at rest and under activating conditions (Brooks 2005). The study of brain receptors in particular requires the use of selective radioligands. These radioligands are labelled with positron emitters (e.g. carbon-11, $t_{1/2}$=20.4 min; fluorine-18, $t_{1/2}$=

109.7 min; bromine-76, $t_{1/2}$=6 hr) produced within a cyclotron. In contrast, single photon emission computed tomography has a coarser spatial and temporal resolution and lesser sensitivity compared to PET. It uses commercially available gamma-emitter radionuclides with relatively long half-lives (e.g. iodine-123, $t_{1/2}$=13.2 hr; technetium-99m, $t_{1/2}$=6 hr).

For a radioligand to be useful, its labelling needs to be stable and have sufficient affinity and high selectivity for the receptor under investigation, and low non-specific binding, rapid permeation into the brain, and few metabolites, if any. If metabolites are present in plasma, then ideally they should be polar so that they cannot cross the blood-brain barrier easily (Heiss and Herholz 2006).

A positron is a positively-charged electron which upon emission from the nucleus of for example an ^{11}C or ^{18}F combines with an electron. This process results in the production of two high energy gamma rays (511 keV) released from the site of annihilation at 180^{o} from each other. These gamma rays exit the body and are detected using a series of highly sensitive external radiation detectors placed in parallel rings around the head. Individual detectors are constructed from scintillating crystals such as bismuth germinate or lutetium oxyorthosilicate and have an amplification circuit. On entering the crystal detector the gamma rays are converted into visible photons which are amplified by a photomultiplier tube and are then converted into an electrical impulse. If the detectors linked in electronic coincidence pick up two emissions within a very short space of time one is able to make an estimate of an annihilation that occurred somewhere along a line joining the two detectors (see Fig. 4.1). With sufficient sampling of lines of events and angles, it is possible to reconstruct a 3

dimensional tomographic distribution of positron annihilation and hence radioactivity in the body. Reconstruction techniques including filter back projection are then used to create the PET emission scan.

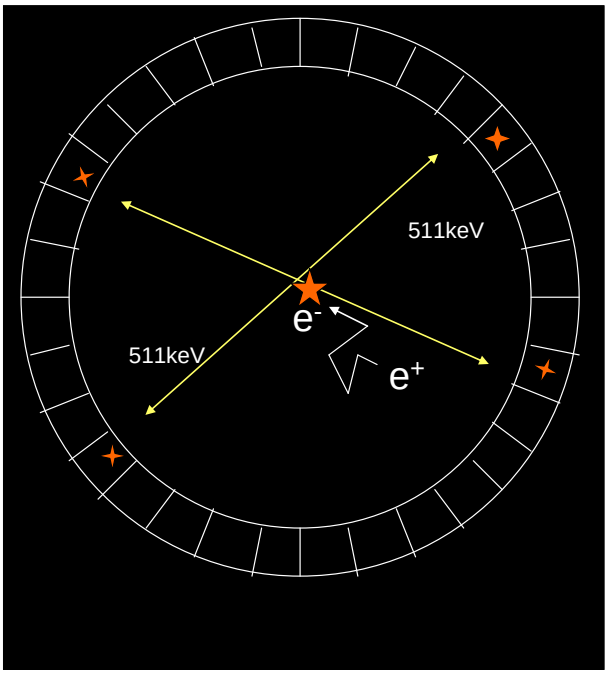


Fig. 4.1. Signal detection in a positron emission tomography camera. Schematic diagram illustrating positron (e+) and electron (e-) annihilation leading to coincident gamma ray (511 keV) release and detection of the released gamma rays by external detectors.

In addition to the emission scan, a transmission scan is usually carried out with the subject positioned in the PET camera before the administration of the radioligand and the emission scan. This usually involves rotating a point or rod source of activity with a long-lived positron emitting source such as germanium 68 / gadolinium 68. These data together with data from when there is no subject in the camera help to produce factors for the correction of attenuation of signal that occurs in the subject's head along each coincidence line of response. The camera's voxel element response can be calibrated against laboratory detectors for counting blood samples and the dose of

activity administered. Hence ligand concentrations measured in brain tissue can be recorded in the same units as those of blood or plasma samples. This enables kinetic models to be operated to derive measures of ligand binding as well as calculation of the percentage of administered dose present in a unit volume of brain tissue.

4.1.1.1. Data reconstruction

Suitable detector collimation and calibration allow the measurement of regional tissue concentration and ligand time course in the brain. From this, the fraction of administered ligand distributed to the tissue of interest and its rate of flux or sequesteration can be quantified. Then, with appropriate kinetic models, absolute rate constants for ligand exchange or turnover can be derived. It is fundamental to establish the mathematical relationship between the input function which is measured as ligand concentration in plasma, and tissue response measured as radioactivity counts in the region of interest (ROI).

4.1.1.2. Kinetic modelling

A number of analytic strategies may be employed for the *in vivo* quantification of receptors in humans (Slifstein and Laruelle 2001). These include the use of irreversible and reversible binding models, tissue ratios, equilibrium analyses, linear compartment models applied to tracer doses, and non-linear models applied to multiple injection data with varying specific activities or blocking agents (Carson et al 1993). Most commonly the brain uptake of PET radioligands is described using compartmental modelling. One of the simplest approaches is to assume that brain regions are composed of a non-displaceable, non-specific freely exchanging compartment (Cn) and a compartment where radioligand is bound specifically (Cb)

(see Fig. 4.2). Measurement of ligand concentrations in peripheral arterial blood is often used as an approximate measure of the delivery of ligand to brain tissue. This can be measured continuously via an indwelling cannula in the radial artery. In addition, serial blood samples can be used to measure ligand parent compound and metabolite components using HPLC. In some circumstances, a reference region devoid of target receptors may provide the measure for non-specific binding and remove the need for arterial sampling. More complex kinetic models might include separate brain compartments representing non-specific ligand binding, freely exchanging pools, ligand metabolism, and ligand diffusion to binding sites (Brooks 2005).

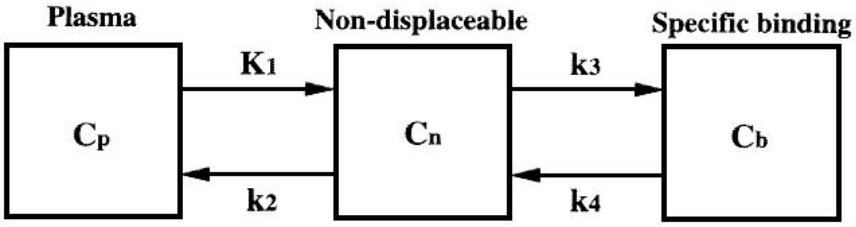


Fig. 4.2. Compartmental modelling. This model contains 3 compartments and 4 parameters (K_1, k_2, k_3 and k_4) for kinetic modelling of labelled neuroreceptor uptake and distribution in the brain. It depicts transfer of activity between the plasma compartment (**Cp**) and the 2 tissue compartments (**Cn** - non-displaceable compartment with non-specific brain uptake including free tracer within the extracellular space and **Cb** – specific binding within the target region). Fractional rate constants (K_1, k_2, k_3 and k_4) are the fractions of the concentration in one compartment moving to another compartment (min^{-1}, K_1 ml min^{-1} ml^{-1}). The parameter of interest, binding potential (BP), is defined as the rate constants k_3/k_4.

At tracer doses, the kinetic behaviour of a ligand can be described via a series of first order rate constants. The delivery rate constant from the plasma compartment (Cp) to compartment Cn is K_1 (ml/min/ml) and equals the product of blood flow and extraction fraction; k_2 (min^{-1}) defines the rate constant of return from Cn to Cp. At true equilibrium, the concentration of free tracer in tissue water equals the concentration in plasma water. The parameter k_3 is the rate constant of transfer from compartment Cn to Cb, while the parameter k_4 is the dissociation rate from the receptor (min^{-1}). A true equilibrium is however never reached after a bolus injection of a ligand.

The concentration ratio between tissue and free tracer in plasma at equilibrium is defined as the total volume of distribution (VD) which can be calculated as:

$$VD = \frac{K_1}{k_2} \cdot \left(1 + \frac{k_3}{k_4}\right)$$

The ratio of the two rate constants describing ligand passage from free to bound brain compartments, k_3/k_4, is known as the binding potential (BP). At ligand tracer doses, binding potential reflects f_2.BP or f_2. B_{max}/K_d where f_2 is the free fraction of radioligand in tissue, B_{max} the receptor availability, and K_d the receptor dissociation constant. The parameter f_2 is not usually determined experimentally, henceforth f_2.BP will simply be described as BP. The BP generally reflects the capacity of the tissue for ligand-binding site interaction (Mintun et al 1984). Also, the measurement of the BP in the presence of different levels of cold ligand together with Scatchard analysis allows the independent estimation of B_{max} and K_d. It is generally assumed that in many circumstances K_d remains unchanged, and hence measurements of BP tend to reflect changes in B_{max}.

Compartmental modelling requires an input function, which is generally a metabolite-corrected arterial plasma curve, and it also requires regional brain uptake time activity curves (TACs). If there is a brain area that can act as a non-specific brain reference region (e.g. cerebellum for NK_1R tracers or occipital cortex for opioid tracers), then arterial cannulation can be avoided as the brain reference region uptake curve can replace the arterial plasma activity input function (Lammertsma and Hume 1996). A reference region then would only be composed of a Cn compartment and there would be no Cb compartment and therefore could be explained by a one-tissue compartment model. The assumption is often also made that the level of free and non-specific binding is equal in the target regions and the reference region. In addition, sometimes graphical approaches are used to linearise brain regional TACs when non-specific uptake has reached an equilibrium with plasma.

For reversible ligands, a state of so-called 'transient equilibrium' can be reached after a bolus injection of the ligand. This occurs when a constant ratio of tissue to tissue, or tissue to blood radioactivity is maintained over time. Here, the ratio is constant because the clearance from plasma and tissue occurs at the same fractional rate (Carson et al 1993).

4.1.1.3. Region of interest analysis

An ROI analysis is often used to sample levels of tracer uptake in target brain regions. The functional PET images are often co-aligned to the subject's magnetic resonance image (MRI). The latter is often used to define ROIs by drawing object maps or by functional images being transformed into standard stereotaxic space and a predefined template of ROIs from a probabilistic atlas being applied (Hammers et al 2003).

4.1.1.4. Sources of error in positron emission tomography

Sources of error in PET (Carson 1991) include errors in ligand preparation, acquisition of tissue response, data analysis and partial volume effects. Firstly to avoid perturbations in receptor density via 'cold' ligand binding, it is important to use high specific activity (ratio of radioactive to cold compound) measurements. Secondly, errors in the recording of the primary PET data include the registration of scattered coincidences when photons scatter within the head with the line through the point of positron annihilation being wrongly defined. However, methods exist to correct for this kind of error. Care is also needed not to exceed the response of the PET camera at higher ligand doses. Thirdly, humans with the disorder of interest may handle PET ligands differently to normal human volunteers. Therefore, care is needed when interpreting PET data processed via models derived in normal tissue versus diseased tissue. Fourthly, partial volume effects may occur when the ROI is smaller than the physical resolution of the PET camera. Furthermore, errors not due to biological variation, but due to methods, can be divided into systematic errors (bias) and random errors (variance). Proper selection of methods helps to decrease errors and increase accuracy.

4.1.1.5. Limitations of positron emission tomography

Successful ligands *in vitro* may not necessarily become successful *in vivo*. This may be due to poor blood-brain-barrier penetration, high non-specific binding or rapid *in vivo* metabolism. Also, the dose of radioactivity required may not be safe in some circumstances or may not allow the study of younger subjects or women. Also, PET is very expensive and so subject numbers are not usually high in studies. Furthermore, imaging of small brain structures is often limited by the resolution of the PET scanner.

4.1.2. NK_1 receptors in the human brain in vivo

4.1.2.1. Positron emission tomography radioligands for NK_1 receptors

With the advent of non-peptide antagonists at neurokinin receptors, the possibility of studying these receptor systems *in vivo* using PET has become a real option. Indeed, so far a number of radioligands for both NK_1Rs and NK_3Rs have been synthesised (Bennacef et al 2004). Some of the radioligands that bind to NK_1Rs include [^{11}C]CP-96,345, [^{125}I]703,606, [^{11}C]CP-99,994, [^{18}F]FTP, [^{11}C]GR 203,040, [^{11}C]GR 205,171, [^{11}C]CP 643,051, [^{11}C]LY 303,870, [^{11}C]R 116,301, *N*-[^{11}C]-CP-643,051, [^{11}C]BME and [^{11}C]BMP (Bagot-Gueret et al 2003; Bender et al 2004; Gao et al 2005). However, many of these radioligands exhibited fairly low brain uptake, significant non-specific binding and extensive metabolism. For example, initial studies with [^{11}C]GR 203,040 and [^{11}C]GR 205,171 in rhesus monkeys yielded discrepant results. With [^{11}C]GR 205,171, the striatum was identified as the area with highest uptake and the signal reduced with increasing doses of cold GR 205,171. In contrast, [^{11}C]GR 203,040 showed highest uptake in the thalamus, indicating a lower ratio of specific to non-specific binding (Bergstrom et al 2000). However, autoradiographic studies with [^{11}C]R 116,301 suggest that it may become a useful PET ligand in the future (Van der Mey et al 2005).

4.1.2.2. [^{18}F]Substance P Antagonist-Receptor Quantifier

The *in vivo* PET imaging of NK_1Rs would benefit from a radioligand with high selectivity for NK_1Rs and a high signal-to-noise ratio. Indeed, [^{18}F]SPA-RQ [2-fluoromethoxy-5-(5-trifluoromethyl-tetrazol-1-yl)-benzyl]-[(2*S*,3*S*)-2-phenyl-piperidin-3-yl)amine] has been developed for imaging NK_1Rs in the living human brain using PET (Hargreaves 2002; Solin et al 2004). This compound is structurally

related to the NK_1RA, GR205,171 and has a very high affinity for NK_1Rs (h-IC_{50} = 67 pM), moderate lipophilicity (log P~1.8) and with a half-life ($t_{1/2}$) for ^{18}F of 110 min (Bergstrom et al 2004; Solin et al 2004). A number of studies indicate that this radioligand may be useful for non-invasive imaging of central NK_1Rs (Bergstrom et al 2004; Hargreaves 2002; Hietala et al 2005; Keller et al 2006; Nyman et al 2006; Solin et al 2004; Wallius et al 2007). For example, initial studies in male guinea-pigs revealed evidence of its utility in the *in vivo* setting. Here [^{18}F]SPA-RQ showed high accumulation in the caudate/putamen and cortex, with very low uptake of radioactivity in the cerebellum. Pre-treatment with an NK_1RA blocked the uptake in the caudate/putamen and cortex, indicating the uptake as specific (Solin et al 2004). Further studies in monkeys and humans have demonstrated that [^{18}F]SPA-RQ has a high ratio of specific to non-specific binding and thus deemed promising for quantitative neuro-receptor studies. Furthermore, the regional distribution of [^{18}F]SPA-RQ uptake was found to be concordant with the known densities of NK_1R sites in the human brain (Hargreaves 2002; Hietala et al 2005). In addition, Bergstrom et al. have shown that the *in vivo* signal in the human cerebellum did not change with high doses of an NK_1RA (Bergstrom et al 2004), suggesting that the cerebellum can act as a suitable reference region.

Recently, the radiation safety profile of [^{18}F]SPA-RQ was studied by quantifying its whole-body biokinetics in 4 male and 3 female healthy volunteers after the intravenous injection of about 192 ± 7 MBq of [^{18}F]SPA-RQ (Sprague et al 2007). [^{18}F]SPA-RQ exhibited very low levels of defluorination in human subjects; only marrow-rich bone structures (e.g. vertebrae, pelvis, and skull) exhibited uptake of the radioligand. In addition, blood pressure, pulse, and respiratory rates showed no

significant change from baseline. Furthermore, blood and urine tests performed 24 hr after the administration of the radioligand also showed no significant changes. Uptake of radioactivity was greatest in the lungs followed by the upper large intestinal wall, small intestine, urinary bladder wall, and kidneys. The excretion of radioactivity from [^{18}F]SPA-RQ via the urine was about twice that of the hepatobiliary route. Whole-body PET with [^{18}F]SPA-RQ suggested that the truest estimate of the effective dose of the radioligand was about 30 μSv/MBq (Sprague et al 2007). This value is not very different from those reported for many other ^{18}F-labeled PET radioligands. Thus the risks from typically injected doses of [^{18}F]SPA-RQ should be well within accepted levels for human volunteers.

4.1.3. Aims of this chapter

In view of the slow kinetics and clearance of [^{18}F]SPA-RQ, quantification based on the first 90 min would not be fully optimal. Thus the aim of the study in this chapter was to develop a PET scanning protocol and an appropriate mathematical model for the study and quantification of brain NK_1R populations in human subjects *in vivo* using the [^{18}F] SPA-RQ radioligand. Regional brain uptake curves were quantified using compartmental analyses and a comparison transient equilibrium ratio method.

4.2. METHODS

4.2.1. Radio-synthesis of [^{18}F]SPA-RQ

The precursor for [^{18}F]SPA-RQ was a gift from Merck Research Laboratories, West Point, Pennsylvania, USA. The synthesis of [^{18}F]SPA-RQ was then carried out by Dr Zhao Yongjun at the MRC Cyclotron Building similar to a published protocol (Solin et al 2004), where SPA-RQ (molecular weight 450) was radiolabelled with the positron emitter fluorine-18 (^{18}F; $t_{1/2}$ =109.8 min) in the *O*-fluoromethyl position (see Appendix A).

4.2.2. Human subjects

Six normal right-handed male volunteers were recruited. Approval was given by the UK Administration of Radioactive Substances Advisory Committee (ARSAC; study number 262-336 (14177)) for i.v. administration of circa 141 MBq of [^{18}F]SPA-RQ resulting in an effective dose of 4.2-4.8 mSv. Ethical approval was also given by the Local Research Ethics Committees of the Hammersmith, Queen Charlotte's & Chelsea and Acton Hospitals (Ethics number 00/5774). All subjects were recruited via advertising in local and national newspapers or magazines. Subjects were interviewed to exclude an Axis I psychiatric disorder on the Diagnostic and Statistical Manual of Mental Disorders-Fourth Edition (DSM-IV) (APA 1994) using the Structured Clinical Interview Schedule for DSM-IV (SCID) (First et al 1997) and were also scored on the 17-item HDRS (Hamilton 1960; Hamilton 1967). In addition, all subjects filled in a Beck Depression Inventory (BDI) (Beck et al 1961) and a Spielberger State-Trait Anxiety Inventory (STAI) (Spielberger 1983).

Only subjects between 30 and 65 years were allowed into the study. Other exclusion criteria included presence of a significant medical condition e.g. a CNS disorder, recent history (4 weeks) of substance abuse or dependence, weekly alcohol consumption > 21 units in the last 4 weeks and the use of > 10 cigarettes per day. In addition, any volunteers who had received significant radiation in the 12 months prior to the study were excluded. Subjects were only recruited after full written informed consent. All subjects were also given a physical examination before they underwent the scanning protocol. In addition, a letter was sent to their General Practitioner asking for any reason why the subject should not take part.

4.2.3. Positron emission tomography and magnetic resonance imaging scanning protocols

All scans were performed at the Hammersmith Hospital in London. All subjects had a 0.5 Tesla T1-weighted MRI scan (three dimensional [3D] image; pulse sequence radiofrequency [RF]=fast; repetition time [TR]=30 ms, echo time [TE]=3 ms; flip angle 30°; number of signal acquisitions [NSA]=1; field of view [FOV]=25 cm; matrix 152 x 256 and voxel dimensions 0.98 mm, 1.65 mm and 1.6 mm – Apollo, Marconi Medical Systems, Cleveland, Ohio, USA) for purposes of co-registration and underwent the PET scanning protocol described below (see Fig. 4.3). PET scans were performed on the high-sensitivity ECAT EXACT 3D HR++ (966) PET scanner (CTI, Knoxville, Tennessee, USA). The scans were acquired in 3D mode with an axial field of view of 23.4 cm and 95 reconstructed trans-axial image planes (Spinks et al 2000). A head-holder was used to ensure comfort and reduce head movements. Subjects were aligned in the scanner using a laser system and positioned parallel to the orbitomeatal line to include the cerebellum. After a 5 min transmission scan for attenuation and

scatter correction of subsequent 3D emission images, an average i.v. bolus of 138 MBq (range 131-149) of [^{18}F]SPA-RQ (M_w = 450 g/mol) was administered by hand over 20 sec and flushed with 10 ml of heparinised saline. The mean specific radioactivity of [^{18}F]SPA-RQ at the time of injection was 122 GBq/μmol (range 69-193) and the mean mass of injected radioligand was 580 ng (range 320-890 ng). In addition, the radiochemical purity of the injected [^{18}F]SPA-RQ ranged from 99.7% to 100%. A first emission scan was acquired in List Mode for 90 min. After 60 min, the subject was repositioned in the scanner using the laser system, skin markers and bed position co-ordinates and a second emission scan of 60 min acquired. This was followed by a further 5 min transmission scan. The transmission scans were acquired to correct for tissue attenuation using a pellet source of ^{137}Cs with 150 MBq of radioactivity (Spinks et al 2000). Post-acquisition frame re-binning was performed as follows: the first emission scan was sorted into 28 frames of variable durations, the second emission scan was framed into 6 frames of 10 min each. The dynamic studies were reconstructed using the analytic reconstruction method of filtered back-projection with a ramp filter. Attenuation and scatter corrections were applied (Spinks et al 2000). The spatial resolution of the reconstructed images in this study was 5.2 mm full width half maximum (FWHM) (trans-axial) and 5.9 mm FWHM (axial).

After injection of [^{18}F]SPA-RQ, arterial blood sampling was carried out continuously online for the first 15 min of the first emission scan with a bismuth germanate coincidence detector, together with discrete arterial blood samples taken throughout at 5, 10, 15, 20, 30, 40, 50, 60, 75, 92, 150, 180 and 210 min (Ranicar et al 1991). In addition in 4 of the 6 volunteers a further 3 discrete venous samples were taken at the last 3 time points. Samples were collected into heparinised syringes which were

dispensed into tubes for centrifugation at 2000 *g* for 2 min. Radioactivity was then measured in the separated plasma by the MRC Cyclotron Quality Control staff (see Appendix B).

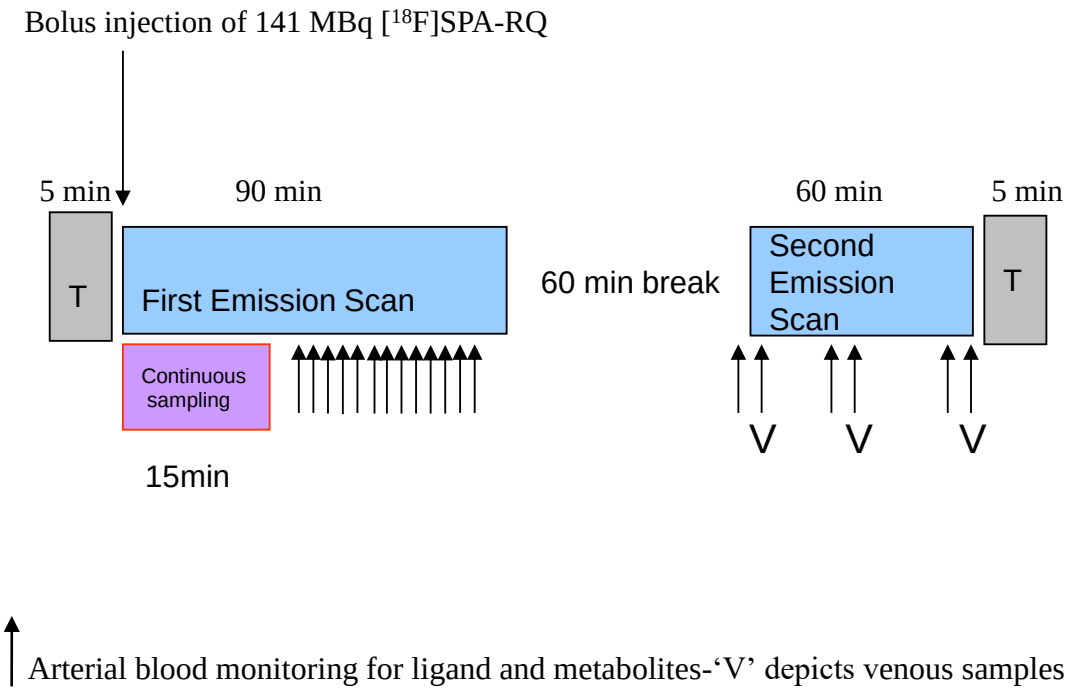


Fig. 4.3. Positron emission tomography scanning protocol for brain NK_1 receptors in normal human subjects *in vivo* using [^{18}F] SPA-RQ. After a baseline blood sample (arrow) and a 5 min transmission scan (T), all subjects were administered circa 141 MBq of [^{18}F]SPA-RQ in a bolus injection and had their first emission scan for 90 min After a break of about 60 min, they were placed in the scanner again for a second emission scan lasting 60 min. For the first 15 min after ligand injection, all subjects underwent continuous arterial sampling for the ligand and its metabolites. This was followed by discrete arterial sampling (arrows). During the second scan 4 of the volunteers underwent both arterial and venous sampling. Blood samples were used for determination of the plasma clearance of the ligand. A second 5 min transmission scan was carried out after the second emission scan.

4.2.4. Image analysis

Data analysis was performed using a ROI approach. For each subject the MRI image was re-sliced and co-registered with the PET image of summed multiple emission time frames using an automated multi-resolution mutual information optimisation procedure (Studholme et al 1997). For the first emission scan, frames were summed from the dynamic time frames acquired over 30 to 90 min. For the second emission scan, all of the time frames acquired over 60 min were summed. Regions were then defined by placing standard volumes on the MRIs.

A total of ten target ROIs were defined in both the left and the right hemispheres using the individual MRIs. These ROIs were the head of caudate (1.11 cm^3), putamen (3.15 cm^3), thalamus (3.32 cm^3), occipital cortex (11.1 cm^3) and frontal cortex (14.7 cm^3). The values in parentheses give the volume for the ROIs with the right and left hemispheres combined. A single reference ROI with a mean volume of 14.74 cm^3 was also created by summing regions placed in the left and right cerebellar hemispheres. Target ROIs were delineated on 3 to 4 consecutive slices and reference region ROIs were delineated on 5 consecutive slices. The ROI data was generated using the medical imaging software Analyze, version 6.0 (Mayo Foundation, Rochester, MN, USA).

4.2.5. Radioligand kinetic modelling

Plasma input function was generated from the continuous and discrete arterial samples and the time course of the activity concentration due to unmetabolised [^{18}F]SPA-RQ. A set of TACs were generated from the dynamic PET images. Estimates of total VDs were obtained from weighted non-linear least square fits of the TACs. A reversible

two-tissue, four rate constants (K1, k2, k3, k4) compartment model using plasma input function was applied. Estimates of micro-parameters were obtained from fits to the measured TACs, minimising the weighted sum of squares of the differences between the data and the model by the simplex method (Gunn et al 1998; Nelder and Mead 1965). Under the assumption that the VD of the free and non-specifically bound tracer is the same throughout the brain and equal to the cerebellar VD, indirect estimates of BP were obtained from f2.BP = (VD_{ROI} / VD cereb) - 1. The performance of the compartmental model was evaluated by comparing the VD and BP estimates calculated from data of emission scan 1 only with those obtained from combined data of emission scans 1 and 2. Hence, compartmental modelling with a blood input function was used to provide a standard estimate of BP.

As an alternative method of analysis, a 'transient equilibrium' calculation of activity ratios was applied (Carson et al 1993). Here the estimates are the apparent volume of distribution (VDa: calculated from the ratio of tissue activity over unmetabolised [^{18}F]SPA-RQ in plasma activity) and apparent binding potential (BPa: obtained from the ratio of activity in the target region over activity in the reference region minus one). In order to account for variations in the sampling rate over time, TAC data was weighted to give each frame equal weight according to the length and total counts in the frame. Apparent estimates using the transient equilibrium ratio method were only based on the second emission scan. Calculations were performed using MATLAB (the Math Works, Inc., Natick, MA, USA) on Sun Ultra 10 workstations (Sun Microsystems, Inc., Santa Clara, CA, USA).

4.2.6. Statistical analysis

Statistical analyses were performed using the Statistical package for Social Sciences (SPSS, Chicago, Il. USA) for windows version 15.0. Mean, standard deviations (SD) and range were calculated for the demographic data and the mood inventories. Estimates of VD and BP are presented for both the compartmental model and the ratio method. A standard error (s.e.) for each estimate was used only with the compartmental model. The mean and SD were used for the average estimates of all 6 subjects for each brain region. In addition, coefficients of variation (CV) were calculated as (SD/mean) x 100 for each brain region and comparisons made between compartmental modeling and the ratio method. A one way analysis of variance (ANOVA) for each separate brain region was used to test for differences in BP estimates obtained via the different models. Arterial versus venous activities were analysed using repeated measures ANOVA within the general linear model (GLM) in SPSS. The Greenhouse-Geisser test was used in cases with a non-significant result on Mauchly's test for sphericity. Significance was set at $p < 0.05$.

PET and MRI figures were captured using a 'snapshot' accessory on a SUN Ultra^{TM} 10 workstation (Sun Microsystems Inc., Santa Clara, CA, USA). TACs and the graph of the average parent fraction against time were produced using 'Clickfit' software in MATLAB (the Math Works, Inc., Natick, MA, USA) and 'snapshot' accessory on the SUN workstations. Other figures, graphs or charts were generated using Microsoft Excel and / or Powerpoint within Microsoft Office 2007.

4.3. RESULTS

4.3.1. Subject demographics and radioligand-related data

The demographics for the 6 healthy white male volunteers were: mean age =51.7 yrs (SD 10.5) [range=31-59]; mean weight =78.0 Kg (SD 10.8) [range=68.0-89.2]. Scores on mood inventories were: mean HDRS score =0.7 (SD 1.0) [range=0-2]; mean BDI =1.5 (SD 1.5) [range=0-4]; mean trait STAI (trait) =29.0 (SD 7.8) [range=22-44] and mean STAI (state) =28.7 (SD 10.8) [range=20-47]. Mean (SD) for activity injected =138 MBq (5.9), for specific activity =122 GBq/µmol (48) [range = 69-193] and for weight of SPA-RQ =0.58 µg (0.22) [range = 0.32-0.89]. See Table 4.1.

Table 4.1. Descriptive statistics for subjects

	Controls (n=6) mean (SD)	
Age range (years)	31-59	
Age Mean (years)	51.7 (10.5)	
Gender	male (n=6)	
Weight (Kg)	78.0 (10.8)	
BDI Score (max =63)	1.5 (1.5)	
HDRS	0.7 (1.0)	
Spielberger Trait Anxiety Score	29.0 (7.8)	(max =80)
Spielberger State Anxiety Score	28.7 (10.8)	(max =80)
Past use of antidepressants	Nil	
Activity Injected (MBq)	138 (5.9)	
Specific Activity (GBq/µmol)	122 (48)	
Specific Activity range (GBq/µmol)	69-193	
Weight of SPA-RQ (µg)	0.58 (0.22)	
Weight of SPA-RQ range (µg)	0.32-0.89	

4.3.2. Brain uptake of [^{18}F]SPA-RQ

4.3.2.1. Summed positron emission tomography scan images and magnetic resonance imaging scans

Summed PET images depicting regions of NK_1R binding with the [^{18}F]SPA-RQ radioligand together with their co-registered T1 weighted MRIs from a normal volunteer are seen in Fig. 4.4. The MRI was used to define the ROIs and co-registered to the summed PET images of the first early scan (30-90 min) and to the summed PET images of the second late scan (150-210 min). PET data was corrected for radioactive decay. The late summed PET image was based on fewer counts and noisier than the earlier summed PET image. However, the late summed PET image provided a better regional contrast. A comparison of the early and late summed PET images revealed a rapid decrease in radioactivity in the cerebellum and an increase in signal in the striatum. The highest [^{18}F]SPA-RQ activity was found in the putamen and caudate, with moderate activity in the occipital and frontal cortices and thalamus. Radioligand labelling was barely detectable in the cerebellum. The order of receptor density was in good agreement with other studies, both postmortem (Hargreaves 2002) and PET (Hietala et al 2005).

4.3.2.2. Regions of interest

The MRI and PET co-registration process allowed for accurate placing of volumes of interest / object maps onto the images. The positions of the object maps for the cerebellum are illustrated on transverse PET images in Fig. 4.5, while the positions of the object maps for target tissues (head of caudate, putamen, occipital cortex, frontal cortex and thalamus) are illustrated on transverse PET images in Fig. 4.6.

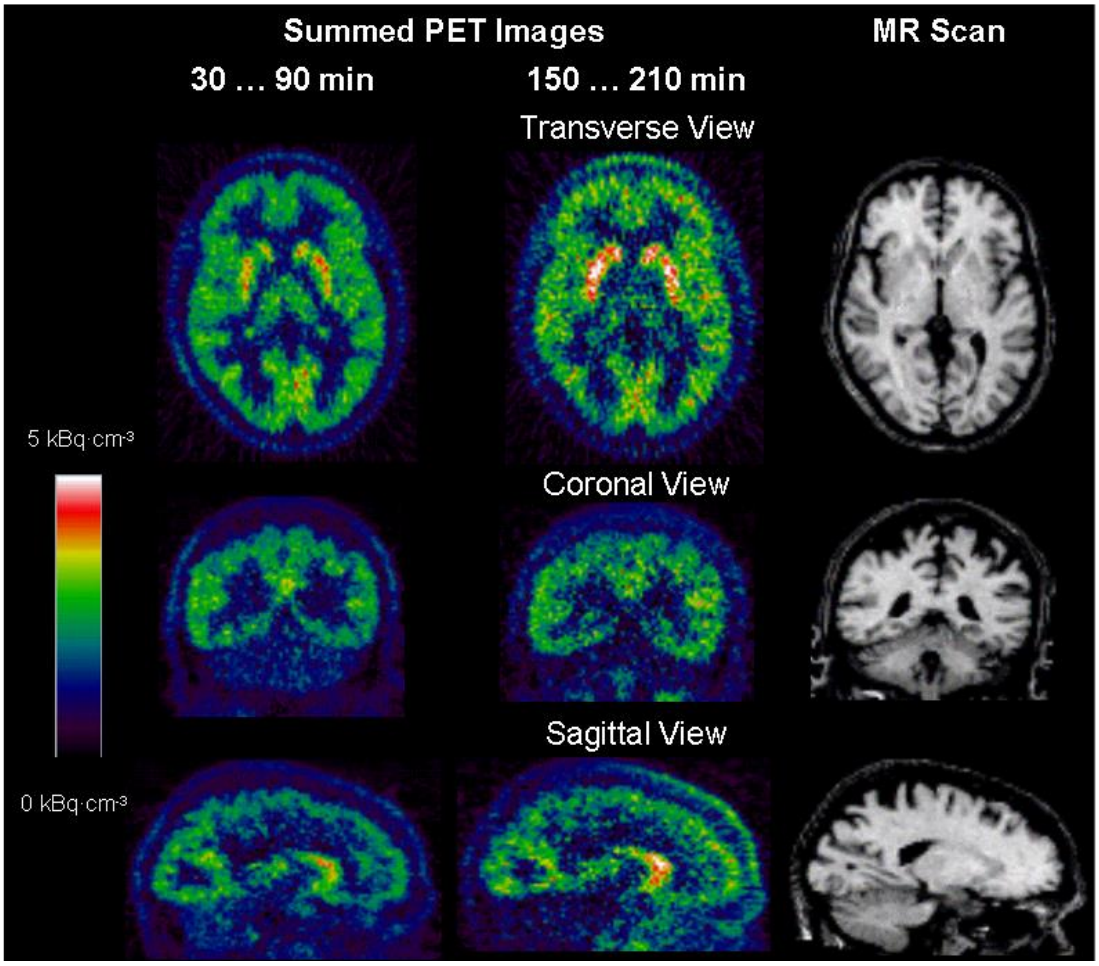


Fig. 4.4. Positron emission tomography images with [^{18}F] SPA-RQ and co-registered magnetic resonance images. PET and MRI images in one subject showing regions with NK_1R binding using [^{18}F] SPA-RQ. On the right hand side, the T1 weighted MR image is shown which was used to define the ROIs. It is co-registered to the summed image (150 … 210 min) of the second PET scan in the middle column. On the left hand side, the summed PET image (30 … 90 min) of the first scan is displayed. The PET data is corrected for radioactive decay. The late summed image is based on fewer counts and therefore noisier than the earlier summed image but provides a better regional contrast. The coronal and sagittal views show a decrease of radioactivity in the cerebellum, which acts as a reference region and an increase of signal in the striatum which is a receptor-rich region.

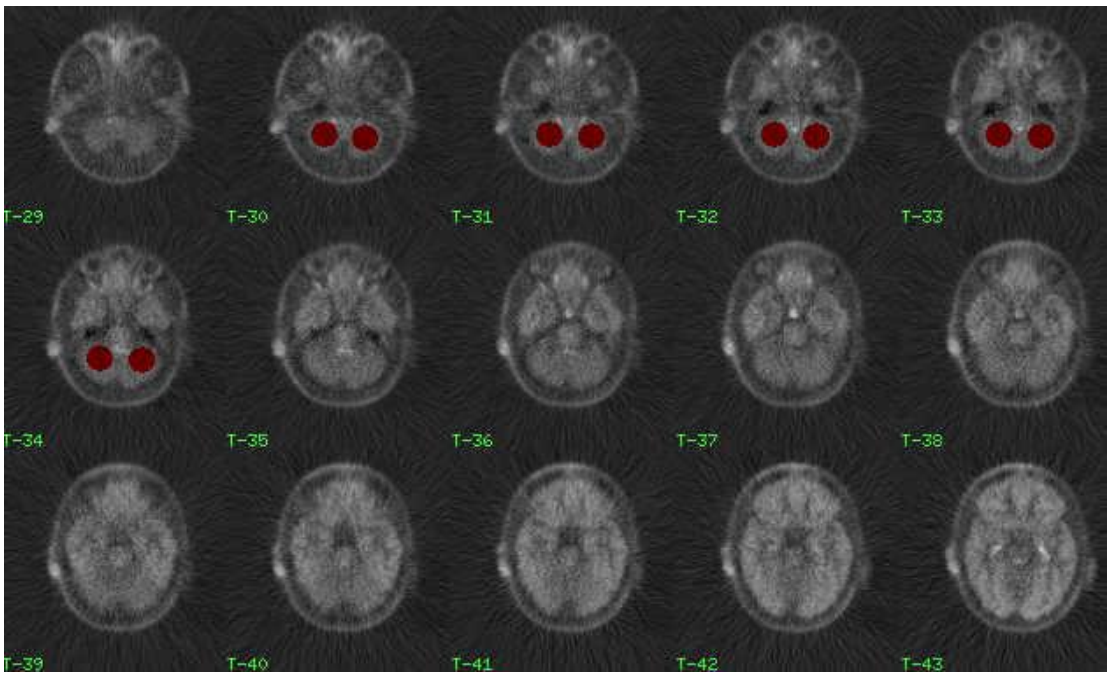


Fig. 4.5. Reference region maps of the cerebellum. Transverse PET images in one subject. The image illustrates the numbers, position and sizes of the object maps for the cerebellum (T30-T34; red).

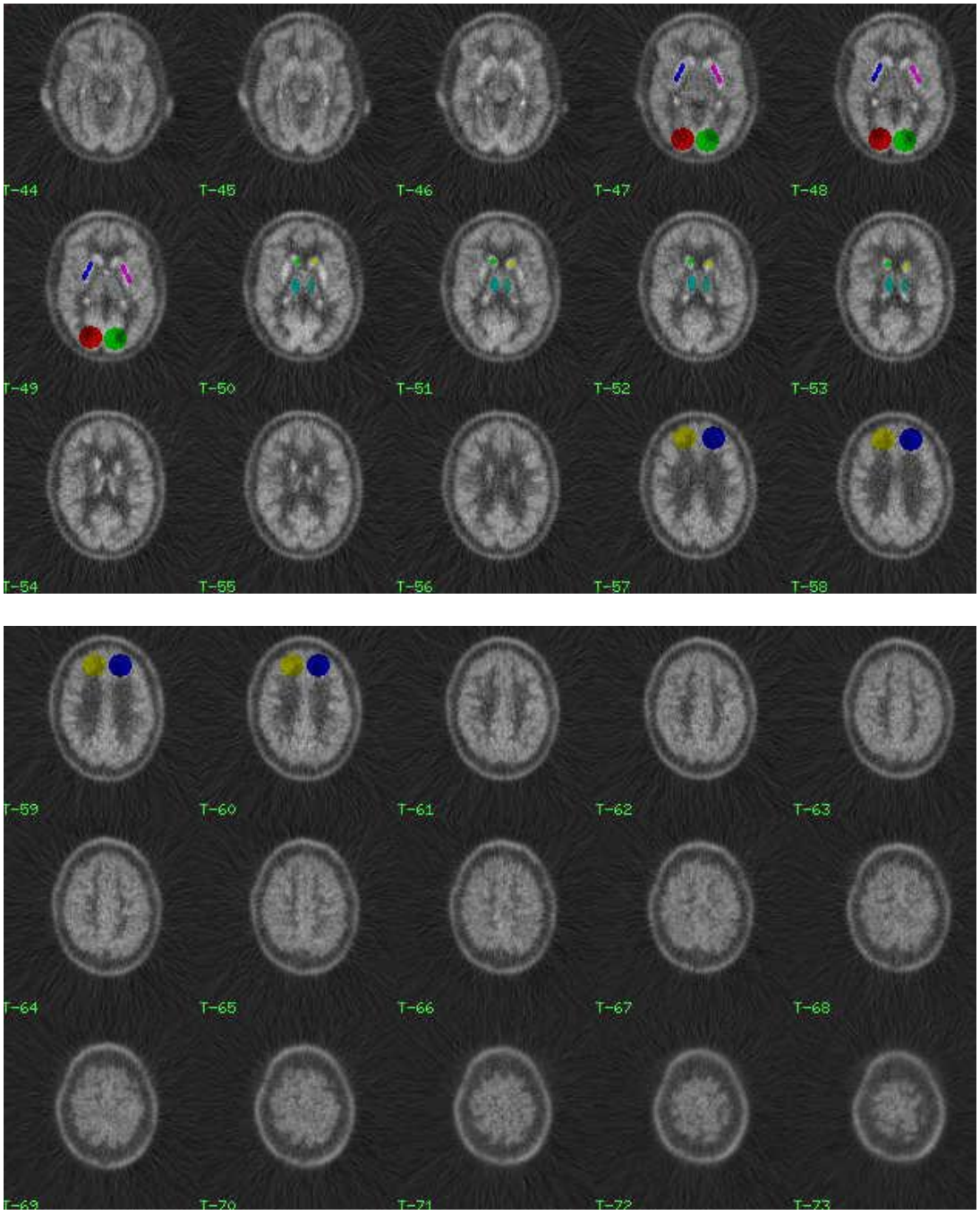


Fig. 4.6. Object maps for regions of interest. Transverse PET images in one subject. The image illustrates the numbers, the position and the sizes of the object maps for the putamen (T47-T49), occipital cortex (T47-T49), head of caudate (T50-T53), thalamus (T50-T53) and frontal cortex (T57-T60).

4.3.2.3. Regional time activity curves

Regional brain uptake of [^{18}F]SPA-RQ was consistent with the known distribution of NK_1Rs: highest in the striatal regions, moderate in cortical regions and thalamus and low in the cerebellum (see Fig. 4.7 to Fig. 4.12). Unlike the rat, a significant cortical signal in the occipital cortex was found in the human brain. Following i.v. injection of [^{18}F]SPA-RQ, during the first emission scan, decay-corrected tissue activity concentrations gradually rose in target regions such as the putamen, occipital cortex, frontal cortex and thalamus. During the second emission scan the activities in the target regions reached a peak, stabilised and then began to reduce very slowly. In contrast, the uptake in the cerebellum was low, with an initial rise and a later slow decrement of radioactivity. By the end of the second PET emission scan, the order of radioligand binding from high to low was: putamen > head of caudate > occipital lobe > frontal lobe > thalamus > cerebellum. However, in subject 1, there was more binding in the frontal lobe than occipital lobe, perhaps due to biological variation. In addition, small volumes such as the head of caudate and putamen were more likely to suffer from variation caused by head movements.

The first emission scan was corrected for attenuation using the first transmission scan. However, the second transmission scan was attenuation corrected with the first transmission scan as well as the second transmission scan. There are limitations to using either transmission scan for the attenuation correction of the second emission scan. The first transmission scan was carried out before the i.v. bolus injection of the radioligand, but with the volunteers having had a break outside of the scanner prior to the second emission scan, it is likely that they would not have been repositioned in exactly the same position as they were in for the first tranmission scan. Therefore, the

attenuation correction would be approximate and would introduce a non-systematic error. There are also errors when correcting for attenuation using the second transmission scan as this was carried out after the second emission scan. At this point radioactivity would still be present in the brain. As can be seen from the TACs, the effect of this was to lead to an overcorrection for attenuation and hence an underestimation of the brain activity. This was most marked in receptor rich regions e.g. caudate or putamen (see Fig. 4.7 to Fig. 4.12).

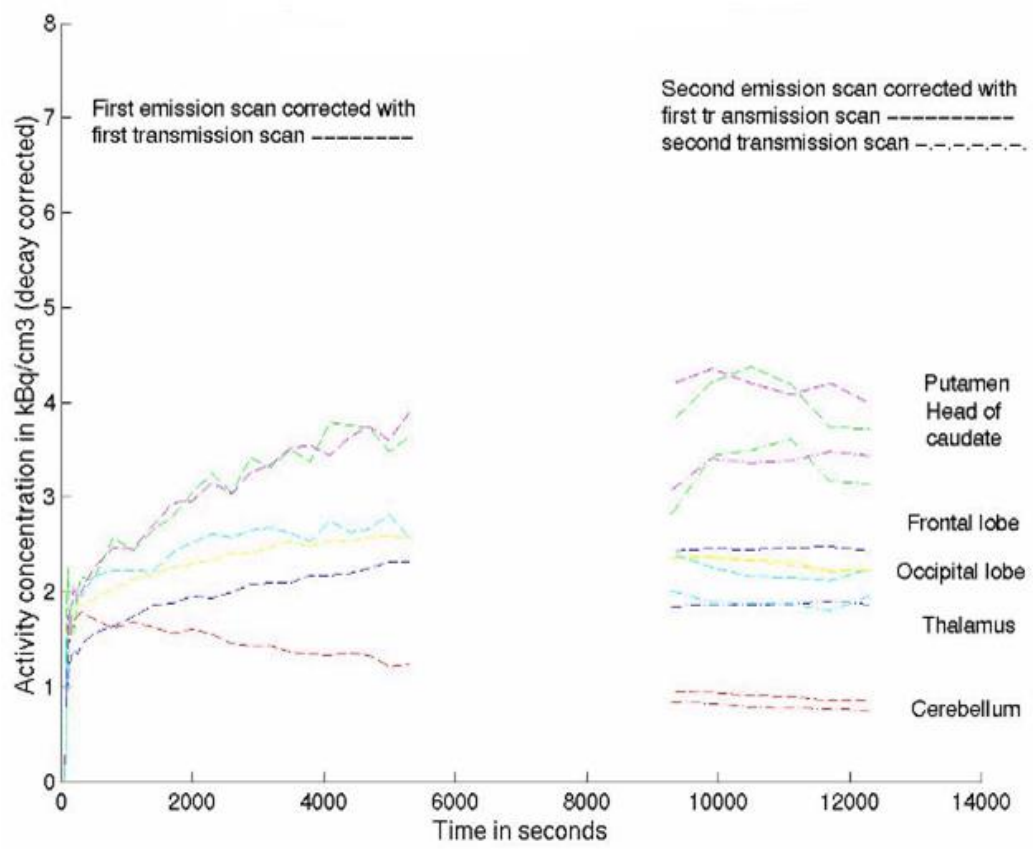


Fig. 4.7. Time activity curve of [^{18}F]SPA-RQ for subject 1. A graph of [^{18}F]SPA-RQ activity (decay-corrected) as seen in different brain ROIs against time. Uptake into the cerebellum is rapid with a small amplitude to the peak of activity and an early washout - typical of a reference region (free and non-specific binding). In contrast uptake into the putamen is much slower, but with a larger amplitude to the peak activity and a slow washout - typical of a receptor-rich area. It is clear that when the second emission scan is corrected for attenuation-correction with the second transmission scan that the activity values are markedly underestimated. This is because the ligand is present during the second transmission scan, while it is absent during the first transmission scan (see also Fig.4.9 to 4.12).

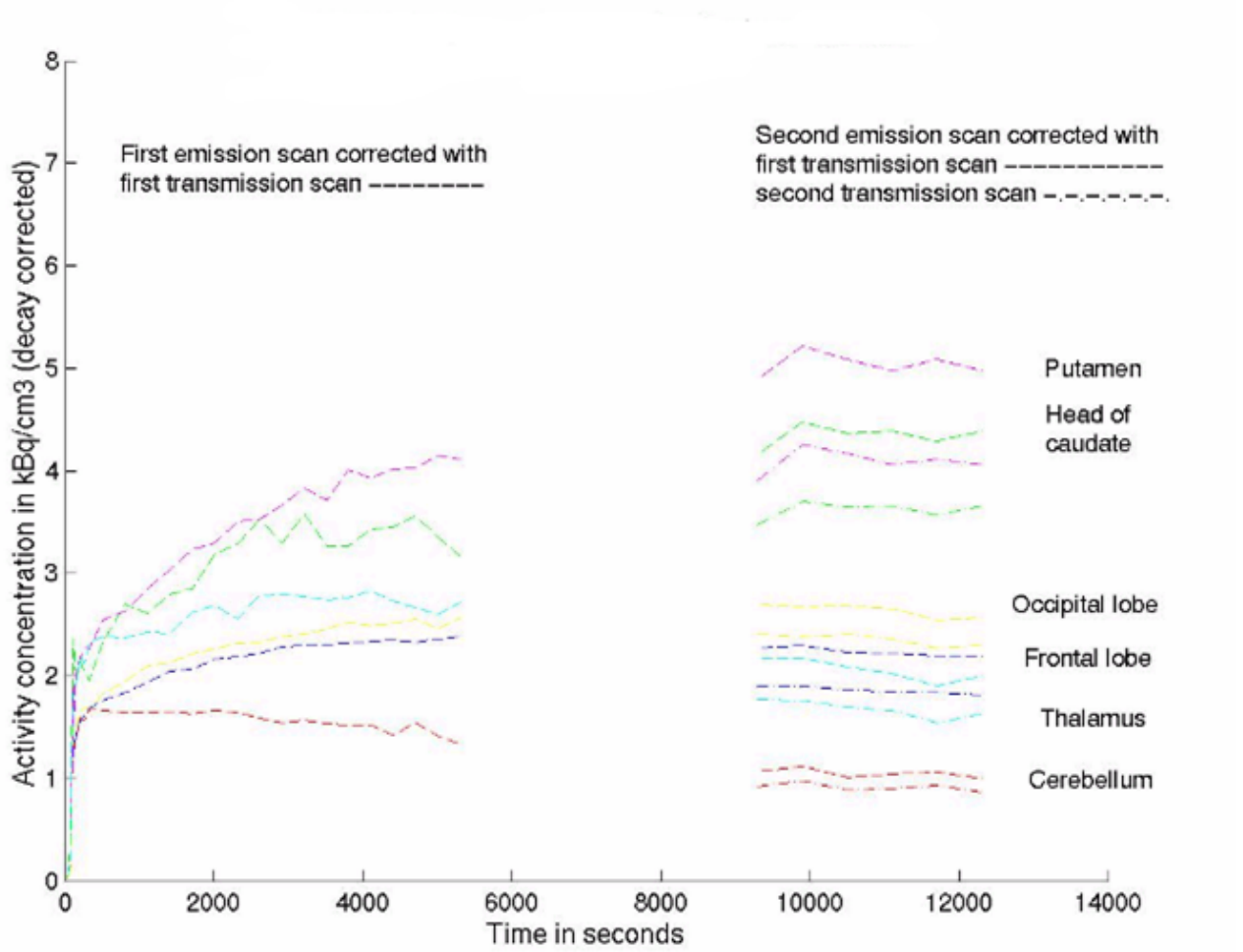


Fig. 4.8. Time activity curve of [^{18}F]SPA-RQ for subject 2.

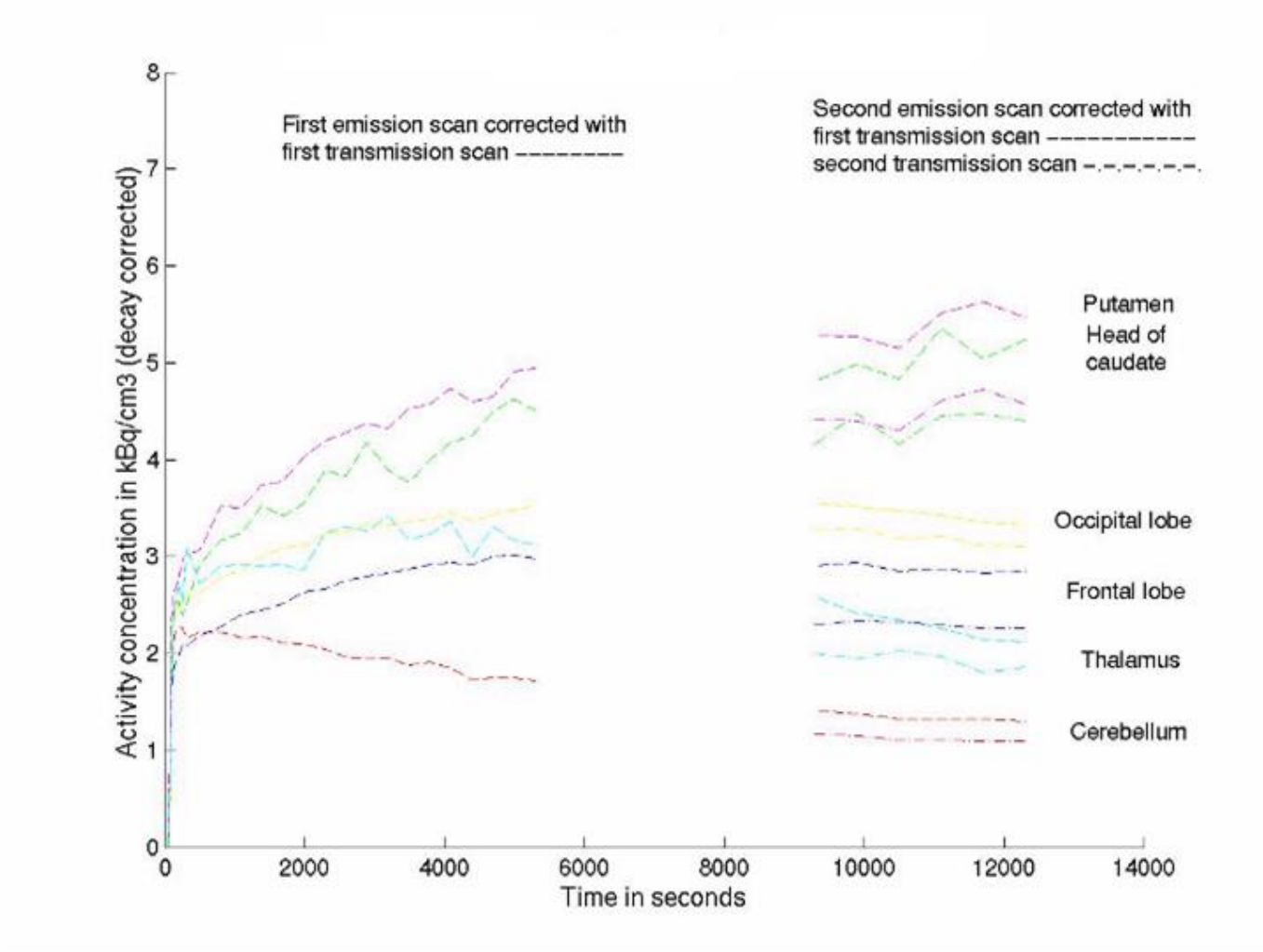


Fig. 4.9. Time activity curve of [^{18}F]SPA-RQ for subject 3.

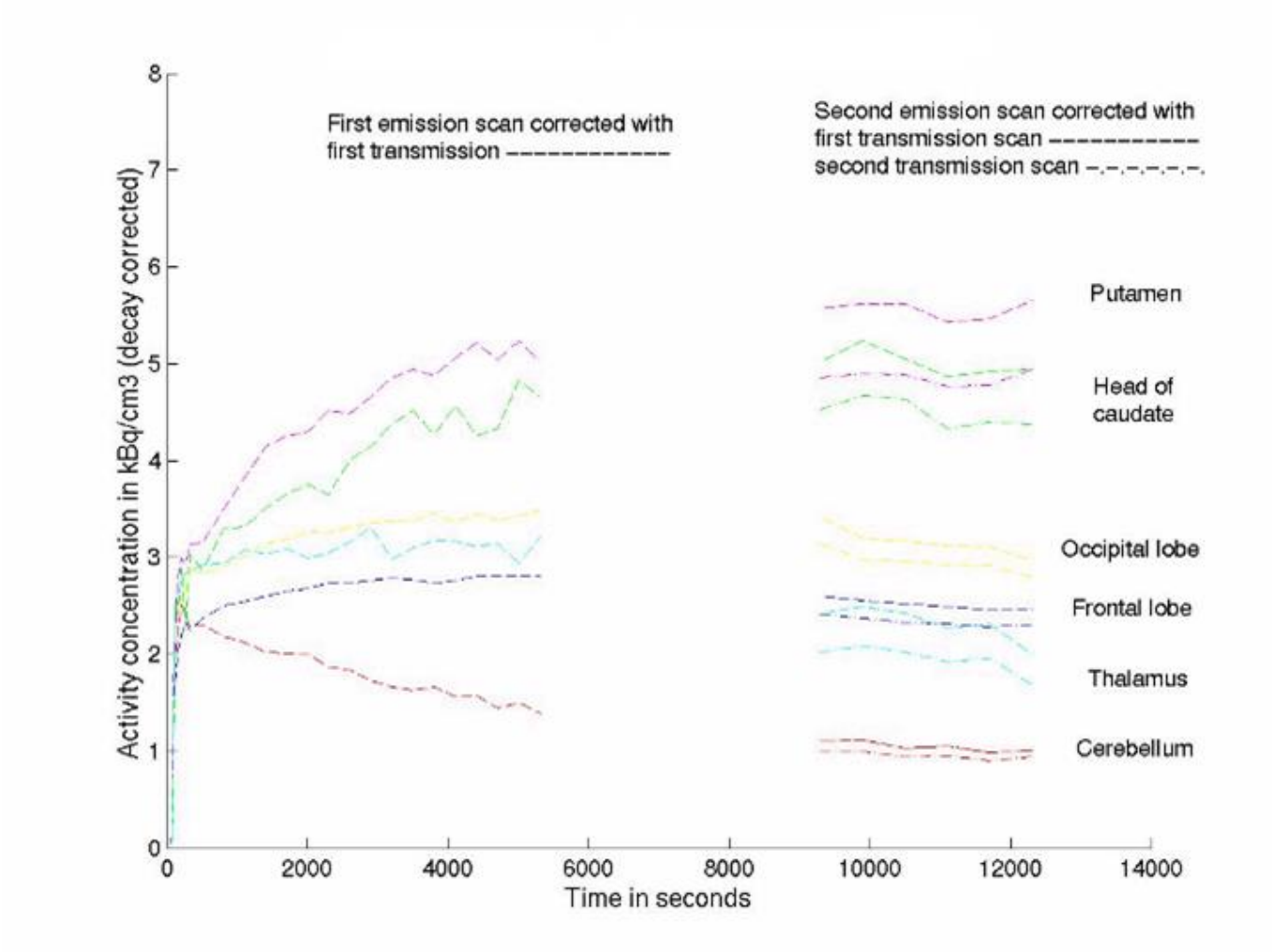


Fig. 4.10. Time activity curve of [^{18}F]SPA-RQ for subject 4.

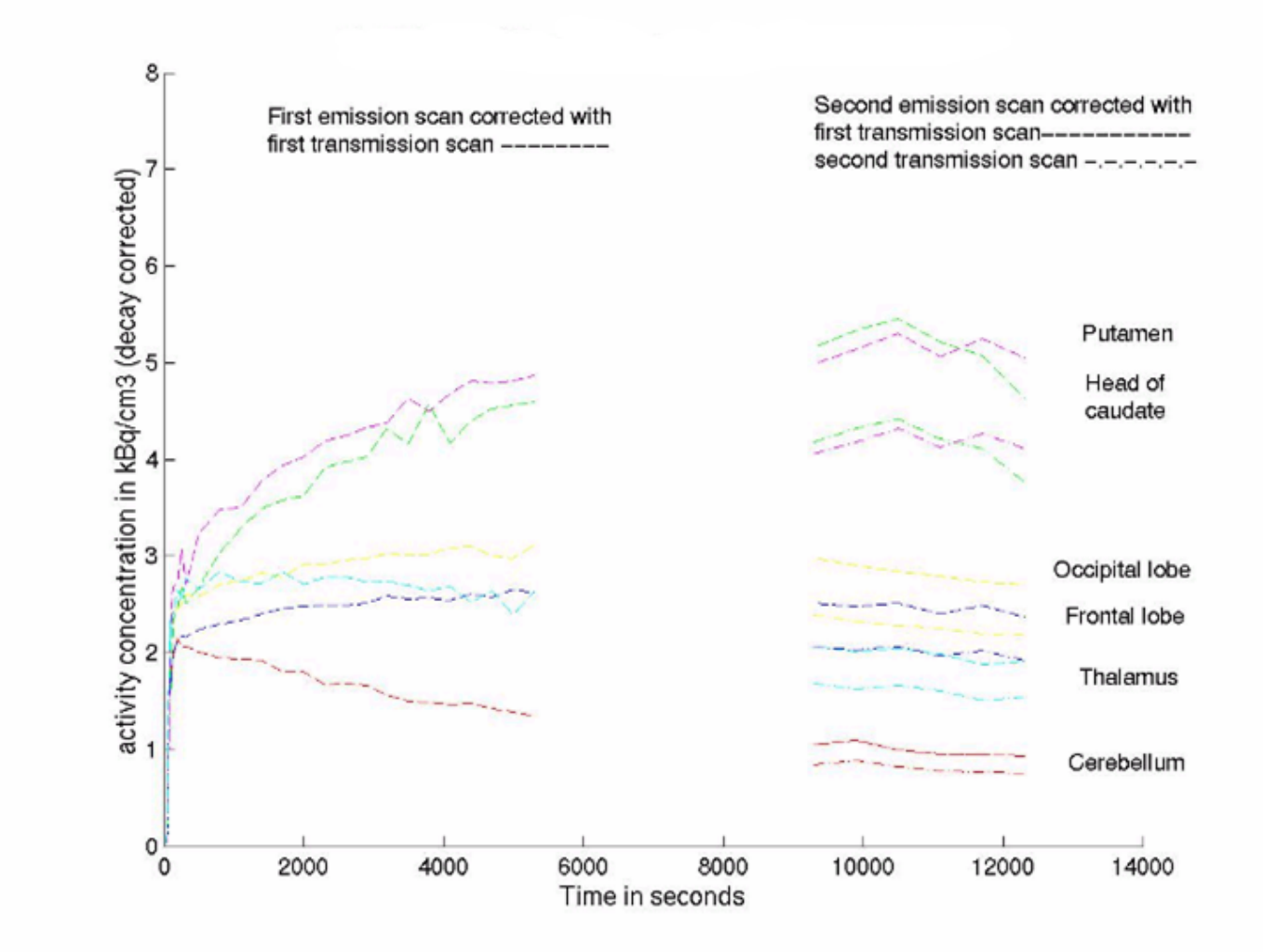


Fig. 4.11. Time activity curve of [^{18}F]SPA-RQ for subject 5.

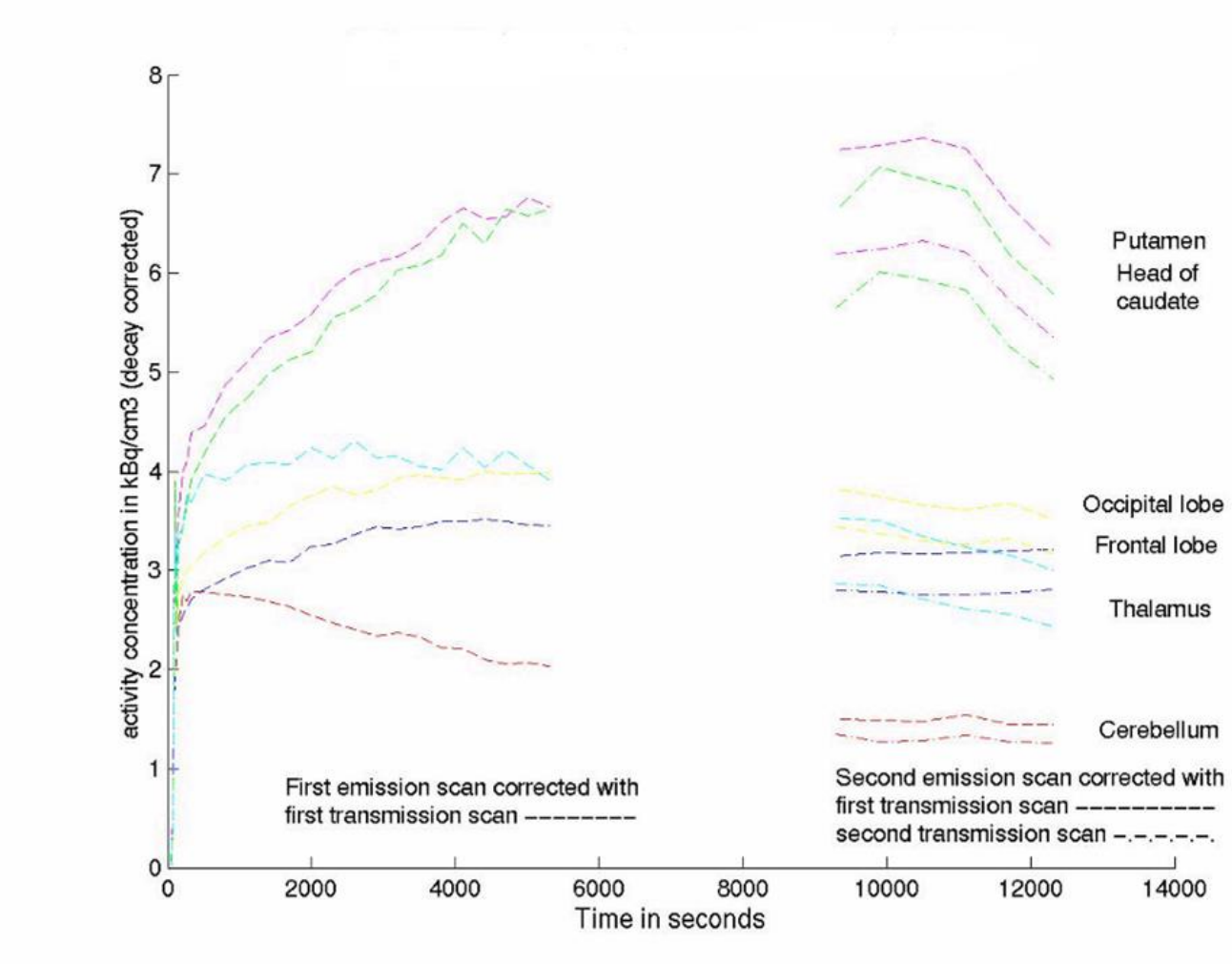


Fig. 4.12. Time activity curve of [^{18}F]SPA-RQ for subject 6.

4.3.3. Plasma analysis of radioligand

The decline in the percentage of the radioligand in plasma over time is illustrated in Fig. 4.13. The mean values could be fitted onto a bi-exponential function.

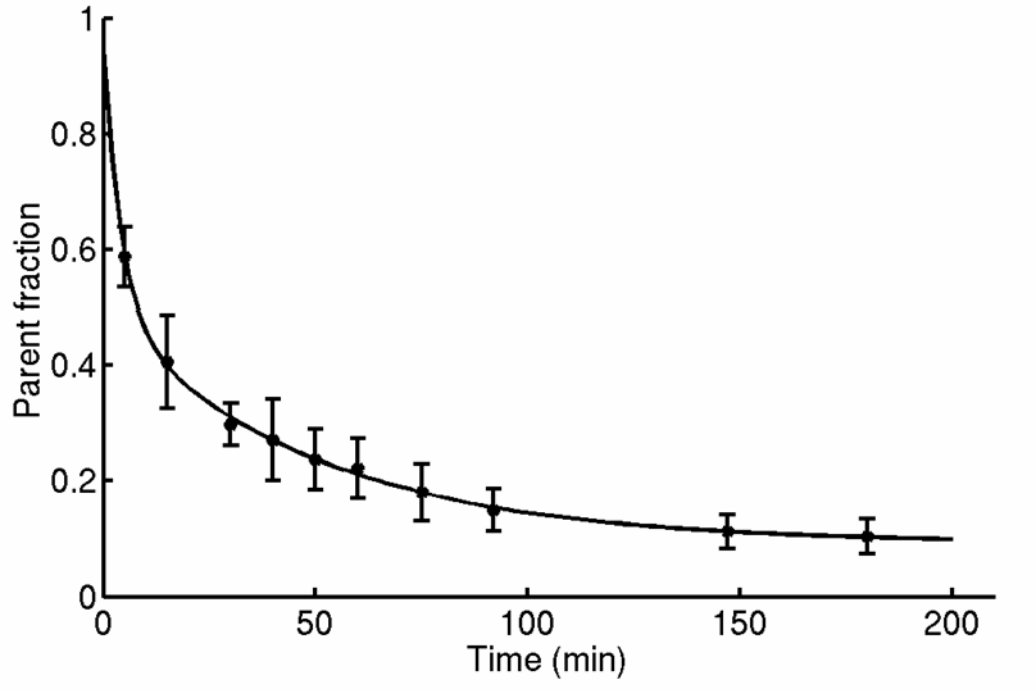


Fig. 4.13. Fraction of unmetabolised [^{18}F]SPA-RQ in arterial plasma. Shown are the mean (SD) of the sample of all 6 volunteers at 5, 15, 30, 40, 50, 60, 75, 92, 147, 180 min. The solid line represents the fit of a bi-exponential function to the mean values.

4.3.3.1. Arterial versus venous radioligand activities

The average arterial and venous radioligand activities obtained in the last three time-points of the second scan (circa 150 min, 180 min and 210 min) for 4 of the subjects appear to converge towards each other as seen in Fig. 4.14. Repeated measures ANOVA revealed that there was no significant difference between the mean arterial and mean venous samples for any of the 3 time points ($F=1.0$; $df=1, 6$; $p=0.36$). However, there was an effect of time ($F=5.7$; $df=2, 12$; $p=0.02$) and a time by sampling interaction ($F=12.3$; $df=2, 12$; $p=0.001$).

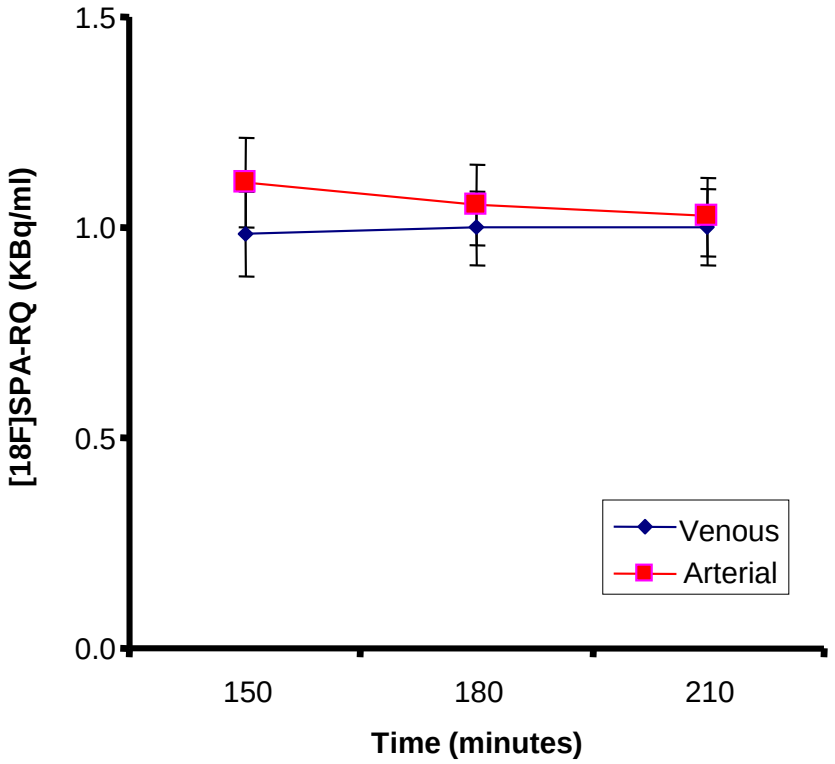


Fig. 4.14. Arterial versus venous [^{18}F]SPA-RQ activity. A graph comparing arterial with venous [^{18}F] SPA-RQ activity in 4 normal human volunteers at the last 3 time points of the second scan (circa 150 min, 180 min and 210 min). Shown are the mean (SD). At these time points venous samples give a good estimate for the plasma clearance of the ligand. Repeated measures ANOVA revealed that there was no significant difference between the mean arterial and the mean venous samples for any of the 3 time points.

4.3.4. Volumes of distribution and binding potential estimates

Table 4.2 compares the VD and BP estimates in different brain regions obtained from compartmental modelling versus the ratio method in each volunteer and also includes the average values for all 6 volunteers. Estimates from compartmental modelling are separated into those based on the first emission scan and those that combine data from both the first and the second emission scans. Apparent estimates using the transient equilibrium 'ratio' method are only based on the second emission scan. All emission scan data here was corrected using the first transmission scan only. The standard errors represent the error generated when applying the experimental data to the kinetic model using weighted non-linear least square fits. Data corrected with the second transmission scan is not presented here as the effect of correction with the second transmission scan is to reduce the BP estimates. This effect is evident in the TACs in Fig. 4.7 to 4.12 where the second emission scan is corrected using the second transmission scan.

It can be seen from Table 4.2 that for each individual subject and for the average of all subjects, the VDa in the cerebellum obtained via the 'ratio' method was higher than with the VD obtained via the compartmental model. In addition, the individual as well as the average BPa for the thalamus, frontal and occipital cortex were similar to the BP values obtained via compartmental modelling. However, for the receptor-rich brain regions such as the caudate and putamen, the BPa values were lower than the BP values obtained from the compartmental models. However, variability of the BP estimates was higher with the compartmental models than with the transient equilibrium 'ratio' method. This is further illustrated in Fig 4.15.

Table 4.2. Volumes of distribution and binding potentials estimates from compartmental modelling versus the ratio method for all 6 subjects.

			Subject 1				Subject 2				Subject 3				Subject 4				Subject 5				Subject 6				Average			
		ROI name	***VD*** ±	*se*	***BP*** ±	*se*	***VD*** ±	*se*	***BP*** ±	*se*	***VD*** ±	*se*	***BP*** ±	*se*	***VD*** ±	*se*	***BP*** ±	*se*	***VD*** ±	*se*	***BP*** ±	*se*	***VD*** ±	*se*	***BP*** ±	*se*	*VD* ±	sd	BP ±	sd
COMPARTMENTAL MODELLING	**Scan 1 only**	Cerebellum	**6.3**	0.1			**8.6**	0.3			**6.2**	0.2			**5.3**	0.1			**8.2**	0.2			**8.5**	0.3			7.2	1.4		
		Thalamus	**16.8**	1.0	**1.67**	0.17	**21.6**	1.3	**1.50**	0.17	**15.5**	1.4	**1.48**	0.23	**12.8**	0.6	**1.41**	0.11	**17.7**	0.9	**1.18**	0.12	**18.6**	1.0	**1.19**	0.14	17.2	3.0	1.41	0.19
		Frontal	**16.2**	0.6	**1.58**	0.11	**22.1**	0.5	**1.56**	0.10	**18.4**	0.7	**1.95**	0.14	**11.8**	0.3	**1.22**	0.07	**25.0**	1.3	**2.06**	0.18	**18.9**	0.5	**1.23**	0.09	**18.7**	4.6	**1.60**	0.35
		Occipital	**16.6**	0.3	**1.64**	0.07	**23.8**	0.8	**1.76**	0.13	**18.8**	0.5	**2.00**	0.12	**14.9**	0.3	**1.81**	0.08	**28.0**	1.3	**2.43**	0.18	**20.8**	0.6	**1.46**	0.10	20.5	4.8	1.85	0.34
		Putamen	**35.8**	6.2	**4.68**	0.99	**81.2**	11.8	**8.43**	1.40	**36.8**	2.5	**4.90**	0.44	**28.7**	1.3	**4.41**	0.25	**92.9**	13.3	**10.4**	1.66	**48.5**	4.1	**4.72**	0.52	54.0	26.7	6.26	2.53
		Caudate	**36.9**	8.7	**4.87**	1.39	**34.4**	4.4	**2.99**	0.53	**24.2**	9.1	**2.87**	1.46	**26.6**	2.4	**4.03**	0.46	**121.3**	25.1	**13.88**	3.11	**80.5**	36.3	**8.50**	4.29	**54.0**	38.9	**6.19**	4.29
	Scans 1 + 2 combined	Cerebellum	**6.7**	0.2			**10.1**	0.3			**13.4**	9.3			**6.2**	0.2			**10.2**	0.3			**9.1**	0.2			9.3	2.6		
		Thalamus	**16.6**	0.8	**1.49**	0.14	**20.1**	0.5	**0.99**	0.07	**14.3**	0.5	**0.07**	0.74	**13.2**	0.3	**1.12**	0.09	**20.1**	0.5	**0.96**	0.08	**20.0**	0.4	**1.19**	0.06	17.4	3.1	0.97	0.48
		Frontal	**10.3**	4.8	**0.55**	0.73	**24.7**	0.3	**1.45**	0.08	**20.3**	0.4	**0.52**	1.05	**15.5**	0.5	**1.50**	0.12	**29.7**	0.7	**1.90**	0.11	**20.4**	0.3	**1.23**	0.05	**20.2**	6.8	**1.19**	0.55
		Occipital	**17.4**	0.3	**1.60**	0.09	**37.2**	2.0	**2.69**	0.23	**29.2**	3.5	**1.18**	1.53	**19.2**	0.5	**2.08**	0.14	**32.5**	0.7	**2.17**	0.12	**23.5**	0.3	**1.57**	0.06	26.5	7.8	1.88	0.54
		Putamen	**39.7**	1.6	**4.96**	0.29	**157**	17.9	**14.6**	1.83	**29.3**	6.2	**1.19**	1.59	**92.9**	225	**13.9**	36.2	**87.0**	3.0	**7.50**	0.40	**52.5**	2.1	**4.75**	0.25	76.5	47.1	7.83	5.39
		Caudate	**36.9**	2.4	**4.52**	0.40	**90.5**	14.9	**7.90**	1.5	**15.5**	24.8	**0.16**	2.02	**37.1**	2.4	**4.97**	0.44	**114.6**	10.0	**10.2**	1.04	**47.6**	2.1	**4.21**	0.24	**57.0**	37.6	**5.34**	3.45
		ROI name	***VD_a***		***BP_a***		***VD_a***		***BP_a***		***VD_a***		***BP_a***		***VD_a***		***BP_a***		***VD_a***		***BP_a***		***VD_a***		***BP_a***		***VDa*** ±	sd	***BPa*** ±	sd
RATIO	**Scan 2 only**	Cerebellum	**10.7**				**17.3**				**16.3**				**8.3**				**15.5**				**11.5**				**13.3**	**3.6**		
		Thalamus	**26.3**		**1.46**		**34.1**		**0.97**		**28.2**		**0.73**		**18.5**		**1.21**		**30.9**		**0.99**		**25.7**		**1.23**		**27.3**	**5.3**	**1.10**	**0.26**
		Frontal	**28.9**		**1.71**		**36.9**		**1.13**		**34.8**		**1.13**		**19.9**		**1.39**		**38.2**		**1.46**		**24.8**		**1.16**		**30.6**	7.3	**1.33**	0.23
		Occipital	**27.3**		**1.56**		**43.7**		**1.52**		**41.7**		**1.56**		**25.1**		**2.01**		**43.9**		**1.83**		**28.5**		**1.48**		**35.0**	**8.9**	**1.66**	**0.21**
		Putamen	**49.3**		**3.62**		**83.2**		**3.80**		**64.9**		**2.99**		**44.0**		**4.27**		**79.5**		**4.11**		**54.7**		**3.75**		**62.6**	**16.1**	**3.76**	**0.45**
		Caudate	**47.3**		**3.44**		**71.7**		**3.14**		**60.8**		**2.73**		**39.7**		**3.75**		**80.1**		**4.15**		**51.3**		**3.45**		**58.5**	15.3	**3.44**	0.49

BP=binding potential; BPa=apparent binding potential; ROI=region of interest; se=standard error; sd=standard deviation; VD=volume of distribution; VDa=apparent volume of distribution. For the average of the 6 subjects, values are mean (sd).

Fig. 4.15 illustrates a chart with the average (SD) BP estimates obtained from all 6 volunteers for the each ROI as obtained using the 3 different models. Analysis using a one way ANOVA for each brain region separately did not reveal a significant difference between the 3 methods of estimation: Thalamus ($F=2.7$; $df=2, 15$; $p=0.10$), frontal cortex ($F=1.6$; $df=2, 15$; $p=0.23$), occipital cortex ($F=0.58$; $df=2, 15$; $p=0.57$), putamen ($F=2.1$; $df=2, 15$; $p=0.15$), head of caudate ($F=1.2$; $df=2, 15$; $p=0.34$). However, clearly the SD was higher in receptor-rich regions when using the compartmental model.

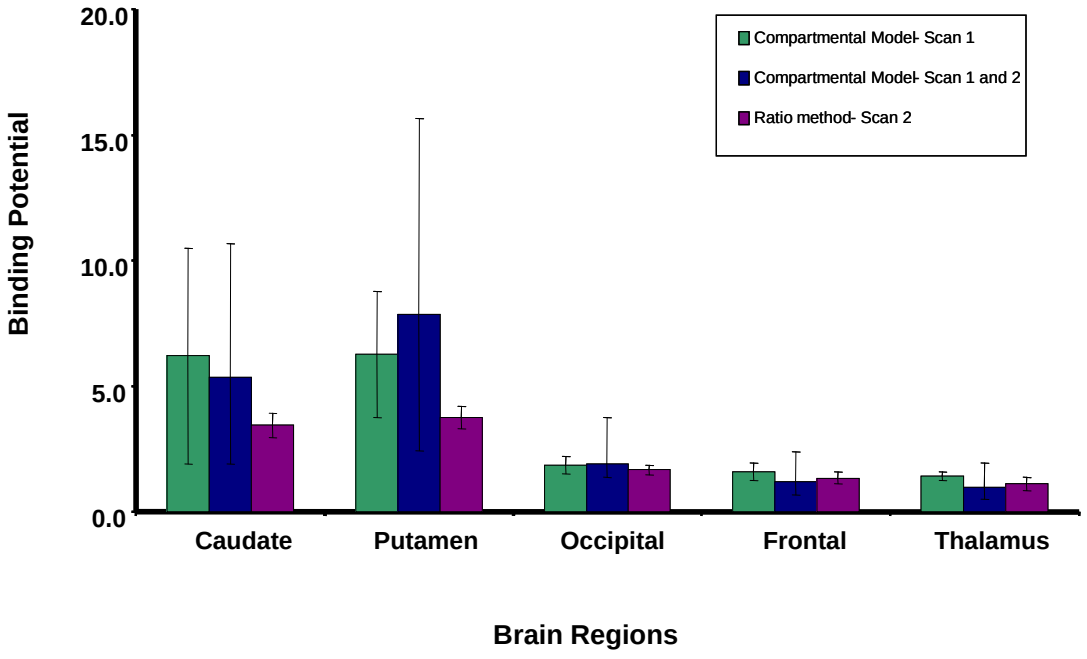


Fig. 4.15. Average binding potential estimates from compartmental modelling and the ratio method. A bar chart comparing the mean (SD) binding potential estimates from 6 volunteers using compartmental modelling (scan1), compartmental modelling (scan1 and 2) and the ratio method (scan 2). Analysis using a one way ANOVA for each brain region separately did not reveal a significant difference between the 3 methods of estimation.

The CV for VD and BP estimates from compartmental modelling versus the ratio method for all 6 subjects is tabulated in Table 4.3. The CV values for both the VD and the BP estimates are generally comparable for the regions with low or moderate binding, but higher for the receptor-rich regions when using the compartmental model. In general, for most regions the CV obtained for the BP estimates were lower using the 'ratio method' that the compartmental models.

Table 4.3. Coefficient of variation for volumes of distribution and binding potentials from compartmental modelling versus the ratio method.

			CV	
		ROI name	***VD***	**BP**
COMPARTMENTAL MODELLING	**Scan 1 only**	**Cerebellum**	19.4	
		Thalamus	17.4	13.6
		Frontal	24.6	22.0
		Occipital	23.4	18.2
		Putamen	49.4	40.4
		Caudate	72.0	69.4
	Scans 1 + 2 combined	**Cerebellum**	28.0	
		Thalamus	17.8	49.5
		Frontal	33.7	46.4
		Occipital	29.4	28.6
		Putamen	61.6	68.9
		Caudate	66.0	64.6
		ROI name	***VDa***	**BPa**
RATIO	**Scan 2 only**	**Cerebellum**	27.1	
		Thalamus	19.4	23.2
		Frontal	23.9	17.6
		Occipital	25.4	12.7
		Putamen	25.7	11.9
		Caudate	26.2	14.2

BP=binding potential; BPa=binding potential (apparent); CV=coefficient of variation (%); ROI=region of interest; VD=volume of distribution; VDa=volume of distribution (apparent).

4.4. DISCUSSION

Both pre-clinical and clinical studies have examined the utility of the radioligand [^{18}F]SPA-RQ for the quantification of NK_1Rs. The aim of this chapter was to make a comparison of different mathematical models for the *in vivo* quantification of NK_1Rs in humans using the radioligand [^{18}F]SPA-RQ and PET. [^{18}F]SPA-RQ has moderate lipophilicity, picomolar affinity for the human NK_1R and can be labelled to a very high specific radioactivity. Here, the injected mass of SPA-RQ per subject was very low and ranged between 0.32 and 0.89 μg.

4.4.1. Comparison of kinetic and transient equilibrium models for [^{18}F]SPA-RQ

A reversible two-tissue, four rate constants (K1, k2, k3, k4) compartment model using plasma input function was compared to a transient equilibrium model. Two PET emission scans were performed: scan 1 (0-90 min) and scan 2 (150-210 min). The TACs revealed that a stable equilibrium state in target brain regions was only reached by the time of scan 2. The BP estimates from both models were comparable for the extra-striatal brain regions examined. In addition, for receptor rich regions such as the striatum, there was no statistically significant difference between the average BP estimates from the different models. However, the BP estimates obtained with the transient equilibrium tended to be lower, but less variable. Thus, in view of the slow kinetics and clearance of [^{18}F]SPA-RQ, quantification based on the first 90 min would not be fully optimal and thus for practical purposes a protocol using the ratio method would be adequate for the *in vivo* quantification of NK_1Rs in the human brain.

The results of this chapter showed that the regional brain uptake of [^{18}F]SPA-RQ was consistent with the known distribution of NK_1Rs: highest in the striatal regions,

moderate in cortical regions and thalamus and low in the cerebellum. In addition, early and late PET emission images and TACs showed the cerebellum to act as a reference region in humans. Similarly, a previous *in vivo* study in guinea-pigs showed [^{18}F]SPA-RQ to have a good signal to noise ratio and also that the non-specific cerebellar signal could not be blocked by a cold NK_1RA (Solin et al 2004). Similarly *in vitro* auto-radiographic studies in postmortem human brain slices showed specific cortical and striatal binding and a non-specific cerebellar signal. In fact, no change in the PET cerebellar signal was seen when high doses of the NK_1RA aprepitant was administered to normal human volunteers *in vivo* (Bergstrom et al 2004).

More recently, Hietala et al. carried out a study to quantify NK_1Rs in normal human volunteers by following the brain radioactivity for up to 6 hrs post-injection (Hietala et al 2005). In the blood they noted free fluoride and a polar radiolabeled metabolite that is unlikely to cross the blood-brain-barrier. Indeed, Hietala et al. 2005 also made a comparison of different mathematical modeling methods. These included one-tissue and two-tissue compartment models and a reference region model. The first utilised estimates of rate constants (K_1, k_2, k_3, k_4) with a fixed 4% vascular volume and calculation of regional BP. They found that the kinetics of [^{18}F]SPA-RQ in the cerebellum could be described by either of the compartmental models and that the kinetic models yielded low BP estimates, but that the reference tissue model using cerebellar input was robust. In addition, they found that total binding peaked at 210 min in the striatum, but peaked earlier in other brain regions indicative of a reversible process of receptor-ligand binding (Hietala et al 2005).

The results in this chapter agree with those of Hietala et al. in that the total uptake was highest in the caudate-putamen region followed by the occipital cortex and the

thalamus and low uptake was seen in the cerebellum. However, Hietala et al. (2005) were able to measure the amounts of unchanged tracer for up to 90 min only, and found that at 80 min, about 30-40% of the parent tracer was unchanged (Hietala et al 2005). However, the results in this chapter show that by 60 min, about 20% of the parent radioligand was unchanged and it was possible to measure the unchanged metabolite for up to 210 min. Here also, the mean values fitted well onto a bi-exponential curve. Similarly, Sprague et al. 2007 found that the average cumulative urine activity in the urine of their subjects would fit a bi-exponential curve (Sprague et al 2007). However, it is clear that because of the slow kinetics of the radioligand, the first 90 min scan on its own is not optimal for the detailed quantification of NK_1R binding. In addition, the average arterial and venous radiotracer activities obtained in the scan 2 appear to converge towards each other and confirm that at these latter time points, venous samples give an adequate estimate of the plasma clearance of the radioligand.

Using the compartmental model, the VDs estimated from the first scan were associated with relatively high standard errors. After only 90 min, the VD in the putamen was still underestimated. In this high uptake region, the standard error on the VD estimate went down when the data from the second scan was also considered. When calculating estimates using the ratio method from data obtained during a transient equilibrium, as occurs during the second scan, then the cerebella VDa gave an overestimation of the VD. BPa however seemed to have an acceptably low bias in the thalamus and cortex. Also although there was wide variability in BP estimates in high uptake regions (e.g. caudate and putamen) between subjects using compartmental modelling, the BPa estimates obtained from all 6 volunteers varied

much less. Similarly, the CV values for both the VD and the BP estimates were generally comparable for the regions with low or moderate binding, but were higher for receptor-rich regions when using the compartmental model. In general for most regions the CV obtained for the BP estimates was lower using the 'ratio method' that the compartmental model.

4.4.2. Limitations of this study

There are a number of limitations with this study. Firstly, for practical reasons imaging data was only obtained up to 210 min versus another study which examined imaging data for up to 300 min. In that study, Yasuno et al. 2007 compared 3 different reference tissue methods for quantification with [^{18}F]SPA-RQ. Eight healthy subjects underwent two [^{18}F]SPA-RQ scans. The models included a simplified reference tissue model, multilinear reference tissue model (MRTM), and multilinear reference tissue model two-parameter version (MRTM2). All three methods generated equivalent values of regional BP. The most temporally stable and reliable values of BP were obtained with the MRTM2 model and with 240 min of imaging data (Yasuno et al 2007). With only 180 min of imaging data, the BP values for the extrastiatal regions were similar to those at 240 min, but with greater variability. However, the BP values for the striatal regions were on average lower than those at 240 min and were more variable.

In comparison, in this chapter, imaging data was obtained for only up to 210 min. It is therefore, likely that the BP estimates in the extra-striatal regions were accurate, but those in the striatal regions were likely to be underestimates. This is probably because

these latter brain regions are so receptor rich that they take longer to rich a transient equilibrium and may also show irreversible kinetics.

Secondly, only the first transmission scan was useful for attenuation correction. When repositioning the subject for the second emission scan, it is likely that the repositioning would not have been exact and so introducing a small error. In addition, head movements may have been more likely to occur by the end of the second emission scan affecting the data obtained for small brain regions such as the caudate and putamen. Also, higher variation in BP estimates is more likely in these smaller structures due to partial volume effects.

Thirdly, ROIs that were drawn were not segmented for grey matter and so for regions with a large amount of white matter such as the cortex, the data obtained may have been slightly different as NK_1Rs are not found in white matter.

4.5. CONCLUSIONS

The results of this chapter showed that [^{18}F]SPA-RQ binds with high affinity to NK_1Rs in the brain. The kinetic analysis employed was a sophisticated approach, but required determination of an arterial input function. The transient equilibrium method thus is suitable for routine clinical research, since it does not require determination of an arterial input function. In fact, a simplified PET scanning protocol for the study of brain NK_1Rs in a clinical population *in vivo* using the [^{18}F] SPA-RQ ligand is illustrated in Fig. 4.16. A single PET emission scan of 60 min duration at 150 min after an i.v. bolus of circa 141 MBq of [^{18}F]SPA-RQ, with discrete venous sampling for the ligand during the emission scan would be adequate. The emission scan would then be followed by a 10 min transmission scan in a scanner that would allow post injection transmission scan. This protocol was used in chapter 5 to study NK_1R in the brains of depressed patients.

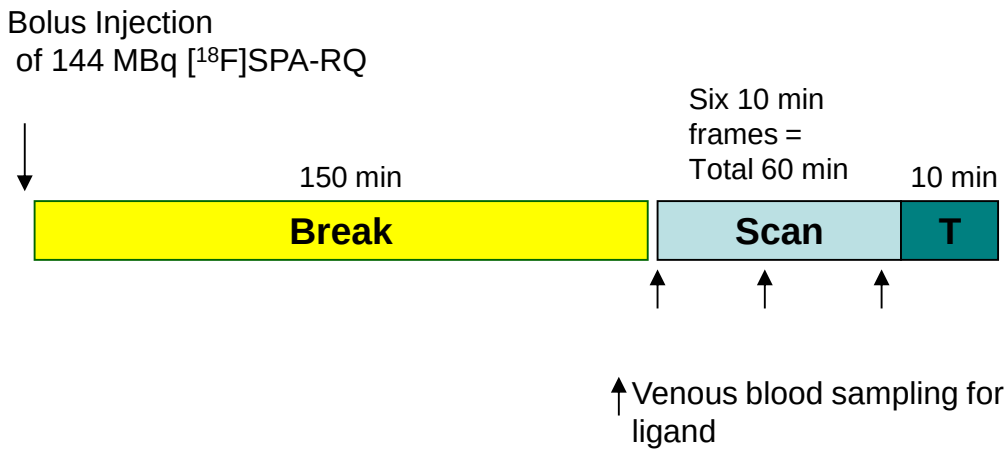


Fig. 4.16. Simplified positron emission tomography scanning protocol for study of brain NK_1 receptors in human subjects *in vivo* using [^{18}F] SPA-RQ. After baseline blood samples (arrows) all subjects to be administered circa 141 MBq of [^{18}F]SPA-RQ in a bolus injection. After a break of 150 min subjects are then placed in the scanner for an emission scan lasting 60 min. This is followed by a 10 min transmission scan. All subjects to undergo discrete venous sampling for the ligand during the emission scan.

CHAPTER 5

IMAGING BRAIN NK_1 RECEPTORS IN DEPRESSION USING POSITRON EMISSION TOMOGRAPHY AND [^{18}F] SPA-RQ

5.1. INTRODUCTION

In chapter 4 data was presented on the measurement of brain NK_1Rs *in vivo* in normal human volunteers using PET and the radioligand [^{18}F]SPA-RQ. BP was calculated, as a quantitative measure for brain NK_1Rs, using a kinetic model and a transient equilibrium model. It was shown that a simplified protocol with a single late scan (150 min after radioligand injection) and venous sampling for the parent ligand would be enough for the calculation of an apparent BP. This chapter presents data using this simplified protocol for the measurement of brain NK_1Rs *in vivo* in depressed subjects.

5.1.1. NK_1 receptors in human depression

As described in the introduction (see section 1.4), substantial evidence from animal studies suggest that NK_1Rs play a role in depression and anxiety, and that NK_1RAs may have antidepressant and anxiolytic properties. Indeed, the animal evidence led to the development of clinical programs for the study of NK_1RAs as novel antidepressants for the treatment of depression. However, the few studies conducted in humans or with human tissue have produced conflicting results, e.g. CSF measurements of SP in depression (Berrettini et al 1985; Geracioti et al 2006; Rimon et al 1984). Nevertheless, a postmortem study showed decreased NK_1R numbers in the orbitofrontal cortex of depressed patients (Stockmeier et al 2002), while another

study which examined the densities of NK_1R binding sites observed a change in the laminar ratio in the anterior cingulate cortex in unipolar depression (Burnet and Harrison 2000). A more recent postmortem study showed a down-regulation of the mRNA for the TAC1 (the gene that codes for both SP and NKA) in the amygdala of patients affected by unipolar or bipolar depression. In contrast, the density of NK_1R binding sites was unchanged in the amygdala in the patient groups (Carletti et al 2005). Furthermore, although initial clinical trials showed NK_1RAs to be effective as antidepressants (Chappell 2002; Kramer et al 1998; Kramer et al 2004), a more recent trial showed that the NK_1RA, aprepitant was no more effective than placebo in the treatment of depression (Keller et al 2006). Despite some of the inconsistent results observed in depression, NK_1RAs are also being investigated in other disorders such as social phobia (Furmark et al 2005).

As shown in chapter 4, the distribution of NK_1Rs in the human brain can be quantified using a simplified protocol that does not involve arterial sampling. The developed protocol allows study of NK_1Rs in clinical populations including depressed patients. In addition, it is important to study NK_1Rs in female subjects as depression is more common in women. Recent data suggest that [^{18}F]SPA-RQ is safe for use in women as radioactivity was not seen to accumulate in the uterus or ovaries after i.v. injection of [^{18}F]SPA-RQ (Sprague et al 2007).

5.1.2. Aims of this chapter

In this chapter, the simplified PET protocol was used to quantify NK_1Rs *in vivo* in antidepressant-free subjects with major depressive disorder (MDD) and subjects recovered from depression (RD). The hypothesis was that the BP for NK_1Rs would be higher in limbic and cortical brain regions as well as the midbrain raphe in MDD patients as compared to RD patients and controls.

As stress may influence NK_1R binding in animals (Duric and McCarson 2005; Hwang et al 2005), physiological measures of stress including blood pressure, pulse and plasma cortisol and subjective measures of mood and stress were collected. Measures of stress were examined for their effect on BP for NK_1Rs.

Previous studies have shown correlations between BP for brain receptors and personality measures (Bhagwagar et al 2006; Meyer et al 2003). In view of this a smaller aim of this chapter was to collect measures of personality and mood and to examine them for correlations with BP for NK_1Rs.

5.2. METHODS

5.2.1. Radiosynthesis of [^{18}F]SPA-RQ

The radiosynthesis for [^{18}F]SPA-RQ was as described in Appendix A.

5.2.2. Human subjects

Ethical approval was given by UK ARSAC {study number RPC 262-336 (18211)} and the Local Research Ethics Committees of the Hammersmith, Queen Charlotte's & Chelsea and Acton Hospitals to study subjects aged 30-70 (Ethics number 03/6690). Additional ethical approval was obtained from the Oxfordshire Psychiatric Research Ethics Committee to allow for recruitment of subjects from Oxford (Ethics number O03.043). All subjects were recruited via advertising in local and national newspapers or magazines. Subjects were initially contacted via telephone by a recruitment psychologist. The exclusion criteria included the presence of a significant medical condition, a recent history of substance abuse or dependence and weekly alcohol consumption > 28 units in the last 4 weeks. In addition, any volunteers who had received significant radiation in the 12 months prior to the study were excluded. Subjects were then interviewed over the telephone for the presence of an Axis I psychiatric disorder using SCID. Those deemed as suitable were contacted again by Psychiatrist (Sepehr Hafizi) to confirm the absence of any exclusion criteria.

RD subjects were classified as having recovered from depression on the basis of 4 criteria: self-reported euthymia following the last major depressive episode (MDE), euthymia based on psychiatric interview, absence of a major depressive episode as judged on SCID and an HRDS score <7 (Frank et al 1991). Only subjects that had met all 4 criteria and free from regular psychotropic medications for > 3 months were

included. Subjects with a current MDE were invited to the PET Psychiatry Unit, Cyclotron Building, MRC Clinical Sciences Centre at the Hammersmith Hospital for an interview to confirm the presence of current MDE. Volunteers and patients deemed suitable were then invited to participate in the study. Subjects were only recruited after full written informed consent. Also, a letter was sent to the General Practitioner asking for any reason why the subject could not take part. An MRI scan was also performed, but in a significant number of cases this was on a different day to the PET scan.

The study protocol for the day of the PET scan is outlined in Fig. 5.1. All subjects were scored on the 17-item HDRS and asked to fill-in BDI and STAI questionnaires. Personality questionnaires included the Eysenck Personality Questionnaire {EPQ-subset scales: extroversion (EPQ-E), lie (EPQ-L), neuroticism (EPQ-N) and psychoticism (EPQ-P)} (Eysenck and Eysenck 1975), 40-item DAS for dysfunctional attitudes (Dozois et al 2003), Barrat Impulsivity Scale (BIS) (Patton et al 1995), a modified Cheek and Buss Shyness and Sociability Scale (Cheek and Buss 1981), the Aggression Questionnaire (TAQ) (Buss and Perry 1992), Cloninger's Tridimensional Personality Questionnaire (TPQ- subsets: novelty seeking, reward dependence and harm avoidance) (Cloninger 1987). Subjects were also asked to fill-in the Parental Bonding Inventory (PBI) (Parker et al 1979). In addition, demographic details including age, gender, handedness, National Adult Reading Test (NART) premorbid full-scale IQ (Nelson 1982), years of education and smoking status were obtained. Female subjects <55 years of age were given a pregnancy test prior to the PET scan. All subjects also had a physical examination including height and weight. One venous cannula was then sited in each forearm. Subjective measures of stress i.e. visual

analogue scales (VAS) for stress and sadness, and objective measures of stress i.e. blood samples for cortisol, blood pressure (mean arterial pressure (MAP= [(2 x diastolic) + systolic] / 3)) and heart rate were carried out at 30 min intervals during the PET scan.

Data was also collected on the MDD and RD subjects with regards to duration of current episode, presence of current melancholic symptoms (MDD patients), age of onset of depression, number of lifetime episodes of depression, total lifetime duration of dysphoria, total lifetime duration of major depression, number of weeks treated with an antidepressant in a lifetime, number of months free from antidepressant medication, classes of antidepressants used in the past, number of episodes of deliberate self harm, family history of depression, number of months of euthymia (RD patients) and the presence of a co-morbid axis I disorder.

Eight subjects who met DSM-IV criteria for a current MDE, and 9 subjects who had met the same criteria for at least 1 previous episode and who were euthymic for > 3 months were initially recruited. A group of 21 normal controls was also recruited at this stage. Only patients off regular psychotropic medications for > 2 weeks prior to the PET scan were included. No subject was ever asked to stop treatment to take part. All patients with a current MDE were advised to seek treatment from their GP. Patients and controls were scanned within an 18 month period: February 2004 to August 2005.

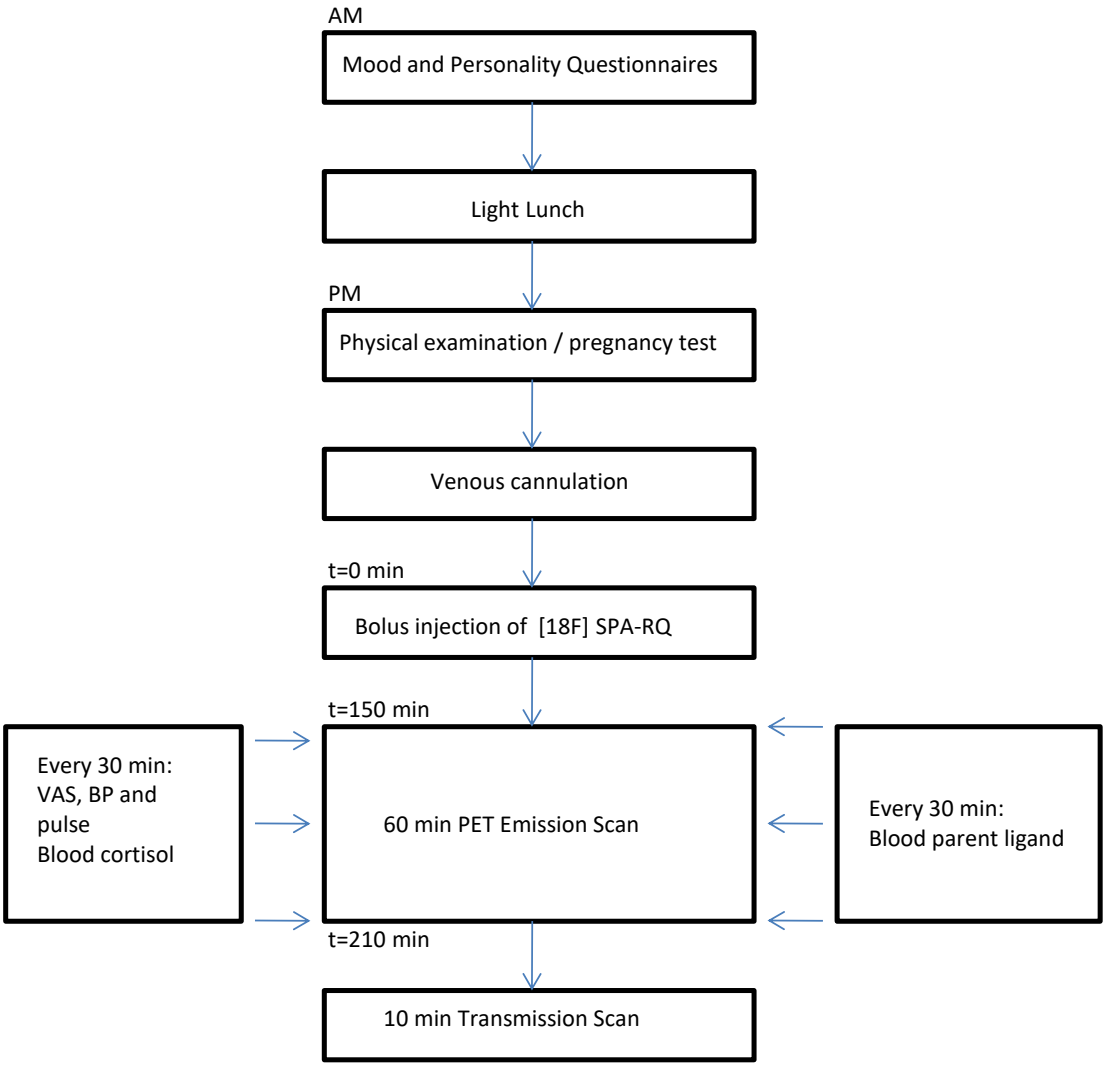


Fig. 5.1. Study protocol on day of the positron emission tomography scan with [^{18}F]SPA-RQ. VAS=Visual Analogue Scale.

5.2.3. Positron emission tomography and magnetic resonance imaging scanning protocols

All scans were performed at the Hammersmith Hospital in London. Depending upon availability, subjects had either a 0.5 T (3D image; pulse sequence RF fast; TR 30 ms, TE 3 ms; flip angle 30°; NSA 1; FOV 25 cm; matrix 152 x 256; voxel dimensions 0.98 mm, 1.65 mm and 1.6 mm - Apollo, Marconi Medical Systems, Cleveland, Ohio, USA), 1.5 T (3D image; pulse sequence RF fast; TR 30 ms, TE 3 ms; flip angle 30°; NSA 1; FOV 25 cm; matrix 156 x 256; voxel dimensions 0.98 mm, 1.6 mm and 1.6 mm- Eclipse, Marconi Medical Systems, Cleveland, Ohio, USA), or 3.0 T (3D image; pulse sequence RF fast; TR 9.6 ms, TE 4.6 ms; flip angle 8°; NSA 1; FOV 240 mm; matrix 208 x 256; voxel dimensions 0.94 mm, 0.94 mm and 1.2 mm, slice thickness 1.2 mm, slices 150- Intera, Philips Medical Systems, Andover, MA, USA) Tesla T1-weighted MRI scan for co-registration purposes and underwent the PET scanning protocol described below (see Fig. 5.1). Subjects were first administered an average i.v. bolus of 144 MBq (range 126-155 MBq) of [^{18}F]SPA-RQ. Subjects then remained in a clinical room until the time of the PET scan (t=0 to t=150 min). PET scans were not performed until 150 min after injection time to allow time for the ligand to reach a transient equilibrium. PET scans were then performed on the ECAT EXACT HR+ (962) PET Camera (CTI, Knoxville, Tennessee, USA) which has a built-in system for carrying out post-injection transmission scans. Subjects were positioned as described for the ECAT EXACT 3D HR++ (966) PET scanner. Head position was checked with a 2 min transmission scan and adjusted accordingly to include the cerebellum. An emission scan of 60 min (t=150 to t=210 min) was then acquired in 3D with an axial FOV of 15.5 cm and 63 reconstructed trans-axial image planes (Brix et al 1997). This

was followed by a 10 min transmission scan to correct for tissue attenuation using three rod sources of ^{68}Ge with circa 100 MBq of radioactivity per rod.

Post-acquisition frame re-binning was performed as follows: the emission scan was divided into 6 frames of 10 minutes each. The dynamic studies were reconstructed using filtered back-projection with a ramp filter. Attenuation and scatter corrections were applied. The spatial resolution of the reconstructed images was 6.0 mm (trans-axial) and 5.0 mm (axial) (Brix et al 1997).

Three venous samples were taken via an indwelling cannula from the opposite arm to where the radioligand injection was given at 150, 180 and 210 min after injection of the radioligand [^{18}F]SPA-RQ. Samples were then treated as described in chapter 4 (section 4.2.3.) for the measurement of parent ligand.

5.2.4. Image analysis

Image analysis was performed similar to that previously described for other radioligands from the Cyclotron Unit (Rabiner et al 2002). Initially, individual MRIs were centred on the anterior commissure and orientated along a line connecting the anterior commissure with the posterior commissure using standard software (Statistical Parametric Mapping 2 [SPM2], online at http://www.fil.ion.ucl.ac.uk/spm) on Matlab version 6.0 (Math Works, Natck, MA, USA). Dynamic PET images were converted into file formats for use in the medical imaging software ANALYZE version 6.0 (Robb et al 1989) and summed [^{18}F]SPA-RQ PET images created. The MRI images were then co-registered to the summed [^{18}F]SPA-RQ PET image using SPM2 and Matlab (Fig. 5.2). Co-registered MRI images were then segmented into

grey matter, white matter and CSF. The threshold for segmentation was set at >65 'intensity' as based on the change in intensity levels between the grey and white matter, measured using MRIcro software version 1.2.9.0 (online at http://www.sph.sc.edu/comd/rorden/mricro.html) (Rorden and Brett 2000). An ROI analysis was employed using a probabilistic atlas (together with a detailed cortical map of subregions) for all brain regions except for the raphe (Hammers et al 2003) to eliminate observer bias for ROI definitions. Only segmented grey matter images were used for normalisation and re-slicing with the summed [^{18}F]SPA-RQ PET image and the probabilistic atlas.

Normalisation and re-slicing was done with Matlab in SPM2 with a 'nearest neighbour' interpolation. The T1 Montreal Neurological Institute (MNI) template (available in SPM2) was normalised to the co-registered segmented grey matter MRI scan and the deformation parameters applied to the probabilistic atlas and the detailed cortical map to create normalised probabilistic atlases. In the stereotaxic standard space, each voxel represented 2.092 x 2.092 x 2.42 mm in volume (equivalent to voxel sizes on the PET image). This was followed by the re-slicing of the segmented grey matter MRI and the normalised probabilistic atlases to PET space (Fig. 5.3).

Every slice on each summed PET image and co-registered MRI slice was examined for the fit of the probabilistic atlas. The ROI for the cerebellum tended to encroach upon the occipital cortex overestimating the activity in the cerebellum (Haneda et al 2007). Thus, care was taken in the sampling of cerebellar slices. Slices where encroachment was evident were excluded and in general only slices in the middle of the cerebellum were used (see Appendix C).

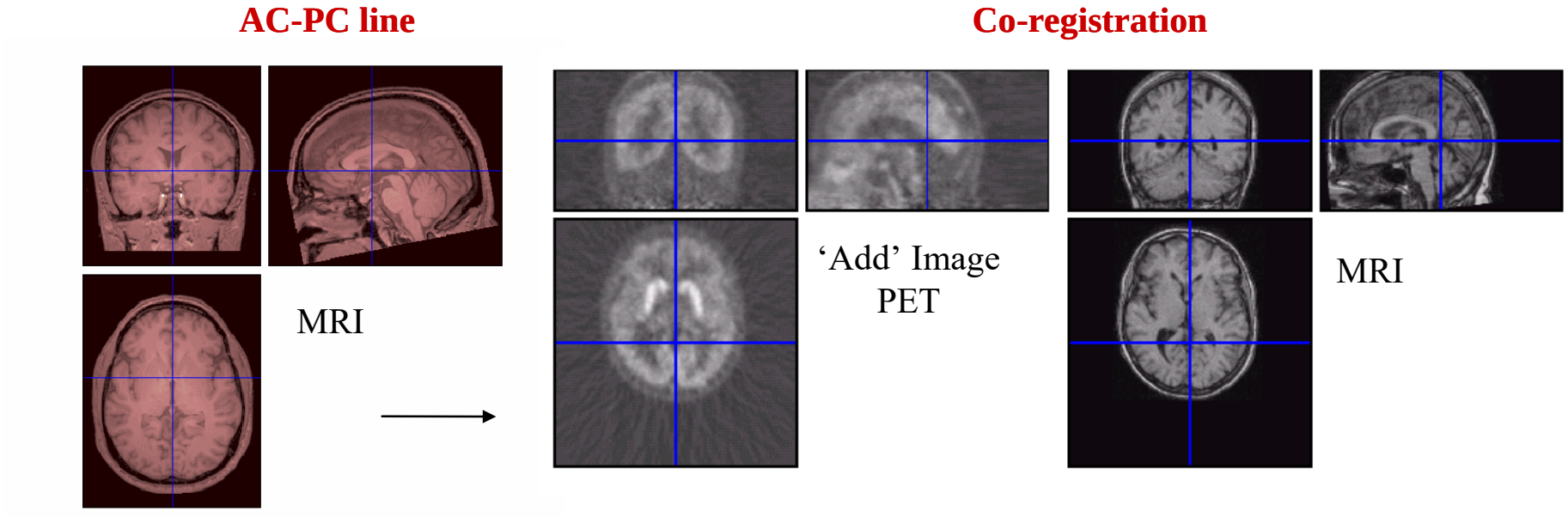


Fig. 5.2. Procedure for image analysis (I). Individual MRIs were initially orientated in a straight line going through the anterior commissure and posterior commissure (AC-PC), and then co-registered with the PET 'add' image.

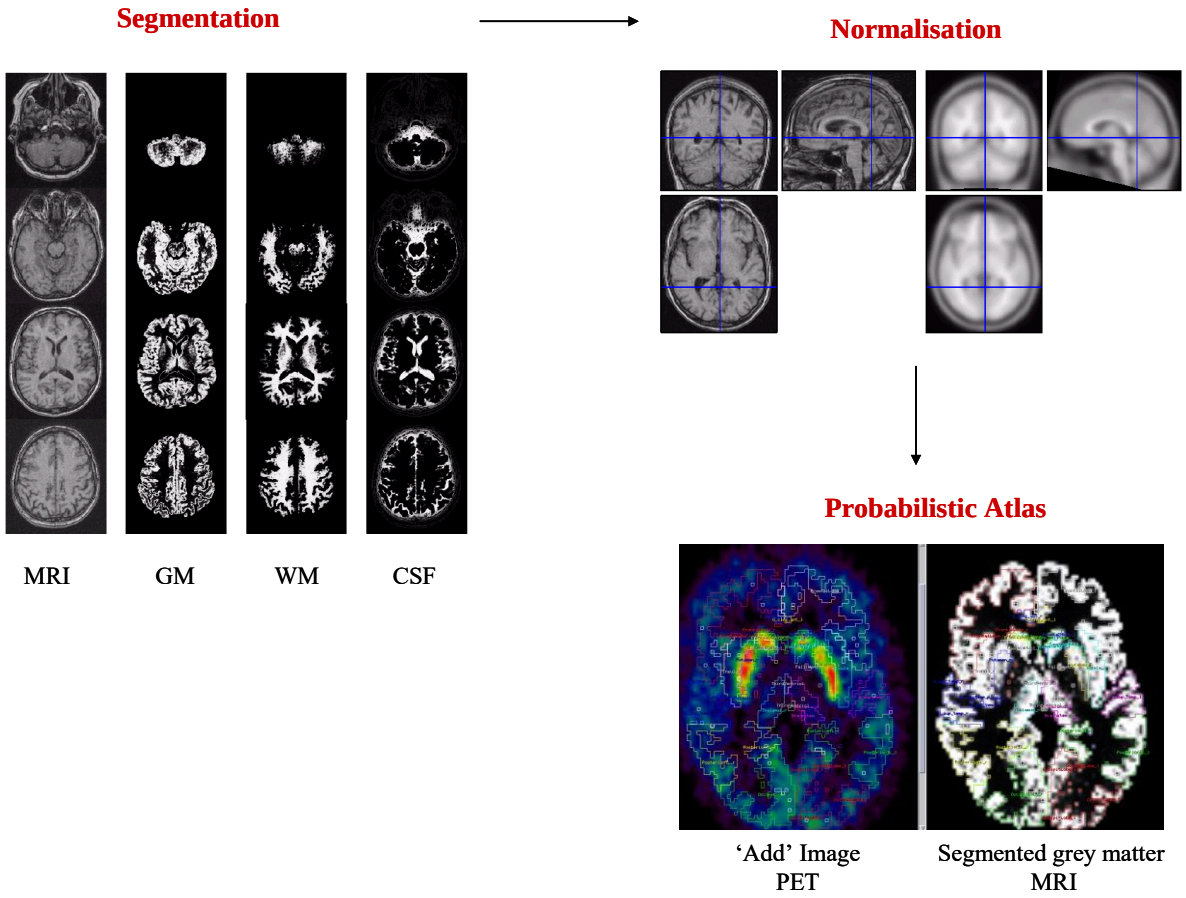


Fig. 5.3. Procedure for image analysis (II). The MRI was then segmented into grey matter (GM), white matter (WM) and cerebrospinal fluid (CSF). The grey-matter segmented MRIs were then normalised with the MNI template and re-sliced with the probabilistic atlas to PET space.

5.2.5. Localisation of the raphe region

The raphe nucleus was initially identified using co-registered and re-sliced summed PET images and MRI from one subject who had had both an [^{11}C] WAY-100635 scan for 5-HT_{1A} receptors (provided by Dr Murthy) and an [^{18}F]SPA-RQ scan for NK_1Rs (Fig. 5.4). This individual was one of the normal male volunteers recruited for the study in chapter 4. PET scans were performed on the high-sensitivity ECAT EXACT 3D HR++ (966) PET scanner (CTI, Knoxville, Tennessee, USA). The position of the raphe was determined on the summed PET [^{11}C] WAY-100635 image. The raphe could be best visualised in a sagittal slice in the midbrain region in the midline, ventral to the cerebral aqueduct. Using these landmarks, the raphe ROI was then delineated on the individual MRIs of all subjects recruited for the current study. Three ROIs were used for the raphe in each subject. The initial ROI was manually placed in the midline with the others on a neighbouring MRI slice on each side of the midline. The volume of each ROI used for the raphe was 444.8 mm^3. ROI placements were made blind to the diagnosis of the subject.

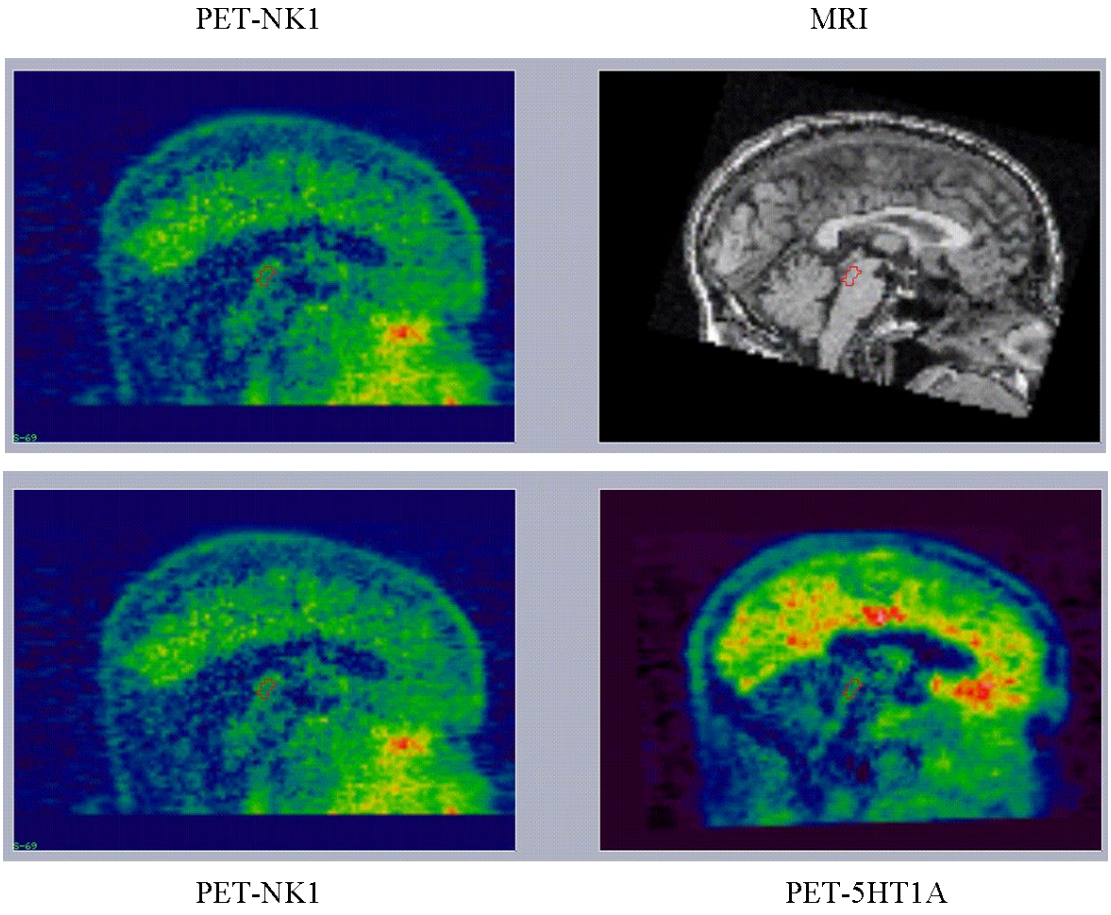


Fig. 5.4. Determination of the position of the raphe nucleus. Sagittal summed PET images for NK_1R ([^{18}F]SPA-RQ) and 5-HT_{1A}Rs ([^{11}C] WAY-100635) co-registered and re-sliced with the 0.5 Tesla MRI in the same individual (normal volunteer recruited for the study in chapter 4). PET scans were performed on the high-sensitivity ECAT EXACT 3D HR++ (966) PET scanner (CTI, Knoxville, Tennessee, USA). An object map (red) represents the position of the raphe as defined on the summed PET [^{11}C] WAY-100635 image.

5.2.6. Generation of time activity curves

Regional TACs were generated by applying the individual ROI atlas on each [^{18}F]SPA-RQ PET dynamic image using an ROI scale factor in ANALYZE version 6.0 (Robb et al 1989). The output from this was then entered into 'Clickfit' software in SPM2 and MATLAB to generate TACs. For all target brain regions, except brainstem and raphe, the activity for each hemisphere was weighted for the volume of the ROI in that hemisphere, summed and divided by the total volume (right and left summed) of the ROIs for the brain region.

For each subject, TACs were plotted for a selected number of brain regions including the putamen, caudate, occipital lobe, amygdala, hippocampus and cerebellum. Right and left hemisphere activities were combined for all regions. Raphe TACs were plotted separately.

5.2.7. Mathematical modeling and binding potential estimates

The ratio method at transient equilibrium was used to obtain estimates of the apparent BP from tissue activity concentration ratios as described in chapter 4. Here BP= (activity in the target region / activity in the cerebellum) -1. In addition, tissue over parent in plasma ratios for [^{18}F] SPA-RQ were generated by Dr Rainer Hinz for comparison of radioligand clearance between tissue and plasma (see Appendix D).

5.2.8. Measurements of stress

Blood pressure, heart rate and plasma cortisol and subjective VAS scores were carried out during the PET emission scan at 30 min intervals (t=150, 180 and 210 min).

5.2.8.1. Physiological measures of stress

5.2.8.1.1. Plasma cortisol measurements

Three blood samples (5 ml) were collected and stored on ice before being centrifuged at 3000 g for 10 min at 4 ºC. The supernatant was separated and stored at -20 ºC at the Hammersmith Hospital. Plasma cortisol levels were then measured by Mrs Alison Reed at the Department of Psychiatry, Oxford University.

5.2.8.1.2. Measurement of blood pressure and heart rate

Systolic and diastolic blood pressure and MAP were measured using an automated sphygmomanometer.

5.2.8.2. Subjective measures of stress

Each subject was asked to rate themselves subjectively, on a scale between 0 and 10, for stress where ‘not stressed at all’=0 and ‘extremely stressed’=10; and for sadness, where ‘not sad at all’=0 and ‘extremely sad’=10.

5.2.9. Statistical analysis

Statistical calculations were performed using SPSS 15.0 (SPSS Inc, Chicago, IL, USA). Group differences in parametric data such as demographics or radioligand variables e.g. specific activity were analysed using a one-way ANOVA and a *post hoc*

Bonferroni test. Differences in categorical data was analysed using the Kruskal-Wallis test.

For BP, initially global BP for each subject was calculated by combining the BP for each region studied as adjusted for region volume (raphe and sub-regions not included). ANOVA was used to examine differences in mean global BP between groups, with and without age as a covariate. To examine the effects of subject group and region on BP measures, 32 ROI measurements (summed values for 15 brain areas (right and left), the brainstem, and the raphe) were entered into repeated-measures ANOVA within GLM in SPSS, with region as the within-subject factor and group as the between-subjects factor. A Greenhouse-Geisser correction was applied as appropriate where the assumptions of sphericity were violated. All values are given as mean (SD) unless specified otherwise and significance level set at $p < 0.05$.

Pearson's product moment correlation coefficients (r) were obtained for mean global BP and regional BP values against PET and clinical variables. These included total injected activity, specific activity, unlabelled 'cold' [18F]SPA-RQ, age, HDRS, BDI, STAI and DAS. Further exploratory correlations between regional and global BP were carried out for the other personality measures. Here correlations were carried out for each group separately and combined. In addition, Spearman's rho correlations were obtained for global BP and regional BP values against number of MDEs, number of episodes of deliberate self harm, and presence of a family history of depression. The significance level for hypothesis-led correlations was set at $p < 0.05$, while exploratory correlations were only accepted at $p < 0.002$ due to multiple comparisons.

With regards to analysis of the measures of stress, MAP was used for further analysis. Area under the curve (AUC) was measured using the trapezoid method. Statistical analysis employed one way ANOVA for comparison of mean AUCs. In addition, a repeated measures ANOVA was used to examine the effects of time, group and group by time interactions. Correlations were carried out using Pearson's product moment. Values are given as mean (SD).

5.3. RESULTS

Three subjects were excluded from the analysis. Two were found to have cerebral atrophy on MRI examination: one from the control group, the other from the MDD group. The third subject excluded was an MDD subject found to be severely anaemic. Furthermore, one control subject had been exposed to an SSRI and diazepam in the past, but on SCID she did not fulfil the criteria for a previous DSM-IV clinical disorder. She was therefore, included in the control group. Thus, the final numbers for statistical comparisons were 20 controls, 6 MDD subjects and 9 RD subjects.

5.3.1. Subject demographics and radioligand-related data

Data on demographic and radioligand-related data for the 3 groups are tabulated in Table 5.1. Analysis of the data with one way ANOVA revealed no significant difference in terms of demographics e.g. age ($F= 0.86$; $df=2, 32$; $p=0.43$), body mass index (BMI) ($F=1.72$; $df=2, 32$; $p=0.20$), NART full-scale IQ ($F=1.28$; $df=2, 32$; $p=0.29$), years of education ($F=0.23$; $df=2, 32$; $p=0.80$), or radioligand-related variables such as the specific activity of the radioligand ($F=0.54$; $df=2, 32$; $p=0.59$), weight of unlabelled SPA-RQ ($F=0.13$; $df=2, 32$; $p=0.88$), injected dose ($F=1.0$; $df=2, 32$; $p=0.38$). Radioligand purity was 100% in all cases.

With the non-parametric Kruskal-Wallis test, the 3 groups did not differ significantly in gender ($\chi^2 =0.47$; $df=2$; $p=0.79$), handedness ($\chi^2 =5.7$; $df=2$; $p=0.06$) or smoking status ($\chi^2 =3.9$; $df=2$; $p=0.14$). However, there was a significant difference between groups in terms of the strength of magnet used for the MRI scan ($\chi^2 =7.6$; $df=2$; $p=0.02$).

5.3.2. Measures of mood and anxiety

One way ANOVA and post-hoc Bonferroni were used to analyse differences between groups on mood and anxiety questionnaires (see Table 5.1). The MDD group had significantly higher scores on the BDI ($F=126$; $df=2, 32$; $p < 0.001$), HDRS ($F=300$; $df=2, 32$; $p < 0.001$), STAI-State ($F=14.8$; $df=2, 31$; $p < 0.001$) and STAI-Trait ($F=46.7$; $df=2, 31$; $p < 0.001$).

5.3.3. Clinical characteristics

In the MDD group (n=6), 6 subjects had previous suicide attempts, 4 had a family history of MDD, 1 met criteria for melancholic depression, 4 had a history of generalised anxiety disorder, 2 had a history of dysthymic disorder and 1 had a history of social phobia. All 6 had been previously exposed to antidepressants. Four had been exposed to an SSRI, one to a tricyclic antidepressant and another subject could not recall. They had all been psychotropic medication-free with a mean period of 34 months (range 7-120 months) prior to the PET scan. However, one of the MDD subjects had taken a single dose of loratidine (an antihistamine that does not readily cross the blood brain barrier) > about 30 hrs before the PET scan.

In the RD group (n=9), 1 subject had a previous history of self harm, 2 had a family history of MDD, 6 met criteria for previous episodes of melancholic depression, 1 had a history of generalised anxiety disorder, 1 had a history for dysthymic disorder and 1 had a history of post-traumatic stress disorder (not otherwise specified). Six had been exposed to antidepressant medications. Three of the subjects had never been treated. The 6 that had been treated were off of medications for a mean period of 53

months (range 6-132 months) prior to the PET scan. The mean period of euthymia for RD subjects prior to the PET scan was 46 months (range 3-132 months).

An independent samples t-test was used to analyse differences in clinical variables between the MDD and RD groups. There was no significant difference with regards to the age of onset (t=1.3; df=13; p=0.22) and number of MDEs (t=0.85; df=13; p=0.41). In addition, in those treated with antidepressants, there was no significant difference in the number of months drug-free (t=-0.85; df=10; p=0.41). However, total lifetime duration of MDEs (t=2.3; df=13; p=0.04), and total lifetime duration of dysphoria (t=2.3; df=13; p=0.04) was significantly higher in the MDD group. Nevertheless, more RD subjects had experienced melancholia (RD=6; MDD=1). However, all 6 MDD subjects had made previous suicide attempts, while only 1 RD subject had done so. Finally, the Kruskal-Wallis test revealed no significant difference between the 3 groups for family history of depression (χ^2 =4.1; df=2; p=0.13).

5.3.4. Measures of personality and parental bonding

One way ANOVA and post-hoc Bonferroni were used to analyse differences between groups on personality and parental bonding scores (see Table 5.2). The control group scored significantly higher on the EPQ-E (F=11.1; df=2, 31; $p < 0.001$) compared to the other two groups. However, the MDD group had significantly higher scores on several measures including the DAS (F=11.5; df=2, 31; $p < 0.001$), TAQ-aggression (F=5.9; df=2, 31; p=0.01), EPQ-P (F=8.1; df=2, 31; p=0.002), EPQ-N (F=31.3; df=2, 31; $p < 0.001$), modified Cheek-Buss Shyness (F=10.7; df=2, 30; $p < 0.001$), and TPQ-harm avoidance (F=10.2; df=2, 30; $p < 0.001$). PBI scores for paternal care were however significantly lower in the MDD group (F=4.27; df=2, 29; p=0.02).

5.3.5. NK_1 receptor binding

5.3.5.1. Effect of gender

Nyman et al. showed that gender may affect NK_1Rs in human brain (Nyman et al 2006). Therefore, the control group in this chapter was separated into males (n=11) and females (n=9), but using an independent samples t-test no difference between men and women was found in BP in brain regions (e.g. for global BP: t=0.37; df=18; p=0.97). Mean (SD) global BP for males was 2.04 (0.32) and for females was 2.05 (0.27). A repeated measure analysis with region as the repeated measure and gender as the between subjects factor revealed a main effect of region (F= 184; df=4, 78; p <0.001), but no effect of gender (F=0.79; df=1, 18; p=0.78) or gender by region interaction (F=1.33; df=4, 78; p=0.26) on NK_1R BP. A repeated measure analysis for all groups, revealed a main effect of region (F=286; df=5, 158; p < 0.001), but no main effect of gender (F=0.01; df=1, 33; p=0.91) or region by gender interaction (F=0.89; df=5, 158; p=0.49) on NK_1R BP. Gender was therefore omitted from subsequent analyses.

5.3.5.2. Activity in the cerebellum

Analysis using one way ANOVA revealed no significant difference between groups in cerebellum activities: healthy controls (mean=0.51 KBq/ml; SD=0.11), RD subjects (mean=0.47 KBq/ml; SD=0.09) and MDD subjects (mean=0.50 KBq/ml; SD=0.17) (F=0.41; df=2, 34; p=0.67).

5.3.5.3. Effect of magnet strength

Subjects had MRI scans using MRI scanners with different magnet strengths. Visual inspection of scans with ROIs mapped onto MRI slices and their co-registered PET

slices did not reveal differences in the mapping of ROIs on MRIs obtained from different scanners. Nevertheless, to check on the effect of MRI magnet strength on BP, the control group was divided into 3 groups according to the MRI magnet strength. Analysis with one way ANOVA did not reveal a significant difference between the groups in any brain region (e.g. for global BP: $F=0.65$; $df=2, 17$; $p=0.54$). A repeated measure analysis for the control group only, with 32 brain regions as the repeated measure and MRI magnet strength as the between subjects factor revealed a main effect of region ($F=115$; $df=5, 77$; $p < 0.001$), but there was no main effect of MRI magnet strength ($F=0.87$; $df=2, 17$; $p=0.44$) or region by MRI magnet strength interaction ($F=1.67$; $df=9, 77$; $p=0.11$).

Table 5.1. Demographics, radioligand-related data and clinical characteristics of healthy controls, subjects with major depressive disorder and subjects recovered from depression

Characteristic	Controls (n=20)	MDD subjects (n=6)	RD subjects (n=9)
	Mean (SD)	Mean (SD)	Mean (SD)
Age range (years)	31-65	32-57	31-58
Age Mean (years)	42.7 (10.1)	43.7 (11.5)	37.8 (9.7)
BMI	27.7 (4.8)	24.6 (4.5)	23.8 (5.0)
Years of Education	16.7 (3.6)	16.2 (3.7)	17.4 (4.3)
Full-scale IQ	117.8 (5.6)	116.5 (4.1)	114.4 (4.9)
BDI Score (max =63)	2.0 (1.8)	27.3 (7.0)**	2.8 (3.3)
HDRS	1.2 (1.3)	20.5 (2.9)**	1.4 (1.7)
STAI-Trait (max=80)	30.9 (5.8) (n=19)	59.2 (8.0)**	35.9 (6.1)
STAI-State (max=80)	28.8 (6.0) (n=19)	51.3 (6.7)**	37.3(14.3)
Activity Injected (MBq)	143 (6)	146 (3)	145 (5)
Specific Activity (GBq/µmol)	194 (163)	217 (173)	142 (92)
Weight of SPA-RQ (µg)	0.59 (0.5)	0.67 (0.8)	0.7 (0.5)
		Mean (range)	Mean (range)
Age of onset (years)		27.7 (18-55)	21.2 (14-27)
Duration of current episode (months)		9.0 (2-17)	-------
Lifetime episodes (months)		45.5 (6-96)*	20.0 (6-48)
Lifetime dysphoria (months)		68.5 (6-156)*	24.3 (6-84)
Number of episodes		3.7 (2-5)	3.1 (1-5)
Euthymic since last episode (months)		-------	46.0 (3-132)
Drug-free (months)		34.2 (7-120)	55.7 (6-132)
	N	N	N
Male	11	4	6
Female	9	2	3
Smoker	2	2	0
Left-Handedness	1	2	0
Past use of antidepressants	1	6	6
Family history of depression	5	4	2
Suicide attempts	-	6	1
Melancholic depression	-	1	6
Co-morbidities:			
Dysthymia		2	1
GAD		4	1
PTSD (NOS)		0	1
Social Phobia		1	0

BDI=Beck Depression Inventory; BMI=body mass index; HDRS=Hamilton Depression Rating Scale; MDD=Major Depressive Disorder; N=number; RD=Recovered Depressed; SD=standard deviation; STAI=Spielberger State Anxiety Inventory; * $p < 0.05$; ** $p < 0.001$.

Table 5.2. Measures on personality and parental bonding for healthy controls, subjects with major depressive disorder and subjects recovered from depression

Characteristic	Controls (n=19)	MDD subject (n=6)	RD subjects (n=9)
	Mean (SD)	Mean (SD)	Mean (SD)
BIS	22.1 (4.8)	19.5 (2.7)	20.2 (3.6)
DAS	96.8 (23.6)	145.3 (23.7)*	95.2 (20.1)
EPQ-Extroversion	15.3 (3.2)*	7.5 (2.2)	12.2 (4.8)
EPQ-Lie	8.4 (4.0)	8.3 (5.4)	8.7 (2.8)
EPQ-Neuroticism	5.6 (3.6)	18.3 (2.5)**	8.2 (3.5)
EPQ-Psychoticism	2.6 (1.5)	6.0 (1.9) *	3.0 (2.3)
Shyness	6.3 (5.2)	18.3 (3.9)**	8.0 (7.1)
Sociability	12.6 (5.0)	10.2 (1.0)	11.0 (4.8)
TAQ	53.4 (12.4)	71.7 (12.2)*	52.9 (10.7)
TPQ-Harm Avoidance	9.6 (5.4)†	21.0 (5.6)**	11.1 (5.3)
TPQ-Novelty Seeking	17.2 (4.8)†	17.5 (3.7)	16.3 (3.2)
TPQ-Reward Dependence	16.8 (3.6)†	19.5 (4.5)	16.7 (4.4)
PBI-maternal care	25.7 (7.1)	17.6 (10.1)	27.3 (6.4)
PBI-maternal protection	12.4 (6.6)	13.6 (8.3)	8.7 (7.4)
PBI-paternal care	24.1 (6.4)†	13.8 (7.0)‡*	18.0 (10.3)
PBI-paternal protection	11.1 (6.5)†	16.2 (8.2)‡	11.9 (9.6)

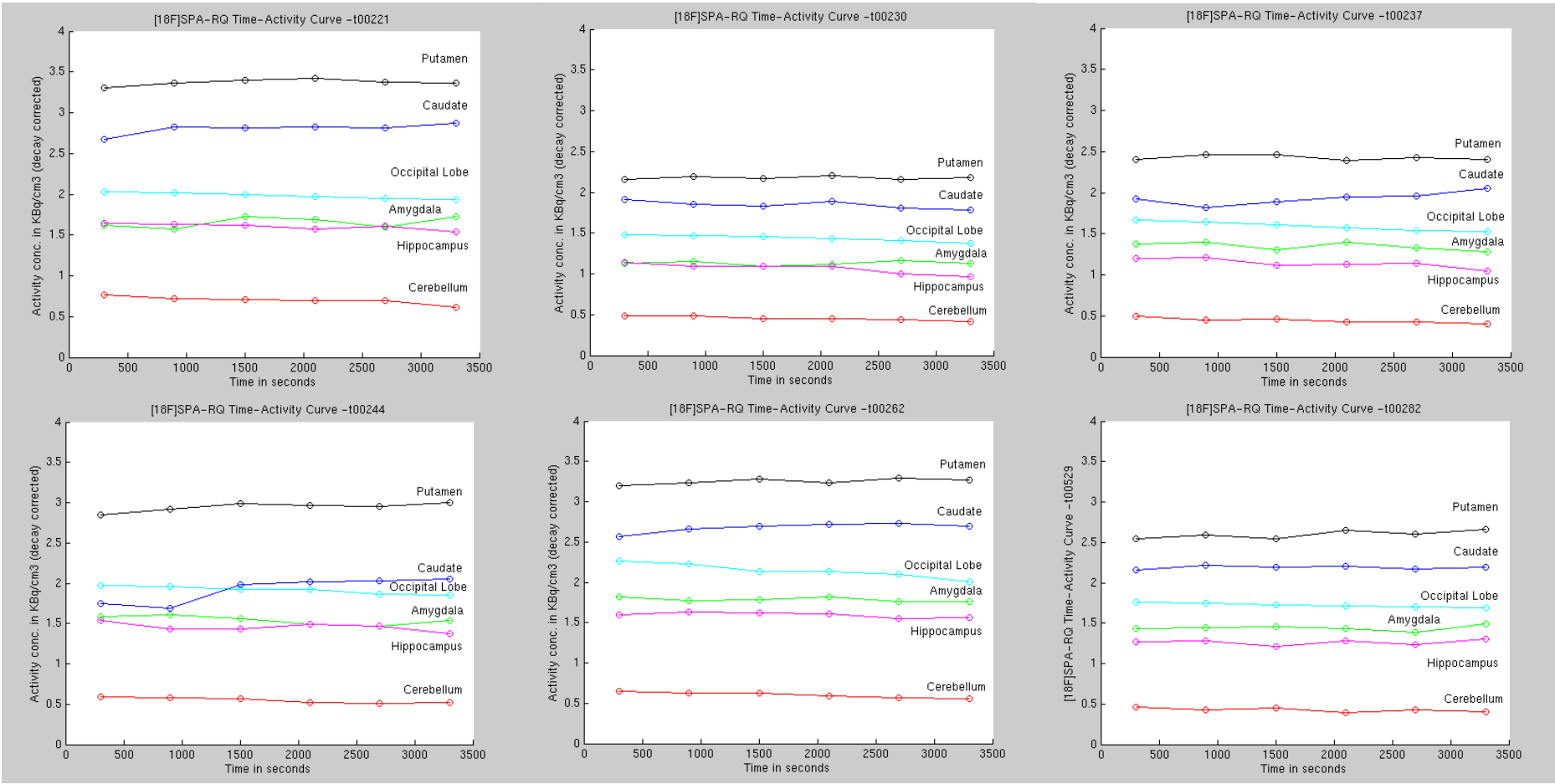
BIS=Baratt Impulsivity Scale; DAS=Dysfunctional Attitudes Scale; EPQ=Eysenck Personality Questionnaire; TAQ=The Aggression Questionnaire; TPQ=Tridimensional Personality Questionnaire; * $p < 0.05$; ** $p < 0.001$ with *post hoc* Bonferroni test; †: n=18; ‡: n=5.

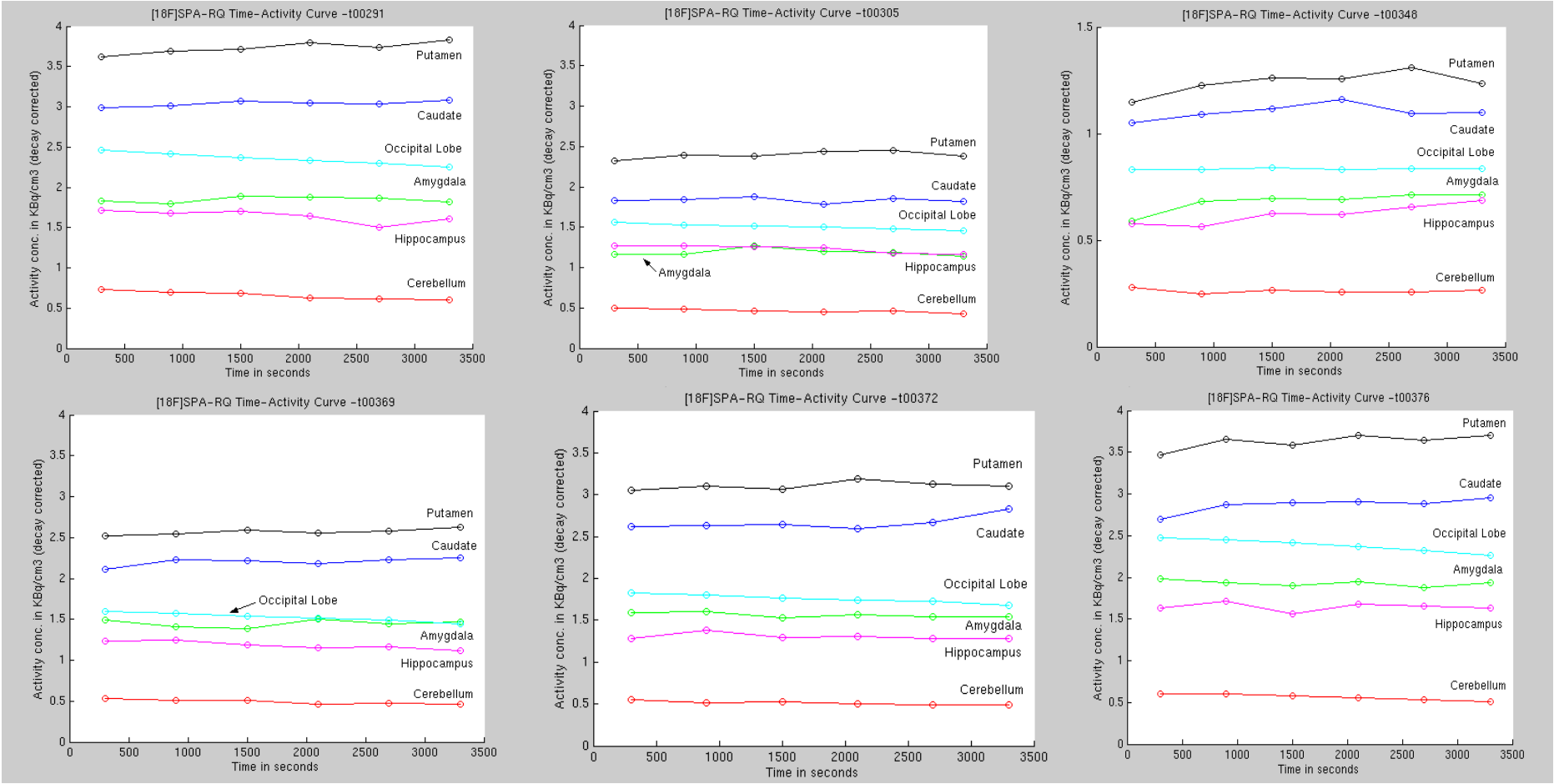
5.3.5.4. Regional time activity curves

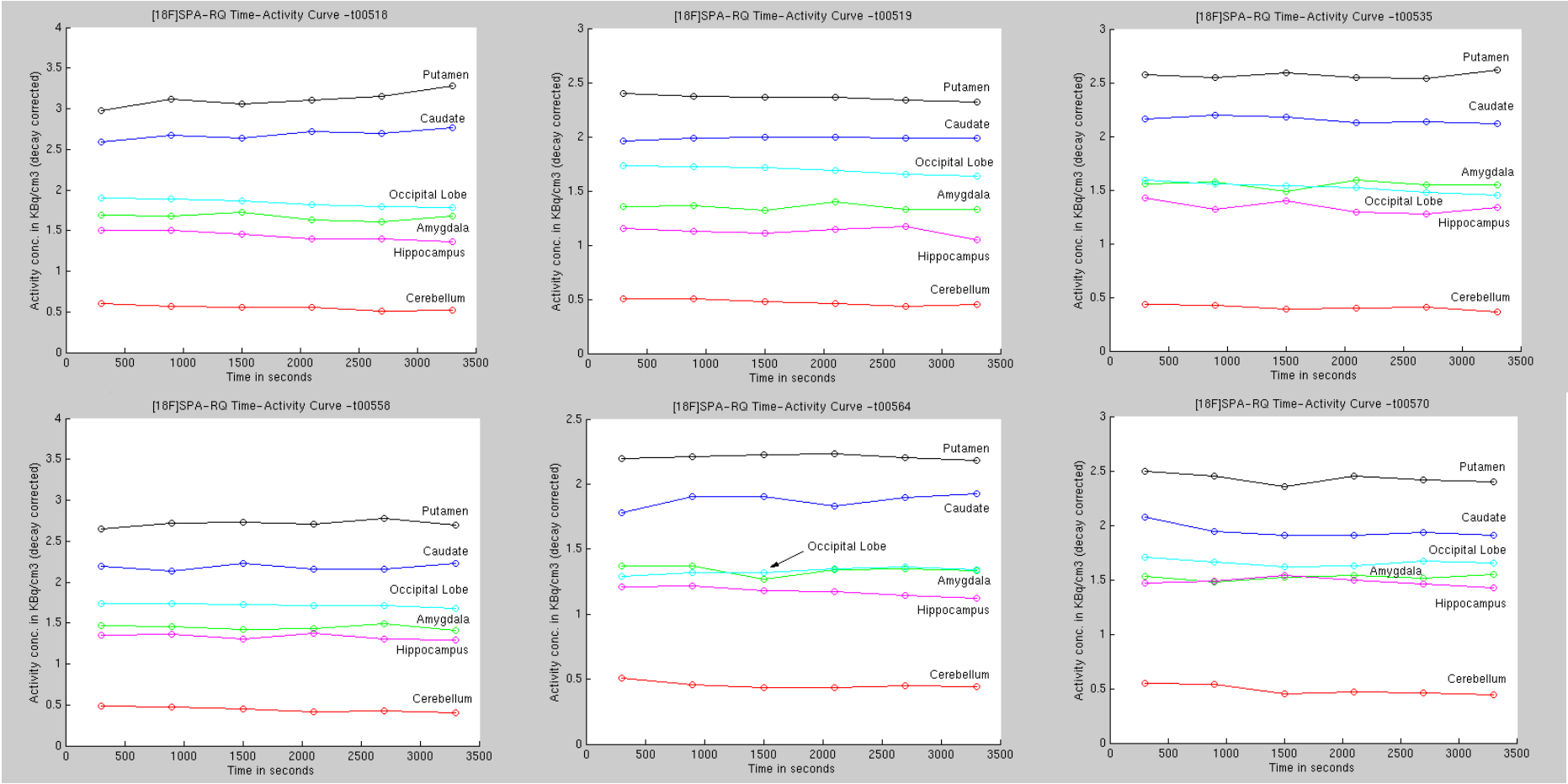
For each individual subject TACs were created for 5 target regions; putamen, caudate, occipital lobe, amygdala and hippocampus, while the cerebellum acted as the reference region (see Fig. 5.5 to Fig. 5.7). The order of radioligand binding from high to low was generally: putamen > caudate > occipital lobe >amygdala > hippocampus> cerebellum. Unlike in chapter 4, the TACs were generally 'flat' as the PET emission scan was carried out at 150-210 min after i.v. injection of [^{18}F]SPA-RQ, when the decay-corrected tissue activity concentrations would have reached close to a transient equilibrium in most target regions. Deviations from a 'flat' line were more likely in small receptor-rich regions such as the putamen and caudate. The order of radioligand binding and the shape of the TACs were very similar in all 3 groups studied (see Fig. 5.5 to Fig. 5.7).

TACs for the raphe were generated separately. There was a moderate amount of radioligand binding in the raphe. An example of a TAC for the raphe in a control subject is shown in Fig. 5.8.

Fig. 5.5. Individual [^{18}F]SPA-RQ time activity curves for control subjects. Comparison of 5 target regions (putamen, caudate, occipital lobe, amygdala and hippocampus) and reference region (cerebellum):




[18F]SPA-RQ Time-Activity Curve -t00291
Activity conc. in KBq/cm3 (decay corrected)
Time in seconds
Putamen
Caudate
Occipital Lobe
Amygdala
Hippocampus
Cerebellum
[18F]SPA-RQ Time-Activity Curve -t00305
Activity conc. in KBq/cm3 (decay corrected)
Time in seconds
Putamen
Caudate
Occipital Lobe
Amygdala
Hippocampus
Cerebellum
[18F]SPA-RQ Time-Activity Curve -t00348
Activity conc. in KBq/cm3 (decay corrected)
Time in seconds
Putamen
Caudate
Occipital Lobe
Amygdala
Hippocampus
Cerebellum
[18F]SPA-RQ Time-Activity Curve -t00369
Activity conc. in KBq/cm3 (decay corrected)
Time in seconds
Putamen
Caudate
Occipital Lobe
Amygdala
Hippocampus
Cerebellum
[18F]SPA-RQ Time-Activity Curve -t00372
Activity conc. in KBq/cm3 (decay corrected)
Time in seconds
Putamen
Caudate
Occipital Lobe
Amygdala
Hippocampus
Cerebellum
[18F]SPA-RQ Time-Activity Curve -t00376
Activity conc. in KBq/cm3 (decay corrected)
Time in seconds
Putamen
Caudate
Occipital Lobe
Amygdala
Hippocampus
Cerebellum


[18F]SPA-RQ Time-Activity Curve -t00518
Activity conc. in KBq/cm3 (decay corrected)
Time in seconds
Putamen
Caudate
Occipital Lobe
Amygdala
Hippocampus
Cerebellum
[18F]SPA-RQ Time-Activity Curve -t00519
Activity conc. in KBq/cm3 (decay corrected)
Time in seconds
Putamen
Caudate
Occipital Lobe
Amygdala
Hippocampus
Cerebellum
[18F]SPA-RQ Time-Activity Curve -t00535
Activity conc. in KBq/cm3 (decay corrected)
Time in seconds
Putamen
Caudate
Amygdala
Occipital Lobe
Hippocampus
Cerebellum
[18F]SPA-RQ Time-Activity Curve -t00558
Activity conc. in KBq/cm3 (decay corrected)
Time in seconds
Putamen
Caudate
Occipital Lobe
Amygdala
Hippocampus
Cerebellum
[18F]SPA-RQ Time-Activity Curve -t00564
Activity conc. in KBq/cm3 (decay corrected)
Time in seconds
Putamen
Caudate
Occipital Lobe
Amygdala
Hippocampus
Cerebellum
[18F]SPA-RQ Time-Activity Curve -t00570
Activity conc. in KBq/cm3 (decay corrected)
Time in seconds
Putamen
Caudate
Occipital Lobe
Amygdala
Hippocampus
Cerebellum

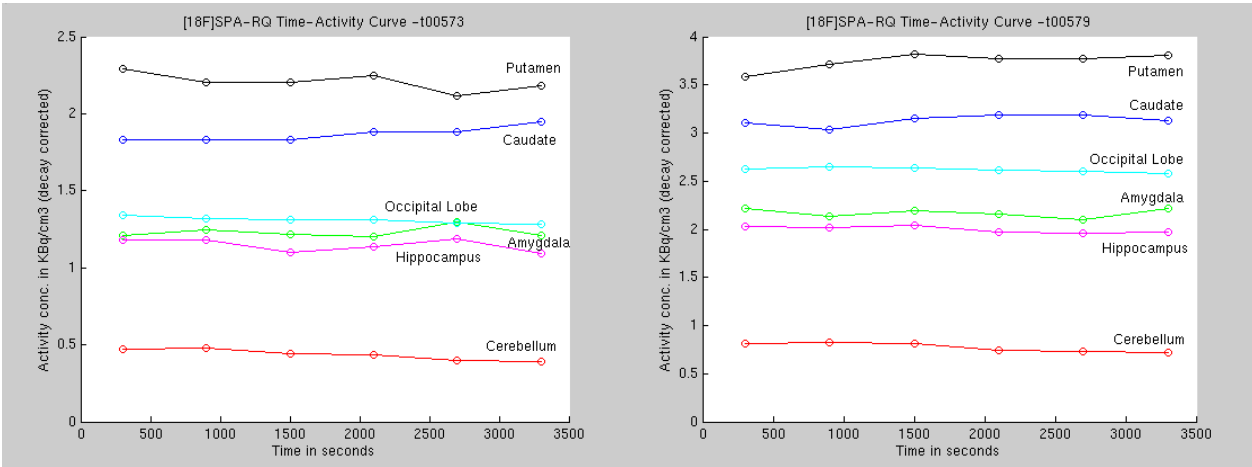

[18F]SPA-RQ Time-Activity Curve -t00573
Activity conc. in KBq/cm3 (decay corrected)
Time in seconds
Putamen
Caudate
Occipital Lobe
Amygdala
Hippocampus
Cerebellum
[18F]SPA-RQ Time-Activity Curve -t00579
Activity conc. in KBq/cm3 (decay corrected)
Time in seconds
Putamen
Caudate
Occipital Lobe
Amygdala
Hippocampus
Cerebellum

Fig. 5.6. Individual [^{18}F]SPA-RQ time activity curves for subjects with major depressive disorder. Comparison of 5 target regions (putamen, caudate, occipital lobe, amygdala and hippocampus) and reference region (cerebellum):

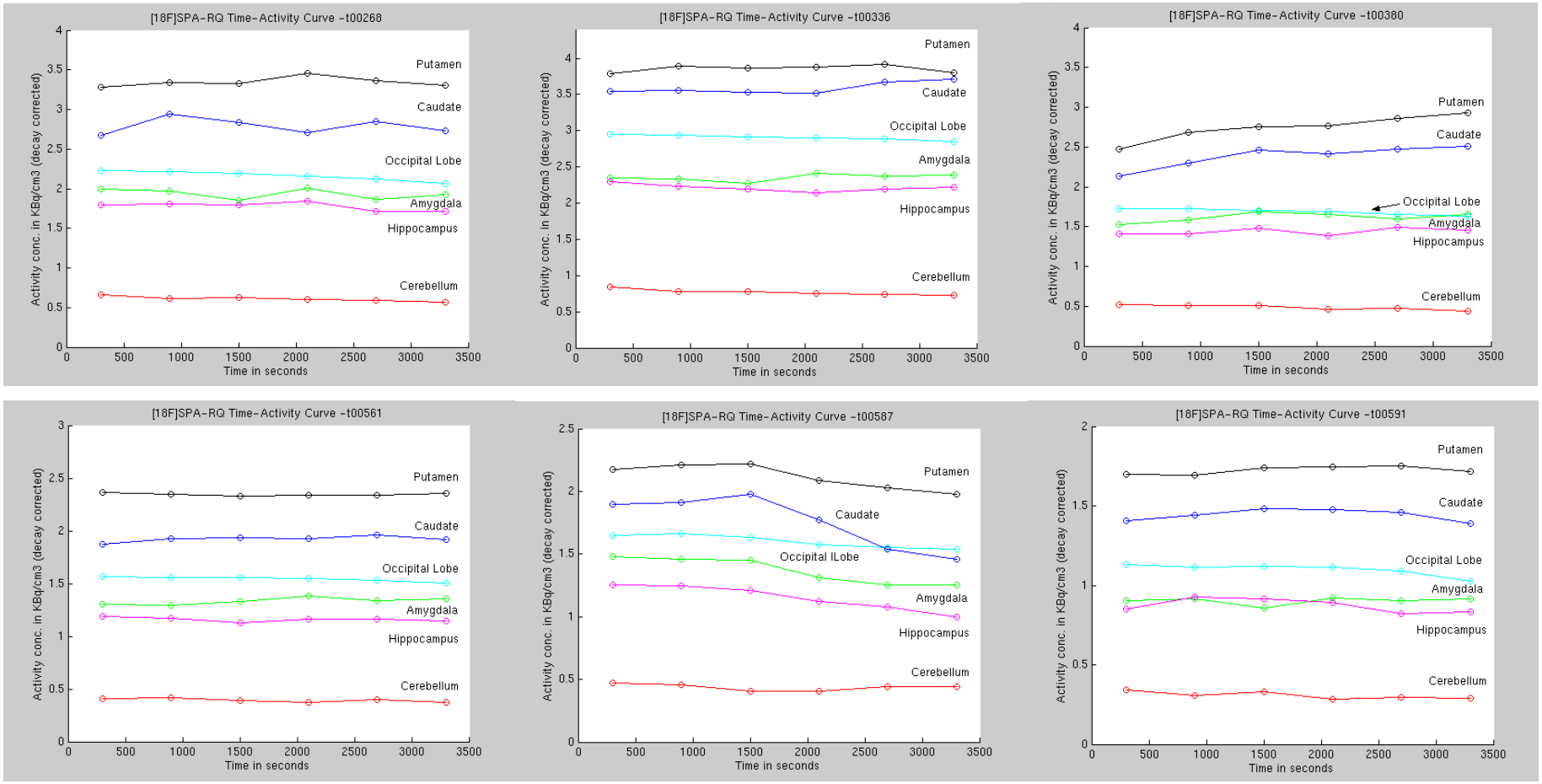
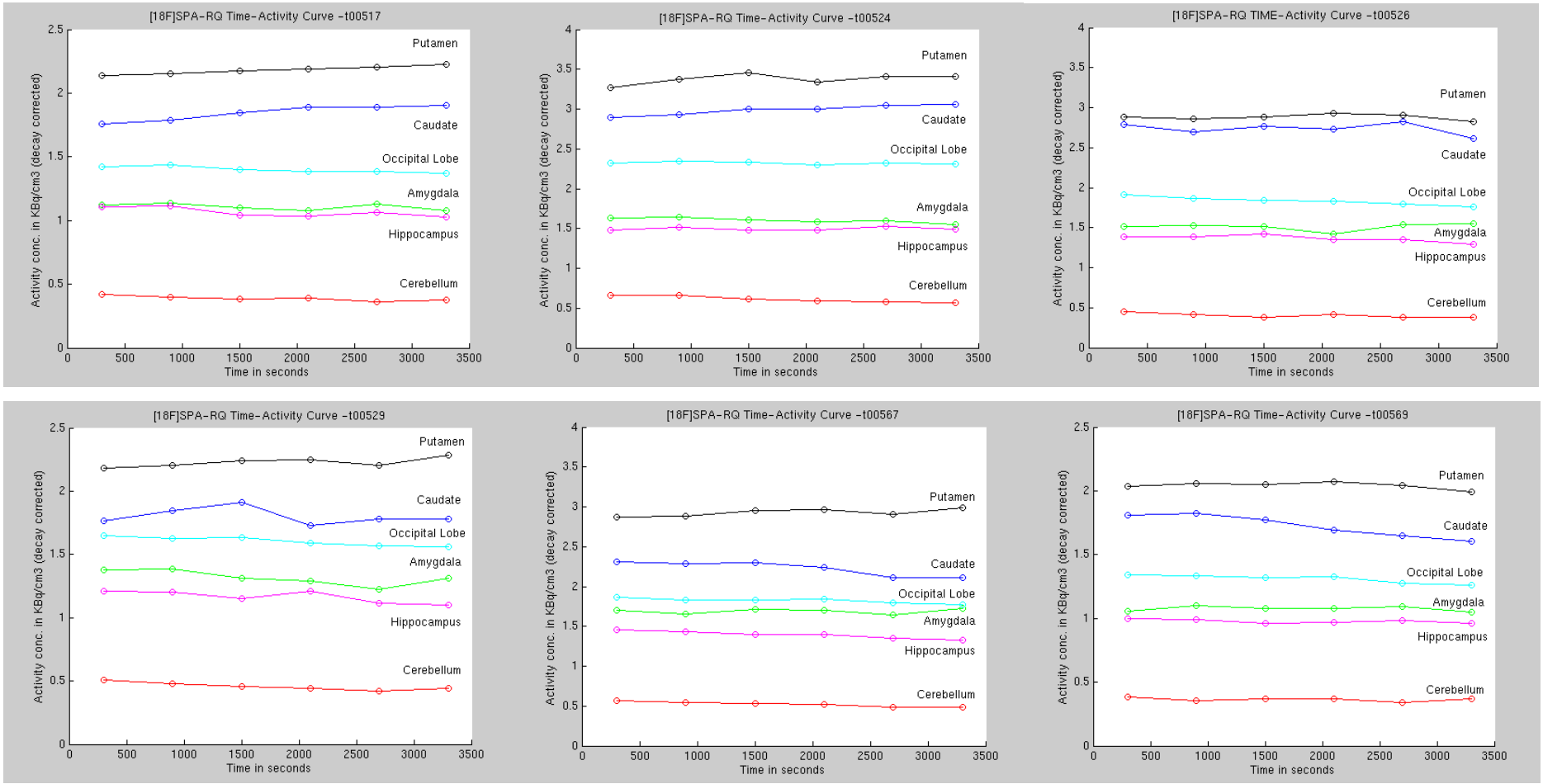
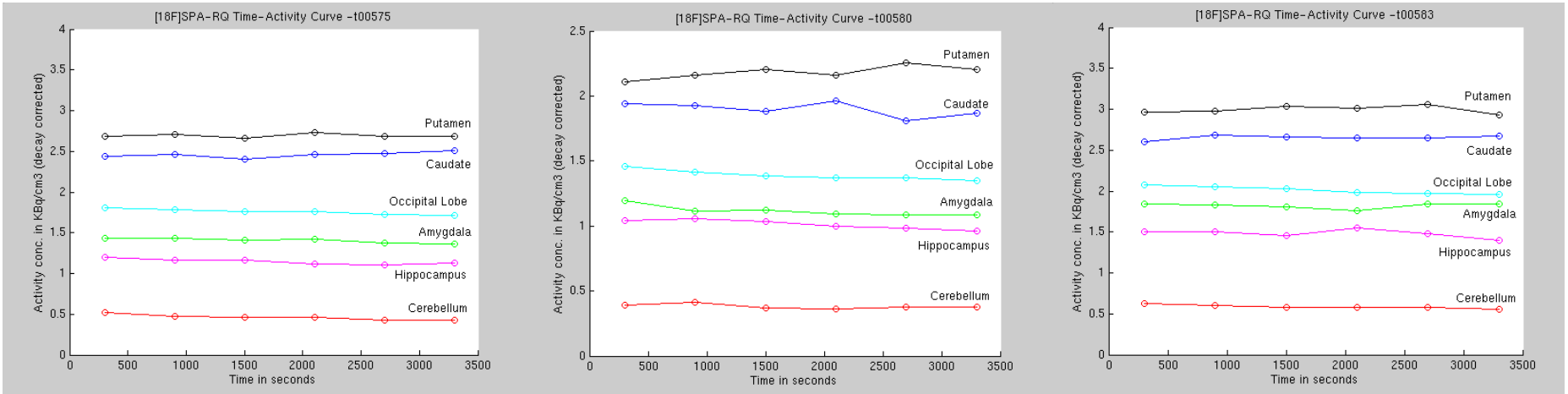


Fig. 5.7. Individual [^{18}F]SPA-RQ time activity curves for subjects recovered from depression. Comparison of 5 target regions (putamen, caudate, occipital lobe, amygdala and hippocampus) and reference region (cerebellum):




[18F]SPA-RQ Time-Activity Curve -t00575
Activity conc. in KBq/cm3 (decay corrected)
Time in seconds
Putamen
Caudate
Occipital Lobe
Amygdala
Hippocampus
Cerebellum
[18F]SPA-RQ Time-Activity Curve -t00580
Activity conc. in KBq/cm3 (decay corrected)
Time in seconds
Putamen
Caudate
Occipital Lobe
Amygdala
Hippocampus
Cerebellum
[18F]SPA-RQ Time-Activity Curve -t00583
Activity conc. in KBq/cm3 (decay corrected)
Time in seconds
Putamen
Caudate
Occipital Lobe
Amygdala
Hippocampus
Cerebellum

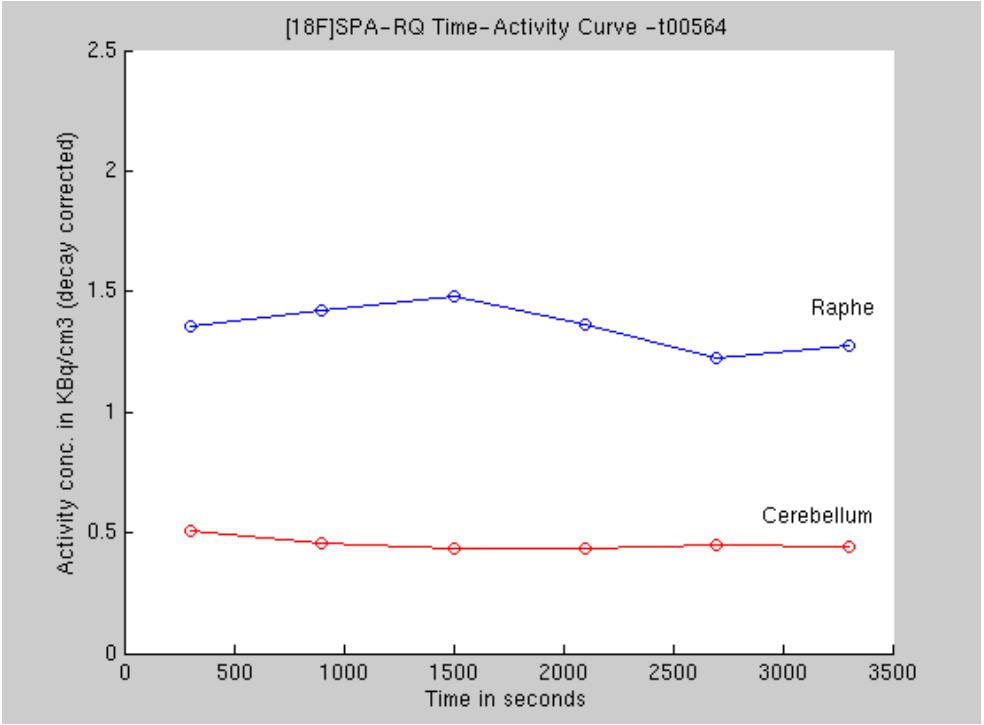


Fig. 5.8. Example of a [^{18}F]SPA-RQ time activity curve for the raphe. Comparison of the target region (raphe) and the reference region (cerebellum) in a normal control subject.

5.3.5.5. NK_1 receptor binding potentials in depressed, recovered depressed and control subjects

The regional BP values for each region and for each group are tabulated in Table 5.3. Repeated measures analysis of regional BP values including sub-regions and the raphe (n=32), with age as a covariate, showed significant main effect of region (F=25.7; df=5, 143; p <0.001), with age as a significant covariate of BP (F=7.7; df=1, 31; p=0.01). However, there was no region by group interaction (F=0.93; df=9,143; p=0.51), region by age interaction (F=1.8; df=5, 143; p=0.12) nor a main effect of group (F=1.3; df=2, 31; p=0.29). With regards to the raphe, there was no significant difference in the mean BP values between the three groups (controls 1.98 (SD 0.36); MDD subjects 2.21 (SD 0.19); RD subjects 2.00 (SD 0.26)) with a one way ANOVA and age as covariate (F=1.3; df=2, 32; p=0.28).

Mean (SD) of the global BP for each group was: controls, 2.04 (0.29); MDD, 2.20 (0.16); RD, 2.22 (0.28). There was no significant difference in mean global BP values between the 3 groups (F=1.7; df=2, 32; p=0.19). However, age was a significant covariate of mean global BP (F=6.9; df=1, 31; p=0.01). The difference in mean global BP between the groups remained non-significant after co-varying for age (F=1.47; df=2, 31; p=0.25).

Fig. 5.9 shows no significant difference between the 3 groups in NK_1R binding potential in the amygdala, while Fig. 5.10 shows that the order of NK_1R density in selected brain regions was the same in all 3 groups: putamen > caudate > occipital lobe > amygdala > hippocampus.

Table 5.3. Binding potentials in brain regions for healthy controls, subjects with major depressive disorder and subjects recovered from depression.

Region	Controls (n=20) BP	MDD subjects (n=6) BP	RD subjects (n=9) BP
Putamen	4.38 (0.55)	4.40 (0.42)	4.64 (0.63)
Caudate	3.42 (0.50)	3.60 (0.32)	3.88 (0.81)
Nucleus accumbens	3.19 (0.49)	3.38 (0.47)	3.52 (0.86)
Pallidum	2.66 (0.73)	2.55 (0.73)	3.07 (0.93)
Cuneus	2.52 (0.43)	2.70 (0.18)	2.75 (0.37)
Lingual gyrus	2.47 (0.36)	2.83 (0.26)	2.80 (0.37)
Occipital lobe	2.42 (0.36)	2.64 (0.17)	2.69 (0.34)
Post cingulate gyrus	2.18 (0.33)	2.28 (0.26)	2.38 (0.42)
Insula	2.17 (0.34)	2.33 (0.23)	2.27 (0.31)
Parietal lobe	2.10 (0.30)	2.26 (0.22)	2.29 (0.31)
Inferior frontal gyrus	2.09 (0.35)	2.26 (0.24)	2.29 (0.24)
Superior parietal gyrus	2.09 (0.28)	2.25 (0.21)	2.31 (0.32)
Superior temporal gyrus	2.06 (0.33)	2.27 (0.18)	2.29 (0.29)
Posterior temporal lobe	2.04 (0.27)	2.26 (0.17)	2.26 (0.32)
Posterior central gyrus	2.04 (0.29)	2.18 (0.29)	2.22 (0.28)
Precentral gyrus	2.03 (0.29)	2.12 (0.25)	2.12 (0.24)
Middle frontal gyrus	2.02 (0.30)	2.19 (0.19)	2.19 (0.24)
Orbitofrontal cortex	1.98 (0.30)	2.18 (0.22)	2.21 (0.27)
Middle temporal gyrus	1.97 (0.28)	2.11 (0.13)	2.09 (0.32)
Frontal lobe	1.95 (0.28)	2.08 (0.20)	2.10 (0.23)
Amygdala	1.94 (0.34)	2.16 (0.17)	2.02 (0.32)
Straight gyrus	1.90 (0.28)	2.17 (0.10)	2.12 (0.39)
Ant cingulate gyrus	1.81 (0.32)	1.91 (0.22)	1.94 (0.27)
Superior frontal gyrus	1.80 (0.26)	1.88 (0.20)	1.92 (0.20)
Ant temporal lobe (lateral)	1.79 (0.30)	1.93 (0.15)	2.01 (0.27)
Lat occipitotemporal	1.72 (0.29)	1.82 (0.09)	1.83 (0.18)
Ant temporal lobe (medial)	1.65 (0.31)	1.74 (0.17)	1.76 (0.25)
Hippocampus	1.64 (0.27)	1.85 (0.11)	1.67 (0.28)
Parahippocampal gyrus	1.51 (0.27)	1.63 (0.12)	1.51 (0.22)
Thalamus	1.39 (0.34)	1.55 (0.36)	1.41 (0.28)
Brainstem	1.00 (0.17)	1.10 (0.17)	1.03 (0.14)
Global	2.04 (0.29)	2.20 (0.16)	2.22 (0.28)
Raphe	1.98 (0.36)	2.21 (0.19)	2.00 (0.26)

Ant=anterior; BP=binding potential; MDD=Major Depressive Disorder; RD= Recovered Depressed; values are mean (SD). Age was a covariate. * $P < 0.05$ (*post hoc* Bonferroni).

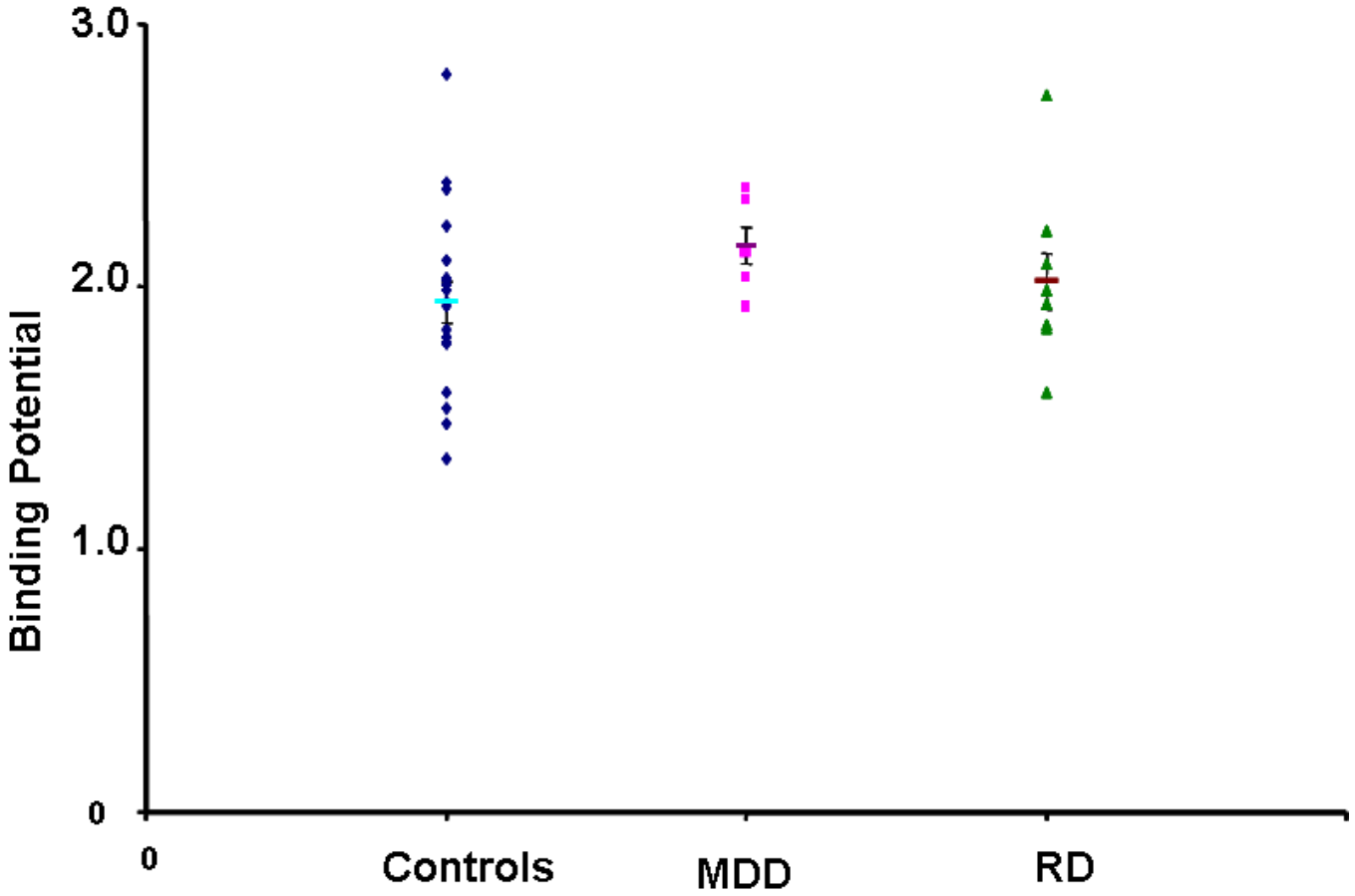


Fig. 5.9. Comparison of NK_1 receptor binding potentials in the amygdala between healthy controls, subjects with major depressive disorder and subjects recovered from depression. Each point represents a subject. For each group, the bars are mean +/- SEM. There was no significant difference between the 3 groups in binding potential in the amygdala.

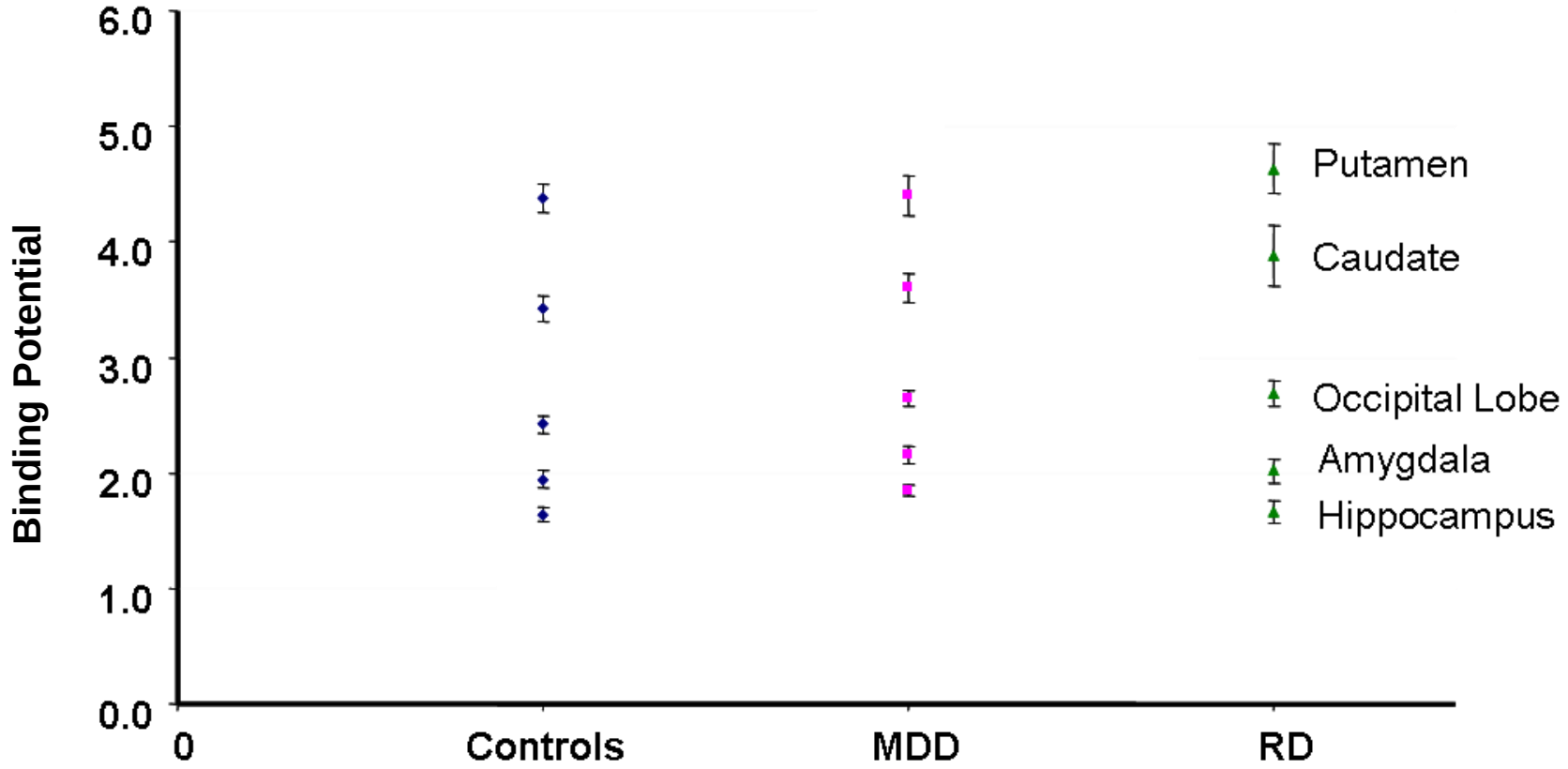


Fig. 5.10. Comparison of NK_1 receptor binding potentials in selected brain regions between healthy controls, subjects with major depressive disorder and subjects recovered from depression. For each region in each group, the bars are mean +/- SEM. There was no significant difference between the 3 groups in binding potential in any of the regions. For each group however, the order of NK_1R density was the same: putamen > caudate > occipital lobe > amygdala > hippocampus.

5.3.5.6. Effect of age on NK_1 receptor binding potential

With the groups examined separately, although there was an inverse correlation between age and mean global BP values, this was not significant: controls (r=-0.398; p=0.08); MDD subjects (r=-0.679; p=0.14); and RD subjects (r=-0.433; p=0.25). Nevertheless, there was an evident age-dependent decline in NK_1Rs when the 3 groups were combined (see Table 5.4). Here, age correlated negatively with global BP (r=-0.439; p=0.01) and with BP in every brain region. The region with the highest negative correlation for NK_1R BP with age was the medial part of the anterior temporal lobe (r=-0.518; p=0.001). Globally the decrease in NK_1R BP was of the order of about 3% per decade, while the rate of decline in the medial part of the anterior temporal lobe was of the order of 8% per decade (see Fig. 5.11).

Table 5.4. Correlations of binding potential with age in brain regions

Region	Pearson's Correlation r	P value
Putamen	-0.417	0.013*
Caudate	-0.444	0.007*
Nucleus accumbens	-.0496	0.002*
Pallidum	-0.331	0.052
Cuneus	-0.254	0.141
Lingual gyrus	-0.284	0.099
Occipital lobe	-0.276	0.108
Posterior cingulate gyrus	-0.380	0.025*
Insula	-0.373	0.027*
Parietal lobe	-0.484	0.003*
Inferior frontal gyrus	-0.457	0.006*
Superior parietal gyrus	-0.460	0.005*
Superior temporal gyrus	-0.421	0.012*
Posterior temporal lobe	-0.334	0.050
Posterior central gyrus	-0.474	0.004*
Precentral gyrus	-0.456	0.006*
Middle frontal gyrus	-0.434	0.009*
Orbitofrontal cortex	-0.438	0.009*
Middle temporal gyrus	-0.367	0.030*
Frontal lobe	-0.446	0.007*
Amygdala	-0.381	0.024*
Straight gyrus	-0.370	0.029*
Anterior cingulate gyrus	-0.470	0.004*
Superior frontal gyrus	-0.408	0.015*
Anterior temporal lobe (lateral)	-0.474	0.004*
Lateral occipitotemporal	-0.438	0.008*
Anterior temporal lobe (medial)	-0.518	0.001**
Hippocampus	-0.299	0.081
Parahippocampal gyrus	-0.315	0.066
Thalamus	-0.103	0.555
Brainstem	-0.491	0.003*
Global	-0.439	0.008*
Raphe	-0.247	0.152

Correlations are for all subjects combined (n=35); * $p < 0.05$; ** $p < 0.002$.

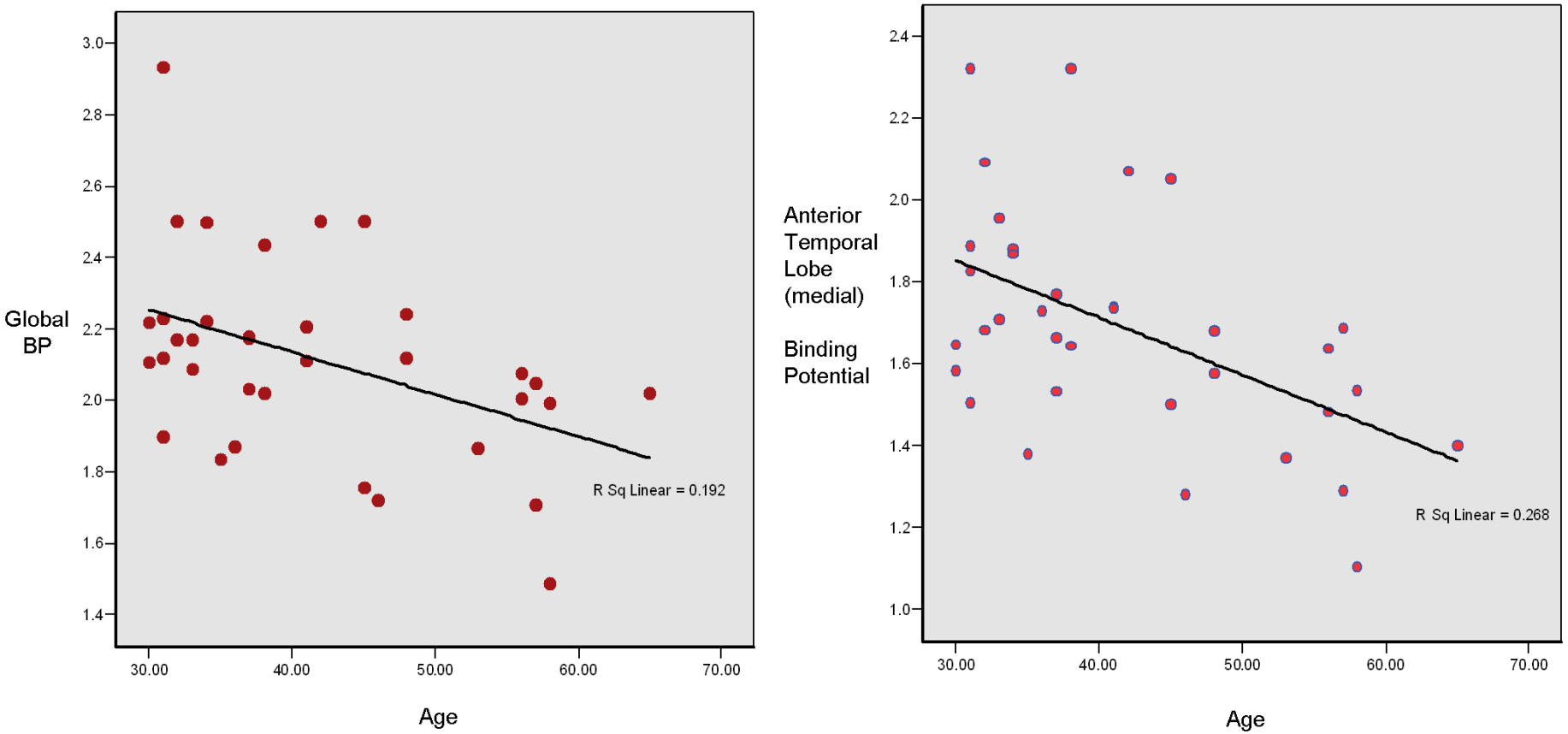


Fig. 5.11. Negative correlations between age and binding potential globally and in anterior temporal lobe (medial). Controls, subjects with major depressive disorder and recovered depressed subjects combined into one group (n=35). Global BP, p=0.008; anterior temporal lobe (medial), p=0.001.

5.3.5.7. Correlation of NK_1 receptor binding potentials with clinical characteristics

Global BP for NK_1Rs did not correlate significantly at $p < 0.002$ in the combined patient groups with any of the clinical characteristics such as age of onset of illness, number of episodes, number of years since first MDD episode, months medication-free, lifetime duration of major depressive episodes or lifetime duration of dysphoria. In addition, there was no significant correlation between the duration of euthymia and BP in brain regions in the RD group.

Not withstanding the small numbers, and with age included as a covariate, there were no significant differences within the combined patient group (MDD and RD subjects-n=15) in global BP and BP in the 32 brain regions, between subjects with melancholia versus without melancholia ($F=0.01$; $df=1, 12$; $p=0.94$), with a history of self-harm versus without a history of self-harm ($F=0.12$; $df=1, 12$; $p=0.74$), with antidepressant exposure versus without antidepressant exposure ($F=0.83$; $df=1, 12$; $p=0.38$).

With all three groups combined (n=35), and with age included as a covariate, there was no significant difference in BP, globally and in the 32 brain regions, between subjects with versus without a family history of depression ($F=0.43$; $df=1, 32$; $p=0.52$). However, there was a significant difference in BP with regards to a history of antidepressant exposure ($F=6.2$, $df=1, 32$; $p=0.02$). Individual t-tests then revealed a significantly higher BP, after correction for multiple comparisons ($p < 0.002$), only in the lingual gyrus ($t=-0.37$; $df=33$; $p=0.001$).

Exclusion of the control subject with previous antidepressant exposure, still did not reveal a significant difference between the 3 groups in BP in any brain region. A

repeated measures analysis of global and regional BP values including sub-regions and the raphe, with age as a covariate, showed a significant main effect of region (F=25.7; df=5, 135; p=0.001), and age was found to be a significant covariate of BP (F=9.2; df=1, 30; p=0.01). There was no region by group interaction (F=0.97; df=9, 135; p=0.48), region by age interaction (F=1.8; df=5, 135; p=0.12), nor a main effect of group (F=2.0; df=2, 30; p=0.15).

5.3.5.8. Correlation of NK_1 receptor binding potentials with mood and personality scores

Isolated correlations were found between PBI (paternal care) and NK_1R BP in the parietal lobe (n=5; r=0.990; p=0.001), in particular the superior parietal gyrus (n=5; r=0.988; p=0.002) in the MDD group. However, this was not replicated in the other groups. Similarly, an isolated negative correlation was found between TPQ-reward dependence and NK_1R BP in the raphe (n=9, r=-0.939; p=0.001) in the RD group, which was not replicated in the other groups. Also, with all groups combined there was a significant negative correlation between EPQ-E and BP for NK_1Rs in posterior temporal lobe (n=34; r=-0.522; p=0.002), straight gyrus (n=34, r=-0.574; p=0.001), orbitofrontal cortex (n=34; r=-0.509; p=0.002) and cuneus (n=34, r=-0.502; p=0.002). However, with removal of an outlier, the correlations were no longer significant.

5.3.6. Measures of stress

A comparison of measures of stress versus time during PET scan can be seen in Fig. 5.12. The physiological measures of stress were the MAP (mm Hg), heart rate and plasma cortisol levels, while the subjective measures were from VAS for stress and sadness. Mean (SD) AUC measures for the 3 groups are tabulated in Table 5.5.

5.3.6.1. Physiological measures of stress

One way ANOVA revealed no significant difference in AUC measures between the groups for plasma cortisol (F=0.34; df=2, 32; p=0.72), MAP (F=1.06; df=2, 31; p=0.37) or heart rate (F=1.18; df=2, 29; p=0.32). For MAP, age was used as a covariate as between subjects there was a main effect of age (F=10.4; df=1, 31; p=0.003). For heart rate, gender was used as a between subjects factor as there was a main effect of gender (F=4.55; df=1, 29; p=0.04).

5.3.6.2. Subjective measures of stress

One way ANOVA revealed a significant difference between the groups in AUC measures for 'sadness' (F=15.0; df=2, 32; $p < 0.001$) and 'stress' (F=5.0; df=2, 32; p=0.01). Repeated measures ANOVA showed there was a main effect of group between subjects for VAS 'sadness' (F=14.2; df=2, 32; $p < 0.001$) and VAS 'stress' (F=5.2; df=2, 32; p=0.01). *Post hoc* Bonferroni revealed the MDD group had higher scores on AUC measures of 'sadness' than the control group ($p < 0.001$) and RD group ($p < 0.001$), and higher scores on AUC measures of 'stress' than the control group (p=0.01) and RD group (p=0.02).

There was no effect of time, group or group by time for any of the stress measures.

5.3.6.3. Correlation of measures of stress with NK_1 receptor binding potential

There were no correlations for brain NK_1R BP with AUC for plasma cortisol, MAP, VAS for sadness or stress. In the MDD group there was an isolated negative correlation (n=6; r=-0.960; p=0.002) between the AUC for heart rate and the superior frontal gyrus, but this was not found in the other two groups.

Table 5.5. Comparison of measures of stress between healthy controls, subjects with major depressive disorder and subjects recovered from depression

Stress measure	Control subjects (n=20)	MDD subjects (n=6)	RD subjects (n=9)
	AUC Mean (SD)	AUC Mean (SD)	AUC Mean (SD)
Plasma cortisol	496 (371)	475 (345)	608 (389)
MAP	298,259 (30,471)	283,020 (12,578)	285,822 (26,987)
Heart rate	3760 (638)	3393 (221)	3575 (606)
VAS sadness	82 (109)	318** (145)	32 (51)
VAS stress	138 (100)	285* (163)	127 (69)

AUC= area under curve (score x min); MAP=mean arterial pressure; VAS=visual analogue scale; * $p < 0.05$; ** $p < 0.001$ with *post hoc* Bonferroni test.

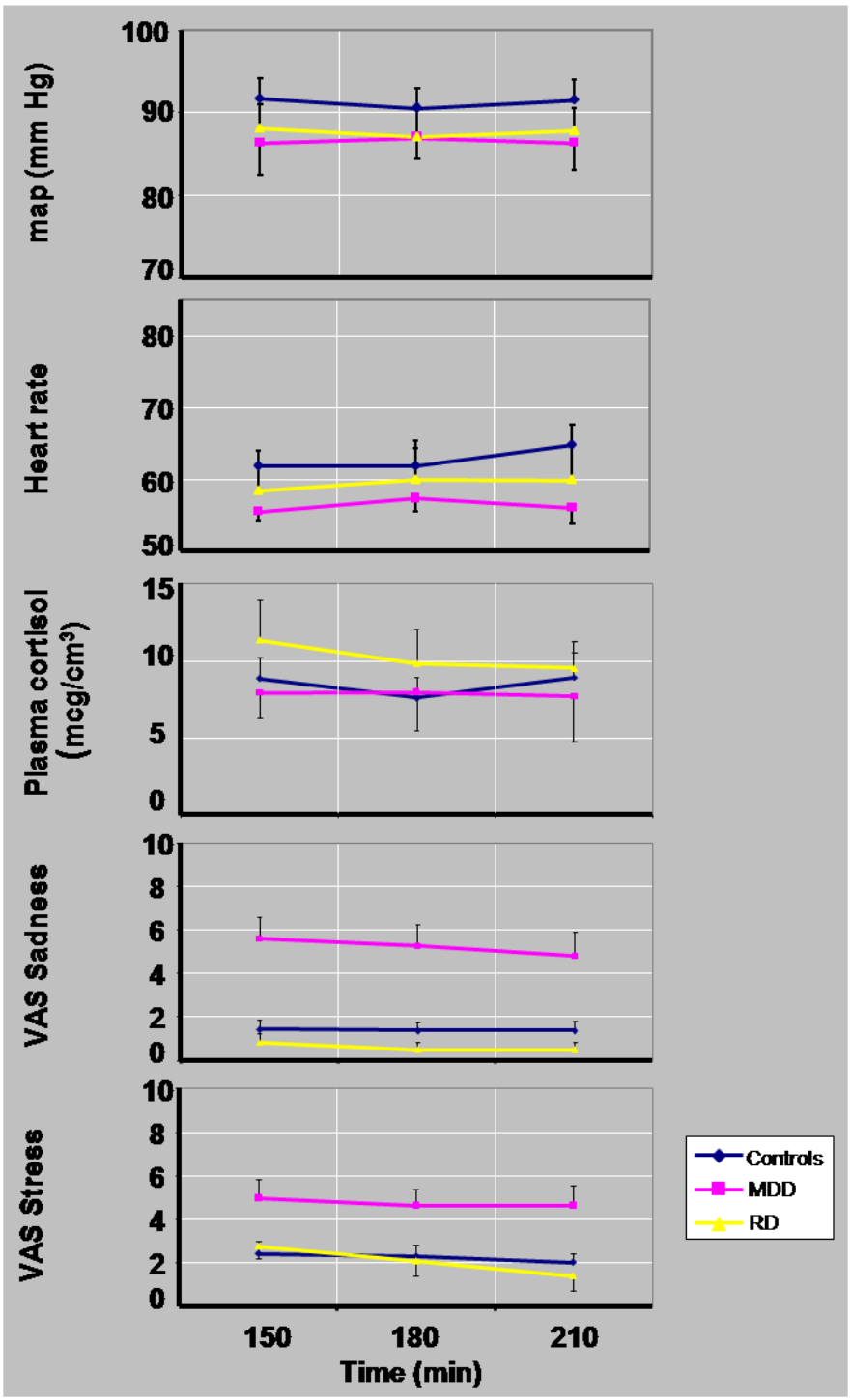


Fig. 5.12. Comparison of measures of stress versus time during PET scan. Physiological measures of stress were map (mm Hg), heart rate and plasma cortisol levels, while subjective measures were VAS scores for stress and sadness. A comparison is made for subjects with MDD, RD subjects and control subjects. Time was measured in min after injection of [^{18}F]SPA-RQ (t=0). Values are mean (SEM).

5.4. DISCUSSION

The main aim of this chapter was to use PET and the radioligand [^{18}F]SPA-RQ to quantify NK_1Rs in antidepressant-free subjects with MDD and RD as compared to control subjects. The hypothesis was that BP for NK_1Rs would be higher in limbic, cortical and midbrain regions in MDD subjects as compared to RD patients and controls.

5.4.1. No difference in NK_1 receptor binding potentials between depressed, recovered depressed and control subjects

Using [^{18}F]SPA-RQ, PET and the 'transient equilibrium' model, there was no difference between MDD patients, RD patients and controls in BP for NK_1Rs in any brain region. This suggests NK_1Rs may not be altered in number in depression. In contrast, animal studies suggest NK_1RAs may exert antidepressant actions. However, a large multicentre trial in depressed patients failed to reveal a benefit of aprepitant over placebo (Keller et al 2006). But it should be noted that the molecular target for treatment may not necessarily be the same as the diseased target. Furthermore, human postmortem studies are inconsistent (see chapter 1) with regards to NK_1Rs in depression. Nevertheless, the findings in this chapter tally with the study which showed no difference in ^{3}H-SP binding in the amygdala in depression (Carletti et al 2005). Another postmortem brain study did however observe a change in the laminar ratio of NK_1Rs in the anterior cingulate cortex in depression (Burnet and Harrison 2000), but PET is not able to measure changes in the laminar ratio of receptors in the brain and so subtle alterations in NK_1Rs in depression such as altered receptor activity would not be detected.

The negative result obtained in this chapter is however fairly robust. In a limbic brain region such as the hippocampus, with the numbers recruited, the minimum difference that could have been detected was 22%. In a receptor-rich brain region such as the posterior cingulate gyrus, with the numbers recruited, it would have been possible to detect a minimum difference of 20% if this had been present. However, in order to detect a 20% difference in NK_1R BP between the MDD group and controls in the hippocampus, with a power of 0.8, at least 12 subjects would have been required in each group. Similarly, with the posterior cingulate, at least 10 subjects would have been required in each group.

It should be noted here that one preliminary *in vivo* PET imaging study did find changes in NK_1R binding in depressed patients (Hietala 2002). This study was presented as an abstract at the American College of Neuropsychopharmacology meeting in Puerto Rico in 2002. In this study, 9 depressed patients (5 females and 4 males; age range=28-48; mean (SD) HDRS scores of 24 (3)) and 9 control subjects (all males; age range 22-48) underwent PET imaging with [^{18}F]SPA-RQ. A simplified reference tissue model with cerebellum as the reference region was applied to estimate BP in 26 brain regions. BP was found to be significantly higher in the caudate, putamen and hippocampus and significantly lower in the posterior cingulate region in the depressed group. This study has never been published as a full paper and the total number of subjects recuited was low which may explain the apparent discrepancy with the results obtained in this chapter.

5.4.2. Comparison of binding potentials in control subjects with Nyman et al (2006)

The 'transient equilibrium' model used in this chapter was found to be robust in terms of the rank order of brain regions for NK_1R BP as compared to another study (Nyman et al 2006). Nyman et al. used a simplified reference tissue model with the cerebellum as the reference region. They scanned 35 male (mean age 27 +/- 8 yr; range 19-55 yr; weight range 55-87 kg) and 20 female (mean age 37 +/- 11 yr; range 21-52 yr; weight range 55-80 kg) normal human volunteers. The normal control subjects in this thesis comprised of 11 male (mean age 43 +/-9 yr; range 31-57 yr) and 9 female (mean age 43 +/- 12 yr; range 31-65). Therefore, the controls in the Nyman et al. study were younger in both gender groups. Table 5.5 outlines the mean and SD of BP estimates together with the CV. The CV values obtained from the data in this chapter ranged from 13-24 (males) and 12-24 (females) versus those of Nyman et al. which ranged from 12-24 (males) and 16-24 (females). There was a significant correlation (see Fig 5.13) between the BP estimates obtained in normal volunteers via the 'transient equilibrium' method in this chapter and those of Nyman et al. in 12 different brain regions (Nyman et al 2006). The correlations for the male subjects were: $r=0.971$, $p < 0.001$; and for the female subjects were: $r=0.952$, $p < 0.001$.

Table 5.6. Comparison of binding potentials in controls versus Nyman et al.

	Transient Equilibrium BP			Nyman et al. (2006) BP		
	Mean	SD	CV	Mean	SD	CV
Males						
Region:						
Putamen	4.35	0.58	13	5.08	0.59	12
Caudate nucleus	3.37	0.57	17	4.47	0.66	15
Occipital lobe	2.39	0.36	15	2.32	0.36	16
Posterior cingulate	2.22	0.35	16	1.95	0.25	13
Raphe	2.11	0.38	18	2.25	0.53	24
Superior Temporal gyrus	2.09	0.37	18	1.87	0.26	14
Orbitofrontal cortex	2.00	0.32	16	1.76	0.26	16
Amygdala	1.97	0.40	20	2.40	0.45	19
Anterior cingulate	1.82	0.34	18	1.55	0.26	17
Hippocampus	1.73	0.30	17	1.63	0.28	17
Parahippocampal gyrus	1.54	0.31	20	1.30	0.19	15
Thalamus	1.46	0.35	24	1.37	0.33	24
Females						
Region:						
Putamen	4.41	0.55	17	4.05	0.67	17
Caudate nucleus	3.47	0.42	12	3.86	0.73	19
Occipital lobe	2.46	0.38	14	1.86	0.41	22
Posterior cingulate	2.12	0.31	15	1.67	0.31	19
Superior Temporal gyrus	2.01	0.30	15	1.46	0.29	20
Orbitofrontal cortex	1.96	0.28	14	1.33	0.28	21
Amygdala	1.90	0.28	15	1.91	0.31	16
Raphe	1.83	0.26	14	1.86	0.41	22
Anterior cingulate	1.80	0.32	18	1.10	0.23	21
Hippocampus	1.53	0.18	12	1.30	0.28	22
Parahippocampal gyrus	1.48	0.21	15	0.98	0.24	24
Thalamus	1.31	0.32	24	1.04	0.25	24

BP=binding potential; CV=coefficient of variation; SD=standard deviation.

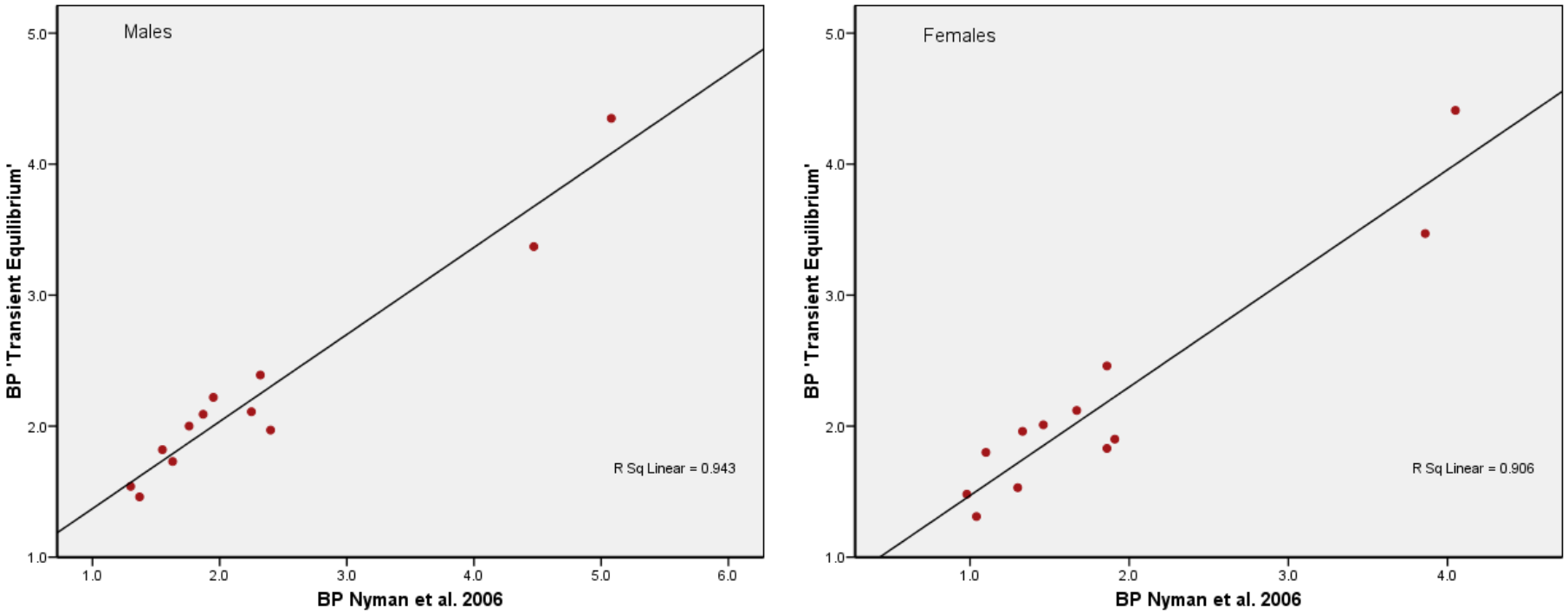


Fig. 5.13. Correlation of binding potentials obtained by transient equilibrium versus those of Nyman et al. (2006) in normal volunteers. Data is for 12 brain regions as outlined in Table 5.5. Males: r=0.971, $p < 0.001$; Females: r=0.952, $p < 0.001$.

5.4.3. Decline of NK_1 receptor binding with age

As there was no difference in BP between the groups studied, then the 3 groups of controls, MDD patients and RD patients were combined into one group of 35 subjects (age range 30-65) to examine the correlation between age and NK_1R binding. Age was found to correlate negatively with global BP and with BP in every brain region. The decline in global BP for NK_1Rs was in the order of 3% per decade. The region with the highest negative correlation for NK_1R BP with age was the medial part of the anterior temporal lobe, a brain region associated with memory function (Henson 2005). An inverse correlation between age and NK_1Rs was also found in another study (Nyman et al 2006). However, in this latter study, all 45 subjects were healthy controls and the age range was from 19 to 55 years. Also, the decline in NK_1R BP with age was restricted to only certain cortical regions, with the average decline being about 7% per decade, and the greatest decline in receptor numbers occurring in the parietal cortex (Nyman et al 2006). Interestingly, a decline in age has also been found using PET imaging with other receptors e.g. $5\text{-}HT_{1A}Rs$ (Bhagwagar et al 2004; Cidis Meltzer et al 2001; Moller et al 2007; Tauscher et al 2001) and $5\text{-}HT_{2A}Rs$ (Adams et al 2004; Meltzer et al 1998; Sheline et al 2002). In contrast, a postmortem study found a positive association between age and NK_1R binding in the anterior cingulate cortex (Burnet and Harrison 2000). However, the different methodologies are probably responsible for the differential results.

Preclinical studies suggest SP (Hasenohrl et al 2000) and NK_1RAs (Kart-Teke et al 2007; Kart et al 2004) may affect memory function. Thus, the finding in this chapter of a decline in NK_1R BP with age, especially in the medial part of the anterior temporal lobe, may support this suggestion.

5.4.4. Effect of gender on NK_1 receptor binding

Unlike the findings of Nyman et al. that gender can affect NK_1Rs in the human brain (Nyman et al 2006), there was no statistically significant difference in brain NK_1R BP between men and women in the control subjects in this thesis. This may be because the two samples were different with respect to age and sample size. In this chapter, all control subjects (n=20) examined were older than 30, while in Nyman et al. (2006), the number of subjects studied totalled 45 and majority of whom were < 30 years old, which may account for the differences. Thus, it is possible that gender differences in NK_1Rs are more evident at a younger age.

5.4.5. NK_1 receptor binding and personality scores

The MDD group scored significantly higher on DAS, EPQ-N, EPQ-P, shyness, TAQ, TPQ-harm avoidance and lower on PBI-paternal care. However, the control group had significantly higher scores on EPQ-E. Previously, DAS scores correlated with 5-HT_{2A}R BPs in cortical regions in recovered depressed patients (Bhagwagar et al 2006) and depressed patients (Meyer et al 2003), while BP for serotonin transporters in depressed patients correlated with severe pessimism (Meyer 2007). In this chapter, isolated significant correlations were found between PBI (paternal care) and NK_1R BP in the parietal lobe, in the MDD group, and an isolated negative correlation between Reward Dependence on the TPQ and NK_1R BP in the raphe in the RD group. However, as the correlations were isolated and did not occur in the other groups or with the groups combined, the findings should be interpreted with caution.

5.4.6. NK_1 receptor binding and clinical parameters

With all three groups combined, there was a significant difference in BP with regards to a history of antidepressant exposure and this was present only in the lingual gyrus. However, this finding may be a false positive as there was no significant difference found in any other brain region. A further analysis of the subjects divided into two groups comprising of those exposed to antidepressants in the past and those never exposed to antidepressants was not possible as the groups were not found to be matched in terms of gender and age. Nevertheless, it is possible that a history of exposure to antidepressants may affect BP for NK_1Rs in the lingual gyrus, a brain region with a role in dreaming (Germain et al 2004) and visual processing (Mather et al 2006). Interestingly, in a study of patients with social anxiety disorder, treatment with the antidepressant nefazodone resulted in greater activity in the bilateral lingual gyri, amongst other brain regions (Kilts et al 2006). Further studies would however be warranted to examine the effects of antidepressants on NK_1Rs in brain regions including the lingual gyrus.

5.4.7. NK_1 receptor binding and measures of stress

The 3 groups did not differ significantly with regards to physiological measures of stress. However, the MDD group did differ significantly from the other 2 groups in VAS for sadness and stress. Also, an isolated significant negative correlation was found between the AUC for heart rate and BP in the superior frontal gyrus of the frontal lobe in the MDD group. However, as the correlation was isolated and did not occur in the other groups or with the groups combined, the finding should be interpreted with caution.

Despite the above, NK_1RAs are being investigated for their therapeutic role in social phobia (Furmark et al 2005), and specific phobias (Michelgard et al 2007). In the latter study, women with a specific phobia for either snakes or spiders, viewed pictures of feared and non-feared animals, while being PET-scanned for 60 min with the NK_1RA [^{11}C]GR205171 PET radioligand. The uptake of the radioligand was significantly reduced in the right amygdala during phobic stimulation, and there was a negative correlation in the right amygdala between subjective anxiety ratings and NK_1R radioligand binding (Michelgard et al 2007).

5.4.8. Strengths and weaknesses of the study

The strengths of this chapter include the large number of healthy controls scanned and matched for age, BMI, years of education and IQ. There were also no significant differences between the groups in terms of gender or handedness. In addition, the MDD subjects were clearly depressed on the BDI and HDRS scores. They were also suffering from anxiety and had significant levels of dysfunctional attitudes and neuroticism.

The results of this study are weakened by the small sample sizes of the MDD group. Also, the clinical data with regards to the number of episodes of depression and age of onset was dependent on subject recall. In addition, PET data can be limited by head movements. Future studies may benefit from the use of realignment software to correct for head movements. Furthermore, receptor BP measures may have been underestimates in receptor-rich brain regions such as the striatum (see section 4.4.2). Finally, changes in the SP system may be present in depression, but may not be reflected in NK_1R binding.

5.5. CONCLUSIONS

Using the PET radioligand [^{18}F]SPA-RQ, there was no difference between MDD patients, RD patients and controls in BP for NK_1Rs in any of the brain regions studied. Also, there was no correlation between measures of stress or personality and BP for NK_1Rs. In addition, there was no effect of gender on BP. However, global and regional BP was found to correlate negatively with age, with the highest correlation present in the medial part of the anterior temporal lobe.

CHAPTER 6

GENERAL DISCUSSION

6.1. REVIEW OF THESIS BACKGROUND

Recent evidence suggests that SP and NK_1Rs may play a role in depression, with NK_1RAs having putative antidepressant properties possibly through interactions with 5-HT. For example, electrophysiological studies have shown that NK_1R blockade or deletion of NK_1Rs can increase 5-HT cell firing in the DRN (Conley et al 2002; Santarelli et al 2001). Also, a human postmortem study showed decreased NK_1Rs in the orbitofrontal cortex of depressed patients (Stockmeier et al 2002). However, interactions between NK_1Rs and 5-HT are poorly defined, and it is not clear if brain NK_1Rs are altered in human depression *in vivo*.

In view of the above, one main aim of this thesis was to examine anatomical interactions between NK_1Rs and the systems pre-synaptic and postsynaptic to 5-HT neurons in the DRN. The other main aim of this thesis was to develop a simplified protocol with the PET ratioligand [^{18}F]SPA-RQ to study NK_1Rs *in vivo* in normal human volunteers and to use this method to investigate if NK_1Rs are altered in medication-free depressed patients. The outcomes of these studies are summarised below and then discussed in more detail.

6.2. SUMMARY OF MAIN AIMS AND FINDINGS

6.2.1. Investigation into colocalisation of NK_1 receptors with 5-HT_{1A} and 5-HT_{2A} receptors in rat forebrain

6.2.1.1. Aim

The aim of these experiments (chapter 2) was to use immunofluorescence to examine cellular colocalisation between NK_1Rs and 5-HT_{1A} as well as 5-HT_{2A} receptors in rat forebrain regions (PFC, septum, hippocampus and amygdala) postsynaptic to the 5-HT neurons in the DRN.

6.2.1.2. Findings

It was found that 5-HT_{1A}R-ir colocalised to a high degree with NK_1R-ir in many forebrain regions, with the highest degree of colocalisation in the MS-DBB and hippocampal sub-regions. Colocalisation was also present in other brain regions including the PFC, frontal cortex and BLA, but to a lesser degree. In contrast, 5-HT_{2A}R-ir colocalised to a low-moderate degree with NK_1R-ir in forebrain regions, with the highest degree of colocalisation occurring in hippocampal sub-regions only. In general, the percentage of neurons demonstrating colocalisation between NK_1Rs and 5-HT_{1A}Rs was much greater than that for NK_1Rs and 5-HT_{2A}Rs.

6.2.2. Investigation of NK_1 receptors on afferent projections to dorsal raphe nucleus

6.2.2.1. Aim

The aim of these experiments (chapter 3) was to use retrograde tracing from DRN to identify afferent neurons in the PFC, LHb and LC and to combine this with

immunohistochemistry at the light microscopic and EM levels to examine for the presence of NK_1Rs on the cell bodies of these afferent neurons.

6.2.1.2. Findings

Retrograde tracing identified neurons afferent to the DRN in the PFC, LHb and LC consistent with previous work. Importantly, NK_1R-ir was found to localise on the cell bodies of some of the afferent neurons within the LHb and the LC at the light microscopic level. This was confirmed at EM in both the LHb and the LC. In the PFC, NK_1R-ir was not found on DRN afferent neurons, but was found on neurons in close proximity.

Put together, the findings provide strong evidence for an anatomical interaction between NK_1Rs and systems both pre-synaptic and post-synaptic to DRN 5-HT neurons.

6.2.3. Methods for quantification of human NK_1 receptors using positron emission tomography and [^{18}F]SPA-RQ

6.2.3.1. Aim

The aim of these experiments (chapter 4) was to develop a PET scanning protocol and an appropriate mathematical model for the study and quantification of brain NK_1Rs in normal human subjects *in vivo* using the [^{18}F] SPA-RQ radioligand.

6.2.3.2. Findings

A transient equilibrium ratio method was found to be comparable to compartmental modelling for the study and quantification of brain NK_1Rs in human subjects *in vivo*

using the [^{18}F] SPA-RQ radioligand. The regional brain uptake of [^{18}F]SPA-RQ was consistent with the known distribution of NK_1Rs; highest in striatum, moderate in cortex and thalamus, and low in cerebellum. On this basis, the cerebellum acted as a suitable reference region in subsequent studies. Moreover, these findings allowed the development of a PET scanning protocol for study of NK_1Rs in clinical populations.

6.2.4. Imaging brain NK_1 receptors in depression using positron emission tomography and [^{18}F] SPA-RQ

6.2.4.1. Aim

The main aim of these experiments (chapter 5) was to use the simplified PET scanning protocol proposed in chapter 4 to quantify human brain NK_1Rs in depression. In view of findings that stress may influence NK_1R binding (Duric and McCarson 2005; Hwang et al 2005), a secondary aim was to examine if NK_1R BP may be related to measures of stress, including physiological measures such as blood pressure, heart rate and plasma cortisol, and subjective measures of mood and stress.

6.2.4.2. Findings

The main finding was that using [^{18}F]SPA-RQ and PET, there was no difference in BP in any of the brain regions studied between MDD patients, RD patients and controls. In addition, although the groups differed with regards to subjective measures of stress, they did not differ significantly in terms of physiological measures of stress. Furthermore, no significant correlations were found between NK_1R BP and stress measures. However, a negative correlation between global NK_1R BP or regional BP with age was discovered. The strongest correlation between age and BP was in the anterior temporal lobe (medial).

6.3. DISCUSSION

6.3.1. Interactions between NK_1 receptors and the 5-HT system in brain regions postsynaptic and presynaptic to the raphe

The main findings of chapter 2 and 3 are summarised in Fig. 6.1. The origin of the 5-HT fibres innervating the forebrain 5-HT receptors is the DRN and MRN, while the origin of the forebrain SP fibres is mostly the hypothalamus and LdTg. NK_1Rs colocalise with 5-HT_{1A}Rs in most forebrain regions except for the LS, while NK_1R colocalisation with 5-HT_{2A}Rs mostly occurred in the hippocampus. In presynaptic regions, NK_1Rs were found on cells afferent to the DRN in the LHb and the LC. The significance of these findings is further discussed below.

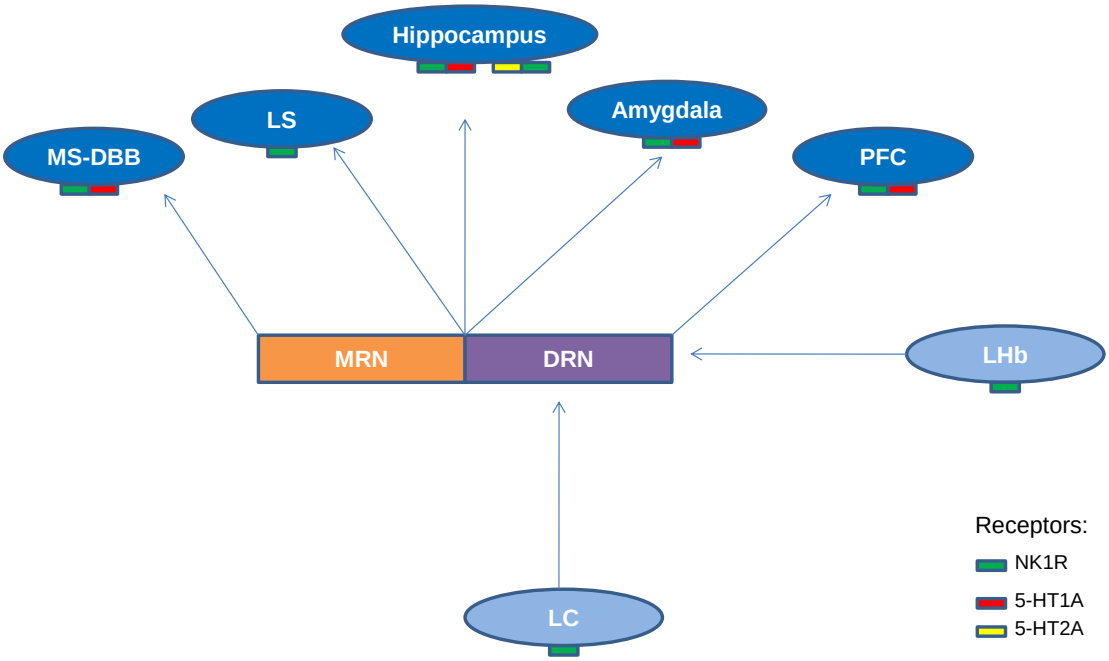


Fig. 6.1. Schematic summary diagram of the interactions between NK_1 receptors and the 5-HT system. 5-HT fibres originate from the MRN and DRN. In postsynaptic regions, NK_1Rs colocalised with 5-HT_{1A}Rs in the MS-DBB, hippocampus, BLA and PFC, but not in the LS. NK_1Rs colocalised with 5-HT_{2A}Rs mostly in the hippocampus. In presynaptic regions, NK_1Rs were found on neurons afferent to the DRN in the LHb and the LC.

In chapter 2, the highest degree of colocalisation (88%) between NK_1Rs and 5-HT_{1A}Rs was found in the MS-DBB. This brain region sends cholinergic and GABAergic projections to the hippocampus to generate theta oscillations (Leranth and Frotscher 1989). These oscillations are thought to play a role in cognition and affect (Degroot and Treit 2004). NK_1R agonists such as SP activate septohippocampal cholinergic neurons via direct post-synaptic mechanisms (Chen et al 2001; Gerfen 1991; Lamour et al 1988; Morozova et al 2008; Pickel et al 2000). On the other hand, 5-HT can exert indirect inhibitory actions on MS-DBB cholinergic neurons via 5-HT_{1A}Rs on PV-positive GABAergic cells (Alreja 1996; Liu and Alreja 1997; Luttgen et al 2005), or via direct activation of 5-HT_{1A}Rs on cholinergic cells (Kia et al 1996a; Luttgen et al 2005). Thus, ultimately 5-HT fibres innervating the MS-DBB exert an inhibitory influence on septal neurons, whereas NK_1Rs are excitatory (Assaf and Miller 1978) (see Fig. 6.2).

In chapter 2, moderate to high levels of colocalisation between NK_1Rs and 5-HT_{1A}Rs were also observed in the hippocampus. Thus, in addition to an indirect action via the MS-DBB, SP and 5-HT may also have direct actions within the hippocampus. Indeed, agonists at NK_1Rs increase GABA release in the CA1 region in rat brain slices (Sloviter et al 2001; Stacey et al 2002), while DRN axons target cells in the hippocampus exerting an inhibitory effect via 5-HT_{1A}Rs (Halasy et al 1992; Kosofsky and Molliver 1987).

Thus, both NK_1Rs and 5-HT_{1A}Rs are localised on neurons in the MS-DBB that form direct cholinergic projections from the MS-DBB to the hippocampus. In addition, NK_1Rs and 5-HT_{1A}Rs are also found colocalised on cells within the hippocampus.

Hence both receptors are in a position to influence hippocampal theta rhythm either indirectly via the MS-DBB or directly via neurons within the hippocampus.

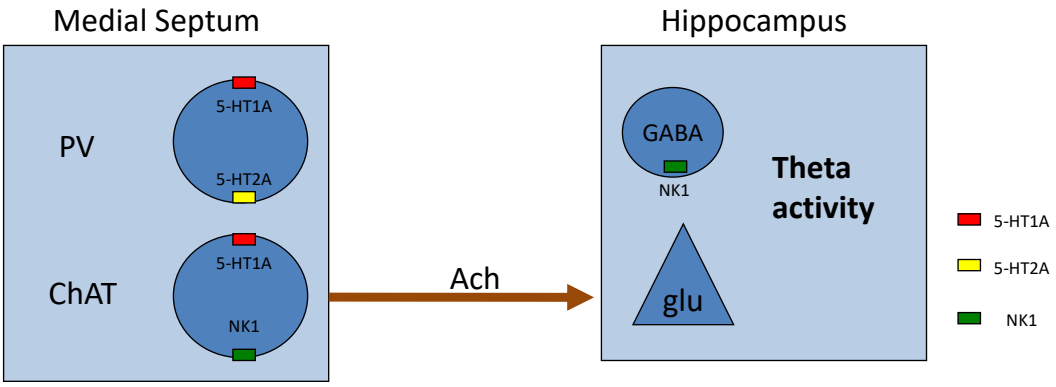


Fig. 6.2. Interactions between NK_1 receptors and the 5-HT system in the septohippocampal pathway of the rat. Within the MS-DBB, 5-HT_{1A}Rs and 5-HT_{2A}Rs are found colocalised to PV cells, while NK_1Rs and 5-HT_{1A}Rs are found on cholinergic cells (ChAT). MS-DBB cholinergic neurons innervate both GABAergic and glutamatergic neurons in the hippocampus to generate hippocampal theta rhythm. Ach=acetylcholine; ChAT=choline acetyl transferase; glu=glutamate; PV=parvalbumin.

Moderate levels of colocalisation between NK_1Rs and 5-HT_{1A}Rs were also seen in the BLA and PFC. The colocalisation is likely to be on GABA interneurons in both regions (Kaneko et al 1994; Levita et al 2003). SP has been shown to stimulate inhibitory synaptic transmission in the BLA (Maubach et al 2001), while the 5-HT_{1A}R agonist, 8-OH-DPAT inhibited firing rate of BLA neurons (Stein et al 2000; Wang et al 1999). Similarly, in the PFC, SP excited cortical neurons (Albus et al 1992; Lamour et al 1983; Phillis and Limacher 1974), while 5-HT acted via 5-HT_{1A}Rs to hyperpolarise PFC neurons (Aghajanian and Marek 1997; Amargos-Bosch et al 2004; Hajos et al 1999; Hajos et al 1998; Zhou and Hablitz 1999).

Thus, in a number of forebrain regions, activation of 5-HT_{1A}Rs and NK_1Rs lead to opposing actions. Therefore, it would be predicted that agonist activation at 5-HT_{1A}Rs by 5-HT targeted antidepressants would lead to similar functional responses as NK_1R blockade by NK_1RAs (see Fig. 6.3).

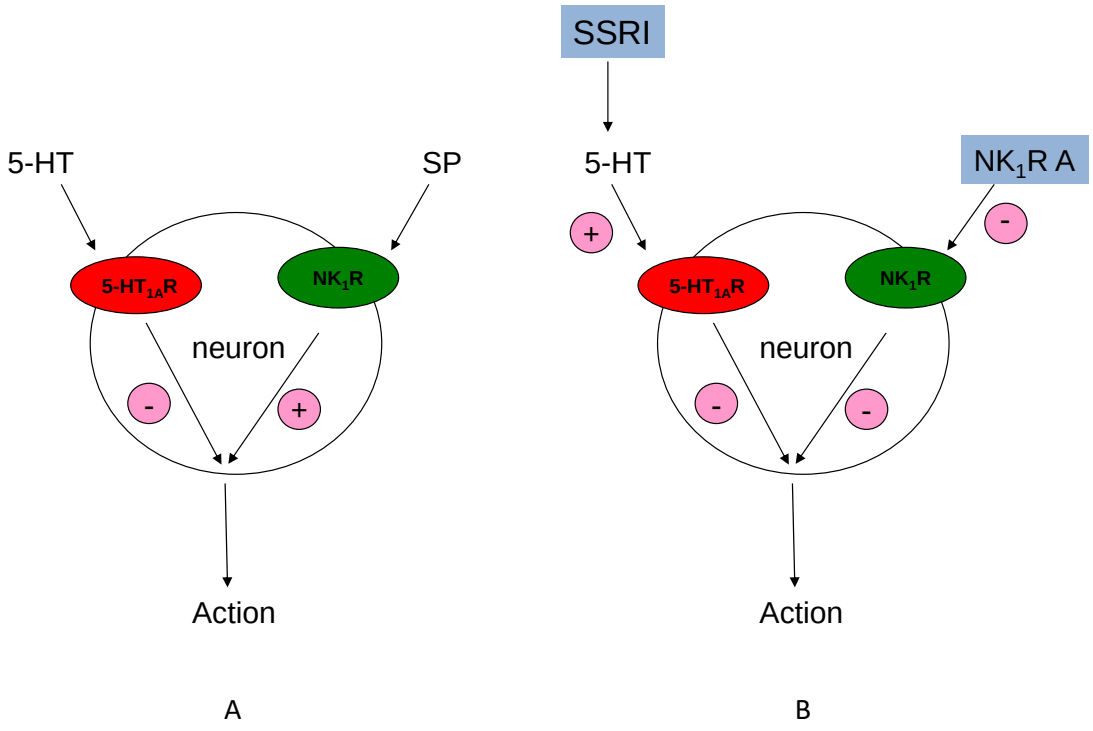


Fig. 6.3. Schematic diagram illustrating agonist and antagonist actions on 5-HT_{1A} and NK_1 receptors on a colocalised cell. A) represents the physiological state where 5-HT acts to hyperpolarise the neuron via 5-HT_{1A}Rs resulting in inhibition. In contrast, SP stimulates the neuron via NK_1Rs. Thus agonist action on 5-HT_{1A}R and NK_1Rs leads to opposing actions. B) represents the effects of pharmacological interventions on the system. SSRI antidepressants enhance 5-HT release in postsynaptic brain regions, leading to hyperpolarisation and resultant inhibition of the neuron via inhibitory 5-HT_{1A}Rs. On the other hand, NK_1RAs block the stimulatory action of SP and thus also result in neuronal inhibition. Thus, antagonism at NK_1Rs results in the same functional response as agonist action at 5-HT_{1A}Rs.

In chapter 3, retrograde tracing from the DRN combined with NK_1R immunohistochemistry at the EM level showed NK_1 Rs to be present in the LHb and LC on neurons afferent to the DRN. Some of the afferent cells in the LC also showed tyrosine hydroxylase-ir. A schematic representation of the possible functional effects of the above finding with regards to NK_1RAs and the DRN is found in Fig. 6.4.

The results of chapter 3 suggest that NK_1Rs are found on LHb neurons afferent to the DRN. Many of these afferent neurons use excitatory neurotransmitters (Kalen et al 1985; Kalen et al 1986), which synapse onto GABA interneurons within the DRN, inhibiting 5-HT projections to the forebrain (Ferraro et al 1997; Kalen et al 1986; Nishikawa and Scatton 1985; Sabatino et al 1991; Speciale et al 1980; Varga et al 2003; Zagami et al 1995). Blockade of NK_1Rs in the LHb with an NK_1RA would therefore lead to enhanced 5-HT release from the DRN as has been shown in the guinea-pig (Conley et al 2002).

With regards to the LC, under stress conditions SP may stimulate NA neurons directly. However, results of at least one study suggest that NK_1RAs can actually increase the firing rate of NA neurons in the LC (Maubach et al 2002) perhaps via a partial agonist effect. This stimulation may be via NK_1Rs located on NA neurons, in turn leading to the stimulation of DRN 5-HT neurons. However, it is also possible that NK_1RAs may block the action of SP via NK_1Rs on GABA interneurons leading to a disinhibition of NA neurons within the LC. Indeed, the finding that intracoerulear $GABA_A$ receptors inhibit NA neurons (Kawahara et al 2000) might suggest such an interaction. However, future studies are required to investigate the presence of NK_1Rs on GABAergic neurons within the LC.

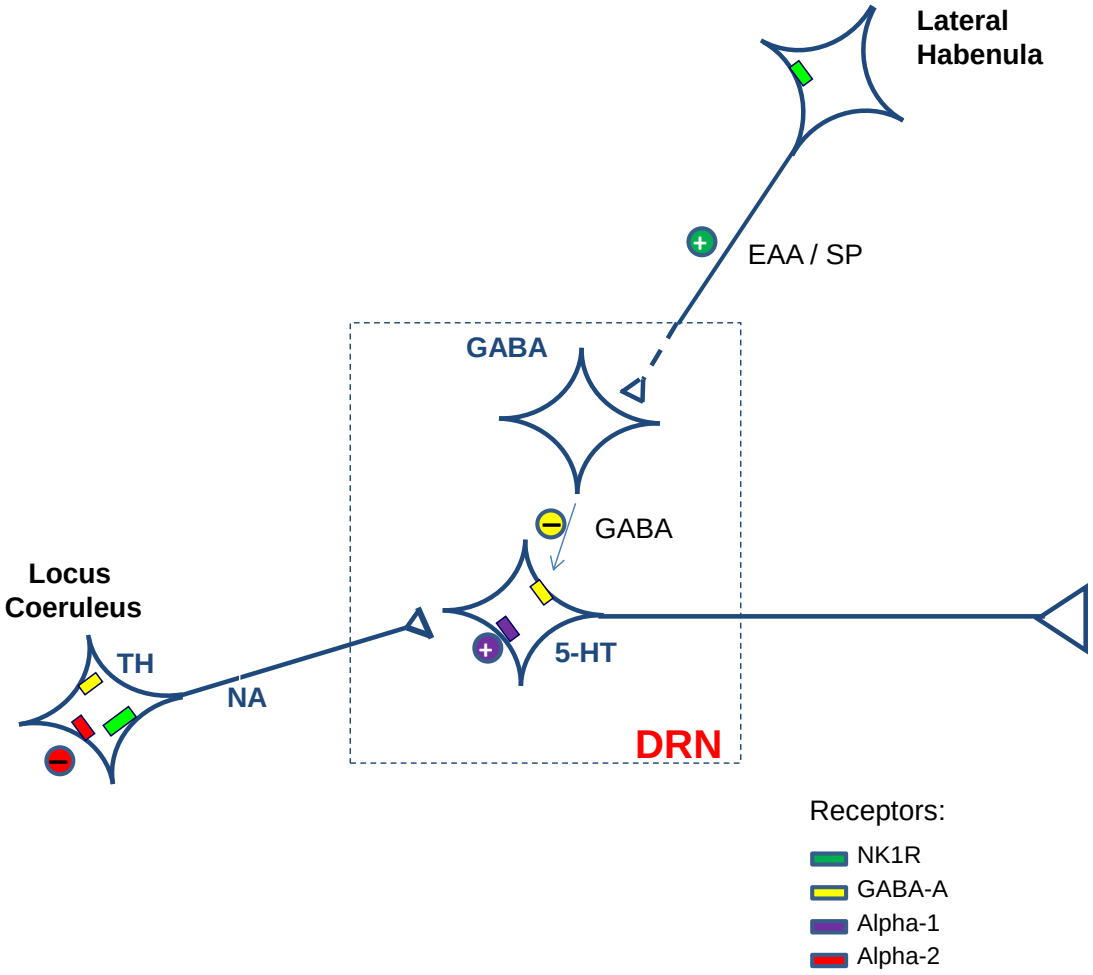


Fig. 6.4. Schematic representation of NK_1 receptors on neurons afferent to the dorsal raphe nucleus 5-HT system. NK_1Rs are found on DRN afferents in the LHb. These neurons use excitatory amino acids (EAA) to synapse onto GABA interneurons within the DRN, inhibiting 5-HT projections from the DRN. Blockade of NK_1Rs in the LHb with an NK_1RA would therefore lead to enhanced 5-HT release from the DRN. Within the LC, under stress conditions SP may stimulate NA neurons directly. NK_1RAs can actually increase the firing rate of NA neurons perhaps via a direct partial agonist effect on NK_1Rs on NA neurons. This would result in stimulation of NA neurons in the LC in turn leading to the stimulation of 5-HT neurons in the DRN via alpha-1 adrenergic receptors. In contrast, alpha-2 adrenergic receptors on LC neurons are inhibitory.

Thus, collectively the results of chapter 2 and 3 suggest that NK_1Rs are located on afferent neurons to the DRN and also colocalise with 5-HT_{1A}Rs (and to some extent 5-HT_{2A}Rs) on neurons in a number of forebrain regions. Therefore, NK_1Rs are in a position to influence the 5-HT system at two levels i.e. presynaptic and postsynaptic to the DRN. Interestingly, in support of the above interaction, the combination of GR 205171 or L-733060 with SSRIs has been shown to potentiate the effects of SSRIs on 5-HT release in postsynaptic cortical regions (Guiard et al 2004). This type of psychopharmacological combination may thus prove therapeutic in the future.

6.3.2. NK_1 receptors in human depression

Chapter 4 showed that [^{18}F]SPA-RQ binds with high affinity to brain NK_1Rs and that NK_1Rs can be quantified with the application of a 'transient equilibrium' model. In fact, there was a significant correlation between the regional BP estimates obtained in chapter 5 from normal volunteers in this thesis and those of Nyman et al. who used a different modelling strategy (Nyman et al 2006). However, the main finding of chapter 5 was that there was no difference in BP for NK_1Rs between normal controls and patients acutely depressed or recovered from depression in any brain region. This suggests that NK_1Rs may not be altered in number in depression. Nevertheless, it is still possible that subtle alterations in NK_1Rs in depression such as altered receptor activity or sensitivity are present, but simply not detectable using PET.

The results of previous human postmortem studies with regards to NK_1Rs in depression are inconsistent. However, the findings of the PET study in chapter 5 agree with the postmortem study which showed no difference in NK_1R binding in the amygdala in depression (Carletti et al 2005), but disagree with the study that found decreased NK_1R numbers in the orbitofrontal cortex (Stockmeier et al 2002). Another postmortem brain study observed a change in the laminar ratio of NK_1Rs in the anterior cingulate cortex in depression (Burnet and Harrison 2000), but this type of change cannot be detected using PET. A small preliminary PET study using a simplified reference tissue model found BP for NK_1Rs to be higher in the caudate, putamen and hippocampus and lower in the posterior cingulate in depressed patients (Hietala 2002). However, this finding has not been published in a full scientific paper and was not replicated in this thesis. Nevertheless, although, NK_1Rs may not be altered in numbers in depression, they may still play a role in other disorders. For

example, SP levels were found to be elevated in the CSF of patients with post-traumatic stress disorder (Geracioti et al 2006), while NK_1RAs have been investigated for their role in social phobia (Furmark et al 2005), and specific phobias (Michelgard et al 2007).

In contrast to the inconsistent studies of NK_1Rs in depression, pharmacological studies in animals suggest that NK_1RAs may have antidepressant actions. However, the results of clinical trials with NK_1RAs have been mixed. Initial phase II trials showed benefits over placebo for NK_1RA, aprepitant (Kramer et al 1998), with the antidepressant efficacy replicated in clinical trials with NK_1RAs: L-759274 (Compound A) (Kramer et al 2004) and CP-122721 (Chappell et al. 2002). However, a more recent large multicentre trial in depressed patients failed to reveal a benefit of aprepitant over placebo (Keller et al 2006). Furthermore, if NK_1RAs indeed do have antidepressant properties it has not been clear to date how they exert their actions. However, the results of the preclinical studies in this thesis suggest novel anatomical substrates for NK_1RAs via an interaction with the 5-HT system at both presynaptic and postsynaptic levels.

Interestingly, similar to the study of Nyman et al. 2006, an inverse correlation between age and brain NK_1Rs was also found in this thesis. The brain region with the highest negative correlation was the medial part of the anterior temporal lobe. This brain region is associated with memory function suggestive of a possible role for NK_1Rs in memory (Henson 2005). Indeed, preclinical studies suggest that SP and NK_1RAs may have influences on memory function (Hasenohrl et al 2000; Kart-Teke

et al 2007; Kart et al 2004). Future studies may thus show NK_1Rs to play a role in memory-related disorders such as dementia.

Although the evidence is inconsistent, studies have suggested that angiotensin I converting enzyme (ACE) insertion/deletion (I/D) polymorphism may influence therapeutic outcome in depression. One of the functions of ACE in the CNS is the degradation of SP. Indeed, the D allele has been associated with higher serum ACE activity (Rigat et al 1990) and higher CNS levels of SP (Arinami et al 1996). The variation in BP for human NK_1Rs, as seen with the PET study in chapter 5, may perhaps be partly explained by the presence of gene polymorphisms, including I/D polymorphism for ACE. Futher studies are needed to test this hypotheis.

Linking the results from immunohistochemistry with those from PET imaging, it may be that NK_1Rs are more important as targets for treatment rather than being disordered in the diseased state. Indeed, NK_1RAs may exert their antidepressant actions via an influence on the 5-HT system at levels both presynaptic and postsynaptic to the DRN. Not withstanding the negative results of the last clinical trial for aprepitant, this might explain why NK_1RAs were found in many pre-clinical studies to have antidepressant and anxiolytic actions, whilst the receptors were not found to be altered in depression using PET in this thesis.

6.4. FUTURE STUDIES

This section notes future studies that may aid in extending understanding of the role of brain NK_1Rs in depression and their interaction with the 5-HT system.

Immunofluorescence studies in chapter 2 found NK_1Rs to colocalise extensively with 5-HT_{1A}Rs in a number of forebrain regions including the MS-DBB. Thus, in the future, it would be useful to observe the effects of medial septal lesions and the local administration of SP, NK_1RA or 5-HT_{1A}R agonists and their effects on behaviour.

Colocalisation of NK_1Rs and 5-HT_{1A}Rs in neurons in the forebrain may also suggest that 5-HT_{1A}R activation could affect results of NK_1R activation. Investigating the effect of pharmacological activation of 5-HT_{1A}R upon NK_1R internalisation, and release of SP from primary afferents might also prove useful. In addition, in brain regions where the degree of colocalisation between NK_1Rs and 5-HT receptors was low, it is still possible that SP is able to modulate 5-HT indirectly, e.g. via NK_1Rs on GABA interneurons, as has been suggested for the LS (Ebner et al 2008). Therefore, further immunohistochemical experiments to study the neuronal connections between NK_1R-ir positive neurons and 5-HT_{2A}Rs in non-hippocampal forebrain regions may yet reveal important anatomical interactions.

Retrograde tracing from the DRN and immunohistochemistry for NK_1Rs in chapter 3 found NK_1Rs within the LHb and LC to localise to neurons afferent to the DRN. Thus, it would be useful to study the effect of specific ablation of NK_1R expressing neurons in the LHb or LC with injections of SP conjugated to saporin upon the DRN and 5-HT function. In addition, although NK_1Rs are mainly found on dendrites and

somas, they have also been occasionally found on axons and axonal terminals (Pickel et al 2000). The results of chapter 3 do not discount the possibility of NK_1Rs on axons in the LC. It is thus possible that NK_1Rs may influence incoming afferents to the LC e.g CRF or peptidergic afferents. This could be investigated using EM studies or whole-cell patch-clamp recording for altered neurotransmitter release upon NK_1R activation or blockade.

The study in chapter 5 showed that there was no differnce in NK_1R BP between MDD, RD and control subjects. However, the patient group sample sizes were quite small. Despite this and in view of the later negative clinical trials of NK_1RAs, it may be that in order to elucidate the subtle effects of novel psychotropic drugs in humans, a different approach may be required (Hafizi et al 2007). This might include studying the effects of novel psychotropic drugs such as the NK_1RA aprepitant on neuropsychological tests and functional brain imaging in normal human volunteers (Norbury et al 2007) as well as in patients with depression or those at high risk of the illness. Indeed, previous studies in normal volunteers have shown a reduction in the amygdala fear response following short-term treatment with the SSRI citalopram (Harmer et al 2006), or the noradrenaline reuptake inhibitor, reboxetine (Norbury et al 2007). It would be interesting to see if aprepitant would show a similar response. Furthermore, the presence of polymorphisms such as I/D polymorpshism for ACE may partly explain the variability in NK_1R BP. Finally, antagonists at NK_1Rs may yet prove therapeutic in anxiety disorders, while antagonists at another neurokinin receptor, the NK_3R, may prove fruitful in the treatment of schizophrenia (Spooren et al 2005).

6.5. CONCLUSIONS

Preclinical studies in this thesis provide neuroanatomical evidence for interactions between NK_1Rs and the 5-HT system. Immunofluorescence studies showed colocalisation of NK_1Rs with 5-HT_{1A}Rs in a number of rat forebrain regions including the MS-DBB, hippocampus, amygdala and medial PFC, and to a lesser extent with 5-HT_{2A}Rs in the hippocampus. Retrograde tracing from the DRN combined with immunohistochemistry for NK_1Rs showed at EM that NK_1Rs may be found on neurons afferent to the DRN, within the LHb and the LC, but not the medial PFC. The above data suggest that the NK_1R and 5-HT systems interact at both the postsynaptic level and the presynaptic levels. These anatomical interactions could explain how NK_1RAs exert their antidepressant actions. For example, NK_1RAs could operate via an influence on postsynaptic cellular targets, that are also the targets of 5-HT enhancing antidepressants, and/or via an action on DRN afferents in the LHb and LC.

The results of the clinical studies in this thesis suggest that brain NK_1Rs can be quantified in normal human volunteers and depressed subjects *in vivo* using the PET radioligand [^{18}F]SPA-RQ and a transient equilibrium model. Although, a clear decline in NK_1R BP was found with age, no difference was found in BP for NK_1Rs between depressed and control subjects. It may be that NK_1R numbers are not changed with depression. Nevertheless, they may be altered in function in depression and future studies may answer this question. These might include observing the effects of NK_1RAs on neuropsychological tests using functional magnetic resonance.

In summary, the findings of this thesis suggest NK_1Rs have important anatomical interactions with the 5-HT system in the rat brain, but are not altered in number in human depression.

BIBLIOGRAPHY

Acsady L, Katona I, Gulyas AI, Shigemoto R, Freund TF (1997): Immunostaining for substance P receptor labels GABAergic cells with distinct termination patterns in the hippocampus. *J Comp Neurol* 378:320-336.

Adams KH, Pinborg LH, Svarer C, Hasselbalch SG, Holm S, Haugbol S, et al (2004): A database of [(18)F]-altanserin binding to 5-HT(2A) receptors in normal volunteers: normative data and relationship to physiological and demographic variables. *Neuroimage* 21:1105-1113.

Adell A (2004): Antidepressant properties of substance P antagonists: relationship to monoaminergic mechanisms? *Curr Drug Targets CNS Neurol Disord* 3:113-121.

Ader JP, Room P, Postema F, Korf J (1980): Bilaterally diverging axon collaterals and contralateral projections from rat locus coeruleus neurons, demonstrated by fluorescent retrograde double labeling and norepinephrine metabolism. *J Neural Transm* 49:207-208.

Aghajanian GK, Marek GJ (1997): Serotonin induces excitatory postsynaptic potentials in apical dendrites of neocortical pyramidal cells. *Neuropharmacology* 36:589-599.

Aghajanian GK, Wang RY (1977): Habenular and other midbrain raphe afferents demonstrated by a modified retrograde tracing technique. *Brain Res* 122:229-242.

Aguiar MS, Brandao ML (1996): Effects of microinjections of the neuropeptide substance P in the dorsal periaqueductal gray on the behaviour of rats in the plus-maze test. *Physiol Behav* 60:1183-1186.

Aicher SA, Punnoose A, Goldberg A (2000): mu-Opioid receptors often colocalize with the substance P receptor (NK1) in the trigeminal dorsal horn. *J Neurosci* 20:4345-4354.

Albus K, Chao HH, Hicks TP (1992): Tachykinins preferentially excite certain complex cells in the infragranular layers of feline striate cortex. *Brain Res* 587:353-357.

Allam D, Girdlestone D, Garret C (1992): Effect of substance P antagonist, RP 67580 on neuronal activity in the rat locus coeruleus. *Br J Pharmacol* 107:227P.

Allen GV, Hopkins DA (1998): Convergent prefrontal cortex and mamillary body projections to the medial pontine nuclei: a light and electron microscopic study in the rat. *J Comp Neurol* 398:347-358.

Alreja M (1996): Excitatory actions of serotonin on GABAergic neurons of the medial septum and diagonal band of Broca. *Synapse* 22:15-27.

Altar CA, Kim H, Marshall JF (1985): Computer imaging and analysis of dopamine (D2) and serotonin (S2) binding sites in rat basal ganglia or neocortex labeled by [3H]spiroperidol. *J Pharmacol Exp Ther* 233:527-538.

Amargos-Bosch M, Bortolozzi A, Puig MV, Serrats J, Adell A, Celada P, et al (2004): Co-expression and in vivo interaction of serotonin1A and serotonin2A receptors in pyramidal neurons of prefrontal cortex. *Cereb Cortex* 14:281-299.

Amat J, Sparks PD, Matus-Amat P, Griggs J, Watkins LR, Maier SF (2001): The role of the habenular complex in the elevation of dorsal raphe nucleus serotonin and the changes in the behavioral responses produced by uncontrollable stress. *Brain Res* 917:118-126.

Anderson CD, Pasquier DA, Forbes WB, Morgane PJ (1977): Locus coeruleus-to-dorsal raphe input examined by electrophysiological and morphological methods. *Brain Res Bull* 2:209-221.

Anthony TE, Azmitia EC (1997): Molecular characterization of antipeptide antibodies against the 5-HT1A receptor: evidence for state-dependent antibody binding. *Brain Res Mol Brain Res* 50:277-284.

APA (1994): *Diagnostic and Statistical Manual of Mental Disorders* Fourth ed. Washington DC: American Psychiatric Association.

Appel NM, Mitchell WM, Garlick RK, Glennon RA, Teitler M, De Souza EB (1990): Autoradiographic characterization of (+-)-1-(2,5-dimethoxy-4-[125I] iodophenyl)-2-aminopropane ([125I]DOI) binding to 5-HT2 and 5-HT1c receptors in rat brain. *J Pharmacol Exp Ther* 255:843-857.

Araki M, McGeer PL, Kimura H (1988): The efferent projections of the rat lateral habenular nucleus revealed by the PHA-L anterograde tracing method. *Brain Res* 441:319-330.

Araneda R, Andrade R (1991): 5-Hydroxytryptamine2 and 5-hydroxytryptamine 1A receptors mediate opposing responses on membrane excitability in rat association cortex. *Neuroscience* 40:399-412.

Arango V, Ernsberger P, Marzuk PM, Chen JS, Tierney H, Stanley M, et al (1990): Autoradiographic demonstration of increased serotonin 5-HT2 and beta-adrenergic receptor binding sites in the brain of suicide victims. *Arch Gen Psychiatry* 47:1038-1047.

Arango V, Underwood MD, Gubbi AV, Mann JJ (1995): Localized alterations in pre- and postsynaptic serotonin binding sites in the ventrolateral prefrontal cortex of suicide victims. *Brain Res* 688:121-133.

Ardelt AA, Karpitskiy VV, Krause JE, Roth KA (1996): The neostriatal mosaic: basis for the changing distribution of neurokinin-1 receptor immunoreactivity during development. *J Comp Neurol* 376:463-475.

Arinami T, Li L, Mitsushio H, Itokawa M, Hamaguchi H, Toru M (1996): An insertion/deletion polymorphism in the angiotensin converting enzyme gene is associated with both brain substance P contents and affective disorders. *Biol Psychiatry* 40:1122-1127.

Arnsten AF, Goldman-Rakic PS (1984): Selective prefrontal cortical projections to the region of the locus coeruleus and raphe nuclei in the rhesus monkey. *Brain Res* 306:9-18.

Arranz B, Eriksson A, Mellerup E, Plenge P, Marcusson J (1994): Brain 5-HT1A, 5-HT1D, and 5-HT2 receptors in suicide victims. *Biol Psychiatry* 35:457-463.

Arvanov VL, Liang X, Magro P, Roberts R, Wang RY (1999a): A pre- and postsynaptic modulatory action of 5-HT and the 5-HT2A, 2C receptor agonist DOB on NMDA-evoked responses in the rat medial prefrontal cortex. *Eur J Neurosci* 11:2917-2934.

Arvanov VL, Liang X, Russo A, Wang RY (1999b): LSD and DOB: interaction with 5-HT2A receptors to inhibit NMDA receptor-mediated transmission in the rat prefrontal cortex. *Eur J Neurosci* 11:3064-3072.

Aschoff A, Hollander H (1982): Fluorescent compounds as retrograde tracers compared with horseradish peroxidase (HRP). I. A parametric study in the central visual system of the albino rat. *J Neurosci Methods* 6:179-197.

Ashby CR, Jr., Edwards E, Wang RY (1994): Electrophysiological evidence for a functional interaction between 5-HT1A and 5-HT2A receptors in the rat medial prefrontal cortex: an iontophoretic study. *Synapse* 17:173-181.

Assaf SY, Miller JJ (1978): The role of a raphe serotonin system in the control of septal unit activity and hippocampal desynchronization. *Neuroscience* 3:539-550.

Azmitia EC, Segal M (1978): An autoradiographic analysis of the differential ascending projections of the dorsal and median raphe nuclei in the rat. *J Comp Neurol* 179:641-667.

Azmitia EC, Yu I, Akbari HM, Kheck N, Whitaker-Azmitia PM, Marshak DR (1992): Antipeptide antibodies against the 5-HT1A receptor. *J Chem Neuroanat* 5:289-298.

Aznar S, Qian Z, Shah R, Rahbek B, Knudsen GM (2003): The 5-HT1A serotonin receptor is located on calbindin- and parvalbumin-containing neurons in the rat brain. *Brain Res* 959:58-67.

Baby S, Nguyen M, Tran D, Raffa RB (1999): Substance P antagonists: the next breakthrough in treating depression? *J Clin Pharm Ther* 24:461-469.

Bagot-Gueret C, Le Bas MD, Tymciu S, Darabantu M, Emond P, Guilloteau D, et al (2003): Synthesis and biological evaluation of halogenated naphthyridone carboxamides as potential ligands for in vivo imaging studies of substance P receptors. *Bioconjug Chem* 14:629-641.

Bajic D, Koike M, Albsoul-Younes AM, Nakajima S, Nakajima Y (2002): Two different inward rectifier K+ channels are effectors for transmitter-induced slow excitation in brain neurons. *Proc Natl Acad Sci U S A* 99:14494-14499.

Baker KG, Halliday GM, Hornung JP, Geffen LB, Cotton RG, Tork I (1991): Distribution, morphology and number of monoamine-synthesizing and substance P-containing neurons in the human dorsal raphe nucleus. *Neuroscience* 42:757-775.

Ballard TM, Sanger S, Higgins GA (2001): Inhibition of shock-induced foot tapping behaviour in the gerbil by a tachykinin NK1 receptor antagonist. *Eur J Pharmacol* 412:255-264.

Bannon MJ, Deutch AY, Tam SY, Zamir N, Eskay RL, Lee JM, et al (1986): Mild footshock stress dissociates substance P from substance K and dynorphin from Met- and Leu-enkephalin. *Brain Res* 381:393-396.

Bannon MJ, Elliott PJ, Alpert JE, Goedert M, Iversen SD, Iversen LL (1983): Role of endogenous substance P in stress-induced activation of mesocortical dopamine neurones. *Nature* 306:791-792.

Baraban JM, Aghajanian GK (1981): Noradrenergic innervation of serotonergic neurons in the dorsal raphe: demonstration by electron microscopic autoradiography. *Brain Res* 204:1-11.

Barbaresi P (1998): Immunocytochemical localization of substance P receptor in rat periaqueductal gray matter: a light and electron microscopic study. *J Comp Neurol* 398:473-490.

Barnes NM, Sharp T (1999): A review of central 5-HT receptors and their function. *Neuropharmacology* 38:1083-1152.

Baulmann J, Spitznagel H, Herdegen T, Unger T, Culman J (2000): Tachykinin receptor inhibition and c-Fos expression in the rat brain following formalin-induced pain. *Neuroscience* 95:813-820.

Beaujouan JC, Saffroy M, Torrens Y, Glowinski J (2000): Different subtypes of tachykinin NK(1) receptor binding sites are present in the rat brain. *J Neurochem* 75:1015-1026.

Beck AT, Ward CH, Mendelson M, Mock J, Erbaugh J (1961): An inventory for measuring depression. *Arch Gen Psychiatry* 4:561-571.

Beckstead RM, Domesick VB, Nauta WJ (1979): Efferent connections of the substantia nigra and ventral tegmental area in the rat. *Brain Res* 175:191-217.

Behzadi G, Kalen P, Parvopassu F, Wiklund L (1990): Afferents to the median raphe nucleus of the rat: retrograde cholera toxin and wheat germ conjugated horseradish peroxidase tracing, and selective D-[3H]aspartate labelling of possible excitatory amino acid inputs. *Neuroscience* 37:77-100.

Beique JC, Campbell B, Perring P, Hamblin MW, Walker P, Mladenovic L, et al (2004): Serotonergic regulation of membrane potential in developing rat prefrontal cortex: coordinated expression of 5-hydroxytryptamine (5-HT)1A, 5-HT2A, and 5-HT7 receptors. *J Neurosci* 24:4807-4817.

Benabid AL, Jeaugey L (1989): Cells of the rat lateral habenula respond to high-threshold somatosensory inputs. *Neurosci Lett* 96:289-294.

Bender D, Olsen AK, Marthi MK, Smith DF, Cumming P (2004): PET evaluation of the uptake of N-[11C]methyl CP-643,051, an NK1 receptor antagonist, in the living porcine brain. *Nucl Med Biol* 31:699-704.

Benkelfat C, Ellenbogen MA, Dean P, Palmour RM, Young SN (1994): Mood-lowering effect of tryptophan depletion. Enhanced susceptibility in young men at genetic risk for major affective disorders. *Arch Gen Psychiatry* 51:687-697.

Bennacef I, Tymciu S, Dhilly M, Lasne MC, Debruyne D, Perrio C, et al (2004): Synthesis and biological evaluation of novel fluoro and iodo quinoline carboxamides as potential ligands of NK-3 receptors for in vivo imaging studies. *Bioorg Med Chem* 12:4533-4541.

Bensaid M, Faucheux BA, Hirsch E, Agid Y, Soubrie P, Oury-Donat F (2001): Expression of tachykinin NK2 receptor mRNA in human brain. *Neurosci Lett* 303:25-28.

Bentivoglio M, Kuypers HG, Catsman-Berrevoets CE, Loewe H, Dann O (1980): Two new fluorescent retrograde neuronal tracers which are transported over long distances. *Neurosci Lett* 18:25-30.

Beresford IJ, Birch PJ, Hagan RM, Ireland SJ (1991): Investigation into species variants in tachykinin NK1 receptors by use of the non-peptide antagonist, CP-96,345. *Br J Pharmacol* 104:292-293.

Bergstrom L, Torrens Y, Saffroy M, Beaujouan JC, Lavielle S, Chassaing G, et al (1987): [3H]neurokinin B and 125I-Bolton Hunter eledoisin label identical tachykinin binding sites in the rat brain. *J Neurochem* 48:125-133.

Bergstrom M, Fasth KJ, Kilpatrick G, Ward P, Cable KM, Wipperman MD, et al (2000): Brain uptake and receptor binding of two [11C]labelled selective high affinity NK1-antagonists, GR203040 and GR205171--PET studies in rhesus monkey. *Neuropharmacology* 39:664-670.

Bergstrom M, Hargreaves RJ, Burns HD, Goldberg MR, Sciberras D, Reines SA, et al (2004): Human positron emission tomography studies of brain neurokinin 1 receptor occupancy by aprepitant. *Biol Psychiatry* 55:1007-1012.

Berod A, Hartman BK, Pujol JF (1981): Importance of fixation in immunohistochemistry: use of formaldehyde solutions at variable pH for the localization of tyrosine hydroxylase. *J Histochem Cytochem* 29:844-850.

Berrettini WH, Rubinow DR, Nurnberger JI, Jr., Simmons-Alling S, Post RM, Gershon ES (1985): CSF substance P immunoreactivity in affective disorders. *Biol Psychiatry* 20:965-970.

Berry SA, Shah MC, Khan N, Roth BL (1996): Rapid agonist-induced internalization of the 5-hydroxytryptamine2A receptor occurs via the endosome pathway in vitro. *Mol Pharmacol* 50:306-313.

Bhagwagar Z, Hinz R, Taylor M, Fancy S, Cowen P, Grasby P (2006): Increased 5-HT2A Receptor Binding in Euthymic, Medication-Free Patients Recovered From Depression: A Positron Emission Study With [11C]MDL 100,907. *Am J Psychiatry* 163:1580-1587.

Bhagwagar Z, Rabiner EA, Sargent PA, Grasby PM, Cowen PJ (2004): Persistent reduction in brain serotonin1A receptor binding in recovered depressed men measured by positron emission tomography with [11C]WAY-100635. *Mol Psychiatry* 9:386-392.

Bilkei-Gorzo A, Racz I, Michel K, Zimmer A (2002): Diminished anxiety- and depression-related behaviors in mice with selective deletion of the Tac1 gene. *J Neurosci* 22:10046-10052.

Blasco-Ibanez JM, Freund TF (1995): Synaptic input of horizontal interneurons in stratum oriens of the hippocampal CA1 subfield: structural basis of feed-back activation. *Eur J Neurosci* 7:2170-2180.

Blier P, de Montigny C (1994): Current advances and trends in the treatment of depression. *Trends Pharmacol Sci* 15:220-226.

Blier P, Gobbi G, Haddjeri N, Santarelli L, Mathew G, Hen R (2004): Impact of substance P receptor antagonism on the serotonin and norepinephrine systems: relevance to the antidepressant/anxiolytic response. *J Psychiatry Neurosci* 29:208-218.

Blier P, Ward NM (2003): Is there a role for 5-HT1A agonists in the treatment of depression? *Biol Psychiatry* 53:193-203.

Block CH, Hoffman G, Kapp BS (1989): Peptide-containing pathways from the parabrachial complex to the central nucleus of the amygdala. *Peptides* 10:465-471.

Bolam JP, Smith Y (1990): The GABA and substance P input to dopaminergic neurones in the substantia nigra of the rat. *Brain Res* 529:57-78.

Bondy B, Baghai TC, Minov C, Schule C, Schwarz MJ, Zwanzger P, et al (2003): Substance P serum levels are increased in major depression: preliminary results. *Biol Psychiatry* 53:538-542.

Boothman LJ, Mitchell SN, Sharp T (2006): Investigation of the SSRI augmentation properties of 5-HT(2) receptor antagonists using in vivo microdialysis. *Neuropharmacology* 50:726-732.

Borhegyi Z, Leranth C (1997a): Distinct substance P- and calretinin-containing projections from the supramammillary area to the hippocampus in rats; a species difference between rats and monkeys. *Exp Brain Res* 115:369-374.

Borhegyi Z, Leranth C (1997b): Substance P innervation of the rat hippocampal formation. *J Comp Neurol* 384:41-58.

Borsini F, Ceci A, Bietti G, Donetti A (1995): BIMT 17, a 5-HT1A receptor agonist/5-HT2A receptor antagonist, directly activates postsynaptic 5-HT inhibitory responses in the rat cerebral cortex. *Naunyn Schmiedebergs Arch Pharmacol* 352:283-290.

Bowker RM, Westlund KN, Sullivan MC, Wilber JF, Coulter JD (1983): Descending serotonergic, peptidergic and cholinergic pathways from the raphe nuclei: a multiple transmitter complex. *Brain Res* 288:33-48.

Boyce S, Smith D, Carlson E, Hewson L, Rigby M, O'Donnell R, et al (2001): Intra-amygdala injection of the substance P [NK(1) receptor] antagonist L-760735 inhibits neonatal vocalisations in guinea-pigs. *Neuropharmacology* 41:130-137.

Brain SD, Cox HM (2006): Neuropeptides and their receptors: innovative science providing novel therapeutic targets. *Br J Pharmacol* 147 Suppl 1:S202-211.

Brix G, Zaers J, Adam LE, Bellemann ME, Ostertag H, Trojan H, et al (1997): Performance evaluation of a whole-body PET scanner using the NEMA protocol. National Electrical Manufacturers Association. *J Nucl Med* 38:1614-1623.

Broadwell RD, Oliver C, Brightman MW (1980): Neuronal transport of acid hydrolases and peroxidase within the lysosomal system or organelles: involvement of agranular reticulum-like cisterns. *J Comp Neurol* 190:519-532.

Brodin E, Ogren SO, Theodorsson-Norheim E (1987): Effects of subchronic treatment with imipramine, zimelidine and alaproclate on regional tissue levels of substance P- and neurokinin A/neurokinin B-like immunoreactivity in the brain and spinal cord of the rat. *Neuropharmacology* 26:581-590.

Brodin E, Rosen A, Schott E, Brodin K (1994): Effects of sequential removal of rats from a group cage, and of individual housing of rats, on substance P, cholecystokinin and somatostatin levels in the periaqueductal grey and limbic regions. *Neuropeptides* 26:253-260.

Brodin K, Rosen A, Iwarsson K, Ogren SO, Brodin E (1989): Increased levels of substance P and cholecystokinin in rat cerebral cortex following repeated electroconvulsive shock and subchronic treatment with a serotonin uptake inhibitor. *Acta Physiol Scand* 136:613-614.

Brooks DJ (2005): Positron emission tomography and single-photon emission computed tomography in central nervous system drug development. *NeuroRx* 2:226-236.

Buck SH, Helke CJ, Burcher E, Shults CW, O'Donohue TL (1986): Pharmacologic characterization and autoradiographic distribution of binding sites for iodinated tachykinins in the rat central nervous system. *Peptides* 7:1109-1120.

Buell G, Schulz MF, Arkinstall SJ, Maury K, Missotten M, Adami N, et al (1992): Molecular characterisation, expression and localisation of human neurokinin-3 receptor. *FEBS Lett* 299:90-95.

Bullier J, Kennedy H, Salinger W (1984): Bifurcation of subcortical afferents to visual areas 17, 18, and 19 in the cat cortex. *J Comp Neurol* 228:309-328.

Burgunder JM, Young WS, 3rd (1989): Neurokinin B and substance P genes are co-expressed in a subset of neurons in the rat habenula. *Neuropeptides* 13:165-169.

Burnet PW, Eastwood SL, Lacey K, Harrison PJ (1995): The distribution of 5-HT1A and 5-HT2A receptor mRNA in human brain. *Brain Res* 676:157-168.

Burnet PW, Harrison PJ (2000): Substance P (NK1) receptors in the cingulate cortex in unipolar and bipolar mood disorder and schizophrenia. *Biol Psychiatry* 47:80-83.

Burnet PW, Miller R, Lewis LJ, Pei Q, Sharp T, Harrison PJ (2001): Electroconvulsive shock increases tachykinin NK(1) receptors, but not the encoding mRNA, in rat cortex. *Eur J Pharmacol* 413:213-219.

Buss AH, Perry M (1992): The aggression questionnaire. *J Pers Soc Psychol* 63:452-459.

Caberlotto L, Hurd YL, Murdock P, Wahlin JP, Melotto S, Corsi M, et al (2003): Neurokinin 1 receptor and relative abundance of the short and long isoforms in the human brain. *Eur J Neurosci* 17:1736-1746.

Cai X, Gu Z, Zhong P, Ren Y, Yan Z (2002): Serotonin 5-HT1A receptors regulate AMPA receptor channels through inhibiting Ca2+/calmodulin-dependent

kinase II in prefrontal cortical pyramidal neurons. *J Biol Chem* 277:36553-36562.

Caldecott-Hazard S, Mazziotta J, Phelps M (1988): Cerebral correlates of depressed behavior in rats, visualized using 14C-2-deoxyglucose autoradiography. *J Neurosci* 8:1951-1961.

Carletti R, Corsi M, Melotto S, Caberlotto L (2005): Down-regulation of amygdala preprotachykinin A mRNA but not H-SP receptor binding sites in subjects affected by mood disorders and schizophrenia. *Eur J Neurosci* 21:1712-1718.

Carlton SM, Coggeshall RE (1997): Immunohistochemical localization of 5-HT2A receptors in peripheral sensory axons in rat glabrous skin. *Brain Res* 763:271-275.

Carson RE (1991): Precision and accuracy considerations of physiological quantitation in PET. *J Cereb Blood Flow Metab* 11:A45-50.

Carson RE, Channing MA, Blasberg RG, Dunn BB, Cohen RM, Rice KC, et al (1993): Comparison of bolus and infusion methods for receptor quantitation: application to [18F]cyclofoxy and positron emission tomography. *J Cereb Blood Flow Metab* 13:24-42.

Casanovas JM, Hervas I, Artigas F (1999): Postsynaptic 5-HT1A receptors control 5-HT release in the rat medial prefrontal cortex. *Neuroreport* 10:1441-1445.

Celada P, Puig MV, Casanovas JM, Guillazo G, Artigas F (2001): Control of dorsal raphe serotonergic neurons by the medial prefrontal cortex: Involvement of serotonin-1A, GABA(A), and glutamate receptors. *J Neurosci* 21:9917-9929.

Chalmers DT, Watson SJ (1991): Comparative anatomical distribution of 5-HT1A receptor mRNA and 5-HT1A binding in rat brain--a combined in situ hybridisation/in vitro receptor autoradiographic study. *Brain Res* 561:51-60.

Chan-Palay V (1981): Evidence for the coexistence of serotonin and substance P in single raphe cells and fiber plexuses: combined immunocytochemistry and autoradiography. *Adv Exp Med Biol* 133:81-97.

Chang MM, Leeman SE (1970): Isolation of a sialogogic peptide from bovine hypothalamic tissue and its characterization as substance P. *J Biol Chem* 245:4784-4790.

Chang MM, Leeman SE, Niall HD (1971): Amino-acid sequence of substance P. *Nat New Biol* 232:86-87.

Chappell P (2002): Effects of CP-122,721, a selective NK-1 receptor antagonist in patients with major depression. *42nd annual meeting of the New Clinical Drug Evaluation Unit (NCDEU)*. Boca Raton, FL.

Chaput Y, de Montigny C, Blier P (1991): Presynaptic and postsynaptic modifications of the serotonin system by long-term administration of antidepressant treatments. An in vivo electrophysiologic study in the rat. *Neuropsychopharmacology* 5:219-229.

Charara A, Parent A (1998): Chemoarchitecture of the primate dorsal raphe nucleus. *J Chem Neuroanat* 15:111-127.

Chastrette N, Pfaff DW, Gibbs RB (1991): Effects of daytime and nighttime stress on Fos-like immunoreactivity in the paraventricular nucleus of the hypothalamus, the habenula, and the posterior paraventricular nucleus of the thalamus. *Brain Res* 563:339-344.

Cheek JH, Buss AH (1981): Shyness and Socialbility. *J Pers Soc Psychol* 41:330-339.

Cheeseman HJ, Pinnock RD, Henderson G (1983): Substance P excitation of rat locus coeruleus neurones. *Eur J Pharmacol* 94:93-99.

Cheeta S, Tucci S, Sandhu J, Williams AR, Rupniak NM, File SE (2001): Anxiolytic actions of the substance P (NK1) receptor antagonist L-760735 and the 5-HT1A agonist 8-OH-DPAT in the social interaction test in gerbils. *Brain Res* 915:170-175.

Chen LW, Wei LC, Liu HL, Qiu Y, Chan YS (2001): Cholinergic neurons expressing substance P receptor (NK(1)) in the basal forebrain of the rat: a double immunocytochemical study. *Brain Res* 904:161-166.

Chen LW, Wei LC, Liu HL, Rao ZR (2000): Noradrenergic neurons expressing substance P receptor (NK1) in the locus coeruleus complex: a double immunofluorescence study in the rat. *Brain Res* 873:155-159.

Cheng LL, Wang SJ, Gean PW (1998): Serotonin depresses excitatory synaptic transmission and depolarization-evoked Ca2+ influx in rat basolateral amygdala via 5-HT1A receptors. *Eur J Neurosci* 10:2163-2172.

Chenu F, Guiard BP, Bourin M, Gardier AM (2006): Antidepressant-like activity of selective serotonin reuptake inhibitors combined with a NK1 receptor antagonist in the mouse forced swimming test. *Behav Brain Res* 172:256-263.

Chowdrey HS, Larsen PJ, Harbuz MS, Lightman SL, Jessop DS (1995): Endogenous substance P inhibits the expression of corticotropin-releasing hormone during a chronic inflammatory stress. *Life Sci* 57:2021-2029.

Cialdai C, Tramontana M, Patacchini R, Lecci A, Catalani C, Catalioto RM, et al (2006): MEN15596, a novel nonpeptide tachykinin NK2 receptor antagonist. *Eur J Pharmacol* 549:140-148.

Cidis Meltzer C, Drevets WC, Price JC, Mathis CA, Lopresti B, Greer PJ, et al (2001): Gender-specific aging effects on the serotonin 1A receptor. *Brain Res* 895:9-17.

Clement Y, Kia KH, Daval G, Verge D (1996): An autoradiographic study of serotonergic receptors in a murine genetic model of anxiety-related behaviors. *Brain Res* 709:229-242.

Cloninger CR (1987): A systematic method for clinical description and classification of personality variants. A proposal. *Arch Gen Psychiatry* 44:573-588.

Coiro V, Capretti L, Volpi R, Davoli C, Marcato A, Cavazzini U, et al (1992): Stimulation of ACTH/cortisol by intravenously infused substance P in normal men: inhibition by sodium valproate. *Neuroendocrinology* 56:459-463.

Collin M, Backberg M, Onnestam K, Meister B (2002): 5-HT1A receptor immunoreactivity in hypothalamic neurons involved in body weight control. *Neuroreport* 13:945-951.

Commons KG, Connolley KR, Valentino RJ (2003): A neurochemically distinct dorsal raphe-limbic circuit with a potential role in affective disorders. *Neuropsychopharmacology* 28:206-215.

Commons KG, Valentino RJ (2002): Cellular basis for the effects of substance P in the periaqueductal gray and dorsal raphe nucleus. *J Comp Neurol* 447:82-97.

Concha ML, Wilson SW (2001): Asymmetry in the epithalamus of vertebrates. *J Anat* 199:63-84.

Conley RK, Cumberbatch MJ, Mason GS, Williamson DJ, Harrison T, Locker K, et al (2002): Substance P (neurokinin 1) receptor antagonists enhance dorsal raphe neuronal activity. *J Neurosci* 22:7730-7736.

Contestabile A, Villani L, Fasolo A, Franzoni MF, Gribaudo L, Oktedalen O, et al (1987): Topography of cholinergic and substance P pathways in the habenulo-interpeduncular system of the rat. An immunocytochemical and microchemical approach. *Neuroscience* 21:253-270.

Coppen A, Shaw DM, Herzberg B, Maggs R (1967): Tryptophan in the treatment of depression. *Lancet* 2:1178-1180.

Cornea-Hebert V, Riad M, Wu C, Singh SK, Descarries L (1999): Cellular and subcellular distribution of the serotonin 5-HT2A receptor in the central nervous system of adult rat. *J Comp Neurol* 409:187-209.

Culman J, Klee S, Ohlendorf C, Unger T (1997): Effect of tachykinin receptor inhibition in the brain on cardiovascular and behavioral responses to stress. *J Pharmacol Exp Ther* 280:238-246.

Czeh B, Simon M, van der Hart MG, Schmelting B, Hesselink MB, Fuchs E (2005): Chronic stress decreases the number of parvalbumin-immunoreactive interneurons in the hippocampus: prevention by treatment with a substance P receptor (NK1) antagonist. *Neuropsychopharmacology* 30:67-79.

Czyrak A, Czepiel K, Mackowiak M, Chocyk A, Wedzony K (2003): Serotonin 5-HT1A receptors might control the output of cortical glutamatergic neurons in rat cingulate cortex. *Brain Res* 989:42-51.

Dableh LJ, Yashpal K, Rochford J, Henry JL (2005): Antidepressant-like effects of neurokinin receptor antagonists in the forced swim test in the rat. *Eur J Pharmacol* 507:99-105.

Dam TV, Escher E, Quirion R (1990a): Visualization of neurokinin-3 receptor sites in rat brain using the highly selective ligand [3H]senktide. *Brain Res* 506:175-179.

Dam TV, Martinelli B, Quirion R (1990b): Autoradiographic distribution of brain neurokinin-1/substance P receptors using a highly selective ligand [3H]-[Sar9,Met(O2)11]-substance P. *Brain Res* 531:333-337.

Dam TV, Takeda Y, Krause JE, Quirion R (1991): Comparative autoradiographic distribution of [125I]-neuropeptide gamma and [125I]-neurokinin A binding sites in guinea pig brain. *Ann N Y Acad Sci* 632:377-381.

Danks JA, Rothman RB, Cascieri MA, Chicchi GG, Liang T, Herkenham M (1986): A comparative autoradiographic study of the distributions of substance P and eledoisin binding sites in rat brain. *Brain Res* 385:273-281.

De Almeida J, Mengod G (2007): Quantitative analysis of glutamatergic and GABAergic neurons expressing 5-HT(2A) receptors in human and monkey prefrontal cortex. *J Neurochem* 103:475-486.

De Almeida RM, Giovenardi M, Charchat H, Lucion AB (1998): 8-OH-DPAT in the median raphe nucleus decreases while in the medial septal area it may increase anxiety in female rats. *Neurosci Biobehav Rev* 23:259-264.

De Almeida RM, Lucion AB (1997): 8-OH-DPAT in the median raphe, dorsal periaqueductal gray and corticomedial amygdala nucleus decreases, but in the medial septal area it can increase maternal aggressive behavior in rats. *Psychopharmacology (Berl)* 134:392-400.

De Araujo JE, Huston JP, Brandao ML (2001a): Opposite effects of substance P fragments C (anxiogenic) and N (anxiolytic) injected into dorsal periaqueductal gray. *Eur J Pharmacol* 432:43-51.

De Araujo JE, Huston JP, Brandao ML (2001b): Place aversion induced by microinjections of C-fragment of substance P into the dorsal periaqueductal gray of rats is mediated by tachykinin NK1 receptors. *Peptides* 22:1447-1452.

De Araujo JE, Silva RC, Huston JP, Brandao ML (1999): Anxiogenic effects of substance P and its 7-11 C terminal, but not the 1-7 N terminal, injected into the dorsal periaqueductal gray. *Peptides* 20:1437-1443.

De Felipe C, Herrero JF, O'Brien JA, Palmer JA, Doyle CA, Smith AJ, et al (1998): Altered nociception, analgesia and aggression in mice lacking the receptor for substance P. *Nature* 392:394-397.

De Montigny C (1984): Electroconvulsive shock treatments enhance responsiveness of forebrain neurons to serotonin. *J Pharmacol Exp Ther* 228:230-234.

Degroot A, Treit D (2004): Anxiety is functionally segregated within the septo-hippocampal system. *Brain Res* 1001:60-71.

Deuschle M, Sander P, Herpfer I, Fiebich BL, Heuser I, Lieb K (2005): Substance P in serum and cerebrospinal fluid of depressed patients: no effect of antidepressant treatment. *Psychiatry Res* 136:1-6.

Dietl MM, Palacios JM (1991): Phylogeny of tachykinin receptor localization in the vertebrate central nervous system: apparent absence of neurokinin-2 and neurokinin-3 binding sites in the human brain. *Brain Res* 539:211-222.

Ding DC, Gabbott PL, Totterdell S (2001): Differences in the laminar origin of projections from the medial prefrontal cortex to the nucleus accumbens shell and core regions in the rat. *Brain Res* 917:81-89.

Ding YQ, Shigemoto R, Takada M, Ohishi H, Nakanishi S, Mizuno N (1996): Localization of the neuromedin K receptor (NK3) in the central nervous system of the rat. *J Comp Neurol* 364:290-310.

Doherty MD, Pickel VM (2000): Ultrastructural localization of the serotonin 2A receptor in dopaminergic neurons in the ventral tegmental area. *Brain Res* 864:176-185.

Dozois DJ, Covin R, Brinker JK (2003): Normative data on cognitive measures of depression. *J Consult Clin Psychol* 71:71-80.

Dreifuss JJ, Raggenbass M (1986): Tachykinins and bombesin excite non-pyramidal neurones in rat hippocampus. *J Physiol* 379:417-428.

Drevets WC, Frank E, Price JC, Kupfer DJ, Holt D, Greer PJ, et al (1999): PET imaging of serotonin 1A receptor binding in depression. *Biol Psychiatry* 46:1375-1387.

Duric V, McCarson KE (2005): Hippocampal neurokinin-1 receptor and brain-derived neurotrophic factor gene expression is decreased in rat models of pain and stress. *Neuroscience* 133:999-1006.

Ebner K, Rupniak NM, Saria A, Singewald N (2004): Substance P in the medial amygdala: emotional stress-sensitive release and modulation of anxiety-related behavior in rats. *Proc Natl Acad Sci U S A* 101:4280-4285.

Ebner K, Singewald GM, Whittle N, Ferraguti F, Singewald N (2008): Neurokinin 1 Receptor Antagonism Promotes Active Stress Coping Via Enhanced Septal 5-HT Transmission. *Neuropsychopharmacology* 33:1929-1941.

Ebner K, Singewald N (2006): The role of substance P in stress and anxiety responses. *Amino Acids* 31:251-272.

Ebner K, Singewald N (2007): Stress-induced release of substance P in the locus coeruleus modulates cortical noradrenaline release. *Naunyn Schmiedebergs Arch Pharmacol* 376:73-82.

Eckenrode TC, Barr GA, Battisti WP, Murray M (1987): Acetylcholine in the interpeduncular nucleus of the rat: normal distribution and effects of deafferentation. *Brain Res* 418:273-286.

Eison AS, Mullins UL (1996): Regulation of central 5-HT2A receptors: a review of in vivo studies. *Behav Brain Res* 73:177-181.

Elde R, Schalling M, Ceccatelli S, Nakanishi S, Hokfelt T (1990): Localization of neuropeptide receptor mRNA in rat brain: initial observations using probes for neurotensin and substance P receptors. *Neurosci Lett* 120:134-138.

Elhwuegi AS (2004): Central monoamines and their role in major depression. *Prog Neuropsychopharmacol Biol Psychiatry* 28:435-451.

Emson PC, Cuello AC, Paxinos G, Jessell T, Iversen LL (1977): The origin of substance P and acetylcholine projections to the ventral tegmental area and interpeduncular nucleus in the rat. *Acta Physiol Scand Suppl* 452:43-46.

Engberg S, Ahlstedt I, Leffler A, Lindstrom E, Kristensson E, Svensson A, et al (2007): Molecular cloning, mutations and effects of NK1 receptor antagonists reveal the human-like pharmacology of gerbil NK1 receptors. *Biochem Pharmacol* 73:259-269.

Eysenck HJ, Eysenck SBG (1975): *The Eysenck Personality Questionnaire*. London: Hodder & Stoughton.

Fehder WP, Sachs J, Uvaydova M, Douglas SD (1997): Substance P as an immune modulator of anxiety. *Neuroimmunomodulation* 4:42-48.

Ferraro G, Montalbano ME, Sardo P, La Grutta V (1996): Lateral habenular influence on dorsal raphe neurons. *Brain Res Bull* 41:47-52.

Ferraro G, Montalbano ME, Sardo P, La Grutta V (1997): Lateral habenula and hippocampus: a complex interaction raphe cells-mediated. *J Neural Transm* 104:615-631.

File SE (2000): NKP608, an NK1 receptor antagonist, has an anxiolytic action in the social interaction test in rats. *Psychopharmacology (Berl)* 152:105-109.

First M, Spitzer RL, Gibbon M, Williams J (1997): *Structured clinical interview for DSM-IV axis I disorders, (SCID-I), clinician version (administration booklet)*. Washington DC: American Psychiatric Press.

Fischette CT, Nock B, Renner K (1987): Effects of 5,7-dihydroxytryptamine on serotonin1 and serotonin2 receptors throughout the rat central nervous system using quantitative autoradiography. *Brain Res* 421:263-279.

Fong TM, Anderson SA, Yu H, Huang RR, Strader CD (1992a): Differential activation of intracellular effector by two isoforms of human neurokinin-1 receptor. *Mol Pharmacol* 41:24-30.

Fong TM, Yu H, Strader CD (1992b): Molecular basis for the species selectivity of the neurokinin-1 receptor antagonists CP-96,345 and RP67580. *J Biol Chem* 267:25668-25671.

Frank E, Prien RF, Jarrett RB, Keller MB, Kupfer DJ, Lavori PW, et al (1991): Conceptualization and rationale for consensus definitions of terms in major depressive disorder. Remission, recovery, relapse, and recurrence. *Arch Gen Psychiatry* 48:851-855.

Freund TF (2003): Interneuron Diversity series: Rhythm and mood in perisomatic inhibition. *Trends Neurosci* 26:489-495.

Freund TF, Buzsaki G (1996): Interneurons of the hippocampus. *Hippocampus* 6:347-470.

Froger N, Gardier AM, Moratalla R, Alberti I, Lena I, Boni C, et al (2001): 5-hydroxytryptamine (5-HT)1A autoreceptor adaptive changes in substance P (neurokinin 1) receptor knock-out mice mimic antidepressant-induced desensitization. *J Neurosci* 21:8188-8197.

Fuchs E, Flugge G (2002): Social stress in tree shrews: effects on physiology, brain function, and behavior of subordinate individuals. *Pharmacol Biochem Behav* 73:247-258.

Furmark T, Appel L, Michelgard A, Wahlstedt K, Ahs F, Zancan S, et al (2005): Cerebral blood flow changes after treatment of social phobia with the neurokinin-1 antagonist GR205171, citalopram, or placebo. *Biol Psychiatry* 58:132-142.

Gall C, Moore RY (1984): Distribution of enkephalin, substance P, tyrosine hydroxylase, and 5-hydroxytryptamine immunoreactivity in the septal region of the rat. *J Comp Neurol* 225:212-227.

Gao DM, Hoffman D, Benabid AL (1996): Simultaneous recording of spontaneous activities and nociceptive responses from neurons in the pars compacta of substantia nigra and in the lateral habenula. *Eur J Neurosci* 8:1474-1478.

Gao M, Mock BH, Hutchins GD, Zheng QH (2005): Synthesis and initial PET imaging of new potential NK1 receptor radioligands 1-[2-(3,5-bis-trifluoromethyl-benzyloxy)-1-phenyl-ethyl]-4-[11C]methyl-pip erazine and {4-[2-(3,5-bis-trifluoromethyl-benzyloxy)-1-phenyl-ethyl]-piperazine-1-yl} -acetic acid [11C]methyl ester. *Nucl Med Biol* 32:543-552.

Garlow SJ, Morilak DA, Dean RR, Roth BL, Ciaranello RD (1993): Production and characterization of a specific 5-HT2 receptor antibody. *Brain Res* 615:113-120.

Gavioli EC, Canteras NS, De Lima TC (2002): The role of lateral septal NK1 receptors in mediating anxiogenic effects induced by intracerebroventricular injection of substance P. *Behav Brain Res* 134:411-415.

Geisler S, Andres KH, Veh RW (2003): Morphologic and cytochemical criteria for the identification and delineation of individual subnuclei within the lateral habenular complex of the rat. *J Comp Neurol* 458:78-97.

Gellman RL, Aghajanian GK (1993): Pyramidal cells in piriform cortex receive a convergence of inputs from monoamine activated GABAergic interneurons. *Brain Res* 600:63-73.

Gentsch C, Cutler M, Vassout A, Veenstra S, Brugger F (2002): Anxiolytic effect of NKP608, a NK1-receptor antagonist, in the social investigation test in gerbils. *Behav Brain Res* 133:363-368.

Geracioti TD, Jr., Carpenter LL, Owens MJ, Baker DG, Ekhator NN, Horn PS, et al (2006): Elevated cerebrospinal fluid substance p concentrations in posttraumatic stress disorder and major depression. *Am J Psychiatry* 163:637-643.

Gerard C, Langlois X, Gingrich J, Doucet E, Verge D, Kia HK, et al (1994): Production and characterization of polyclonal antibodies recognizing the intracytoplasmic third loop of the 5-hydroxytryptamine1A receptor. *Neuroscience* 62:721-739.

Gerard NP, Eddy RL, Jr., Shows TB, Gerard C (1990): The human neurokinin A (substance K) receptor. Molecular cloning of the gene, chromosome localization, and isolation of cDNA from tracheal and gastric tissues. *J Biol Chem* 265:20455-20462.

Gerfen CR (1991): Substance P (neurokinin-1) receptor mRNA is selectively expressed in cholinergic neurons in the striatum and basal forebrain. *Brain Res* 556:165-170.

Germain A, Nofzinger EA, Kupfer DJ, Buysse DJ (2004): Neurobiology of non-REM sleep in depression: further evidence for hypofrontality and thalamic dysregulation. *Am J Psychiatry* 161:1856-1863.

Geurts FJ, De Schutter E, Timmermans JP (2002): Localization of 5-HT2A, 5-HT3, 5-HT5A and 5-HT7 receptor-like immunoreactivity in the rat cerebellum. *J Chem Neuroanat* 24:65-74.

Giardina GA, Gagliardi S, Martinelli M (2003): Antagonists at the neurokinin receptors--recent patent literature. *IDrugs* 6:758-772.

Gitter BD, Waters DC, Bruns RF, Mason NR, Nixon JA, Howbert JJ (1991): Species differences in affinities of non-peptide antagonists for substance P receptors. *Eur J Pharmacol* 197:237-238.

Gobbi G, Blier P (2005): Effect of neurokinin-1 receptor antagonists on serotoninergic, noradrenergic and hippocampal neurons: comparison with antidepressant drugs. *Peptides* 26:1383-1393.

Gobbi G, Cassano T, Radja F, Morgese MG, Cuomo V, Santarelli L, et al (2007): Neurokinin 1 receptor antagonism requires norepinephrine to increase serotonin function. *Eur Neuropsychopharmacol* 17:328-338.

Gonatas NK, Harper C, Mizutani T, Gonatas JO (1979): Superior sensitivity of conjugates of horseradish peroxidase with wheat germ agglutinin for studies of retrograde axonal transport. *J Histochem Cytochem* 27:728-734.

Grady EF, Baluk P, Bohm S, Gamp PD, Wong H, Payan DG, et al (1996): Characterization of antisera specific to NK1, NK2, and NK3 neurokinin receptors and their utilization to localize receptors in the rat gastrointestinal tract. *J Neurosci* 16:6975-6986.

Gray JA, Roth BL (2001): Paradoxical trafficking and regulation of 5-HT(2A) receptors by agonists and antagonists. *Brain Res Bull* 56:441-451.

Gross-Isseroff R, Israeli M, Biegon A (1989): Autoradiographic analysis of tritiated imipramine binding in the human brain post mortem: effects of suicide. *Arch Gen Psychiatry* 46:237-241.

Gross C, Zhuang X, Stark K, Ramboz S, Oosting R, Kirby L, et al (2002): Serotonin1A receptor acts during development to establish normal anxiety-like behaviour in the adult. *Nature* 416:396-400.

Guiard BP, Froger N, Hamon M, Gardier AM, Lanfumey L (2005): Sustained pharmacological blockade of NK1 substance P receptors causes functional desensitization of dorsal raphe 5-HT 1A autoreceptors in mice. *J Neurochem* 95:1713-1723.

Guiard BP, Przybylski C, Guilloux JP, Seif I, Froger N, De Felipe C, et al (2004): Blockade of substance P (neurokinin 1) receptors enhances extracellular serotonin when combined with a selective serotonin reuptake inhibitor: an in vivo microdialysis study in mice. *J Neurochem* 89:54-63.

Gulyas AI, Acsady L, Freund TF (1999): Structural basis of the cholinergic and serotonergic modulation of GABAergic neurons in the hippocampus. *Neurochem Int* 34:359-372.

Gunn RN, Sargent PA, Bench CJ, Rabiner EA, Osman S, Pike VW, et al (1998): Tracer kinetic modeling of the 5-HT1A receptor ligand [carbonyl-11C]WAY-100635 for PET. *Neuroimage* 8:426-440.

Guyenet PG, Aghajanian GK (1977): Excitation of neurons in the nucleus locus coeruleus by substance P and related peptides. *Brain Res* 136:178-184.

Haddjeri N, Blier P (2000): Effect of neurokinin-I receptor antagonists on the function of 5-HT and noradrenaline neurons. *Neuroreport* 11:1323-1327.

Haddjeri N, Blier P (2001): Sustained blockade of neurokinin-1 receptors enhances serotonin neurotransmission. *Biol Psychiatry* 50:191-199.

Haddjeri N, Blier P, de Montigny C (1998): Long-term antidepressant treatments result in a tonic activation of forebrain 5-HT1A receptors. *J Neurosci* 18:10150-10156.

Hafizi S, Chandra P, Cowen J (2007): Neurokinin-1 receptor antagonists as novel antidepressants: trials and tribulations. *Br J Psychiatry* 191:282-284.

Hahn MK, Bannon MJ (1999): Stress-induced C-fos expression in the rat locus coeruleus is dependent on neurokinin 1 receptor activation. *Neuroscience* 94:1183-1188.

Hajos M, Gartside SE, Varga V, Sharp T (2003a): In vivo inhibition of neuronal activity in the rat ventromedial prefrontal cortex by midbrain-raphe nuclei: role of 5-HT1A receptors. *Neuropharmacology* 45:72-81.

Hajos M, Hajos-Korcsok E, Sharp T (1999): Role of the medial prefrontal cortex in 5-HT1A receptor-induced inhibition of 5-HT neuronal activity in the rat. *Br J Pharmacol* 126:1741-1750.

Hajos M, Hoffmann WE, Robinson DD, Yu JH, Hajos-Korcsok E (2003b): Norepinephrine but not serotonin reuptake inhibitors enhance theta and gamma activity of the septo-hippocampal system. *Neuropsychopharmacology* 28:857-864.

Hajos M, Richards CD, Szekely AD, Sharp T (1998): An electrophysiological and neuroanatomical study of the medial prefrontal cortical projection to the midbrain raphe nuclei in the rat. *Neuroscience* 87:95-108.

Halasy K, Miettinen R, Szabat E, Freund TF (1992): GABAergic Interneurons are the Major Postsynaptic Targets of Median Raphe Afferents in the Rat Dentate Gyrus. *Eur J Neurosci* 4:144-153.

Halasz J, Toth M, Mikics E, Hrabovszky E, Barsy B, Barsvari B, et al (2008): The effect of neurokinin1 receptor blockade on territorial aggression and in a model of violent aggression. *Biol Psychiatry* 63:271-278.

Hamada S, Senzaki K, Hamaguchi-Hamada K, Tabuchi K, Yamamoto H, Yamamoto T, et al (1998): Localization of 5-HT2A receptor in rat cerebral cortex and olfactory system revealed by immunohistochemistry using two antibodies raised in rabbit and chicken. *Brain Res Mol Brain Res* 54:199-211.

Hamilton M (1960): A rating scale for depression. *J Neurol Neurosurg Psychiatry* 23:56-62.

Hamilton M (1967): Development of a rating scale for primary depressive illness. *Br J Soc Clin Psychol* 6:278-296.

Hamke M, Herpfer I, Lieb K, Wandelt C, Fiebich BL (2006): Substance P induces expression of the corticotropin-releasing factor receptor 1 by activation of the neurokinin-1 receptor. *Brain Res* 1102:135-144.

Hammers A, Allom R, Koepp MJ, Free SL, Myers R, Lemieux L, et al (2003): Three-dimensional maximum probability atlas of the human brain, with particular reference to the temporal lobe. *Hum Brain Mapp* 19:224-247.

Haneda E, Higuchi M, Maeda J, Inaji M, Okauchi T, Ando K, et al (2007): In vivo mapping of substance P receptors in brains of laboratory animals by high-resolution imaging systems. *Synapse* 61:205-215.

Harding A, Paxinos G, Halliday G (2004): The Serotonin and Tachykinin Systems. In: Paxinos G editor. *The Rat Nervous System*, 3rd ed. San Diego: Elsevier Academic Press, pp 1205-1256.

Hargreaves R (2002): Imaging substance P receptors (NK1) in the living human brain using positron emission tomography. *J Clin Psychiatry* 63 Suppl 11:18-24.

Harlan RE, Garcia MM, Krause JE (1989): Cellular localization of substance P- and neurokinin A-encoding preprotachykinin mRNA in the female rat brain. *J Comp Neurol* 287:179-212.

Harmer CJ, Mackay CE, Reid CB, Cowen PJ, Goodwin GM (2006): Antidepressant drug treatment modifies the neural processing of nonconscious threat cues. *Biol Psychiatry* 59:816-820.

Harrison S, Geppetti P (2001): Substance p. *Int J Biochem Cell Biol* 33:555-576.

Harro J, Oreland L (2001): Depression as a spreading adjustment disorder of monoaminergic neurons: a case for primary implication of the locus coeruleus. *Brain Res Brain Res Rev* 38:79-128.

Hasenohrl RU, Jentjens O, De Souza Silva MA, Tomaz C, Huston JP (1998): Anxiolytic-like action of neurokinin substance P administered systemically or

into the nucleus basalis magnocellularis region. *Eur J Pharmacol* 354:123-133.

Hasenohrl RU, Souza-Silva MA, Nikolaus S, Tomaz C, Brandao ML, Schwarting RK, et al (2000): Substance P and its role in neural mechanisms governing learning, anxiety and functional recovery. *Neuropeptides* 34:272-280.

Hauptman JS, DeSalles AA, Espinoza R, Sedrak M, Ishida W (2008): Potential surgical targets for deep brain stimulation in treatment-resistant depression. *Neurosurg Focus* 25:E3.

Hayashi K, Sato H, Kaise T, Ohmori K, Ishii A, Sano J, et al (2001): Roles of mast cells and sensory nerves in cutaneous vascular hyperpermeability and scratching behavior induced by poly-L-arginine in rats. *Eur J Pharmacol* 425:219-227.

Hayashi M (1992): Ontogeny of some neuropeptides in the primate brain. *Prog Neurobiol* 38:231-260.

Hayat MA (2000): Applications of microwave heating to microscopy. *Principles and Techniques of Electron Microscopy- Biological Applications*, Fourth ed. Cambridge: Cambridge University Press, pp 472-482.

Heiss WD, Herholz K (2006): Brain receptor imaging. *J Nucl Med* 47:302-312.

Helke CJ, Thor KB, Sasek CA (1990): Distribution and coexistence of neuropeptides in bulbospinal and medullary autonomic pathways. *Ann N Y Acad Sci* 579:149-159.

Henson R (2005): A mini-review of fMRI studies of human medial temporal lobe activity associated with recognition memory. *Q J Exp Psychol B* 58:340-360.

Herkenham M, Nauta WJ (1979): Efferent connections of the habenular nuclei in the rat. *J Comp Neurol* 187:19-47.

Herpfer I, Hunt SP, Stanford SC (2005): A comparison of neurokinin 1 receptor knock-out (NK1-/-) and wildtype mice: exploratory behaviour and extracellular noradrenaline concentration in the cerebral cortex of anaesthetised subjects. *Neuropharmacology* 48:706-719.

Herpfer I, Lieb K (2005): Substance p receptor antagonists in psychiatry: rationale for development and therapeutic potential. *CNS Drugs* 19:275-293.

Hietala J (2002): Pet neuroimaging studies of substance P NK1 receptors in depression. *41st Annual meeting of the American College of Neuropsychopharmacology*. San Juan, Puerto Rico.

Hietala J, Nyman MJ, Eskola O, Laakso A, Gronroos T, Oikonen V, et al (2005): Visualization and quantification of neurokinin-1 (NK1) receptors in the human brain. *Mol Imaging Biol* 7:262-272.

Hodges H, Green S, Glenn B (1987): Evidence that the amygdala is involved in benzodiazepine and serotonergic effects on punished responding but not on discrimination. *Psychopharmacology (Berl)* 92:491-504.

Hokfelt T, Bartfai T, Bloom F (2003): Neuropeptides: opportunities for drug discovery. *Lancet Neurol* 2:463-472.

Hokfelt T, Kellerth JO, Nilsson G, Pernow B (1975): Substance p: localization in the central nervous system and in some primary sensory neurons. *Science* 190:889-890.

Hokfelt T, Ljungdahl A, Steinbusch H, Verhofstad A, Nilsson G, Brodin E, et al (1978): Immunohistochemical evidence of substance P-like immunoreactivity in some 5-hydroxytryptamine-containing neurons in the rat central nervous system. *Neuroscience* 3:517-538.

Hokfelt T, Pernow B, Wahren J (2001): Substance P: a pioneer amongst neuropeptides. *J Intern Med* 249:27-40.

Holstege JC (1987): Brainstem projections to lumbar motoneurons in rat--II. An ultrastructural study by means of the anterograde transport of wheat germ agglutinin coupled to horseradish peroxidase and using the tetramethyl benzidine reaction. *Neuroscience* 21:369-376.

Hong JS, Tilson HA, Yoshikawa K (1983): Effects of lithium and haloperidol administration on the rat brain levels of substance P. *J Pharmacol Exp Ther* 224:590-593.

Hong JS, Yang HY, Racagni G, Costa E (1977): Projections of substance P containing neurons from neostriatum to substantia nigra. *Brain Res* 122:541-544.

Honkaniemi J, Pelto-Huikko M, Rechardt L, Isola J, Lammi A, Fuxe K, et al (1992): Colocalization of peptide and glucocorticoid receptor immunoreactivities in rat central amygdaloid nucleus. *Neuroendocrinology* 55:451-459.

Hopkins B, Powell SJ, Danks P, Briggs I, Graham A (1991): Isolation and characterisation of the human lung NK-1 receptor cDNA. *Biochem Biophys Res Commun* 180:1110-1117.

Hoyer D, Hannon JP, Martin GR (2002): Molecular, pharmacological and functional diversity of 5-HT receptors. *Pharmacol Biochem Behav* 71:533-554.

Hrdina PD, Demeter E, Vu TB, Sotonyi P, Palkovits M (1993): 5-HT uptake sites and 5-HT2 receptors in brain of antidepressant-free suicide victims/depressives: increase in 5-HT2 sites in cortex and amygdala. *Brain Res* 614:37-44.

Hurd YL, Keller E, Sotonyi P, Sedvall G (1999): Preprotachykinin-A mRNA expression in the human and monkey brain: An in situ hybridization study. *J Comp Neurol* 411:56-72.

Hurley KM, Herbert H, Moga MM, Saper CB (1991): Efferent projections of the infralimbic cortex of the rat. *J Comp Neurol* 308:249-276.

Hussain Z, Johnson LR, Totterdell S (1996): A light and electron microscopic study of NADPH-diaphorase-, calretinin- and parvalbumin-containing neurons in the rat nucleus accumbens. *J Chem Neuroanat* 10:19-39.

Husum H, Vasquez PA, Mathe AA (2001): Changed concentrations of tachykinins and neuropeptide Y in brain of a rat model of depression: lithium treatment normalizes tachykinins. *Neuropsychopharmacology* 24:183-191.

Hwang BH, Katner J, Iyengar S (2005): Corticotropin-releasing factor mRNA and substance P receptor binding in the paraventricular hypothalamic nucleus, central nucleus of the amygdala, and locus coeruleus of Sprague-Dawley rats following restraint-induced stress. *J Mol Neurosci* 25:239-250.

Ihara N, Ueda S, Kawata M, Sano Y (1988): Immunohistochemical demonstration of serotonin-containing nerve fibers in the mammalian hippocampal formation. *Acta Anat (Basel)* 132:335-346.

Iijima K, Ohtomo K (1988): Immunocytochemical study using a GABA antiserum for the demonstration of inhibitory neurons in the rat locus ceruleus. *The American journal of anatomy* 181:43-52.

Imai H, Steindler DA, Kitai ST (1986): The organization of divergent axonal projections from the midbrain raphe nuclei in the rat. *J Comp Neurol* 243:363-380.

Invernizzi RW, Garattini S (2004): Role of presynaptic alpha2-adrenoceptors in antidepressant action: recent findings from microdialysis studies. *Prog Neuropsychopharmacol Biol Psychiatry* 28:819-827.

Iritani S, Fujii M, Satoh K (1989): The distribution of substance P in the cerebral cortex and hippocampal formation: an immunohistochemical study in the monkey and rat. *Brain Res Bull* 22:295-303.

Itaya SK, van Hoesen GW (1982): WGA-HRP as a transneuronal marker in the visual pathways of monkey and rat. *Brain Res* 236:199-204.

Jakab RL, Goldman-Rakic PS (1998): 5-Hydroxytryptamine2A serotonin receptors in the primate cerebral cortex: possible site of action of hallucinogenic and antipsychotic drugs in pyramidal cell apical dendrites. *Proc Natl Acad Sci U S A* 95:735-740.

Jakab RL, Goldman-Rakic PS (2000): Segregation of serotonin 5-HT2A and 5-HT3 receptors in inhibitory circuits of the primate cerebral cortex. *J Comp Neurol* 417:337-348.

Jakab RL, Hazrati LN, Goldman-Rakic P (1996): Distribution and neurochemical character of substance P receptor (SPR)-immunoreactive striatal neurons of

the macaque monkey: accumulation of SP fibers and SPR neurons and dendrites in "striocapsules" encircling striosomes. *J Comp Neurol* 369:137-149.

Jankowski MP, Sesack SR (2004): Prefrontal cortical projections to the rat dorsal raphe nucleus: ultrastructural features and associations with serotonin and gamma-aminobutyric acid neurons. *J Comp Neurol* 468:518-529.

Jansson A, Tinner B, Bancila M, Verge D, Steinbusch HW, Agnati LF, et al (2001): Relationships of 5-hydroxytryptamine immunoreactive terminal-like varicosities to 5-hydroxytryptamine-2A receptor-immunoreactive neuronal processes in the rat forebrain. *J Chem Neuroanat* 22:185-203.

Jansson A, Tinner B, Steinbusch HW, Agnati LF, Fuxe K (1998): On the relationship of 5-hydroxytryptamine neurons to 5-hydroxytryptamine 2A receptor-immunoreactive neuronal processes in the brain stem of rats. A double immunolabelling analysis. *Neuroreport* 9:2505-2511.

Jones BE, Cuello AC (1989): Afferents to the basal forebrain cholinergic cell area from pontomesencephalic--catecholamine, serotonin, and acetylcholine--neurons. *Neuroscience* 31:37-61.

Jones RS, Mondadori C, Olpe HR (1985): Neuronal sensitivity to substance P is increased after repeated treatment with tranylcypromine, carbamazepine or oxaprotaline, but decreased after repeated electroconvulsive shock. *Neuropharmacology* 24:627-633.

Joyce JN, Shane A, Lexow N, Winokur A, Casanova MF, Kleinman JE (1993): Serotonin uptake sites and serotonin receptors are altered in the limbic system of schizophrenics. *Neuropsychopharmacology* 8:315-336.

Kalen P, Karlson M, Wiklund L (1985): Possible excitatory amino acid afferents to nucleus raphe dorsalis of the rat investigated with retrograde wheat germ agglutinin and D-[3H]aspartate tracing. *Brain Res* 360:285-297.

Kalen P, Pritzel M, Nieoullon A, Wiklund L (1986): Further evidence for excitatory amino acid transmission in the lateral habenular projection to the rostral raphe nuclei: lesion-induced decrease of high affinity glutamate uptake. *Neurosci Lett* 68:35-40.

Kanazawa I, Mogaki S, Muramoto O, Kuzuhara S (1980): On the origin of substance P-containing fibres in the entopeduncular nucleus and the substantia nigra of the rat. *Brain Res* 184:481-485.

Kaneko T, Shigemoto R, Nakanishi S, Mizuno N (1994): Morphological and chemical characteristics of substance P receptor-immunoreactive neurons in the rat neocortex. *Neuroscience* 60:199-211.

Kart-Teke E, Dere E, Brandao ML, Huston JP, De Souza Silva MA (2007): Reinstatement of episodic-like memory in rats by neurokinin-1 receptor antagonism. *Neurobiol Learn Mem* 87:324-331.

Kart E, Jocham G, Muller CP, Schlomer C, Brandao ML, Huston JP, et al (2004): Neurokinin-1 receptor antagonism by SR140333: enhanced in vivo ACh in the hippocampus and promnestic post-trial effects. *Peptides* 25:1959-1969.

Kawahara H, Kawahara Y, Westerink BH (2000): The role of afferents to the locus coeruleus in the handling stress-induced increase in the release of noradrenaline in the medial prefrontal cortex: a dual-probe microdialysis study in the rat brain. *Eur J Pharmacol* 387:279-286.

Kawahara Y, Kawahara H, Westerink BH (1999): Tonic regulation of the activity of noradrenergic neurons in the locus coeruleus of the conscious rat studied by dual-probe microdialysis. *Brain Res* 823:42-48.

Keller M, Montgomery S, Ball W, Morrison M, Snavely D, Liu G, et al (2006): Lack of efficacy of the substance p (neurokinin1 receptor) antagonist aprepitant in the treatment of major depressive disorder. *Biol Psychiatry* 59:216-223.

Khawaja X (1995): Quantitative autoradiographic characterisation of the binding of [3H]WAY-100635, a selective 5-HT1A receptor antagonist. *Brain Res* 673:217-225.

Kia HK, Brisorgueil MJ, Daval G, Langlois X, Hamon M, Verge D (1996a): Serotonin1A receptors are expressed by a subpopulation of cholinergic neurons in the rat medial septum and diagonal band of Broca--a double immunocytochemical study. *Neuroscience* 74:143-154.

Kia HK, Brisorgueil MJ, Hamon M, Calas A, Verge D (1996b): Ultrastructural localization of 5-hydroxytryptamine1A receptors in the rat brain. *J Neurosci Res* 46:697-708.

Kia HK, Miquel MC, Brisorgueil MJ, Daval G, Riad M, El Mestikawy S, et al (1996c): Immunocytochemical localization of serotonin1A receptors in the rat central nervous system. *J Comp Neurol* 365:289-305.

Kilts CD, Kelsey JE, Knight B, Ely TD, Bowman FD, Gross RE, et al (2006): The neural correlates of social anxiety disorder and response to pharmacotherapy. *Neuropsychopharmacology* 31:2243-2253.

Kim DS, Kim JE, Kwak SE, Kim DW, Choi SY, Kwon OS, et al (2007): Seizure activity selectively reduces 5-HT1A receptor immunoreactivity in CA1 interneurons in the hippocampus of seizure-prone gerbils. *Brain Res* 1154:181-193.

Kim MA, Lee HS, Lee BY, Waterhouse BD (2004): Reciprocal connections between subdivisions of the dorsal raphe and the nuclear core of the locus coeruleus in the rat. *Brain Res* 1026:56-67.

Kiss J, Csaki A, Bokor H, Kocsis K, Kocsis B (2002): Possible glutamatergic/aspartatergic projections to the supramammillary nucleus and their origins in the rat studied by selective [(3)H]D-aspartate labelling and immunocytochemistry. *Neuroscience* 111:671-691.

Klemm WR (2004): Habenular and interpeduncularis nuclei: shared components in multiple-function networks. *Med Sci Monit* 10:RA261-273.

Kohler C, Chan-Palay V, Steinbusch H (1982): The distribution and origin of serotonin-containing fibers in the septal area: a combined immunohistochemical and fluorescent retrograde tracing study in the rat. *J Comp Neurol* 209:91-111.

Kolta A, Dubuc R, Lund JP (1993): An immunocytochemical and autoradiographic investigation of the serotoninergic innervation of trigeminal mesencephalic and motor nuclei in the rabbit. *Neuroscience* 53:1113-1126.

Koshiya K, Kato T (1983): Acute changes in nigral substance P content induced by drugs acting on dopamine, muscarine and GABA receptors. *Naunyn Schmiedebergs Arch Pharmacol* 324:223-227.

Kosofsky BE, Molliver ME (1987): The serotoninergic innervation of cerebral cortex: different classes of axon terminals arise from dorsal and median raphe nuclei. *Synapse* 1:153-168.

Kostowski W, Plaznik A, Stefanski R (1989): Intra-hippocampal buspirone in animal models of anxiety. *Eur J Pharmacol* 168:393-396.

Koutcherov Y, Ashwell KW, Paxinos G (2000a): The distribution of the neurokinin B receptor in the human and rat hypothalamus. *Neuroreport* 11:3127-3131.

Koutcherov Y, Mai JK, Ashwell KW, Paxinos G (2000b): Organization of the human paraventricular hypothalamic nucleus. *J Comp Neurol* 423:299-318.

Kowall NW, Quigley BJ, Jr., Krause JE, Lu F, Kosofsky BE, Ferrante RJ (1993): Substance P and substance P receptor histochemistry in human neurodegenerative diseases. *Regul Pept* 46:174-185.

Koyano K, Velimirovic BM, Grigg JJ, Nakajima S, Nakajima Y (1993): Two signal transduction mechanisms of substance P-induced depolarization in locus coeruleus neurons. *Eur J Neurosci* 5:1189-1197.

Kramer MS, Cutler N, Feighner J, Shrivastava R, Carman J, Sramek JJ, et al (1998): Distinct mechanism for antidepressant activity by blockade of central substance P receptors. *Science* 281:1640-1645.

Kramer MS, Winokur A, Kelsey J, Preskorn SH, Rothschild AJ, Snavely D, et al (2004): Demonstration of the efficacy and safety of a novel substance P (NK1) receptor antagonist in major depression. *Neuropsychopharmacology* 29:385-392.

Kreiss DS, Lucki I (1995): Effects of acute and repeated administration of antidepressant drugs on extracellular levels of 5-hydroxytryptamine measured in vivo. *J Pharmacol Exp Ther* 274:866-876.

Kuang P, Lang S, Liu J, Zhang F, Wu W (1991): The investigation of antiepileptic action of qingyangshen (QYS)--effect of QYS on the concentrations of neuropeptides in rat brain. *J Tradit Chin Med* 11:40-46.

Lacoste B, Riad M, Descarries L (2006): Immunocytochemical evidence for the existence of substance P receptor (NK1) in serotonin neurons of rat and mouse dorsal raphe nucleus. *Eur J Neurosci* 23:2947-2958.

Lafaille F, Welner SA, Suranyi-Cadotte BE (1991): Regulation of serotonin type 2 (5-HT2) and beta-adrenergic receptors in rat cerebral cortex following novel and classical antidepressant treatment. *J Psychiatry Neurosci* 16:209-214.

Lai JP, Cnaan A, Zhao H, Douglas SD (2008): Detection of full-length and truncated neurokinin-1 receptor mRNA expression in human brain regions. *J Neurosci Methods* 168:127-133.

Lammertsma AA, Hume SP (1996): Simplified reference tissue model for PET receptor studies. *Neuroimage* 4:153-158.

Lamour Y, Dutar P, Jobert A (1983): Effects of neuropeptides on rat cortical neurons: laminar distribution and interaction with the effect of acetylcholine. *Neuroscience* 10:107-117.

Lamour Y, Senut MC, Dutar P, Bassant MH (1988): Neuropeptides and septo-hippocampal neurons: electrophysiological effects and distributions of immunoreactivity. *Peptides* 9:1351-1359.

Lanciego JL, Wouterlood FG, Erro E, Gimenez-Amaya JM (1998): Multiple axonal tracing: simultaneous detection of three tracers in the same section. *Histochem Cell Biol* 110:509-515.

Lanfumey L, Hamon M (2004): 5-HT1 receptors. *Curr Drug Targets CNS Neurol Disord* 3:1-10.

Langlois X, Wintmolders C, te Riele P, Leysen JE, Jurzak M (2001): Detailed distribution of Neurokinin 3 receptors in the rat, guinea pig and gerbil brain: a comparative autoradiographic study. *Neuropharmacology* 40:242-253.

Laruelle M, Abi-Dargham A, Casanova MF, Toti R, Weinberger DR, Kleinman JE (1993): Selective abnormalities of prefrontal serotonergic receptors in schizophrenia. A postmortem study. *Arch Gen Psychiatry* 50:810-818.

Lecourtier L, Kelly PH (2007): A conductor hidden in the orchestra? Role of the habenular complex in monoamine transmission and cognition. *Neurosci Biobehav Rev* 31:658-672.

Lee HS, Kim MA, Valentino RJ, Waterhouse BD (2003): Glutamatergic afferent projections to the dorsal raphe nucleus of the rat. *Brain Res* 963:57-71.

Lee HS, Kim MA, Waterhouse BD (2005): Retrograde double-labeling study of common afferent projections to the dorsal raphe and the nuclear core of the locus coeruleus in the rat. *J Comp Neurol* 481:179-193.

Lee T, Kaneko T, Shigemoto R, Nomura S, Mizuno N (1997): Collateral projections from striatonigral neurons to substance P receptor-expressing intrinsic neurons in the striatum of the rat. *J Comp Neurol* 388:250-264.

Leger L, Gay N, Cespuglio R (2002): Neurokinin NK1- and NK3-immunoreactive neurons in serotonergic cell groups in the rat brain. *Neurosci Lett* 323:146-150.

Lejeune F, Gobert A, Millan MJ (2002): The selective neurokinin (NK)(1) antagonist, GR205,171, stereospecifically enhances mesocortical dopaminergic transmission in the rat: a combined dialysis and electrophysiological study. *Brain Res* 935:134-139.

Leranth C, Frotscher M (1989): Organization of the septal region in the rat brain: cholinergic-GABAergic interconnections and the termination of hippocampo-septal fibers. *J Comp Neurol* 289:304-314.

Levesque M, Parent R, Parent A (2006): Cellular and subcellular localization of neurokinin-1 and neurokinin-3 receptors in primate globus pallidus. *Eur J Neurosci* 23:2760-2772.

Levesque M, Wallman MJ, Parent R, Sik A, Parent A (2007): Neurokinin-1 and neurokinin-3 receptors in primate substantia nigra. *Neurosci Res* 57:362-371.

Levita L, Mania I, Rainnie DG (2003): Subtypes of substance P receptor immunoreactive interneurons in the rat basolateral amygdala. *Brain Res* 981:41-51.

Leysen JE (2004): 5-HT2 receptors. *Curr Drug Targets CNS Neurol Disord* 3:11-26.

Leysen JE, Niemegeers CJ, Van Nueten JM, Laduron PM (1982): [3H]Ketanserin (R 41 468), a selective 3H-ligand for serotonin2 receptor binding sites. Binding properties, brain distribution, and functional role. *Mol Pharmacol* 21:301-314.

Leyton M, Ghadirian AM, Young SN, Palmour RM, Blier P, Helmers KF, et al (2000): Depressive relapse following acute tryptophan depletion in patients with major depressive disorder. *J Psychopharmacol* 14:284-287.

Li H, Li YQ (2000): Collateral projection of substance P receptor expressing neurons in the medullary dorsal horn to bilateral parabrachial nuclei of the rat. *Brain Res Bull* 53:163-169.

Li JL, Wang D, Kaneko T, Shigemoto R, Nomura S, Mizuno N (2000a): The relationship between neurokinin-1 receptor and substance P in the medullary dorsal horn: a light and electron microscopic immunohistochemical study in the rat. *Neurosci Res* 36:327-334.

Li JL, Wang D, Kaneko T, Shigemoto R, Nomura S, Mizuno N (2000b): Relationship between neurokinin-1 receptor and substance P in the striatum: light and electron microscopic immunohistochemical study in the rat. *J Comp Neurol* 418:156-163.

Li Q, Brownfield MS, Levy AD, Battaglia G, Cabrera TM, Van de Kar LD (1994): Attenuation of hormone responses to the 5-HT1A agonist ipsapirone by long-term treatment with fluoxetine, but not desipramine, in male rats. *Biol Psychiatry* 36:300-308.

Li X, Inoue T, Abekawa T, Weng S, Nakagawa S, Izumi T, et al (2006): 5-HT1A receptor agonist affects fear conditioning through stimulations of the postsynaptic 5-HT1A receptors in the hippocampus and amygdala. *Eur J Pharmacol* 532:74-80.

Li YQ, Jia HG, Rao ZR, Shi JW (1990a): Serotonin-, substance P- or leucine-enkephalin-containing neurons in the midbrain periaqueductal gray and nucleus raphe dorsalis send projection fibers to the central amygdaloid nucleus in the rat. *Neurosci Lett* 120:124-127.

Li YQ, Rao ZR, Shi JW (1990b): Midbrain periaqueductal gray neurons with substance P- or enkephalin-like immunoreactivity send projection fibers to the nucleus accumbens in the rat. *Neurosci Lett* 119:269-271.

Lieb K, Ahlvers K, Dancker K, Strohbusch S, Reincke M, Feige B, et al (2002): Effects of the neuropeptide substance P on sleep, mood, and neuroendocrine measures in healthy young men. *Neuropsychopharmacology* 27:1041-1049.

Lieb K, Fiebich BL, Herpfer I, Mantovani M, Loffler M, Feuerstein TJ (2005): No modulatory effect of neurokinin-1 receptor antagonists on serotonin uptake in human and rat brain synaptosomes. *Eur Neuropsychopharmacol* 15:641-646.

Lieb K, Treffurth Y, Hamke M, Akundi RS, von Kleinsorgen M, Fiebich BL (2003): Valproic acid inhibits substance P-induced activation of protein kinase C epsilon and expression of the substance P receptor. *J Neurochem* 86:69-76.

Lieb K, Walden J, Grunze H, Fiebich BL, Berger M, Normann C (2004): Serum levels of substance P and response to antidepressant pharmacotherapy. *Pharmacopsychiatry* 37:238-239.

Lisoprawski A, Blanc G, Glowinski J (1981): Activation by stress of the habenulo-interpeduncular substance P neurons in the rat. *Neurosci Lett* 25:47-51.

Liu HL, Cao R, Jin L, Chen LW (2002a): Immunocytochemical localization of substance P receptor in hypothalamic oxytocin-containing neurons of C57 mice. *Brain Res* 948:175-179.

Liu R, Ding Y, Aghajanian GK (2002b): Neurokinins activate local glutamatergic inputs to serotonergic neurons of the dorsal raphe nucleus. *Neuropsychopharmacology* 27:329-340.

Liu W, Alreja M (1997): Atypical antipsychotics block the excitatory effects of serotonin in septohippocampal neurons in the rat. *Neuroscience* 79:369-382.

Liu YY, Wong-Riley MT, Liu JP, Wei XY, Jia Y, Liu HL, et al (2004): Substance P and enkephalinergic synapses onto neurokinin-1 receptor-immunoreactive neurons in the pre-Botzinger complex of rats. *Eur J Neurosci* 19:65-75.

Ljungdahl A, Hokfelt T, Nilsson G (1978a): Distribution of substance P-like immunoreactivity in the central nervous system of the rat--I. Cell bodies and nerve terminals. *Neuroscience* 3:861-943.

Ljungdahl A, Hokfelt T, Nilsson G, Goldstein M (1978b): Distribution of substance P-like immunoreactivity in the central nervous system of the rat--II. Light microscopic localization in relation to catecholamine-containing neurons. *Neuroscience* 3:945-976.

Login GR, Dvorak AM (1993): A review of rapid microwave fixation technology: its expanding niche in morphologic studies. *Scanning* 15:58-66.

Lopez-Gimenez JF, Mengod G, Palacios JM, Vilaro MT (1997): Selective visualization of rat brain 5-HT2A receptors by autoradiography with [3H]MDL 100,907. *Naunyn Schmiedebergs Arch Pharmacol* 356:446-454.

Lotstra F, Mailleux P, Vanderhaeghen JJ (1988): Substance P neurons in the human hippocampus: an immunohistochemical analysis in the infant and adult. *J Chem Neuroanat* 1:111-123.

Lucas LR, Pompei P, McEwen BS (1997): Effects of deoxycorticosterone acetate and diazepam on neuropeptidergic neurons in rat striatum. *Neuroreport* 8:811-816.

Luttgen M, Ogren SO, Meister B (2005): 5-HT(1A) receptor mRNA and immunoreactivity in the rat medial septum/diagonal band of Broca-relationships to GABAergic and cholinergic neurons. *J Chem Neuroanat* 29:93-111.

Luttgen M, Ove Ogren S, Meister B (2004): Chemical identity of 5-HT(2A) receptor immunoreactive neurons of the rat septal complex and dorsal hippocampus. *Brain Res* 1010:156-165.

Ma QP, Bleasdale C (2002): Modulation of brain stem monoamines and gamma-aminobutyric acid by NK1 receptors in rats. *Neuroreport* 13:1809-1812.

Maciewicz R, Foote WE, Bry J (1981): Excitatory projection from the interpeduncular nucleus to central superior raphe neurons. *Brain Res* 225:179-183.

Maeno H, Kiyama H, Tohyama M (1993): Distribution of the substance P receptor (NK-1 receptor) in the central nervous system. *Brain Res Mol Brain Res* 18:43-58.

Maeshima T, Ito R, Hamada S, Senzaki K, Hamaguchi-Hamada K, Shutoh F, et al (1998a): The cellular localization of 5-HT2A receptors in the spinal cord and spinal ganglia of the adult rat. *Brain Res* 797:118-124.

Maeshima T, Shutoh F, Hamada S, Senzaki K, Hamaguchi-Hamada K, Ito R, et al (1998b): Serotonin2A receptor-like immunoreactivity in rat cerebellar Purkinje cells. *Neurosci Lett* 252:72-74.

Malek-Ahmadi P (1992): Substance P and neuropsychiatric disorders: an overview. *Neurosci Biobehav Rev* 16:365-369.

Malmgren L, Olsson Y (1978): A sensitive method for histochemical demonstration of horseradish peroxidase in neurons following retrograde axonal transport. *Brain Res* 148:279-294.

Mantyh PW (2002): Neurobiology of substance P and the NK1 receptor. *J Clin Psychiatry* 63 Suppl 11:6-10.

Mantyh PW, Allen CJ, Ghilardi JR, Rogers SD, Mantyh CR, Liu H, et al (1995): Rapid endocytosis of a G protein-coupled receptor: substance P evoked internalization of its receptor in the rat striatum in vivo. *Proc Natl Acad Sci U S A* 92:2622-2626.

Mantyh PW, Gates T, Mantyh CR, Maggio JE (1989): Autoradiographic localization and characterization of tachykinin receptor binding sites in the rat brain and peripheral tissues. *J Neurosci* 9:258-279.

Mantyh PW HSMJ (1984): Substance P receptors: localization by light microscopic autoradiography in rat brain using [3H]SP as the radioligand. *Brain Research* 307:147-165.

Mantyh PW, Pinnock RD, Downes CP, Goedert M, Hunt SP (1984): Correlation between inositol phospholipid hydrolysis and substance P receptors in rat CNS. *Nature* 309:795-797.

Mantyh PW, Rogers SD, Ghilardi JR, Maggio JE, Mantyh CR, Vigna SR (1996): Differential expression of two isoforms of the neurokinin-1 (substance P) receptor in vivo. *Brain Res* 719:8-13.

Marek GJ, Aghajanian GK (1996): LSD and the phenethylamine hallucinogen DOI are potent partial agonists at 5-HT2A receptors on interneurons in rat piriform cortex. *J Pharmacol Exp Ther* 278:1373-1382.

Marksteiner J, Sperk G, Krause JE (1992): Distribution of neurons expressing neurokinin B in the rat brain: immunohistochemistry and in situ hybridization. *J Comp Neurol* 317:341-356.

Marlier L, Teilhac JR, Cerruti C, Privat A (1991): Autoradiographic mapping of 5-HT1, 5-HT1A, 5-HT1B and 5-HT2 receptors in the rat spinal cord. *Brain Res* 550:15-23.

Martensson B, Nyberg S, Toresson G, Brodin E, Bertilsson L (1989): Fluoxetine treatment of depression. Clinical effects, drug concentrations and monoamine metabolites and N-terminally extended substance P in cerebrospinal fluid. *Acta Psychiatr Scand* 79:586-596.

Martin-Ruiz R, Puig MV, Celada P, Shapiro DA, Roth BL, Mengod G, et al (2001): Control of serotonergic function in medial prefrontal cortex by serotonin-2A receptors through a glutamate-dependent mechanism. *J Neurosci* 21:9856-9866.

Martin KF, Mason R (1987): Isapirone is a partial agonist at 5-hydroxytryptamine 1A (5-HT1A) receptors in the rat hippocampus: electrophysiological evidence. *Eur J Pharmacol* 141:479-483.

Martin P, Tissier MH, Adrien J, Puech AJ (1991): Antidepressant-like effects of buspirone mediated by the 5-HT1A post-synaptic receptors in the learned helplessness paradigm. *Life Sci* 48:2505-2511.

Massi M, Panocka I, de Caro G (2000): The psychopharmacology of tachykinin NK-3 receptors in laboratory animals. *Peptides* 21:1597-1609.

Mateo Y, Ruiz-Ortega JA, Pineda J, Ugedo L, Meana JJ (2000): Inhibition of 5-hydroxytryptamine reuptake by the antidepressant citalopram in the locus coeruleus modulates the rat brain noradrenergic transmission in vivo. *Neuropharmacology* 39:2036-2043.

Mathe AA, Jousisto-Hanson J, Stenfors C, Theodorsson E (1990): Effect of lithium on tachykinins, calcitonin gene-related peptide, and neuropeptide Y in rat brain. *J Neurosci Res* 26:233-237.

Mather M, Mitchell KJ, Raye CL, Novak DL, Greene EJ, Johnson MK (2006): Emotional arousal can impair feature binding in working memory. *J Cogn Neurosci* 18:614-625.

Matsuda Y, Fujimura K (1992): Action of habenular efferents on ventral tegmental area neurons studied in vitro. *Brain Res Bull* 28:743-749.

Maubach KA, Martin K, Chicchi G, Harrison T, Wheeldon A, Swain CJ, et al (2002): Chronic substance P (NK1) receptor antagonist and conventional antidepressant treatment increases burst firing of monoamine neurones in the locus coeruleus. *Neuroscience* 109:609-617.

Maubach KA, Martin K, Smith DW, Hewson L, Frankshun RA, Harrison T, et al (2001): Substance P stimulates inhibitory synaptic transmission in the guinea pig basolateral amygdala in vitro. *Neuropharmacology* 40:806-817.

Mazzone SB, Geraghty DP (2000): Characterization and regulation of tachykinin receptors in the nucleus tractus solitarius. *Clin Exp Pharmacol Physiol* 27:939-942.

Mazzone SB, Hinrichsen CF, Geraghty DP (1997): Substance P receptors in brain stem respiratory centers of the rat: regulation of NK1 receptors by hypoxia. *J Pharmacol Exp Ther* 282:1547-1556.

McDonald AJ, Mascagni F (2007): Neuronal localization of 5-HT type 2A receptor immunoreactivity in the rat basolateral amygdala. *Neuroscience* 146:306-320.

McKenna DJ, Nazarali AJ, Hoffman AJ, Nichols DE, Mathis CA, Saavedra JM (1989): Common receptors for hallucinogens in rat brain: a comparative autoradiographic study using [125I]LSD and [125I]DOI, a new psychotomimetic radioligand. *Brain Res* 476:45-56.

McQuade R, Sharp T (1997): Functional mapping of dorsal and median raphe 5-hydroxytryptamine pathways in forebrain of the rat using microdialysis. *J Neurochem* 69:791-796.

Meltzer CC, Price JC, Mathis CA, Butters MA, Ziolko SK, Moses-Kolko E, et al (2004): Serotonin 1A receptor binding and treatment response in late-life depression. *Neuropsychopharmacology* 29:2258-2265.

Meltzer CC, Smith G, Price JC, Reynolds CF, 3rd, Mathis CA, Greer P, et al (1998): Reduced binding of [18F]altanserin to serotonin type 2A receptors in aging: persistence of effect after partial volume correction. *Brain Res* 813:167-171.

Meltzer HY, Li Z, Kaneda Y, Ichikawa J (2003): Serotonin receptors: their key role in drugs to treat schizophrenia. *Prog Neuropsychopharmacol Biol Psychiatry* 27:1159-1172.

Menard J, Treit D (1998): The septum and the hippocampus differentially mediate anxiolytic effects of R(+)-8-OH-DPAT. *Behav Pharmacol* 9:93-101.

Mengod G, Pompeiano M, Martinez-Mir MI, Palacios JM (1990): Localization of the mRNA for the 5-HT2 receptor by in situ hybridization histochemistry. Correlation with the distribution of receptor sites. *Brain Res* 524:139-143.

Meyer JH (2007): Imaging the serotonin transporter during major depressive disorder and antidepressant treatment. *J Psychiatry Neurosci* 32:86-102.

Meyer JH, McMain S, Kennedy SH, Korman L, Brown GM, DaSilva JN, et al (2003): Dysfunctional attitudes and 5-HT2 receptors during depression and self-harm. *Am J Psychiatry* 160:90-99.

Micheau J, Van Marrewijk B (1999): Stimulation of 5-HT1A receptors by systemic or medial septum injection induces anxiogenic-like effects and facilitates acquisition of a spatial discrimination task in mice. *Prog Neuropsychopharmacol Biol Psychiatry* 23:1113-1133.

Michelgard A, Appel L, Pissiota A, Frans O, Langstrom B, Bergstrom M, et al (2007): Symptom provocation in specific phobia affects the substance P neurokinin-1 receptor system. *Biol Psychiatry* 61:1002-1006.

Mick G, Maeno H, Kiyama H, Tohyama M (1994): Marginal topography of neurons expressing the substance P receptor in the rat suprachiasmatic nucleus. *Brain Res Mol Brain Res* 21:157-161.

Mick G, Shigemoto R, Kitahama K (1995): Localization of substance P receptors in central neural structures controlling daily rhythms in nocturnal rodents. *C R Acad Sci III* 318:209-217.

Mijnster MJ, Raimundo AG, Koskuba K, Klop H, Docter GJ, Groenewegen HJ, et al (1997): Regional and cellular distribution of serotonin 5-hydroxytryptamine2a receptor mRNA in the nucleus accumbens, olfactory tubercle, and caudate putamen of the rat. *J Comp Neurol* 389:1-11.

Mileusnic D, Lee JM, Magnuson DJ, Hejna MJ, Krause JE, Lorens JB, et al (1999a): Neurokinin-3 receptor distribution in rat and human brain: an immunohistochemical study. *Neuroscience* 89:1269-1290.

Mileusnic D, Magnuson DJ, Hejna MJ, Lorens JB, Lorens SA, Lee JM (1999b): Age and species-dependent differences in the neurokinin B system in rat and human brain. *Neurobiol Aging* 20:19-35.

Millan MJ (2003): The neurobiology and control of anxious states. *Prog Neurobiol* 70:83-244.

Millan MJ, Lejeune F, De Nanteuil G, Gobert A (2001): Selective blockade of neurokinin (NK)(1) receptors facilitates the activity of adrenergic pathways projecting to frontal cortex and dorsal hippocampus in rats. *J Neurochem* 76:1949-1954.

Milner TA, Pickel VM (1986): Ultrastructural localization and afferent sources of substance P in the rat parabrachial region. *Neuroscience* 17:687-707.

Miner LA, Backstrom JR, Sanders-Bush E, Sesack SR (2003): Ultrastructural localization of serotonin2A receptors in the middle layers of the rat prelimbic prefrontal cortex. *Neuroscience* 116:107-117.

Mintun MA, Raichle ME, Kilbourn MR, Wooten GF, Welch MJ (1984): A quantitative model for the in vivo assessment of drug binding sites with positron emission tomography. *Ann Neurol* 15:217-227.

Miquel MC, Doucet E, Riad M, Adrien J, Verge D, Hamon M (1992): Effect of the selective lesion of serotoninergic neurons on the regional distribution of 5-HT1A receptor mRNA in the rat brain. *Brain Res Mol Brain Res* 14:357-362.

Mitsuhashi M, Ohashi Y, Shichijo S, Christian C, Sudduth-Klinger J, Harrowe G, et al (1992): Multiple intracellular signaling pathways of the neuropeptide substance P receptor. *J Neurosci Res* 32:437-443.

Mitsushio H, Takashima M, Mataga N, Toru M (1988): Effects of chronic treatment with trihexyphenidyl and carbamazepine alone or in combination with haloperidol on substance P content in rat brain: a possible implication of substance P in affective disorders. *J Pharmacol Exp Ther* 245:982-989.

Moller M, Jakobsen S, Gjedde A (2007): Parametric and regional maps of free serotonin 5HT1A receptor sites in human brain as function of age in healthy humans. *Neuropsychopharmacology* 32:1707-1714.

Morcuende S, Gadd CA, Peters M, Moss A, Harris EA, Sheasby A, et al (2003): Increased neurogenesis and brain-derived neurotrophic factor in neurokinin-1 receptor gene knockout mice. *Eur J Neurosci* 18:1828-1836.

Morgane PJ, Jacobs MS (1979): Raphe projections to the locus coeruleus in the rat. *Brain Res Bull* 4:519-534.

Morilak DA, Garlow SJ, Ciaranello RD (1993): Immunocytochemical localization and description of neurons expressing serotonin2 receptors in the rat brain. *Neuroscience* 54:701-717.

Morilak DA, Somogyi P, Lujan-Miras R, Ciaranello RD (1994): Neurons expressing 5-HT2 receptors in the rat brain: neurochemical identification of cell types by immunocytochemistry. *Neuropsychopharmacology* 11:157-166.

Morozova E, Wu M, Dumalska I, Alreja M (2008): Neurokinins robustly activate the majority of septohippocampal cholinergic neurons. *Eur J Neurosci* 27:114-122.

Morris JS, Smith KA, Cowen PJ, Friston KJ, Dolan RJ (1999): Covariation of activity in habenula and dorsal raphe nuclei following tryptophan depletion. *Neuroimage* 10:163-172.

Mounir S, Parent A (2002): The expression of neurokinin-1 receptor at striatal and pallidal levels in normal human brain. *Neurosci Res* 44:71-81.

Murakami S, Inagaki S, Shimada S, Kubota Y, Kito S, Ogawa N, et al (1989): The colocalization of substance P- and somatostatin-like peptides in neurons of the entopeduncular nucleus of rats. *Peptides* 10:973-977.

Murray CJ, Lopez AD (1997): Alternative projections of mortality and disability by cause 1990-2020: Global Burden of Disease Study. *Lancet* 349:1498-1504.

Murtra P, Sheasby AM, Hunt SP, De Felipe C (2000): Rewarding effects of opiates are absent in mice lacking the receptor for substance P. *Nature* 405:180-183.

Myohanen TT, Venalainen JI, Garcia-Horsman JA, Mannisto PT (2008): Spatial association of prolyl oligopeptidase, inositol 1,4,5-triphosphate type 1 receptor, substance P and its neurokinin-1 receptor in the rat brain: An immunohistochemical colocalization study. *Neuroscience* 153:1177-1189.

Nagano M, Saitow F, Haneda E, Konishi S, Hayashi M, Suzuki H (2006): Distribution and pharmacological characterization of primate NK-1 and NK-3 tachykinin receptors in the central nervous system of the rhesus monkey. *Br J Pharmacol* 147:316-323.

Nakajima Y, Tsuchida K, Negishi M, Ito S, Nakanishi S (1992): Direct linkage of three tachykinin receptors to stimulation of both phosphatidylinositol hydrolysis and cyclic AMP cascades in transfected Chinese hamster ovary cells. *J Biol Chem* 267:2437-2442.

Nakamura H, Moroji T, Nohara S, Nakamura H, Okada A (1990): Effects of whole-body vibration stress on substance P- and neurotensin-like immunoreactivity in the rat brain. *Environ Res* 52:155-163.

Nakanishi S (1991): Mammalian tachykinin receptors. *Annu Rev Neurosci* 14:123-136.

Nakaya Y, Kaneko T, Shigemoto R, Nakanishi S, Mizuno N (1994): Immunohistochemical localization of substance P receptor in the central nervous system of the adult rat. *J Comp Neurol* 347:249-274.

Nalivaiko E, Michaud JC, Soubrie P, Le Fur G, Feltz P (1997): Tachykinin neurokinin-1 and neurokinin-3 receptor-mediated responses in guinea-pig substantia nigra: an in vitro electrophysiological study. *Neuroscience* 78:745-757.

Nazarali AJ, McKenna DJ, Saavedra JM (1989): Autoradiographic localization of 5HT2 receptors in rat brain using [125I]-DOI, a selective psychotomimetic radioligand. *Prog Neuropsychopharmacol Biol Psychiatry* 13:573-581.

Neckers LM, Schwartz JP, Wyatt RJ, Speciale SG (1979): Substance P afferents from the habenula innervate the dorsal raphe nucleus. *Exp Brain Res* 37:619-623.

Nelder JA, Mead R (1965): A simplex method for function minimization. *Comput J* 7:308-313.

Nelson DL (2004): 5-HT5 receptors. *Curr Drug Targets CNS Neurol Disord* 3:53-58.

Nelson HE (1982): *National Adult Reading Test*. Windsor, UK: NFER-Nelson.

Neumeister A, Nugent AC, Waldeck T, Geraci M, Schwarz M, Bonne O, et al (2004): Neural and behavioral responses to tryptophan depletion in unmedicated

patients with remitted major depressive disorder and controls. *Arch Gen Psychiatry* 61:765-773.

Nikolaus S, Huston JP, Hasenohrl RU (1999): The neurokinin-1 receptor antagonist WIN51,708 attenuates the anxiolytic-like effects of ventralpallidal substance P injection. *Neuroreport* 10:2293-2296.

Nikolaus S, Huston JP, Hasenohrl RU (2000): Anxiolytic-like effects in rats produced by ventral pallidal injection of both N- and C-terminal fragments of substance P. *Neurosci Lett* 283:37-40.

Nilsson L, Winblad B, Volkmann I, Alafuzoff I, Berstrom L (1991): Characterization and quantification of ^{125}I-Bolton Hunter substance P binding sites in human brain *Neurochem Int* 18:399-404.

Nishikawa T, Scatton B (1985): Inhibitory influence of GABA on central serotonergic transmission. Raphe nuclei as the neuroanatomical site of the GABAergic inhibition of cerebral serotonergic neurons. *Brain Res* 331:91-103.

Nitsch R, Leranth C (1994): Substance P-containing hypothalamic afferents to the monkey hippocampus: an immunocytochemical, tracing, and coexistence study. *Exp Brain Res* 101:231-240.

Nocjar C, Roth BL, Pehek EA (2002): Localization of 5-HT(2A) receptors on dopamine cells in subnuclei of the midbrain A10 cell group. *Neuroscience* 111:163-176.

Norbury R, Mackay CE, Cowen PJ, Goodwin GM, Harmer CJ (2007): Short-term antidepressant treatment and facial processing. Functional magnetic resonance imaging study. *Br J Psychiatry* 190:531-532.

Nordstrom P, Asberg M (1992): Suicide risk and serotonin. *Int Clin Psychopharmacol* 6 Suppl 6:12-21.

Nussdorfer GG, Malendowicz LK (1998): Role of tachykinins in the regulation of the hypothalamo-pituitary-adrenal axis. *Peptides* 19:949-968.

Nyman MJ, Eskola O, Kajander J, Vahlberg T, Sanabria S, Burns D, et al (2006): Gender and age affect NK1 receptors in the human brain - a positron emission tomography study with [18 F]SPA-RQ. *Int J Neuropsychopharmacol*:1-11.

Ogier R, Raggenbass M (2003): Action of tachykinins in the rat hippocampus: modulation of inhibitory synaptic transmission. *Eur J Neurosci* 17:2639-2647.

Otsuka M, Yoshioka K (1993): Neurotransmitter functions of mammalian tachykinins. *Physiol Rev* 73:229-308.

Ou XM, Lemonde S, Jafar-Nejad H, Bown CD, Goto A, Rogaeva A, et al (2003): Freud-1: A neuronal calcium-regulated repressor of the 5-HT1A receptor gene. *J Neurosci* 23:7415-7425.

Owens MJ, Nemeroff CB (1994): Role of serotonin in the pathophysiology of depression: focus on the serotonin transporter. *Clin Chem* 40:288-295.

Page NM (2005): New challenges in the study of the mammalian tachykinins. *Peptides* 26:1356-1368.

Papp M, Vassout A, Gentsch C (2000): The NK1-receptor antagonist NKP608 has an antidepressant-like effect in the chronic mild stress model of depression in rats. *Behav Brain Res* 115:19-23.

Parent A, Cicchetti F, Beach TG (1995): Striatal neurones displaying substance P (NK1) receptor immunoreactivity in human and non-human primates. *Neuroreport* 6:721-724.

Paris JM, Cunningham KA (1994): Habenula lesions decrease the responsiveness of dorsal raphe serotonin neurons to cocaine. *Pharmacol Biochem Behav* 49:555-560.

Park MR (1987): Monosynaptic inhibitory postsynaptic potentials from lateral habenula recorded in dorsal raphe neurons. *Brain Res Bull* 19:581-586.

Parker G, Tupling H, Brown LG (1979): A parental bonding instrument. *Br J Med Psychol* 52:1-10.

Pasquier DA, Kemper TL, Forbes WB, Morgane PJ (1977): Dorsal raphe, substantia nigra and locus coeruleus: interconnections with each other and the neostriatum. *Brain Res Bull* 2:323-339.

Patel TD, Azmitia EC, Zhou FC (1996): Increased 5-HT1A receptor immunoreactivity in the rat hippocampus following 5,7-dihydroxytryptamine lesions in the cingulum bundle and fimbria-fornix. *Behav Brain Res* 73:319-323.

Patton JH, Stanford MS, Barratt ES (1995): Factor structure of the Barratt impulsiveness scale. *J Clin Psychol* 51:768-774.

Paxinos G, Watson C (1998): *The rat brain in streretaxic coordinates*, 3rd ed: Academic Press.

Pazos A, Cortes R, Palacios JM (1985): Quantitative autoradiographic mapping of serotonin receptors in the rat brain. II. Serotonin-2 receptors. *Brain Res* 346:231-249.

Pazos A, Palacios JM (1985): Quantitative autoradiographic mapping of serotonin receptors in the rat brain. I. Serotonin-1 receptors. *Brain Res* 346:205-230.

Pazos A, Probst A, Palacios JM (1987): Serotonin receptors in the human brain--IV. Autoradiographic mapping of serotonin-2 receptors. *Neuroscience* 21:123-139.

Peddie CJ, Davies HA, Colyer FM, Stewart MG, Rodriguez JJ (2008): Colocalisation of serotonin2A receptors with the glutamate receptor subunits NR1 and GluR2 in the dentate gyrus: an ultrastructural study of a modulatory role. *Exp Neurol* 211:561-573.

Pennefather JN, Lecci A, Candenas ML, Patak E, Pinto FM, Maggi CA (2004): Tachykinins and tachykinin receptors: a growing family. *Life Sci* 74:1445-1463.

Pernow B (1983): Substance P. *Pharmacol Rev* 35:85-141.

Peterson GM, Shurlow CL (1992): Morphological evidence for a substance P projection from medial septum to hippocampus. *Peptides* 13:509-517.

Petrov T, Krukoff TL, Jhamandas JH (1994): Chemically defined collateral projections from the pons to the central nucleus of the amygdala and hypothalamic paraventricular nucleus in the rat. *Cell Tissue Res* 277:289-295.

Peyron C, Luppi PH, Fort P, Rampon C, Jouvet M (1996): Lower brainstem catecholamine afferents to the rat dorsal raphe nucleus. *J Comp Neurol* 364:402-413.

Peyron C, Luppi PH, Kitahama K, Fort P, Hermann DM, Jouvet M (1995): Origin of the dopaminergic innervation of the rat dorsal raphe nucleus. *Neuroreport* 6:2527-2531.

Peyron C, Petit JM, Rampon C, Jouvet M, Luppi PH (1998): Forebrain afferents to the rat dorsal raphe nucleus demonstrated by retrograde and anterograde tracing methods. *Neuroscience* 82:443-468.

Phillis JW, Limacher JJ (1974): Excitation of cerebral cortical neurons by various polypeptides. *Exp Neurol* 43:414-423.

Pickel VM, Douglas J, Chan J, Gamp PD, Bunnett NW (2000): Neurokinin 1 receptor distribution in cholinergic neurons and targets of substance P terminals in the rat nucleus accumbens. *J Comp Neurol* 423:500-511.

Pickel VM, Joh TH, Reis DJ, Leeman SE, Miller RJ (1979): Electron microscopic localization of substance P and enkephalin in axon terminals related to dendrites of catecholaminergic neurons. *Brain Res* 160:387-400.

Piggins HD, Samuels RE, Coogan AN, Cutler DJ (2001): Distribution of substance P and neurokinin-1 receptor immunoreactivity in the suprachiasmatic nuclei and intergeniculate leaflet of hamster, mouse, and rat. *J Comp Neurol* 438:50-65.

Piguet P, Galvan M (1994): Transient and long-lasting actions of 5-HT on rat dentate gyrus neurones in vitro. *J Physiol* 481 (Pt 3):629-639.

Pompeiano M, Palacios JM, Mengod G (1992): Distribution and cellular localization of mRNA coding for 5-HT1A receptor in the rat brain: correlation with receptor binding. *J Neurosci* 12:440-453.

Pompeiano M, Palacios JM, Mengod G (1994): Distribution of the serotonin 5-HT2 receptor family mRNAs: comparison between 5-HT2A and 5-HT2C receptors. *Brain Res Mol Brain Res* 23:163-178.

Przegalinski E, Tatarczynska E, Klodzinska A, Chojnacka-Wojcik E (1994): The role of postsynaptic 5-HT1A receptors in the anticonflict effect of ipsapirone. *Neuropharmacology* 33:1109-1115.

Quartara L, Maggi CA (1998): The tachykinin NK1 receptor. Part II: Distribution and pathophysiological roles. *Neuropeptides* 32:1-49.

Quirion R, Dam TV (1986): Ontogeny of substance P receptor binding sites in rat brain. *J Neurosci* 6:2187-2199.

Rabiner EA, Messa C, Sargent PA, Husted-Kjaer K, Montgomery A, Lawrence AD, et al (2002): A database of [(11)C]WAY-100635 binding to 5-HT(1A) receptors in normal male volunteers: normative data and relationship to methodological, demographic, physiological, and behavioral variables. *Neuroimage* 15:620-632.

Rahman S, McLean JH, Darby-King A, Paterno G, Reynolds JN, Neuman RS (1995): Loss of cortical serotonin2A signal transduction in senescent rats: reversal following inhibition of protein kinase C. *Neuroscience* 66:891-901.

Rahman S, Neuman RS (1993): Activation of 5-HT2 receptors facilitates depolarization of neocortical neurons by N-methyl-D-aspartate. *Eur J Pharmacol* 231:347-354.

Rainnie DG (1999): Serotonergic modulation of neurotransmission in the rat basolateral amygdala. *J Neurophysiol* 82:69-85.

Raley JM (2006): A Pharmacological and Neuroanatomical study of 5-HT and GABA interactions in the brain. *Univ Dept of Pharmacology*, Vol D.Phil. Thesis. Oxford: University of Oxford, pp 9-10.

Ramboz S, Oosting R, Amara DA, Kung HF, Blier P, Mendelsohn M, et al (1998): Serotonin receptor 1A knockout: an animal model of anxiety-related disorder. *Proc Natl Acad Sci U S A* 95:14476-14481.

Ranicar AS, Williams CW, Schnorr L, Clark JC, Rhodes CG, Bloomfield PM, et al (1991): The on-line monitoring of continuously withdrawn arterial blood during PET studies using a single BGO/photomultiplier assembly and non-stick tubing. *Med Prog Technol* 17:259-264.

Raurich A, Mengod G, Artigas F, Cortes R (1999): Displacement of the binding of 5-HT(1A) receptor ligands to pre- and postsynaptic receptors by (-)pindolol. A comparative study in rodent, primate and human brain. *Synapse* 34:68-76.

Renoldi G, Invernizzi RW (2006): Blockade of tachykinin NK1 receptors attenuates stress-induced rise of extracellular noradrenaline and dopamine in the rat and gerbil medial prefrontal cortex. *J Neurosci Res* 84:961-968.

Reynolds ES (1963): The use of lead citrate at high pH as an electron-opaque stain in electron microscopy. *J Cell Biol* 17:208-212.

Ribeiro-da-Silva A, Hokfelt T (2000): Neuroanatomical localisation of Substance P in the CNS and sensory neurons. *Neuropeptides* 34:256-271.

Ricciardi KH, Blaustein JD (1994): Projections from ventrolateral hypothalamic neurons containing progestin receptor- and substance P-immunoreactivity to specific forebrain and midbrain areas in female guinea pigs. *J Neuroendocrinol* 6:135-144.

Rigat B, Hubert C, Alhenc-Gelas F, Cambien F, Corvol P, Soubrier F (1990): An insertion/deletion polymorphism in the angiotensin I-converting enzyme gene accounting for half the variance of serum enzyme levels. *J Clin Invest* 86:1343-1346.

Rigby M, O'Donnell R, Rupniak NM (2005): Species differences in tachykinin receptor distribution: further evidence that the substance P (NK1) receptor predominates in human brain. *J Comp Neurol* 490:335-353.

Riley LA, Walker PD, Hart RP, Jonakait GM (1991): Alterations of preprotachykinin (PPT) mRNA in medullary raphe occur following manipulation of serotonin. *Ann N Y Acad Sci* 632:455-456.

Rimon R, Le Greves P, Nyberg F, Heikkila L, Salmela L, Terenius L (1984): Elevation of substance P-like peptides in the CSF of psychiatric patients. *Biol Psychiatry* 19:509-516.

Robb RA, Hanson DP, Karwoski RA, Larson AG, Workman EL, Stacy MC (1989): Analyze: a comprehensive, operator-interactive software package for multidimensional medical image display and analysis. *Comput Med Imaging Graph* 13:433-454.

Roberts GW, Woodhams PL, Polak JM, Crow TJ (1982): Distribution of neuropeptides in the limbic system of the rat: the amygdaloid complex. *Neuroscience* 7:99-131.

Ronnekleiv OK, Kelly MJ (1984): Distribution of substance P neurons in the epithalamus of the rat: an immunohistochemical investigation. *J Pineal Res* 1:355-370.

Rorden C, Brett M (2000): Stereotaxic display of brain lesions. *Behav Neurol* 12:191-200.

Rosen A, Brodin K, Eneroth P, Brodin E (1992): Short-term restraint stress and s.c. saline injection alter the tissue levels of substance P and cholecystokinin in the peri-aqueductal grey and limbic regions of rat brain. *Acta Physiol Scand* 146:341-348.

Rosen A, Franck J, Brodin E (1995): Effects of acute systemic treatment with the 5 HT-uptake blocker alaproclate on tissue levels and release of substance P in rat periaqueductal grey. *Neuropeptides* 28:317-324.

Rosene DL, Mesulam MM (1978): Fixation variables in horseradish peroxidase neurohistochemistry. I. The effect of fixation time and perfusion procedures upon enzyme activity. *J Histochem Cytochem* 26:28-39.

Rowan MJ, Anwyl R (1986): Neurophysiological effects of buspirone and isapirone in the hippocampus: comparison with 5-hydroxytryptamine. *Eur J Pharmacol* 132:93-96.

Rupniak NM, Carlson EC, Harrison T, Oates B, Seward E, Owen S, et al (2000): Pharmacological blockade or genetic deletion of substance P (NK(1)) receptors attenuates neonatal vocalisation in guinea-pigs and mice. *Neuropharmacology* 39:1413-1421.

Rupniak NM, Carlson EJ, Shepheard S, Bentley G, Williams AR, Hill A, et al (2003): Comparison of the functional blockade of rat substance P (NK1) receptors by GR205171, RP67580, SR140333 and NKP-608. *Neuropharmacology* 45:231-241.

Rupniak NM, Carlson EJ, Webb JK, Harrison T, Porsolt RD, Roux S, et al (2001): Comparison of the phenotype of NK1R-/- mice with pharmacological blockade of the substance P (NK1) receptor in assays for antidepressant and anxiolytic drugs. *Behav Pharmacol* 12:497-508.

Rupniak NM, Kramer MS (1999): Discovery of the antidepressant and anti-emetic efficacy of substance P receptor (NK1) antagonists. *Trends Pharmacol Sci* 20:485-490.

Ryckmans T, Balancon L, Berton O, Genicot C, Lamberty Y, Lallemand B, et al (2002a): First dual NK(1) antagonists-serotonin reuptake inhibitors: synthesis and SAR of a new class of potential antidepressants. *Bioorg Med Chem Lett* 12:261-264.

Ryckmans T, Berton O, Grimee R, Kogej T, Lamberty Y, Pasau P, et al (2002b): Dual NK(1) antagonists--serotonin reuptake inhibitors as potential antidepressants. Part 2: SAR and activity of benzyloxyphenethyl piperazine derivatives. *Bioorg Med Chem Lett* 12:3195-3198.

Sabatino M, Ferraro G, La Grutta V (1991): Relay stations and neurotransmitters between the pallidal region and the hippocampus. *Electroencephalogr Clin Neurophysiol* 78:302-310.

Sachais BS, Snider RM, Lowe JA, 3rd, Krause JE (1993): Molecular basis for the species selectivity of the substance P antagonist CP-96,345. *J Biol Chem* 268:2319-2323.

Saffroy M, Beaujouan JC, Petitet F, Torrens Y, Glowinski J (1994): Differential localization of 3H-[Pro9]SP binding sites in the guinea pig and rat brain. *Brain Res* 633:317-325.

Saffroy M, Beaujouan JC, Torrens Y, Besseyre J, Bergstrom L, Glowinski J (1988): Localization of tachykinin binding sites (NK1, NK2, NK3 ligands) in the rat brain. *Peptides* 9:227-241.

Saffroy M, Torrens Y, Glowinski J, Beaujouan JC (2001): Presence of NK2 binding sites in the rat brain. *J Neurochem* 79:985-996.

Saffroy M, Torrens Y, Glowinski J, Beaujouan JC (2003): Autoradiographic distribution of tachykinin NK2 binding sites in the rat brain: comparison with NK1 and NK3 binding sites. *Neuroscience* 116:761-773.

Sakai K, Salvert D, Touret M, Jouvet M (1977a): Afferent connections of the nucleus raphe dorsalis in the cat as visualized by the horseradish peroxidase technique. *Brain Res* 137:11-35.

Sakai K, Touret M, Salvert D, Leger L, Jouvet M (1977b): Afferent projections to the cat locus coeruleus as visualized by the horseradish peroxidase technique. *Brain Res* 119:21-41.

Sakanaka M, Inagaki S, Shiosaka S, Senba E, Takagi H, Takatsuki K, et al (1982a): Ontogeny of substance P-containing neuron system of the rat: immunohistochemical analysis--II. Lower brain stem. *Neuroscience* 7:1097-1126.

Sakanaka M, Shiosaka S, Takatsuki K, Inagaki S, Hara Y, Kawai Y, et al (1982b): Origins of substance P-containing fibers in the lateral septal area of young rats: immunohistochemical analysis of experimental manipulations. *J Comp Neurol* 212:268-277.

Sakanaka M, Shiosaka S, Takatsuki K, Inagaki S, Takagi H, Senba E, et al (1981a): Evidence for the existence of a substance P-containing pathway from the nucleus laterodorsalis tegmenti (Castaldi) to the lateral septal area of the rat. *Brain Res* 230:351-355.

Sakanaka M, Shiosaka S, Takatsuki K, Inagaki S, Takagi H, Senba E, et al (1981b): Experimental immunohistochemical studies on the amygdalofugal peptidergic (substance P and somatostatin) fibers in the stria terminalis of the rat. *Brain Res* 221:231-242.

Sakanaka M, Shiosaka S, Takatsuki K, Tohyama M (1983): Evidence for the existence of a substance P-containing pathway from the nucleus laterodorsalis tegmenti (Castaldi) to the medial frontal cortex of the rat. *Brain Res* 259:123-126.

Salome N, Stemmelin J, Cohen C, Griebel G (2006): Selective blockade of NK2 or NK3 receptors produces anxiolytic- and antidepressant-like effects in gerbils. *Pharmacol Biochem Behav* 83:533-539.

Santana N, Bortolozzi A, Serrats J, Mengod G, Artigas F (2004): Expression of serotonin1A and serotonin2A receptors in pyramidal and GABAergic neurons of the rat prefrontal cortex. *Cereb Cortex* 14:1100-1109.

Santarelli L, Gobbi G, Blier P, Hen R (2002): Behavioral and physiologic effects of genetic or pharmacologic inactivation of the substance P receptor (NK1). *J Clin Psychiatry* 63 Suppl 11:11-17.

Santarelli L, Gobbi G, Debs PC, Sibille ET, Blier P, Hen R, et al (2001): Genetic and pharmacological disruption of neurokinin 1 receptor function decreases anxiety-related behaviors and increases serotonergic function. *Proc Natl Acad Sci U S A* 98:1912-1917.

Santarelli L, Saxe M, Gross C, Surget A, Battaglia F, Dulawa S, et al (2003): Requirement of hippocampal neurogenesis for the behavioral effects of antidepressants. *Science* 301:805-809.

Sargent PA, Kjaer KH, Bench CJ, Rabiner EA, Messa C, Meyer J, et al (2000): Brain serotonin1A receptor binding measured by positron emission tomography with [11C]WAY-100635: effects of depression and antidepressant treatment. *Arch Gen Psychiatry* 57:174-180.

Saria A (1999): The tachykinin NK1 receptor in the brain: pharmacology and putative functions. *Eur J Pharmacol* 375:51-60.

Sartori SB, Burnet PW, Sharp T, Singewald N (2004): Evaluation of the effect of chronic antidepressant treatment on neurokinin-1 receptor expression in the rat brain. *Neuropharmacology* 46:1177-1183.

Sartorius A, Henn FA (2007): Deep brain stimulation of the lateral habenula in treatment resistant major depression. *Med Hypotheses* 69:1305-1308.

Satake H, Kawada T (2006): Overview of the primary structure, tissue-distribution, and functions of tachykinins and their receptors. *Curr Drug Targets* 7:963-974.

Schotte A, Leysen JE (1988): Distinct autoradiographic labelling of serotonin 5-HT2 receptors, alpha 1-adrenoceptors and histamine-H1 receptors and of tetrabenazine-displaceable ketanserin binding sites in rodent brain with [125I]7-amino-8-iodo-ketanserin. *Eur J Pharmacol* 145:213-216.

Schreiber R, De Vry J (1993): Neuroanatomical basis for the antidepressant-like effects of the 5-HT(1A) receptor agonists 8-OH-DPAT and ipsapirone in the rat forced swimming test. *Behav Pharmacol* 4:625-636.

Segal M (1979): Serotonergic innervation of the locus coeruleus from the dorsal raphe and its action on responses to noxious stimuli. *J Physiol* 286:401-415.

Segrave R, Nathan PJ (2005): Pindolol augmentation of selective serotonin reuptake inhibitors: accounting for the variability of results of placebo-controlled double-blind studies in patients with major depression. *Hum Psychopharmacol* 20:163-174.

Seress L, Leranth C (1996): Distribution of substance P-immunoreactive neurons and fibers in the monkey hippocampal formation. *Neuroscience* 71:633-650.

Sergeyev V, Fetissov S, Mathe AA, Jimenez PA, Bartfai T, Mortas P, et al (2005): Neuropeptide expression in rats exposed to chronic mild stresses. *Psychopharmacology (Berl)* 178:115-124.

Sergeyev V, Hokfelt T, Hurd Y (1999): Serotonin and substance P co-exist in dorsal raphe neurons of the human brain. *Neuroreport* 10:3967-3970.

Serres F, Sartori SB, Halton A, Pei Q, Rochat C, Singewald N, et al (2006): Stereoselective and region-specific induction of immediate early gene expression in rat parietal cortex by blockade of neurokinin 1 receptors. *J Psychopharmacol* 20:570-576.

Sesack SR, Deutch AY, Roth RH, Bunney BS (1989): Topographical organization of the efferent projections of the medial prefrontal cortex in the rat: an anterograde tract-tracing study with Phaseolus vulgaris leucoagglutinin. *J Comp Neurol* 290:213-242.

Severini C, Improta G, Falconieri-Erspamer G, Salvadori S, Erspamer V (2002): The tachykinin peptide family. *Pharmacol Rev* 54:285-322.

Sheldon PW, Aghajanian GK (1990): Serotonin (5-HT) induces IPSPs in pyramidal layer cells of rat piriform cortex: evidence for the involvement of a 5-HT2-activated interneuron. *Brain Res* 506:62-69.

Sheline YI, Mintun MA, Moerlein SM, Snyder AZ (2002): Greater loss of 5-HT(2A) receptors in midlife than in late life. *Am J Psychiatry* 159:430-435.

Shelton RC, Tollefson GD, Tohen M, Stahl S, Gannon KS, Jacobs TG, et al (2001): A novel augmentation strategy for treating resistant major depression. *Am J Psychiatry* 158:131-134.

Shen KZ, North RA (1992): Substance P opens cation channels and closes potassium channels in rat locus coeruleus neurons. *Neuroscience* 50:345-353.

Shen RY, Andrade R (1998): 5-Hydroxytryptamine2 receptor facilitates GABAergic neurotransmission in rat hippocampus. *J Pharmacol Exp Ther* 285:805-812.

Shigemoto R, Nakaya Y, Nomura S, Ogawa-Meguro R, Ohishi H, Kaneko T, et al (1993): Immunocytochemical localization of rat substance P receptor in the striatum. *Neurosci Lett* 153:157-160.

Shimada S, Inagaki S, Kubota Y, Ogawa N, Shibasaki T, Takagi H (1989): Coexistence of peptides (corticotropin releasing factor/neurotensin and substance P/somatostatin) in the bed nucleus of the stria terminalis and central amygdaloid nucleus of the rat. *Neuroscience* 30:377-383.

Shinoda K, Inagaki S, Shiosaka S, Kohno J, Tohyama M (1984): Experimental immunohistochemical studies on the substance P neuron system in the lateral habenular nucleus of the rat: distribution and origins. *J Comp Neurol* 222:578-588.

Shirayama Y, Mitsushio H, Takashima M, Ichikawa H, Takahashi K (1996): Reduction of substance P after chronic antidepressants treatment in the striatum, substantia nigra and amygdala of the rat. *Brain Res* 739:70-78.

Shughrue PJ, Lane MV, Merchenthaler I (1996): In situ hybridization analysis of the distribution of neurokinin-3 mRNA in the rat central nervous system. *J Comp Neurol* 372:395-414.

Shults CW, Quirion R, Chronwall B, Chase TN, O'Donohue TL (1984): A comparison of the anatomical distribution of substance P and substance P receptors in the rat central nervous system. *Peptides* 5:1097-1128.

Shults CW, Quirion R, Jensen RT, Moody TW, O'Donohue TL, Chase TN (1982): Autoradiographic localization of substance P receptors using 125I substance P. *Peptides* 3:1073-1075.

Shumake J, Conejo-Jimenez N, Gonzalez-Pardo H, Gonzalez-Lima F (2004): Brain differences in newborn rats predisposed to helpless and depressive behavior. *Brain Res* 1030:267-276.

Shumake J, Edwards E, Gonzalez-Lima F (2003): Opposite metabolic changes in the habenula and ventral tegmental area of a genetic model of helpless behavior. *Brain Res* 963:274-281.

Siegel RA, Duker EM, Pahnke U, Wuttke W (1987): Stress-induced changes in cholecystokinin and substance P concentrations in discrete regions of the rat hypothalamus. *Neuroendocrinology* 46:75-81.

Siemion IZ, Kluczyk A, Cebrat M (2005): The peptide molecular links between the central nervous and the immune systems. *Amino Acids* 29:161-176.

Sim LJ, Joseph SA (1989): Opiocortin and catecholamine projections to raphe nuclei. *Peptides* 10:1019-1025.

Sivam SP, Krause JE (1992): Tachykinin systems in the spinal cord and basal ganglia: influence of neonatal capsaicin treatment or dopaminergic intervention on levels of peptides, substance P-encoding mRNAs, and substance P receptor mRNA. *J Neurochem* 59:2278-2284.

Sivam SP, Krause JE, Takeuchi K, Li S, McGinty JF, Hong JS (1989): Lithium increases rat striatal beta- and gamma-preprotachykinin messenger RNAs. *J Pharmacol Exp Ther* 248:1297-1301.

Slifstein M, Laruelle M (2001): Models and methods for derivation of in vivo neuroreceptor parameters with PET and SPECT reversible radiotracers. *Nucl Med Biol* 28:595-608.

Sloviter RS, Ali-Akbarian L, Horvath KD, Menkens KA (2001): Substance P receptor expression by inhibitory interneurons of the rat hippocampus: enhanced detection using improved immunocytochemical methods for the preservation and colocalization of GABA and other neuronal markers. *J Comp Neurol* 430:283-305.

Smith DW, Hewson L, Fuller P, Williams AR, Wheeldon A, Rupniak NM (1999): The substance P antagonist L-760,735 inhibits stress-induced NK(1) receptor internalisation in the basolateral amygdala. *Brain Res* 848:90-95.

Smith KA, Fairburn CG, Cowen PJ (1997): Relapse of depression after rapid depletion of tryptophan. *Lancet* 349:915-919.

Solin O, Eskola O, Hamill TG, Bergman J, Lehikoinen P, Gronroos T, et al (2004): Synthesis and characterization of a potent, selective, radiolabeled substance-P antagonist for NK1 receptor quantitation: ([18F]SPA-RQ). *Mol Imaging Biol* 6:373-384.

Speciale SG, Neckers LM, Wyatt RJ (1980): Habenular modulation of raphe indoleamine metabolism. *Life Sci* 27:2367-2372.

Spielberger CD (1983): *Manual for the state-trait anxiety inventory*. Palo Alto, CA: Consulting Psychologists Press: STAI.

Spinks TJ, Jones T, Bloomfield PM, Bailey DL, Miller M, Hogg D, et al (2000): Physical characteristics of the ECAT EXACT3D positron tomograph. *Phys Med Biol* 45:2601-2618.

Spooren W, Riemer C, Meltzer H (2005): Opinion: NK3 receptor antagonists: the next generation of antipsychotics? *Nat Rev Drug Discov* 4:967-975.

Sprague DR, Chin FT, Liow JS, Fujita M, Burns HD, Hargreaves R, et al (2007): Human biodistribution and radiation dosimetry of the tachykinin NK1 antagonist radioligand [18F]SPA-RQ: comparison of thin-slice, bisected, and 2-dimensional planar image analysis. *J Nucl Med* 48:100-107.

Stacey AE, Woodhall GL, Jones RS (2002): Activation of neurokinin-1 receptors promotes GABA release at synapses in the rat entorhinal cortex. *Neuroscience* 115:575-586.

Staley JK, Malison RT, Innis RB (1998): Imaging of the serotonergic system: interactions of neuroanatomical and functional abnormalities of depression. *Biol Psychiatry* 44:534-549.

Stefanski R, Palejko W, Bidzinski A, Kostowski W, Plaznik A (1993): Serotonergic innervation of the hippocampus and nucleus accumbens septi and the anxiolytic-like action of midazolam and 5-HT1A receptor agonists. *Neuropharmacology* 32:977-985.

Stein C, Davidowa H, Albrecht D (2000): 5-HT(1A) receptor-mediated inhibition and 5-HT(2) as well as 5-HT(3) receptor-mediated excitation in different subdivisions of the rat amygdala. *Synapse* 38:328-337.

Steinbusch HW (1981): Distribution of serotonin-immunoreactivity in the central nervous system of the rat-cell bodies and terminals. *Neuroscience* 6:557-618.

Steinbusch HW, Nieuwenhuys R (1983): The raphe nuclei of the rat brainstem; A cytoarchitectonic and immunocytochemical study. In: Emson PC editor. *Chemical Neuroanatomy*. New York: Raven Press, pp 131-207.

Stenfors C, Srinivasan GR, Theodorsson E, Mathe AA (1992): Electroconvulsive stimuli and brain peptides: effect of modification of seizure duration on neuropeptide Y, neurokinin A, substance P and neurotensin. *Brain Res* 596:251-258.

Stern WC, Johnson A, Bronzino JD, Morgane PJ (1979): Effects of electrical stimulation of the lateral habenula on single-unit activity of raphe neurons. *Exp Neurol* 65:326-342.

Stern WC, Johnson A, Bronzino JD, Morgane PJ (1981): Neuropharmacology of the afferent projections from the lateral habenula and substantia nigra to the anterior raphe in the rat. *Neuropharmacology* 20:979-989.

Stockmeier CA (2003): Involvement of serotonin in depression: evidence from postmortem and imaging studies of serotonin receptors and the serotonin transporter. *J Psychiatr Res* 37:357-373.

Stockmeier CA, Shapiro LA, Dilley GE, Kolli TN, Friedman L, Rajkowska G (1998): Increase in serotonin-1A autoreceptors in the midbrain of suicide victims with major depression-postmortem evidence for decreased serotonin activity. *J Neurosci* 18:7394-7401.

Stockmeier CA, Shi X, Konick L, Overholser JC, Jurjus G, Meltzer HY, et al (2002): Neurokinin-1 receptors are decreased in major depressive disorder. *Neuroreport* 13:1223-1227.

Stratton SC, Beresford IJ, Hagan RM (1996): Autoradiographic localization of tachykinin NK2 receptors in adult rat brain using [^{3}H]SR48968. *Br J Pharmacol* 117:295P.

Studholme C, Hill DL, Hawkes DJ (1997): Automated three-dimensional registration of magnetic resonance and positron emission tomography brain images by multiresolution optimization of voxel similarity measures. *Med Phys* 24:25-35.

Swain CJ (1998): Neurokinin receptor antagonists. *Prog Med Chem* 35:57-81.

Szabo ST, Blier P (2001a): Effect of the selective noradrenergic reuptake inhibitor reboxetine on the firing activity of noradrenaline and serotonin neurons. *Eur J Neurosci* 13:2077-2087.

Szabo ST, Blier P (2001b): Functional and pharmacological characterization of the modulatory role of serotonin on the firing activity of locus coeruleus norepinephrine neurons. *Brain Res* 922:9-20.

Takahashi K, Tanaka A, Hara M, Nakanishi S (1992): The primary structure and gene organization of human substance P and neuromedin K receptors. *Eur J Biochem* 204:1025-1033.

Takayama H, Ota Z, Ogawa N (1986): Effect of immobilization stress on neuropeptides and their receptors in rat central nervous system. *Regul Pept* 15:239-248.

Takeda Y, Chou KB, Takeda J, Sachais BS, Krause JE (1991): Molecular cloning, structural characterization and functional expression of the human substance P receptor. *Biochem Biophys Res Commun* 179:1232-1240.

Takeuchi Y, Kojima M, Matsuura T, Sano Y (1983): Serotonergic innervation on the motoneurons in the mammalian brainstem. Light and electron microscopic immunohistochemistry. *Anat Embryol (Berl)* 167:321-333.

Tamiya R, Inoue K, Takagi H (1994): GABA-ergic and substance P-ergic double-innervation to noradrenergic neurons in the rat locus coeruleus. *Osaka City Med J* 40:1-11.

Tan PZ, Baldwin RM, Van Dyck CH, Al-Tikriti M, Roth B, Khan N, et al (1999): Characterization of radioactive metabolites of 5-HT2A receptor PET ligand [18F]altanserin in human and rodent. *Nucl Med Biol* 26:601-608.

Tanaka E, North RA (1993): Actions of 5-hydroxytryptamine on neurons of the rat cingulate cortex. *J Neurophysiol* 69:1749-1757.

Tanaka M, Yoshida M, Emoto H, Ishii H (2000): Noradrenaline systems in the hypothalamus, amygdala and locus coeruleus are involved in the provocation of anxiety: basic studies. *Eur J Pharmacol* 405:397-406.

Tauscher J, Verhoeff NP, Christensen BK, Hussey D, Meyer JH, Kecojevic A, et al (2001): Serotonin 5-HT1A receptor binding potential declines with age as measured by [11C]WAY-100635 and PET. *Neuropsychopharmacology* 24:522-530.

Teixeira RM, Santos AR, Ribeiro SJ, Calixto JB, Rae GA, De Lima TC (1996): Effects of central administration of tachykinin receptor agonists and antagonists on plus-maze behavior in mice. *Eur J Pharmacol* 311:7-14.

Thomas DR, Hagan JJ (2004): 5-HT7 receptors. *Curr Drug Targets CNS Neurol Disord* 3:81-90.

Thornton EW, Evans JA, Harris C (1985): Attenuated response to nomifensine in rats during a swim test following lesion of the habenula complex. *Psychopharmacology (Berl)* 87:81-85.

Timofeeva E, Richard D (2001): Activation of the central nervous system in obese Zucker rats during food deprivation. *J Comp Neurol* 441:71-89.

Tooney PA, Au GG, Chahl LA (2000a): Localisation of tachykinin NK1 and NK3 receptors in the human prefrontal and visual cortex. *Neurosci Lett* 283:185-188.

Tooney PA, Au GG, Chahl LA (2000b): Tachykinin NK1 and NK3 receptors in the prefrontal cortex of the human brain. *Clin Exp Pharmacol Physiol* 27:947-949.

Tooney PA, Crawter VC, Chahl LA (2001): Increased tachykinin NK(1) receptor immunoreactivity in the prefrontal cortex in schizophrenia. *Biol Psychiatry* 49:523-527.

Tork I (1990): Anatomy of the serotonergic system. *Ann N Y Acad Sci* 600:9-34; discussion 34-35.

Toth K, Wittner L, Urban Z, Doyle WK, Buzsaki G, Shigemoto R, et al (2007): Morphology and synaptic input of substance P receptor-immunoreactive interneurons in control and epileptic human hippocampus. *Neuroscience* 144:495-508.

Totterdell S, Ingham CA, Bolam JP (1992): Immunocytochemistry I: pre-embedding staining. In: Bolam JP editor. *Experimental Neuroanatomy: A Practical Approach*. Oxford: Oxford University Press (IRL), pp 103-128.

Turcatti G, Zoffmann S, Lowe JA, 3rd, Drozda SE, Chassaing G, Schwartz TW, et al (1997): Characterization of non-peptide antagonist and peptide agonist binding sites of the NK1 receptor with fluorescent ligands. *J Biol Chem* 272:21167-21175.

Turecki G, Briere R, Dewar K, Antonetti T, Lesage AD, Seguin M, et al (1999): Prediction of level of serotonin 2A receptor binding by serotonin receptor 2A

genetic variation in postmortem brain samples from subjects who did or did not commit suicide. *Am J Psychiatry* 156:1456-1458.

Unger T, Carolus S, Demmert G, Ganten D, Lang RE, Maser-Gluth C, et al (1988): Substance P induces a cardiovascular defense reaction in the rat: pharmacological characterization. *Circ Res* 63:812-820.

Usher M, Cohen JD, Servan-Schreiber D, Rajkowski J, Aston-Jones G (1999): The role of locus coeruleus in the regulation of cognitive performance. *Science* 283:549-554.

Valentino RJ, Bey V, Pernar L, Commons KG (2003): Substance P Acts through local circuits within the rat dorsal raphe nucleus to alter serotonergic neuronal activity. *J Neurosci* 23:7155-7159.

Valentino RJ, Commons KG (2005): Peptides that fine-tune the serotonin system. *Neuropeptides* 39:1-8.

Van Bockstaele EJ (1998): Morphological substrates underlying opioid, epinephrine and gamma-aminobutyric acid inhibitory actions in the rat locus coeruleus. *Brain Res Bull* 47:1-15.

Van der Does AJ (2001): The effects of tryptophan depletion on mood and psychiatric symptoms. *J Affect Disord* 64:107-119.

van der Hart MG, Czeh B, de Biurrun G, Michaelis T, Watanabe T, Natt O, et al (2002): Substance P receptor antagonist and clomipramine prevent stress-induced alterations in cerebral metabolites, cytogenesis in the dentate gyrus and hippocampal volume. *Mol Psychiatry* 7:933-941.

van der Hart MG, de Biurrun G, Czeh B, Rupniak NM, den Boer JA, Fuchs E (2005): Chronic psychosocial stress in tree shrews: effect of the substance P (NK1 receptor) antagonist L-760735 and clomipramine on endocrine and behavioral parameters. *Psychopharmacology (Berl)* 181:207-216.

Van der Mey M, Janssen CG, Janssens FE, Jurzak M, Langlois X, Sommen FM, et al (2005): Synthesis and biodistribution of [(11)C]R116301, a promising PET ligand for central NK(1) receptors. *Bioorg Med Chem* 13:1579-1586.

van der Want JJ, Klooster J, Cardozo BN, de Weerd H, Liem RS (1997): Tract-tracing in the nervous system of vertebrates using horseradish peroxidase and its conjugates: tracers, chromogens and stabilization for light and electron microscopy. *Brain Res Brain Res Protoc* 1:269-279.

van Kampen M, Kramer M, Hiemke C, Flugge G, Fuchs E (2002): The chronic psychosocial stress paradigm in male tree shrews: evaluation of a novel animal model for depressive disorders. *Stress* 5:37-46.

van Praag HM, Plutchik R (1984): Depression type and depression severity in relation to risk of violent suicide attempt. *Psychiatry Res* 12:333-338.

Vandermaelen CP, Aghajanian GK (1983): Electrophysiological and pharmacological characterization of serotonergic dorsal raphe neurons recorded extracellularly and intracellularly in rat brain slices. *Brain Res* 289:109-119.

Varga V, Kocsis B, Sharp T (2003): Electrophysiological evidence for convergence of inputs from the medial prefrontal cortex and lateral habenula on single neurons in the dorsal raphe nucleus. *Eur J Neurosci* 17:280-286.

Varga V, Szekely AD, Csillag A, Sharp T, Hajos M (2001): Evidence for a role of GABA interneurones in the cortical modulation of midbrain 5-hydroxytryptamine neurones. *Neuroscience* 106:783-792.

Varty GB, Cohen-Williams ME, Hunter JC (2003): The antidepressant-like effects of neurokinin NK1 receptor antagonists in a gerbil tail suspension test. *Behav Pharmacol* 14:87-95.

Varty GB, Cohen-Williams ME, Morgan CA, Pylak U, Duffy RA, Lachowicz JE, et al (2002): The gerbil elevated plus-maze II: anxiolytic-like effects of selective neurokinin NK1 receptor antagonists. *Neuropsychopharmacology* 27:371-379.

Vassout A, Veenstra S, Hauser K, Ofner S, Brugger F, Schilling W, et al (2000): NKP608: a selective NK-1 receptor antagonist with anxiolytic-like effects in the social interaction and social exploration test in rats. *Regul Pept* 96:7-16.

Vendruscolo LF, Takahashi RN, Bruske GR, Ramos A (2003): Evaluation of the anxiolytic-like effect of NKP608, a NK1-receptor antagonist, in two rat strains that differ in anxiety-related behaviors. *Psychopharmacology (Berl)* 170:287-293.

Verastegui C, Fernandez-Vivero J, Prada A, Rodriguez F, Romero A, Gonzalez-Moreno M, et al (1997): Presence and distribution of 5HT-, VIP-, NPY-, and SP-immunoreactive structures in adult mouse lung. *Histol Histopathol* 12:909-918.

Verge D, Daval G, Marcinkiewicz M, Patey A, el Mestikawy S, Gozlan H, et al (1986): Quantitative autoradiography of multiple 5-HT1 receptor subtypes in the brain of control or 5,7-dihydroxytryptamine-treated rats. *J Neurosci* 6:3474-3482.

Vertes RP (1991): A PHA-L analysis of ascending projections of the dorsal raphe nucleus in the rat. *J Comp Neurol* 313:643-668.

Vertes RP, Crane AM (1997): Distribution, quantification, and morphological characteristics of serotonin-immunoreactive cells of the supralemniscal nucleus (B9) and pontomesencephalic reticular formation in the rat. *J Comp Neurol* 378:411-424.

Vertes RP, Fortin WJ, Crane AM (1999): Projections of the median raphe nucleus in the rat. *J Comp Neurol* 407:555-582.

Vertes RP, Martin GF (1988): Autoradiographic analysis of ascending projections from the pontine and mesencephalic reticular formation and the median raphe nucleus in the rat. *J Comp Neurol* 275:511-541.

Vetter DE, Mugnaini E (1992): Distribution and dendritic features of three groups of rat olivocochlear neurons. A study with two retrograde cholera toxin tracers. *Anat Embryol (Berl)* 185:1-16.

Vicentic A, Francis D, Moffett M, Lakatos A, Rogge G, Hubert GW, et al (2006): Maternal separation alters serotonergic transporter densities and serotonergic 1A receptors in rat brain. *Neuroscience* 140:355-365.

Vigna SR, Bowden JJ, McDonald DM, Fisher J, Okamoto A, McVey DC, et al (1994): Characterization of antibodies to the rat substance P (NK-1) receptor and to a chimeric substance P receptor expressed in mammalian cells. *J Neurosci* 14:834-845.

Vincent SR, Satoh K, Armstrong DM, Fibiger HC (1983): Substance P in the ascending cholinergic reticular system. *Nature* 306:688-691.

Vincent SR, Staines WA, McGeer EG, Fibiger HC (1980): Transmitters contained in the efferents of the habenula. *Brain Res* 195:479-484.

Walker PD, Riley LA, Hart RP, Jonakait GM (1991): Serotonin regulation of neostriatal tachykinins following neonatal 6-hydroxydopamine lesions. *Brain Res* 557:31-36.

Wallace-Boone TL, Newton AE, Wright RN, Lodge NJ, McElroy JF (2008): Behavioral and pharmacological validation of the gerbil forced-swim test: effects of neurokinin-1 receptor antagonists. *Neuropsychopharmacology* 33:1919-1928.

Wallius E, Nyman M, Oikonen V, Hietala J, Ruotsalainen U (2007): Voxel-based NK1 receptor occupancy measurements with [(18)F]SPA-RQ and positron emission tomography: a procedure for assessing errors from image reconstruction and physiological modeling. *Mol Imaging Biol* 9:284-294.

Wang RY, Aghajanian GK (1977): Physiological evidence for habenula as major link between forebrain and midbrain raphe. *Science* 197:89-91.

Wang SJ, Cheng LL, Gean PW (1999): Cross-modulation of synaptic plasticity by beta-adrenergic and 5-HT1A receptors in the rat basolateral amygdala. *J Neurosci* 19:570-577.

Warden MK, Young WS, 3rd (1988): Distribution of cells containing mRNAs encoding substance P and neurokinin B in the rat central nervous system. *J Comp Neurol* 272:90-113.

Wegener G, Bandpey Z, Heiberg IL, Mork A, Rosenberg R (2003): Increased extracellular serotonin level in rat hippocampus induced by chronic citalopram

is augmented by subchronic lithium: neurochemical and behavioural studies in the rat. *Psychopharmacology (Berl)* 166:188-194.

Weidenhofer J, Yip J, Zavitsanou K, Huang XF, Chahl LA, Tooney PA (2006): Immunohistochemical localisation of the NK1 receptor in the human amygdala: preliminary investigation in schizophrenia. *Prog Neuropsychopharmacol Biol Psychiatry* 30:1313-1321.

Weinberg RJ, van Eyck SL (1991): A tetramethylbenzidine/tungstate reaction for horseradish peroxidase histochemistry. *J Histochem Cytochem* 39:1143-1148.

Weisstaub NV, Zhou M, Lira A, Lambe E, Gonzalez-Maeso J, Hornung JP, et al (2006): Cortical 5-HT2A receptor signaling modulates anxiety-like behaviors in mice. *Science* 313:536-540.

Welner SA, De Montigny C, Desroches J, Desjardins P, Suranyi-Cadotte BE (1989): Autoradiographic quantification of serotonin1A receptors in rat brain following antidepressant drug treatment. *Synapse* 4:347-352.

Whitaker-Azmitia PM, Clarke C, Azmitia EC (1993): Localization of 5-HT1A receptors to astroglial cells in adult rats: implications for neuronal-glial interactions and psychoactive drug mechanism of action. *Synapse* 14:201-205.

Whitton P, Curzon G (1990): Anxiogenic-like effect of infusing 1-(3-chlorophenyl) piperazine (mCPP) into the hippocampus. *Psychopharmacology (Berl)* 100:138-140.

Whitty CJ, Paul MA, Bannon MJ (1997): Neurokinin receptor mRNA localization in human midbrain dopamine neurons. *J Comp Neurol* 382:394-400.

Whitty CJ, Walker PD, Goebel DJ, Poosch MS, Bannon MJ (1995): Quantitation, cellular localization and regulation of neurokinin receptor gene expression within the rat substantia nigra. *Neuroscience* 64:419-425.

Wiklund L, Behzadi G, Kalen P, Headley PM, Nicolopoulos LS, Parsons CG, et al (1988): Autoradiographic and electrophysiological evidence for excitatory amino acid transmission in the periaqueductal gray projection to nucleus raphe magnus in the rat. *Neurosci Lett* 93:158-163.

Willins DL, Berry SA, Alsayegh L, Backstrom JR, Sanders-Bush E, Friedman L, et al (1999): Clozapine and other 5-hydroxytryptamine-2A receptor antagonists alter the subcellular distribution of 5-hydroxytryptamine-2A receptors in vitro and in vivo. *Neuroscience* 91:599-606.

Willins DL, Deutch AY, Roth BL (1997): Serotonin 5-HT2A receptors are expressed on pyramidal cells and interneurons in the rat cortex. *Synapse* 27:79-82.

Wirtshafter D, Asin KE, Pitzer MR (1994): Dopamine agonists and stress produce different patterns of Fos-like immunoreactivity in the lateral habenula. *Brain Res* 633:21-26.

Wittner L, Henze DA, Zaborszky L, Buzsaki G (2006): Hippocampal CA3 pyramidal cells selectively innervate aspiny interneurons. *Eur J Neurosci* 24:1286-1298.

Woods CI, Azeredo WJ (1999): Noradrenergic and serotonergic projections to the superior olive: potential for modulation of olivocochlear neurons. *Brain Res* 836:9-18.

Woolley ML, Haman M, Higgins GA, Ballard TM (2006): Investigating the effect of bilateral amygdala lesions on fear conditioning and social interaction in the male Mongolian gerbil. *Brain Res* 1078:151-158.

Wright DE, Seroogy KB, Lundgren KH, Davis BM, Jennes L (1995): Comparative localization of serotonin1A, 1C, and 2 receptor subtype mRNAs in rat brain. *J Comp Neurol* 351:357-373.

Wu C, Yoder EJ, Shih J, Chen K, Dias P, Shi L, et al (1998): Development and characterization of monoclonal antibodies specific to the serotonin 5-HT2A receptor. *J Histochem Cytochem* 46:811-824.

Xu T, Pandey SC (2000): Cellular localization of serotonin(2A) (5HT(2A)) receptors in the rat brain. *Brain Res Bull* 51:499-505.

Yamaguchi K, Nakajima Y, Nakajima S, Stanfield PR (1990): Modulation of inwardly rectifying channels by substance P in cholinergic neurones from rat brain in culture. *J Physiol* 426:499-520.

Yamano M, Hillyard CJ, Girgis S, MacIntyre I, Emson PC, Tohyama M (1988): Presence of a substance P-like immunoreactive neurone system from the parabrachial area to the central amygdaloid nucleus of the rat with reference to coexistence with calcitonin gene-related peptide. *Brain Res* 451:179-188.

Yang LM, Hu B, Xia YH, Zhang BL, Zhao H (2008): Lateral habenula lesions improve the behavioral response in depressed rats via increasing the serotonin level in dorsal raphe nucleus. *Behav Brain Res* 188:84-90.

Yasuno F, Sanabria SM, Burns D, Hargreaves RJ, Ghose S, Ichise M, et al (2007): PET imaging of neurokinin-1 receptors with [(18)F]SPA-RQ in human subjects: assessment of reference tissue models and their test-retest reproducibility. *Synapse* 61:242-251.

Yip J, Chahl LA (2001): Localization of NK1 and NK3 receptors in guinea-pig brain. *Regul Pept* 98:55-62.

Yokota Y, Sasai Y, Tanaka K, Fujiwara T, Tsuchida K, Shigemoto R, et al (1989): Molecular characterization of a functional cDNA for rat substance P receptor. *J Biol Chem* 264:17649-17652.

Zachrisson O, Mathe AA, Lindefors N (1997): Decreased levels of preprotachykinin-A and tachykinin NK1 receptor mRNA in specific region of the rat striatum after electroconvulsive stimuli. *Eur J Pharmacol* 319:191-195.

Zagami MT, Ferraro G, Montalbano ME, Sardo P, La Grutta V (1995): Lateral habenula and hippocampal units: electrophysiological and iontophoretic study. *Brain Res Bull* 36:539-543.

Zangrossi H, Jr., Viana MB, Graeff FG (1999): Anxiolytic effect of intra-amygdala injection of midazolam and 8-hydroxy-2-(di-n-propylamino)tetralin in the elevated T-maze. *Eur J Pharmacol* 369:267-270.

Zhang Y, Lu L, Furlonger C, Wu GE, Paige CJ (2000): Hemokinin is a hematopoietic-specific tachykinin that regulates B lymphopoiesis. *Nat Immunol* 1:392-397.

Zhou FM, Hablitz JJ (1999): Activation of serotonin receptors modulates synaptic transmission in rat cerebral cortex. *J Neurophysiol* 82:2989-2999.

Zocchi A, Varnier G, Arban R, Griffante C, Zanetti L, Bettelini L, et al (2003): Effects of antidepressant drugs and GR 205171, an neurokinin-1 (NK1) receptor antagonist, on the response in the forced swim test and on monoamine extracellular levels in the frontal cortex of the mouse. *Neurosci Lett* 345:73-76.

Zoli M, Torri C, Ferrari R, Jansson A, Zini I, Fuxe K, et al (1998): The emergence of the volume transmission concept. *Brain Res Brain Res Rev* 26:136-147.

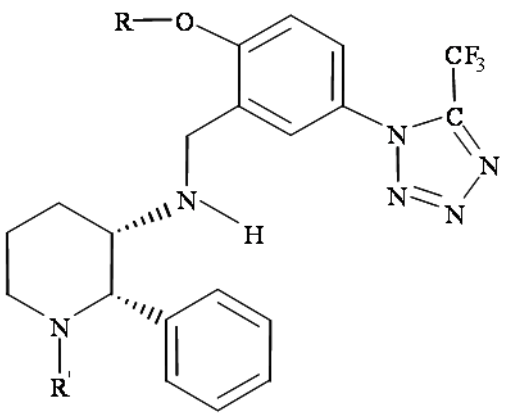
APPENDICES

APPENDIX A: *Radio-synthesis of [^{18F}]SPA-RQ*

Radio-synthesis of [^{18F}]SPA-RQ was carried out by chemists Sajinder Luthra and Zhao Yongjun (Fig. A.1). Essentially, the *O*-desfluoromethyl protected precursor, L-825,058 (*circa* 0.8-1.0 mg) was alkylated using [^{18}F]fluorobromomethane in a mixture solvent of Acetonitrile (100μl) and *N,N*-dimethylformamide (250 μl) containing ceasium carbonate (3.0-4.0 mg). [^{18}F]Fluorobromomethane itself was prepared from dibromomethane *via* a nucleophilic displacement reaction using [^{18}F]fluoride in the presence of potassium carbonate and kryptofix 2.2.2. The alkylation reaction was performed at 95 ˚C for 8 min to enhance the fluoromethylation process and yield the fluorine-18 labelled intermediate [^{18}F]L-832,045. After removal of reaction solvent, the protected intermediate [^{18}F]L-832,045 was deprotected from its *tert*-butoxycarbonyl (Boc) protecting group using trifluoroacetic acid (*circa* 200 μl). The crude product was taken up in a mixture of water and acetonitrile [50:50] and injected onto a semi-preparative HPLC column. [^{18}F]SPA-RQ was isolated using isocratic HPLC (μ–Bondapak C_{18} column, 30 x 0.78 mm i.d.; solvent: 40% / 60%, Acetonitrile / phosphoric acid [0.01M]; flow rate – 2.0 ml/min). The peak containing [^{18}F]SPA-RQ (retention time 12.0-13.0 min) was collected and the HPLC mobile phase removed under reduced pressure. The final residue was formulated for human injection using a solution of sterile 5% aqueous dextrose containing 1% ethanol with the pH adjusted to 6.8-7.6 using 0.1 M phosphate buffer (*circa* 500 μl, pH 7.4).

The radiosynthesis took place *circa* 1.5 hrs from end of bombardment. Typically, the average radiochemical yield of [^{18}F]SPA-RQ was between 6-10% from [^{18}F]fluoride

with an average specific radioactivity of *circa* 100 GBq/μmol at end of radiosynthesis and *circa* 200 GBq/μmol at end of bombardment. Stable SPA-RQ (< 4.5 μg/injection) and total unknown impurities (< 2.0 μg/injection) were within Quality Control specifications. The radiochemical purity was > 95%.



O-desfluoromethyl precursor (I): R = H; R' = *t*.Boc
[^{18}F]fluoro protected intermediate (II): R = [^{18}F]FCH$_2$; R' = *t*.Boc
[^{18}F]SPA-RQ (III): R = [^{18}F]FCH$_2$; R' = H

Fig. A.1. Structure of [^{18}F]SPA-RQ, its precursor and its intermediate. *O*-desfluoromethyl *tert*-butoxycarbonyl (Boc) protected precursor is alkylated to give the [^{18}F] fluoroprotected intermediate and later deprotection with trifluoroacetic acid yields [^{18}F]SPA-RQ.

APPENDIX B: *Measurement of [^{18}F]SPA-RQ and its metabolites in plasma*

Measurement of [^{18}F]SPA-RQ and its metabolites in plasma were made by Safiye Osman and her team. Plasma samples were analysed for metabolites using a semi-automated system with on-line solid-phase extraction (SPE; small column packed with C-18) followed by reverse-phase chromatography (Luthra et al., 1993). Briefly, the plasma samples were loaded onto the SPE column and eluted with di-ammoniumhydrogen phosphate (0.01 M) and further analysed using reverse-phase column (μ–Bondapak C_{18} column, 30 x 0.78 cm i.d.) eluted with a mixture of ammonium acetate (10 mM), acetonitrile and trifluoroacetic acid [55:45; 0.1 v/v] at a flow rate of 3 ml/min. The eluate was monitored for ultraviolet absorbance at 210 nm and radioactivity and subsequent data captured on a PC-based integrator. The radio-chromatogram showed two radioactive components, a minor component at 5.5 min and second component at 11.7 min which represented [^{18}F]SPA-RQ. The polar radioactive components eluted from the SPE and the radioactivity in the SPE eluate increased with time. The amount of [^{18}F]SPA-RQ and its radioactive metabolites at a given time point was calculated from the decay-corrected integrated radio-chromatogram and the levels of radioactivity in the SPE eluate and expressed as a percentage of total plasma sample injected.

APPENDIX C: *Correction of activity concentrations in the cerebellum*

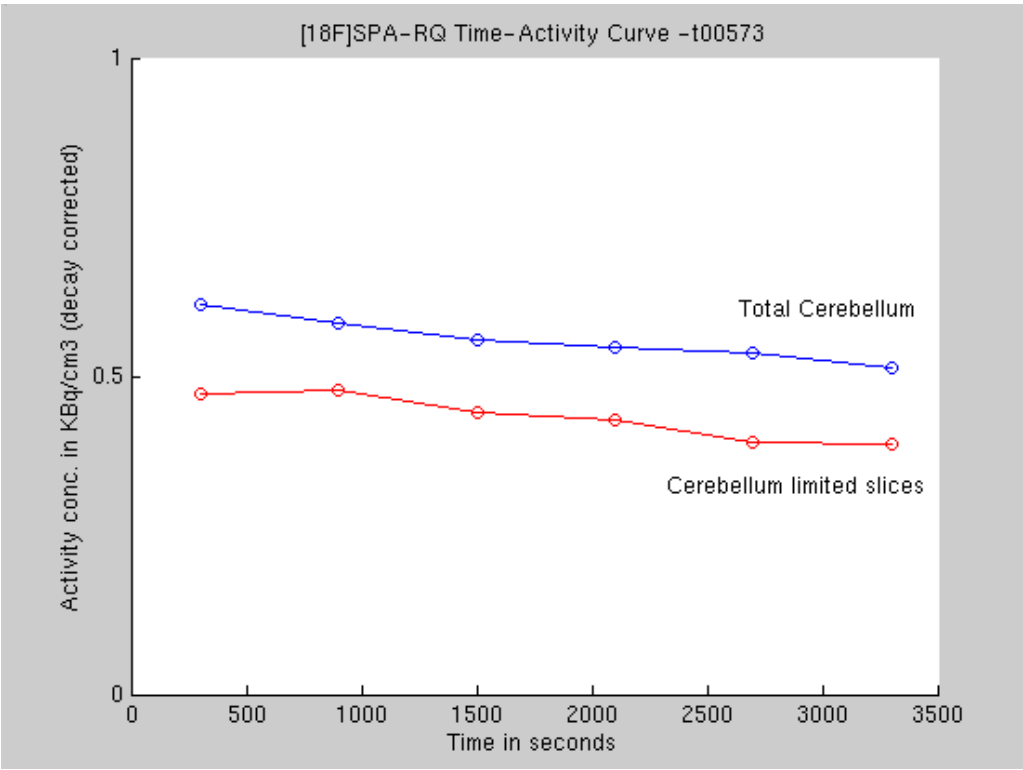


Fig. C.1. Example of [^{18}F] SPA-RQ time activity curves for the whole cerebellum compared to central cerebellum only in one subject. As the [^{18}F] SPA-RQ PET signal in the occipital lobe (a region with moderate binding) tended to encroach upon the cerebellum, the activity concentration in the cerebellum was found to be falsely high, over the time of the PET scan (0-3500 sec), when the whole of the cerebellum was sampled (blue line). By limiting the sampling of the slices to the middle of the cerebellum (10-16 slices) the activity concentration in the cerebellum was corrected (red line).

APPENDIX D: *Tissue over parent in plasma ratios for [^{18}F]SPA-RQ*

Tissue over parent in plasma ratios for [^{18}F]SPA-RQ were generated by Dr Rainer Hinz for comparison of radioligand clearance between tissue and plasma. Some examples are shown in Fig. D.1. The ratios were generally similar and stable over the time of the PET scan in most brain regions in all 3 groups.

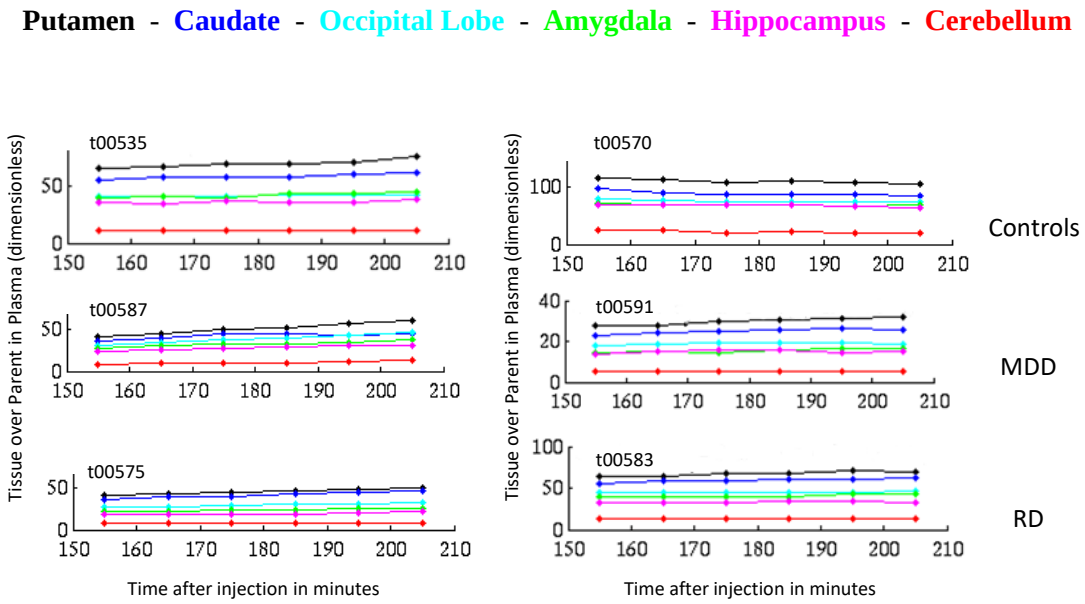


Fig. D.1. Tissue over parent in plasma ratio versus time for [^{18}F] SPA-RQ in controls, depressed and recovered depressed subjects. Examples of tissue over parent ligand in plasma ratios versus time for different brain regions in the 3 different groups: Control subjects, subjects with MDD (major depressive disorder), and RD (recovered depressed) subjects. The examples illustrate that the ratios are generally stable over the time of the scan (150-210 min) in all 3 groups especially in the moderately receptor-rich brain regions (occipital lobe, amygdala and hippocampus).